

# Scleractinian coral morphogenesis: searching for stem cells and precursors of the skeletogenic calicodermis

THÈSE N° 7170 (2016)

PRÉSENTÉE LE 2 NOVEMBRE 2016

À LA FACULTÉ DE L'ENVIRONNEMENT NATUREL, ARCHITECTURAL ET CONSTRUIT  
LABORATOIRE DE GÉOCHIMIE BIOLOGIQUE  
PROGRAMME DOCTORAL EN GÉNIE CIVIL ET ENVIRONNEMENT

ÉCOLE POLYTECHNIQUE FÉDÉRALE DE LAUSANNE

POUR L'OBTENTION DU GRADE DE DOCTEUR ÈS SCIENCES

PAR

**Agathe Eliette Marie LECOINTE**

acceptée sur proposition du jury:

Prof. T. I. Battin, président du jury  
Prof. A. Meibom, Dr I. Domart-Coulon, directeurs de thèse  
Prof. M. Fine, rapporteur  
Prof. E. Houliston, rapporteuse  
Prof. R. Bernier-Latmani, rapporteuse



ÉCOLE POLYTECHNIQUE  
FÉDÉRALE DE LAUSANNE

Suisse  
2016



# Acknowledgements/Remerciements

Ces quatre années de doctorat ont été aussi l'occasion de faire belles rencontres et collaborations et n'aurait pas été possible sans de nombreuses personnes que je souhaiterai remercier ici.

I would like to thank the members of the thesis jury, Prof. Tom Battin, the president, Prof. Rizlan Bernier-Latmani, internal examiner, Prof. Evelyne Houliston, external examiner and Prof. Maoz Fine, external examiner, for having accepting to review this manuscript.

Je remercie bien entendu mon directeur de thèse, le Prof. Anders Meibom, de m'avoir offert l'opportunité de travailler sur ce passionnant sujet. Je le remercie pour son soutien et salue sa capacité à motiver les troupes par son enthousiasme.

Je remercie ma co-directrice de thèse, le Dr Isabelle Domart-Coulon. J'ai beaucoup appris à ses côtés aussi bien sur le plan scientifique qu'humain.

Je voudrais remercier l'ancienne directrice de l'unité MCAM, Prof. Sylvie Rebuffat, ainsi que son successeur, Prof. Philippe Grellier, mais aussi les cheffes de l'équipe MDCEM, YanYan Li et Marie-Lise Bourguet-Kondracki de m'avoir accueilli dans les locaux de l'unité au Muséum National d'Histoire Naturelle (MNHN).

Durant ces quatre années j'ai eu la chance de travailler avec deux aquariums l'un privé l'autre public. Je remercie donc chaleureusement Dr Michel Hignette, directeur de l'Aquarium Tropical du Palais de la Porte Dorée (ATPD, Paris) et Dr Dominique Duché, directeur adjoint, pour non seulement nous avoir donné accès aux locaux et aménagé un espace de travail mais aussi pour ces échanges si intéressants. Un grand merci à l'équipe d'aquariologistes de l'ATPD, Jean-Daniel Galois, Thierry Carré, Fabrice Césari Colonna, Sylvain Joumier, Nicolas Luys, Salem Amazouz, Franck Daloux, Déodat Manchon et Laurent Petit, pour nous avoir fait bénéficier de leur savoir-faire et avoir partagé avec nous leur connaissance et leur grande curiosité du monde aquatique ! Merci au responsable aquariologie de l'aquarium d'Océanopolis, Dominique Barthélémy, pour nous avoir permis de venir travailler à Brest nous sauvant plus d'une fois la mise. Je remercie aussi l'équipe d'aquariologiste d'Océanopolis et notamment Sébastien Delaporte et Estelle Lesage en charge des bacs coraux pour leur aide précieuse.

Durant cette thèse deux semaines de terrain ont été possible et je voudrais remercier les membres de l'Interuniversity Institute for marine science d'Eilat en Mer Rouge et notamment le Prof. Maoz Fine pour leur accueil et leur aide sur place.

La recherche ne serait pas possible sans les plateformes et leurs formidables ingénieurs. Je remercie donc le Dr Chakib Djediat de la Plateforme de microscopie électronique du MNHN de m'avoir initié et formé à la microscopie électronique et tout ce qui entoure cette fascinante discipline. Et ce, toujours dans la bonne

humeur :) Je remercie l'équipe de la bioimaging and optics platform de l'EPFL et plus particulièrement Romain Guiet, Olivier Burri pour m'avoir donné goût à l'analyse d'images et initié au Java, mais aussi Thierry Laroche et José Artacho. Ce fut en vrai plaisir de travailler avec vous ! Merci à Marc Gèze et Cyril Willig pour l'accès au centre de microscopie de fluorescence et d'imagerie numérique du MNHN. Autre aide ponctuelle mais précieuse, celle de Manon Vandervennet et du Dr Carine Lombard.

Merci au Dr Nicolas Rabet pour m'avoir initié à la phylogénie !

Ces quatre ans entre le Muséum et l'EPFL m'ont permis de faire de belles rencontres parmi mes collègues dont certain(e)s sont maintenant des ami(e)s.

Du Muséum je pense à Mehdi, Jimmy, Anaïs, Alison, Benjamin, Isidora, Sévrine (x2), Amandine, Christine, Carine, Manon, Alain, Alexandre, Michel, Arlette, Natacha, Françoise. Ainsi qu'à mon fournisseur officiel de café Brice Molinelli. Je remercie aussi mon voisin de bureau, le Dr René Bensasson de m'avoir fait partager sa curiosité et son goût de la lecture. Merci au Dr Adrienne Kish pour son soutien et ses précieux conseils.

De l'EPFL je pense à la merveilleuse Stéphanie, à la géniale Melany, à Charlotte, Emma, Louise, Mustafa, Christophe, Julia et enfin à Thomas avec qui j'ai eu de passionnantes conversations.

Du Muséum puis de l'EPFL, je remercie Béa, les deux dernières années n'aurait pas été pareilles sans elle ! Travailler avec elle fut un réel plaisir, une belle rencontre :)

En dehors du labo, des amis fidèles, Lulu, Flo, Marine, Apo, Jade, Chloé, Sarah, les Phoks (et les phokesses ;)), Matthieu, Fabien, Malalatiana, William, Cyril, Salomé, Manu et tous les autres merci pour avoir maintenu à flots ma vie sociale en-dehors du labo ;)

Je remercie aussi ma famille pour leur soutien, dont ma sœur Morgane pour avoir fait les dessins de corail du chapitre 2 et ma sœur Alice pour m'avoir aidé à corriger mon anglais ;)

Et enfin un énorme merci à Adrien pour son soutien, ses conseils et tout le reste qui font que ces dernières années comptent parmi les plus belles de ma vie.

Lausanne, le 18 juillet 2016

# Preface

This thesis manuscript is the result of four years of PhD research on the establishment of the calicodermis cell layer in the metamorphosing scleractinian coral larva. The work presented here was realized at the laboratory for biological geochemistry at EPFL in close collaboration with the laboratory of communication molecules and micro-organisms adaptation at the National Muséum of Natural History in Paris, France. Field experiments at the Inter University Institute (Red Sea, Eilat, Israel) were also achieved and are part of this work.



# Abstract

Metamorphosis is a crucial step in the life cycle of a scleractinian coral: The swimming coral larva, the planula, settles, and metamorphoses into a sessile calcifying primary polyp, which subsequently grows into an adult colony. Importantly, morphogenesis into a primary polyp involves the establishment of the skeletogenic cell layer, the so-called calicodermis, but the cellular mechanisms that support this process are not well understood. In the work presented here, calicodermis establishment was studied in two scleractinian corals, *Pocillopora damicornis* and *Stylophora pistillata* using cell proliferation and apoptosis assays, electron microscopy, molecular biology tools, and isotopic imaging using NanoSIMS.

Cell proliferation during coral metamorphosis was evaluated with BrdU (5-bromo-2'-deoxyuridine) incubation pulses (24 h). In the primary polyp stage, cell migration was observed in the chase phase for several days (48 to 64 h) after the incubation pulse. A number of key observations were made: 1) Right after settlement, during the earliest metamorphosis stage that includes initial skeletal formation and therefore requires a fully functional calicodermis, cell proliferation rate in this tissue layer is in fact not significantly higher than in the preceding planula larval stage. This indicates that calicodermis establishment is primarily happening through transdifferentiation of cells from the aboral pseudostratified epithelium of the planula into calicodermis cells. 2) Later, in the growing primary polyp local cell proliferation in the calicodermis remains low, indicating that these cells do not originate in the calicodermis itself. 3) At the same time, it is observed in *S. pistillata* that the pharynx is the most proliferative area with up to 19% of cells dividing, and that cells migrate from this area through pseudostratified epithelium and/or mesenterial filaments to reach the expanding calicodermis, which is actively forming skeleton at this stage. 4) In order to identify potential stem cells and calicodermis precursor cells locations, biological markers were developed. Potential stem cells expressing *piwi* genes were localized in the mesenteries and below tentacle tips of *P. damicornis*. These sites contain proliferative areas involved in gametogenesis and nematogenesis, respectively. 5) Pdcyst-rich is a protein localized in the adult calicodermis and potentially involved in skeleton formation. The related gene was observed to be expressed at the early metamorphosis stage, when skeleton deposition commences. Preliminary results indicate that Pdcyst-rich proteins are also located in the calicodermis of the forming polyp and skeleton of the primary polyp stage. This suggests a role of Pdcyst-rich in skeletogenesis but it is not clear if it acts as a protein of the skeletal organic matrix or as an adhesion protein.

**Keywords:** *Scleractinia* – metamorphosis – calicodermis – cell proliferation – stem cells –

# Résumé

La métamorphose est une étape cruciale du cycle de vie des coraux scléactiniaires : la larve planctonique, la planula, se fixe au substrat et se métamorphose en un polype primaire sessile qui donnera la colonie adulte. Cette morphogénèse en polype primaire implique la mise en place de la couche cellulaire formant le squelette, appelée calicoderme, mais les mécanismes cellulaires sous-jacents ne sont pas bien compris. Dans la présente étude la mise en place du calicoderme a été étudiée chez deux espèces de coraux, *Pocillopora damicornis* et *Stylophora pistillata*, en évaluant la prolifération cellulaire et l'apoptose ainsi que par l'utilisation de méthodes de microscopies électroniques, d'outils de biologie moléculaire et d'imagerie isotopique par NanoSIMS.

La prolifération cellulaire pendant la métamorphose du corail a été évaluée par incubation en présence de BrdU (5-bromo-2'-deoxyuridine) durant 24 h. De plus, au stade polype primaire, la migration des cellules marquées a été suivie sur plusieurs jours (48 à 64 h) après le pulse initial. Plusieurs observations ont été faites : 1) Au stade précoce de la métamorphose, pendant lequel débute la formation du squelette et donc qui requiert un calicoderme fonctionnel, le taux de prolifération des cellules dans ce tissu n'est pas significativement plus élevé que dans le stade précédent, la planula. Cela indique que la mise en place du calicoderme se fait via transdifférentiation des cellules de l'épithélium pseudostratifié aboral de la planula en cellules du calicoderme. 2) Plus tard, dans le polype primaire en croissance, le taux de division des cellules reste bas dans le calicoderme ce qui indique que les cellules qui le composent ne proviennent pas directement du calicoderme. 3) Au même stade, le pharynx du polype primaire présente le taux de prolifération cellulaire le plus élevé avec 19% de ses cellules marquées au BrdU. Ces cellules migrent ensuite du pharynx jusqu'au calicoderme en passant par l'épithélium pseudostratifié et/ou les filaments mésentériques. 4) De façon à identifier de potentielles cellules souches ainsi que le lieu de la différenciation des cellules en cellules du calicoderme, des marqueurs biologiques ont été développés. Des cellules souches potentielles exprimant le gène *piwi* ont été localisées dans les mésentères et sous le bulbe des tentacules de *P. damicornis*. Ces zones correspondent à des sites de prolifération et sont associées respectivement avec la gamétogenèse et la nématogenèse. 5) Pdcyst-rich est une protéine spécifique du calicoderme des polypes adultes et est potentiellement impliquée dans la formation du squelette. Le gène associé s'exprime au stade précoce de la métamorphose, au moment où le squelette commence à se former. Les résultats préliminaires indiquent que la protéine est aussi présente lors de la formation du polype primaire ainsi que dans le squelette du polype primaire. Cela suggère un rôle de Pdcyst-rich dans la squeletogenèse, potentiellement en tant que protéine de la matrice organique du squelette ou que protéine d'adhésion au squelette.

**Mots-clés :** *Scleractinia* – métamorphose – calicoderme – prolifération cellulaire – cellules souches



# Contents

Acknowledgements/Remerciements .....	i
Preface .....	iii
Abstract .....	v
Résumé .....	vi
Contents .....	vii
List of Figures .....	x
List of Tables .....	xi
List of abbreviations and symbols .....	xii
Introduction .....	1
Literature review .....	5
I.    The coral holobiont .....	5
A.    Phylogeny of the <i>Cnidaria</i> .....	5
B.    Polyp: functional life unit.....	6
C.    Coral symbiont: <i>Symbiodinium sp.</i> .....	8
II.   The metamorphosing coral larva as a model to study calicodermis establishment .....	10
A.    Diversity of reproduction modes and life cycle .....	10
B.    Inducing metamorphosis .....	12
C.    Calicodermis establishment during metamorphosis .....	14
D.    Alternative study model: coral explant cultures .....	14
III.  Role of the calicodermis in coral biomineralization .....	15
A.    Calicodermis and the skeletal organic matrix.....	15
B.    Carbon source of biomineralization .....	17
C.    Calcium source of biomineralization .....	18
IV.  Stem cell in <i>Cnidaria</i> and corals .....	18
A.    Stem cell lineages in <i>Cnidaria</i> .....	18
B.    Stem cell related genes.....	21
Chapter 1: Explant formation in primary coral cell culture .....	23
I. Context .....	23
II. Publication.....	23
III. Conclusion .....	45
Chapter 2: Cell proliferation hot spots and cell migration during primary polyp morphogenesis.....	47

I. Context .....	47
II. Publication.....	47
III. Supplementary material.....	58
IV. Conclusion.....	61
Chapter 3: Calicodermis establishment during <i>Pocillopora damicornis</i> metamorphosis: towards the development of precursor cell markers .....	63
I. Abstract .....	63
II. Introduction.....	63
III. Materials and Methods .....	65
A. Biological material .....	65
B. BrdU pulse to assess cell proliferation .....	65
C. Immunolocalisation of BrdU and Pdcyst-rich protein .....	65
D. Bioinformatics identification of <i>piwi</i> gene related sequences in <i>Pocillopora damicornis</i> transcriptome and phylogenetic study. ....	66
E. Semi-quantitative RT-PCR.....	66
F. Whole-mount <i>in situ</i> hybridization (ISH) of <i>piwi 1</i> and <i>piwi 2</i> mRNA.....	67
IV. Results.....	68
A. Cell proliferation in the different tissues through metamorphosis.....	68
B. Identification and expression localization of <i>piwi</i> genes from <i>P. damicornis</i> .....	70
C. <i>pdcyst-rich</i> gene expression and protein localization .....	73
V. Discussion.....	76
A. Proliferation and candidate precursor cells .....	76
B. Pdcyst-rich protein and calicodermis differentiation.....	78
VI. Supplementary material .....	79
Chapter 4: Tracing isotopically labeled biofilm compounds into coral host tissue during settlement .....	85
I. Abstract .....	85
II. Introduction.....	85
III. Material and methods.....	86
A. Biofilm labeling with stable isotopes and larvae exposure .....	86
B. Histological procedures .....	87
C. Scanning electron microscopy in backscattered electron mode (SEM, BSE) .....	87
D. NanoSIMS isotopic imaging .....	87
E. Transmission electron microscopy (TEM).....	88
IV. Results.....	88

V. Discussion.....	91
VI. Supplementary material .....	93
General discussion and conclusion.....	95
I. Metamorphosis induction .....	95
II. Calicodermis establishment during metamorphosis.....	96
III. Stem cells in <i>Scleractinia</i> .....	97
IV. Symbiont regulation during metamorphosis .....	98
V. Conclusion .....	99
References .....	101
Curriculum Vitae .....	113

## List of Figures

Figure 1-1: Simplified phylogenetic tree of Metazoa with inset on <i>Cnidaria</i> .....	6
Figure 1-2: <i>Pocillopora damicornis</i> adult polyps. ....	7
Figure 1-3: Tissue organization of a primary polyp. ....	8
Figure 1-4: Schematic Pocilloporidae life cycle. ....	11
Figure 1-5: Schematic summary of the physical and chemical cues that induce planula metamorphosis. ....	13
Figure 1-6: Tissue ball formation.....	15
Figure 1-7: Dissolved inorganic carbon pathways.....	17
Figure 1-8: Stem cell systems in <i>Cnidaria</i> .....	20
Figure 2-1: <i>In vitro</i> cell aggregation and the formation of tissue balls in primary cultures from <i>P. damicornis</i> scleractinian coral.....	32
Figure 2-2: Structure of tissue ball (TB) compared to polyp.....	34
Figure 2-3: Histological organization of coral tissue balls compared to polyp.....	35
Figure 2-4: Ultrastructure of tissue balls.....	36
Figure 2-5: Compared autofluorescence of a live polyp and a tissue ball.....	37
Figure 2-6: BrdU-labeled nuclei in polyp and in tissue ball formed in 2 days primary cell culture.....	38
Figure 2-7: Compared BrdU incorporation rates of coral cells and dinoflagellates in polyps and in tissue balls obtained in 2 days primary culture.....	40
Figure 2-8: Cell Specific Density of dinoflagellate symbionts at initiation of coral primary cultures.....	41
Figure 3-1: Tissue organization during <i>Stylophora pistillata</i> metamorphosis.....	50
Figure 3-2: Distribution of BrdU-labeled nuclei in coral tissue from planula to adult polyp.....	52
Figure 3-3: Tissue-specific cell turnover during metamorphosis.....	53
Figure 3-4: Chase of the BrdU label in the ectoderm-derived epithelia.....	54
Figure 3-5: Dinoflagellate turnover in host gastrodermis during metamorphosis.....	55
Figure 3-S1: Imaging method for quantification of BrdU-labeled nuclei immunodetected in the coral tissue layers. ....	58
Figure 3-S2: Skeleton deposition during metamorphosis. ....	59
Figure 3-S3: Chase of the BrdU labeling in the gastrodermis .....	59
Figure 4-1: Cell proliferation through metamorphosis. ....	69
Figure 4-2: Piwi maximum-likelihood phylogeny. ....	71
Figure 4-3: <i>piwi 1</i> and <i>piwi 2</i> expressions through metamorphosis. ....	72
Figure 4-4: <i>piwi</i> expressions in <i>P. damicornis</i> adult polyps.....	73
Figure 4-5: <i>pdcyst-rich</i> expression through metamorphosis.....	74
Figure 4-6: Pdcyst-rich protein localization through coral metamorphosis.....	75

Figure 4-7: Pdcyst-rich protein localization in the forming polyp stage in thicker section and using an HRP amplification system.....	76
Figure 4-S1: Probe sequences used to target <i>piwi</i> mRNA in whole mount <i>in situ</i> hybridization .....	80
Figure 4-S2: Piwi-like Eukaryote domain alignment .....	81-82
Figure 4-S3: Pdcyst-rich associated protein maximum likelihood tree.....	83
Figure 5-1: Isotopic enrichment in bacteria from biofilm after 5 days incubation with stable isotopes (t=0 h) and 16 h after transfer in normal seawater in the presence of planulae.....	88
Figure 5-2: <sup>13</sup> C enrichment in <i>Symbiodinium</i> sp. of both planula and metamorphosed larvae.....	89
Figure 5-3: Isotopic ratios in the unsettled planula. ....	90
Figure 5-4: Isotopic enrichment in the metamorphosed larva. ....	91
Figure 5-S1: Mature biofilm grown on underwater paper in aquaria conditions at the Aquarium Tropical du Palais de la Porte Dorée (Paris, France).....	93
Figure 5-S2: Early metamorphosis calicodermis with some of its cnidocyte and mucous cells.....	93

## List of Tables

Table 2-I: Primary culture yield and viability, depending on collagenase type and commercial origin....	33
Table 2-II: BrdU labeling index of nuclei of coral cells and dinoflagellate symbionts in the different tissue layers of the polyp and <i>in vitro</i> , during (2d) formation of the tissue balls.....	39
Table 3-S I: BrdU 24h-labeling index of coral and dinoflagellate cells.....	60
Table 3-S II: Apoptotic index of coral and dinoflagellate cells .....	60
Table 3-S III: BrdU labeling index during the chase experiment.....	60
Table 3-S IV: Nuclei BrdU-labeling intensity.....	60
Table 3-S V: Mitotic index of dinoflagellates .....	60
Table 4-S I: PCR primers sequences used in semi-quantitative RT-PCR.....	79

## List of abbreviations and symbols

<b>AB-AM:</b> antibiotics-antimycotics	<b>HRP:</b> horseradish peroxidase
<b>ATPD:</b> Aquarium Tropical, Palais de la Porte Dorée	<b>i-cell:</b> interstitial cell
<b>BrdU:</b> 5-Bromo-2'-deoxyuridine analogue of deoxy-thymidine	<b>ISH:</b> <i>in situ</i> hybridization
<b>c:</b> calicodermis	<b>KRTAP:</b> cysteine-rich keratin-associated protein
<b>C:</b> carbon	<b>m:</b> mesenteries
<b>CA:</b> carbonic anhydrase	<b>Ma:</b> Million years
<b>Ca<sup>2+</sup>:</b> calcium ion	<b>MALDI-TOF:</b> matrix-assisted laser desorption/ionization time-of-flight
<b>CaCO<sub>3</sub>:</b> calcium carbonate	<b>MNHN:</b> Muséum National d'Histoire Naturelle
<b>CARP:</b> coral acid-rich protein	<b>N:</b> nitrogen
<b>CCA:</b> crustose coralline algae	<b>OsO<sub>4</sub>:</b> osmium tetroxide
<b>CDU:</b> Collagen degrading units	<b>PAR:</b> photosynthetically available radiation
<b>CeMiM:</b> Centre de Microscopie de fluorescence et d'Imagerie numérique	<b>PBS:</b> Phosphate buffered saline
<b>CO<sub>2</sub>:</b> carbone dioxide	<b>PBST:</b> Phosphate buffered saline + TritonX100
<b>CO<sub>3</sub><sup>2-</sup>:</b> carbonate ion	<b>PGC:</b> primordial germ cell
<b>CSD:</b> cell-specific density	<b>PMCA:</b> plasma-membrane calcium pump
<b>DIC:</b> dissolved inorganic carbon	<b>POM:</b> particulate organic matter
<b>DIN:</b> dissolved inorganic nitrogen	<b>pse:</b> pseudostratified epithelium
<b>DOM:</b> dissolved organic matter	<b>rpm:</b> rounds per minute
<b>ECM:</b> extracellular matrix	<b>RT-PCR:</b> reverse transcriptase polymerase chain reaction
<b>EDCRP:</b> epidermal differentiation cysteine-rich protein	<b>sk:</b> skeleton
<b>EST:</b> expressed sequence tag	<b>SC:</b> stem cell
<b>FSW:</b> filtered sea water	<b>SCRiP:</b> small cysteine-rich protein
<b>g:</b> gastrodermis	<b>SEM:</b> scanning electron microscopy
<b>GABA:</b> gamma-aminobutyric acid	<b>SOM:</b> skeletal organic matrix
<b>GBR:</b> Great Barrier Reef	<b>t:</b> tentacle
<b>GLW-amide:</b> amidated glycine-leucine-tryptophan C-terminus motif	<b>TBP:</b> tetrabromopyrrole
<b>H<sup>+</sup>:</b> hydrogen ion	<b>TBs:</b> tissue balls
<b>H<sub>2</sub>O<sub>2</sub>:</b> Hydrogen peroxide	<b>TBx:</b> toluidine blue/sodium borate
<b>HCO<sub>3</sub><sup>-</sup>:</b> bicarbonate ion	<b>TEM:</b> transmission electron microscopy
	<b>v/v:</b> volume/volume
	<b>w/v:</b> weight/volume

# Introduction

Coral reefs are the most diverse ecosystems in the oceans. Often considered “oases in the desert” or “rainforests of the sea” these biostructures provide shelter for at least 25% of all known marine species while occupying less than 0.1% of ocean surface (Spalding et al., 2001). In addition, coral reefs are economically important for tourism, fisheries, and coastline protection representing an estimated 30-375 billion US\$ (Cesar, 2002; Cooper et al., 2008; Costanza et al., 1997; Sarkis et al., 2010). But today these impressive ecosystems are threatened by global stress from increasing sea surface temperature (SST) and ocean acidification related to increasing atmospheric CO<sub>2</sub> concentrations (Cohen and Holcomb, 2009; Hoegh-Guldberg et al., 2007). Moreover, urbanization of coastal environments is adding pressure from local pollution and sedimentation that affect coral health (Carpenter et al., 2008). Today the world has effectively lost 19% of its coral reefs areas since 1998; another 15% are in serious danger of being lost in the next 10–20 years; and further 20% considered under threat of loss over a timescale of 20–40 years (Wilkinson, 2008). Given this situation, it is urgent to improve our knowledge of the organisms that constitute the basis of coral reefs, the *Scleractinia*.

Scleractinian corals are marine animals that, aided by photosynthetic dinoflagellate algae (light enhanced calcification; Allemand et al., 2004) continuously form an external hard skeleton of calcium carbonate (aragonite), which accumulates and forms vast reef structures in shallow-waters of the (sub-)tropics. The largest coral reef system in the world is the Great Barrier Reef (GBR), which extends over an amazing 2,300 km along the north north-east coast of Australia. More than 90% of the shallow water coral species live in the Indo-Pacific region (from Pacific to southern Asia, including Australia and the Red Sea); the rest are located primarily in the Caribbean and Atlantic (Spalding et al., 2001). Most of these corals live under oligotrophic conditions, i.e. in waters very poor in nutrients. How corals exist (not only survive, but flourish) in such low nutrient conditions initially gave rise to “Darwin’s paradox” (Darwin, 1897). The ecological success of coral reef have been since attributed to the endosymbiosis with unicellular dinoflagellates of the genus *Symbiodinium* (McLaughlin and Zahl, 1959). Through photosynthesis and translocation of photosynthates from symbionts to host, these algae can supply up to 90% of a corals nutrient requirements (Muscatine, 1990) and are thus critically important for the vitality of corals. As a consequence, coral bleaching, i.e. the process of losing the symbiont algae, e.g. due to stress in the form of elevated SST, which reveals the white skeleton underneath the coral tissue (hence the term bleaching), is very often catastrophic for the coral. Because this event is simple to observe, it has been used in coral health monitoring for years (e.g. by the Australian Institute of Marine Science). After major bleaching events of 1998, 2002 and 2010, the Australia’s Great Barrier Reef have undergone, during the spring of 2016, a new bleaching event, which is the most severe on recorded history (Cressey, 2016). In the coming years, bleaching events are expected to be more and more frequent as SST will continue to increase (Berkelmans et al., 2004).

Major axes of research on scleractinian corals are symbiosis establishment and disruption (i.e. coral bleaching), coral disease, and biomineralization. But large gaps still exist in our basic physiology knowledge about the coral organism and how it responds to environmental changes, which is essential in a reef conservation and restoration perspective. This thesis work has focused on coral physiology, i.e. tissue homeostasis with emphasis on the skeletogenic tissue, the calicodermis, in an attempt to understand its establishment through polyp morphogenesis: from stem cells to differentiated calicodermis cells. More precisely, the objectives were the followings:

1. Understand the dynamics of cell division and death, i.e. cell turnover, in the different cell layers of the metamorphosing larva and, alternatively, in a primary cell culture model.
2. Determine the cellular mechanisms, cell division and/or differentiation, by which the calicodermis is formed at early metamorphosis stage.
3. Design specific cell markers to localize tissue hosting potential stem cells in the adult polyp.
4. Investigate the use of a cysteine-rich peptide specific to the *Scleractinia*, as a marker to assess spatial and temporal calicoblast differentiation during metamorphosis.
5. Investigate the pathway/mechanism for metamorphosis induced by natural cues, via visualization of metabolite translocation from the settlement biofilm.

Two scleractinians from the Pocilloporidae family, which are among the most studied species, have been systematically used:

- *Pocillopora damicornis* (Linnaeus, 1758) was made available for study through a fruitful collaboration with two public aquaria, the Aquarium Tropical du Palais de la Porte Dorée (ATPD, Paris, France) and Océanopolis (Brest, France). Colonies of *P. damicornis* from both facilities were releasing planula larvae on a regular basis, rendering effective studies of metamorphosis feasible.
- *Stylophora pistillata* (Esper, 1797), a dominant coral species in the Gulf of Aqaba (Red Sea), was made available at the Inter-University Institute of Marine Sciences (Eilat, Israel) through the ASSEMBLE call 6 program.

Furthermore, the availability of EST (expressed sequence tag) databases for both species provided the opportunity to search for specific genes during method development (Karako-Lampert et al., 2014; Traylor-Knowles et al., 2011).

This thesis manuscript is composed of a literature review followed by four chapters presenting results and a global discussion.



Chapter 1 presents a published study on coral cell proliferation in polyps of *Pocillopora damicornis* adult colonies and derived explant tissue cultures (Lecoïnte et al., 2013). Coral cell cultures are alternative models to *in vivo* laboratory settings, to study in simplified, controlled conditions, applied or fundamental coral research topics, including calicodermis establishment. Cell proliferation was assessed through BrdU pulse-labeling experiments in polyps from adult colonies and their forming tissue explants, during the initiation of coral primary cell cultures.

Chapter 2 is a published paper on *S. pistillata* cell proliferation and apoptosis during metamorphosis (Lecoïnte et al., 2016). It focuses on tissue turnover and cell migration in the polyp as well as *Symbiodinium* sp. symbiont density regulation during metamorphosis.

Chapter 3 presents results focused on the identification of cellular markers of calicodermis differentiation from precursor cells. Cell proliferation is assessed at tissue scale in *P. damicornis* during metamorphosis, coupled with investigations of spatial and temporal expression of *piwi* gene family expressing putative stem cells as well as a Pdcyst-rich protein marker of the calicodermis, specific to the *Scleractinia*. The objectives are to develop precursors of the calicodermis lineage. These results will contribute to a manuscript in preparation

Chapter 4 presents a study of transfer of isotopically labeled molecules from a biofilm to the metamorphosed larva and thus to test the hypothesis of a molecular transfer inducing metamorphosis in settled larva.

Finally, a chapter is dedicated to discussion of the obtained results attempting to place the work into a larger perspective.



# Literature review

## I. The coral holobiont

### A. Phylogeny of the *Cnidaria*

Scleractinian corals belong to the phylum *Cnidaria*, which is characterized by an epithelial “stinging cell”, the cnidocyte. This cell possesses a particular organelle, the cnidocyst (or cnida) that is discharged after mechanical stimuli of the cnidocil. *Cnidaria* possess neurons and muscle cells and thus belong to the Metazoa phylum. The phylogenetical position of *Cnidaria*, as a sister-group of *Bilateria*, makes it a very interesting phylum for studies of either basal mechanisms proper to *Bilateria* such as the establishment of the anterior-posterior axis and *hox* genes (Finnerty et al., 2004) or metazoan common traits such as stem cells and their related genes like *piwi* (detailed later).

The *Cnidaria* phylum is composed of the class *Anthozoa*, which includes *Hexacorallia* (including *Scleractinia*) and *Octocorallia* and are characterized by the presence of a reproductive polyp and the absence of medusa stage, and the subphylum *Medusozoa*, which includes four classes *Hydrozoa*, *Scyphozoa*, *Cubozoa* and *Staurozoa* that possess a reproductive medusa stage in addition to their sessile polyp. Life cycle of medusozoans can be very diverse and the presence of polyp or medusa stage secondarily lost. *Cnidaria* is an ancient phylum, among the most basal metazoan phyla. Scleractinian corals arose about 240 Million years ago (Ma) during the Triassic (Stolarski et al., 2011). Its phylogeny is in constant evolution and is currently undergoing intense discussion. For example, the recent use of mitochondrial protein coding genomes evoke the possibility that *Octocorallia* could be reattached to medusozoan, challenging the concept of *Anthozoa* monophyly (Kayal et al., 2013). In contrast, other phylogenetic analyses, combining genomic and transcriptomic databases, confirm the “traditional” phylogenetic tree (Zapata et al., 2015). Genomic and transcriptomic analysis are cheaper and faster than ever and will continue to develop. We are now in the –omic era and the multiplication of data will allow us to further refine the analysis of the phylogenetic relationships between metazoans and, more generally, the phylogenetic tree of *Cnidaria*. Meanwhile, in this document, we will consider the “traditional” phylogenetic tree as represented in Figure 1-1.

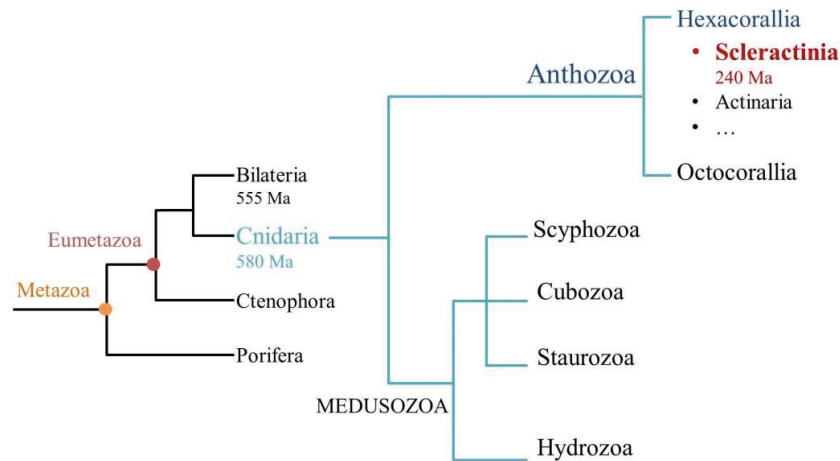


Figure 1-1: Simplified phylogenetic tree of *Metazoa* with inset on *Cnidaria*.

Branches are not scaled. The view of *Cnidaria* most widely accepted today sees *Anthozoa* as a monophyletic group with two subclasses *Octocorallia* and *Hexacorallia* that includes the reef-building species, the scleractinians. *Medusozoa* subphylum is characterized by the presence of a reproductive medusa stage, which is subsequently lost in some classes. Adapted from Zapata et al. 2015.

## B. Polyp: functional life unit

The coral life cycle is dominated by the time spent as a benthic, sessile animal. Members of the Pocilloporidae family are branching colonies of many polyps connected through the coenosarc tissue (Veron, 2000).

Polyps are radially symmetric and cylindrical in shape, with a mouth in the middle of the oral disc externally delimited by a single row of tentacles. *Hexacorallia* are characterized by a multiple of 6 tentacles. *P. damicornis* and *S. pistillata* both have 12, which all end in a terminal bulb (Figure 1-2) (Peters, 2016). The visible part of the polyp, extending outwards from the skeleton, is referred to as “body column”. The polyp mouth opens into the gastrovascular cavity, which is internally delimited by mesenteries; folds of tissue that extends from the external body wall into the middle of the polyp. Between the mouth and the actual gastrovascular cavity is situated the pharynx (or actinopharynx, gullet, or stomodeum), which is an invagination of the oral epithelium formed during embryogenesis. In *Scleractinia*, mesenteries are arranged in pairs of complete (i.e. extending from the column wall to the pharynx) and incomplete (i.e. not connected to the pharynx with an unilobed end) (Daly et al., 2003). Mesenteries, the site of gametogenesis, are composed of two parts: The mesenterial filament which is present all along the column and is of endodermal origin (locally these filaments have lobed structures), and the mesenterial bulbs or cnidoglandular bands, of ectodermal origin (Peters, 2016) (Figure 1-3). Externally, mesenteries are visible because the absence of endosymbiotic algae in the ectoderm derived part of this tissue makes them appear as uncolored lines on the oral disc between tentacles and on the body column (Figure 1-2).

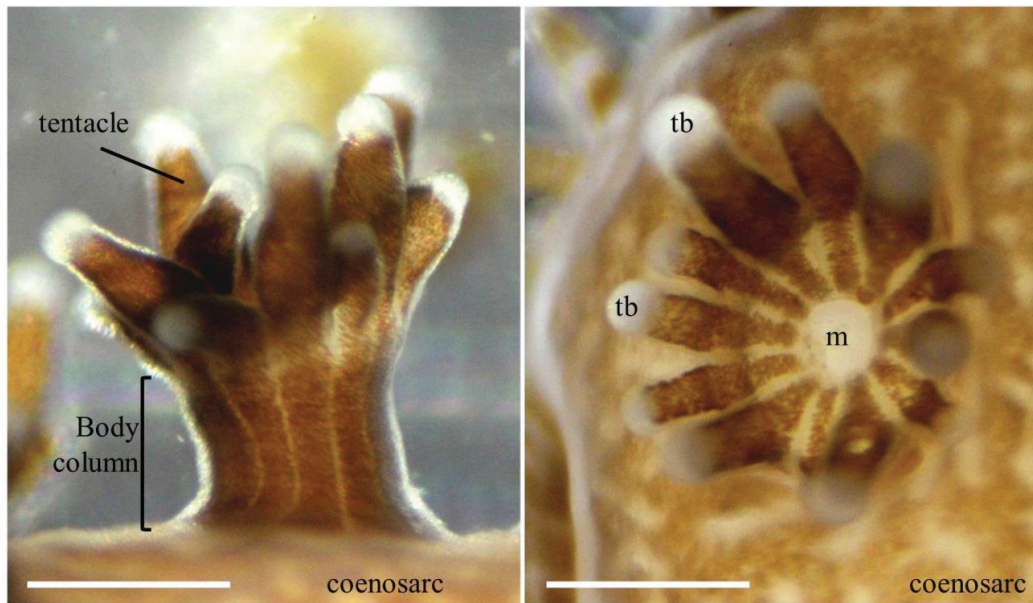


Figure 1-2: *Pocillopora damicornis* adult polyps.

A circle of 12 tentacles surrounds the mouth aperture. Tentacle terminal bulbs are clearly visible as they are not pigmented due to the absence of endosymbiont dinoflagellates. tb: tentacle terminal bulb, m: mouth aperture. Scale bars: 500  $\mu\text{m}$ .

Polyps and coenosarc are composed of two tissues, both made of two epithelia separated by an amorphous gel, the mesoglea (Figure 1-3). The oral tissue facing the seawater is composed of a pseudostratified epithelium (pse) also called epidermis, and oral gastrodermis. The aboral tissue, in contact with the skeleton is composed of the aboral gastrodermis and the skeletogenic epithelium, the calicodermis. Both calicodermis and pse are derived from the ectoderm while the gastrodermis is derived from the endoderm. The gastrodermis is also the principal location of endosymbiosis, with gastrodermal cells frequently hosting one or more unicellular dinoflagellates.

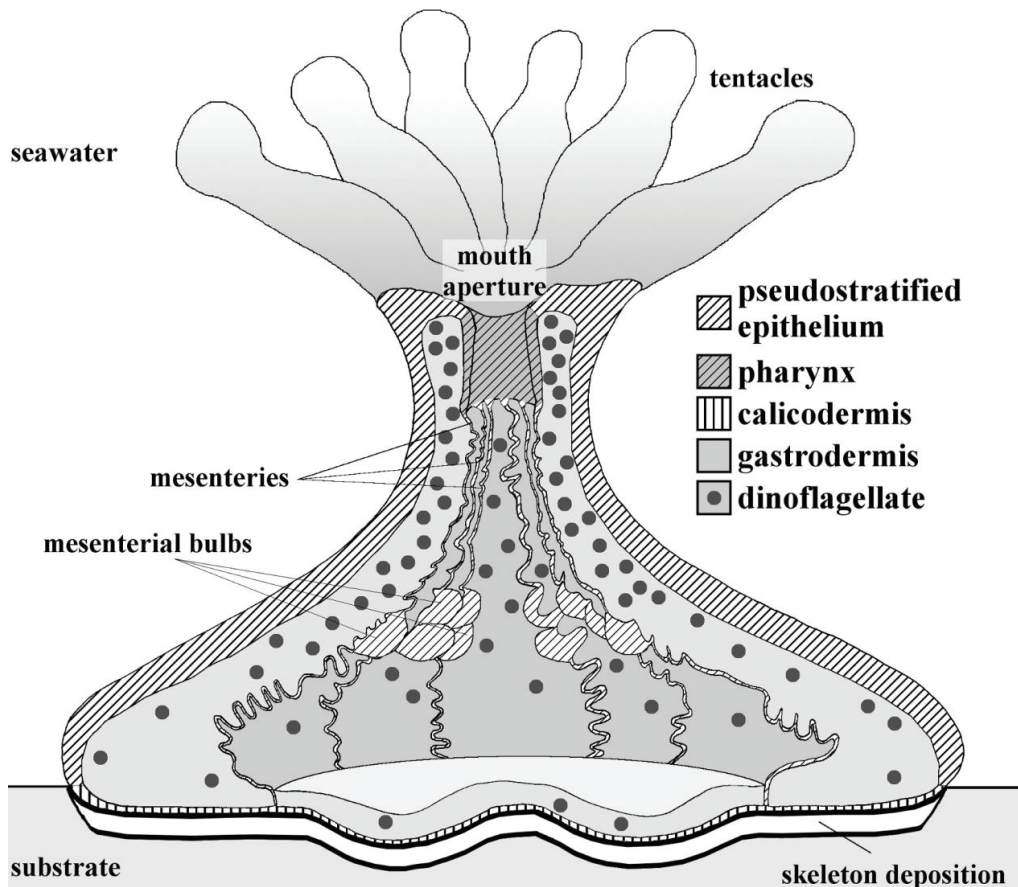


Figure 1-3: Tissue organization of a primary polyp.

Tissues are composed of two epithelia separated by an acellular gel, the mesoglea. Oral tissue is composed of the pseudostratified epithelium and the oral gastrodermis. The aboral tissue facing the skeleton is composed of the oral gastrodermis and the skeletogenic tissue, the calicodermis. Inside the gastrodermis are found unicellular symbiotic algae of *Symbiodinium* genus, the dinoflagellates. Adapted from Lecoq et al. 2016.

### C. Coral symbiont: *Symbiodinium* sp.

The success of scleractinian corals in oligotrophic-, shallow-waters is attributed to the presence of endosymbiotic dinoflagellates of the genus *Symbiodinium* in their gastrodermis. This symbiosis has received large interest as the bleaching, resulting from symbiosis disruption, is an important indicator of coral decreasing health. Cnidaria-dinoflagellate endosymbiosis is mutualistic meaning that it benefits both organisms. Corals are heterotroph with a double capability to take up nutrients (dissolved and particulate organic matter; DOM and POM) from the ambient seawater and capture plankton using their tentacles, respectively. The symbiosis with the autotroph dinoflagellates offer them an additional source of nutrients, in the form of photosynthates (Davy et al., 2012). As this work focus on the calicodermis establishment during coral morphogenesis, we were interested in dinoflagellate proliferation and population regulation during metamorphosis. Symbiont acquisition is a necessary step before talking about population regulation and is thus also discussed in this literature review.

Symbionts can be maternally inherited, i.e. by vertical transmission or acquired from the environment i.e. by horizontal transmission, independently of the reproduction mode; either brooder or spawner. Spawners release gametes in water and form an azooxanthellate planula larva by fertilization in the water column. This larva acquires symbionts from its environment but the spawned egg can also contain dinoflagellates upon release (Hirose et al., 2000). Such colonization by dinoflagellates can occur after settlement, during primary polyp development as it is the case in several *Acropora* sp. (Gómez-Cabrera et al., 2008). In brooders, fertilization occurs inside the polyp where the planula larva develops before being ejected in the water-column; this is referred to as planulation. When the planula already contains dinoflagellates at the moment of planulation (examples are *P. damicornis* and *S. pistillata*) these symbionts are assumed to be maternally inherited. However it has been shown that *S. pistillata* but also *Pocillopora meandrina* can obtain their symbionts from both parent colony and the environment (Byler et al., 2013; Magalon et al., 2005), exhibiting a certain flexibility in symbiont acquisition strategy.

Both modes of symbiont acquisition have pros and cons. Maternal inheritance ensure a high host-symbiont specificity and thus a holobiont more adapted to their environment but also more sensitive to environmental changes, whereas environmental inheritance allows to adjust the symbiosis to the environment. Indeed *Symbiodinium* is highly diverse and today are subdivided into 9 clades (A-I) and multiple sub-clades (Lajeunesse, 2001; Rowan and Powers, 1991). Different clades and sometimes sub-clades have different tolerance to temperature and irradiance and thus are suitable for different depth and/or environment. For example, in the Caribbean, genotyping of *Symbiodinium* in 25 scleractinian corals have shown that there are species with symbiont zonation, i.e. the same coral species can harbor different symbiont clades depending on the water depth (Bongaerts et al., 2015). Clade B and C are the most abundant and found at all depths whereas clades A, D, and H are only present in corals from shallow habitats (<5 m). Symbiont zonation has also been shown in *S. pistillata* from the Gulf of Aqaba, Red Sea, with clade A dominant in the shallow-water and clade C in the deep water (Byler et al., 2013). Flexibility in symbiont acquisition allows corals to select the most suitable clade according to environmental conditions.

This raises the question of how the dinoflagellate population is regulated *in hospite*. In *P. damicornis* and *S. pistillata*, the number of symbionts per host cell is usually one. This number can reach 12 in certain *Anthozoa*, including a few reef-building corals (Muscatine et al., 1998). The host regulates its symbiont population using pre- or post-mitosis mechanisms (Davy et al., 2012). One way to inhibit dinoflagellate proliferation is through nutrient limitation. *In hospite* the dissolved inorganic nitrogen is limited by the host, avoiding dinoflagellates cell division (Cook et al., 1988; Hoegh-Guldberg and Smith, 1989). High nitrogen levels, e.g. from local eutrophication, can disrupt the symbiosis due to lose of control by the host on dinoflagellates proliferation but also make coral more sensitive to thermal stress (Fabricius, 2005; Wiedenmann et al., 2013). Similarly phosphorus limitations have been observed in *Symbiodinium* from *Acropora Formosa* (Jackson et al.,

1989). Also, addition of sodium bicarbonate in seawater increases dinoflagellate photosynthetic rates in *P. damicornis* and *Aiptasia pulchella* revealing carbon limitation in these organisms (Lesser et al., 1994; Weis, 1993). When dinoflagellates are expelled or artificially extracted from their host, their proliferation rate increases showing loss of host control of their population density (Baghdasarian and Muscatine, 2000).

The other way to control symbiont population is by using post-mitotic controls via degradation and/or expulsion of unwanted dinoflagellates (Davy et al., 2012). Expulsion can involve both healthy or degraded dinoflagellates, and in some cases the symbiont is released intact within its host endoderm as observed in *P. damicornis* and *Aiptasia pulchella* (Gates et al., 1992). Degradation of symbiont occurs through two cell death pathways, apoptosis or autophagy. It is thought that both pathways are used to eliminate dinoflagellates (Dunn et al., 2007; Titlyanov et al., 1998). If symbiont expulsion and degradation are completely normal in order to balance the symbiosis, under certain circumstances (including environmental stress) it can lead to total loss of the dinoflagellate population, i.e. coral bleaching.

## **II. The metamorphosing coral larva as a model to study calicodermis establishment**

### **A. Diversity of reproduction modes and life cycle**

Like other *Cnidaria*, scleractinian corals can reproduce sexually and asexually (Fautin, 2002; Fox et al., 2003). Asexual reproduction occurs through formation of new polyps by budding. In solitary organisms polyps are separated by fission whereas in colonial species polyps are connected through tissue called the coenosarc or coenenchyme. Scleractinian corals, being *Anthozoa*, do not have a medusa stage. Sexual reproduction starts with the polyp that can either spawn gametes in water where the fertilization occurs (spawning species or spawners) or only the sperm is released and fertilization occurs inside polyps where the egg develops (brooding species or brooders). In both cases, planula larvae are formed, with brooders releasing them during the planulation. In several brooding species the existence of asexually produced planulae was shown (Ayre and Resing, 1986; Stoddart, 1983). Ecological advantages of this surprising aspect of coral reproduction are still unclear.

Diverse sexual patterns exist: Colonies can have separated sexes, i.e. being gonochoric, or have both male and female polyps, i.e. being hermaphroditic (Harrison, 2011). In the latter case, hermaphroditism can also occur within the same polyp, which has the capacity to produce both sperm and oocyte. It was thought that the dominant pattern was the gonochoric brooding species but the discovery of mass coral spawning on the GBR in the early 1980s changed this perception (Harrison, 2011). It is interesting to notice that on a total of 444 coral species studied around the world, the majority (354) are hermaphroditic broadcast spawners (Harrison, 2011). The advantage of broadcasting gametes is an increase of the dispersal potential. While fertilization and planula development occurs inside a brooding coral, gametes and developing planulae of spawners



are carried by water currents. This greater dispersal capacity allows planulae to reach distant reefs, colonize new environments or even re-colonize bleached reefs, as first demonstrated with a gene flow study (Nishikawa et al., 2003).

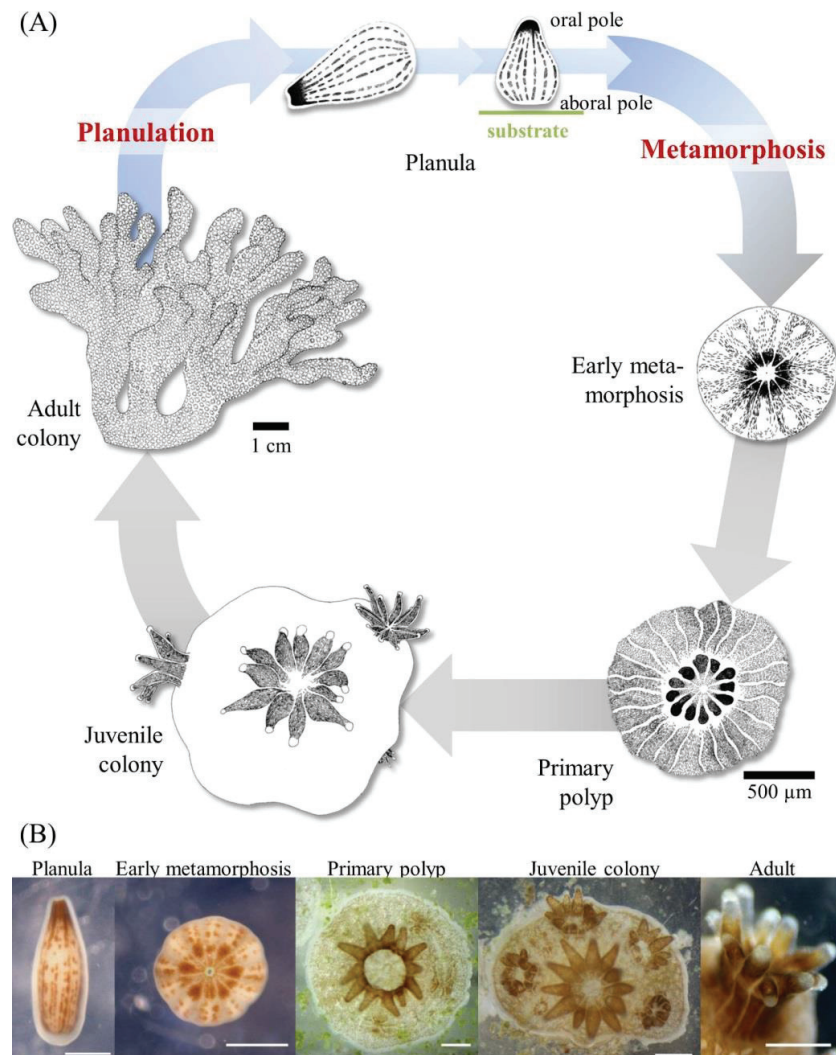


Figure 1-4: Schematic Pocilloporidae life cycle.

(A) Fertilization occurs inside adult polyp gastric cavity and planulae are released when fully developed (Brooding coral). The planulae probe the substrate before they settle and undergo metamorphosis. At early metamorphosis, tentacles are not formed yet but skeleton deposition starts. Then the primary polyp is formed with tentacles and body column fully developed. Finally secondary polyps bud around the primary polyp, forming the juvenile colony. (B) Picture of *P. damicornis* larvae at the different stages illustrated in the life cycle. Scale bars 500 µm. Adapted from Lecoq et al., 2016.

Both models used in this thesis work (i.e. *Pocillopora damicornis* and *Stylophora pistillata*) are brooding scleractinian corals. Their life cycle is presented in Figure 1-4. Fertilization occurs inside the polyp. The released, mature planula larva probes new surfaces with its oral pole. When a suitable substrate is encountered metamorphosis starts. During metamorphosis the planula larva flips to present its aboral pole to the substrate, makes contact and then flattens into a disc. In this early metamorphosis stage, the coral does not

yet possess tentacles but is already able to secrete skeleton and immediately starts forming its basal plate (Gillis et al., 2014, 2015; Vandermeulen and Watabe, 1973). Tentacle buds appear 24-72 hours after settlement as the larva continues to spread on the surface during developing polyp stage. When tentacles are developed and the body column is extended vertically, the primary polyp is formed. Secondary polyps bud around the primary polyp starting from 6 to 12 days after metamorphosis of *P. damicornis* (personal observations). Metamorphosis is not synchronized and different levels of development co-exist even within a same batch of larvae that initiated metamorphosis at the same time.

## **B. Inducing metamorphosis**

Scleractinians are benthic organisms. Following the settling step of the larva, the coral lives fixed onto a substrate during its remaining life. Survival of the future colony relies on the settlement location and thus is critical. As mentioned above, the dispersal capacity of corals is different depending on the reproductive mode. Once fully developed and ready to settle, planulae are described as having an “explorative behavior”: They probe the surface before settlement. The ideal emplacement has to be found and planulae are sensitive to several environmental cues, physical as well as chemical.

Physical cues include a large variety of environmental factors that influence planula settlement and metamorphosis. First scleractinian planulae respond to light intensity (e.g. *Goniastrea aspera*, *Acropora tenuis*) and/or quality, i.e. light spectrum (e.g. *Goniastrea favulus*, *Montipora peltiformis*) and search light conditions similar to those of experienced by their parent colony, indicating that optimal light conditions are species specific (Mundy and Babcock, 1998). Planula from *Porites astreoides* and *Acropora palmata* have been shown to settle preferentially on red substratum (Mason et al., 2011). Temperature effect is less clear, as high temperatures increase settlement rate but in the meantime decreases recruits survival in *Acropora solitaryensis* and *Favites chinensis* corals (Nozawa and Harrison, 2007). Surface also matters, as coral larvae settle less on completely flat surfaces (Nozawa et al., 2011) compared to surfaces with holes or topography. *Acropora millepora* and *Ctenactis crassa* planulae have been observed to settle preferentially on surfaces with micro-perforation closely matching their own size (Whalan et al., 2015). More surprisingly, sounds can influence planulae. *Montastraea faveolata* planulae are attracted by speaker playing reef sounds (Vermeij et al., 2010). Principal physical cues are summary in Figure 1-5.

Chemical cues that induce planula settlement have been studied with the hope to provide biotechnological tools for reef re-seeding, aquaculture, and research. Such chemical cues are collectively called morphogen because they induce polyp morphogenesis. Crustose coralline algae (CCA) and associated biofilms are known to chemically induce planula settlement and metamorphosis in several coral species, including *A. millepora* or *Agaricia* sp. (Heyward and Negri, 1999; Morse et al., 1988). For example, tetrabromopyrrole (TBP) produced by the bacteria genus *Pseudoalteromonas* has been shown to induce (in a dose-dependent manner)

planula metamorphosis in *Orbicella franksi* (formerly *Montastraea franksi*), *Acropora palmata*, and *A. millepora* even without settlement (Sneed et al., 2014; Tebben et al., 2011), indicating a decoupling between settlement and metamorphosis in scleractinian larvae (Tebben et al. 2015). Gene expression patterns of *A. millepora* metamorphosis induced by either CCA or TBP alone have been shown to differ significantly. Interestingly, GABA (gamma-aminobutyric acid) neurotransmitter-related genes are up-regulated in presence of TBP whereas they are not involved in CCA-induced metamorphosis (Siboni et al., 2014), again emphasizing the difference in morphogenic induction by CCA vs TBP alone and the dissociation between larval settlement and metamorphosis. CCA and their chemical extracts can induce proper metamorphosis even if pre-treated with antibiotics, excluding a prominent role of CCA-associated biofilms (Tebben et al., 2015). Morphogenic compounds associated with CCA are glycolipids and polysaccharides identified in *Porolithon onkodes* (Tebben et al., 2015).

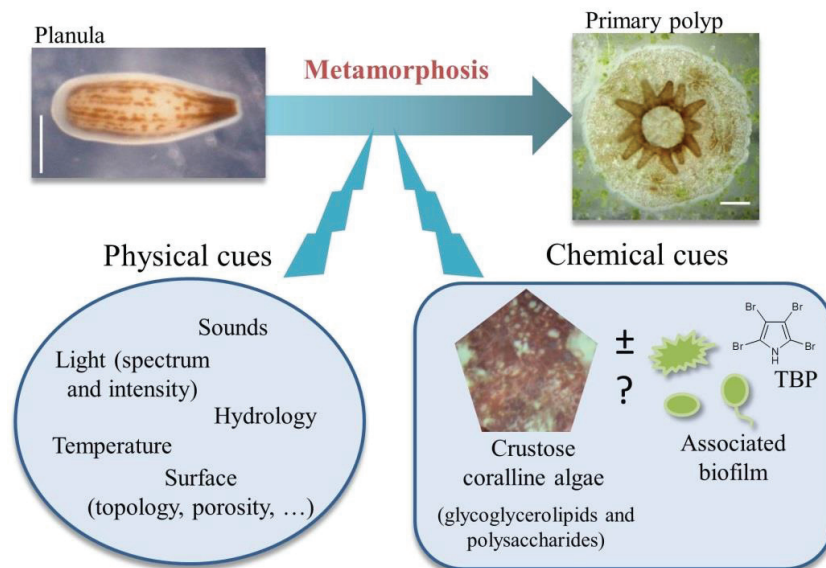


Figure 1-5: Schematic summary of the physical and chemical cues that induce planula metamorphosis.

Physical cues are mostly environmental. Chemical cues are related to the substrate. A crustose coralline algae is known to induce settlement and metamorphosis but the molecules responsible are less known, it could be glycolipids and polysaccharides (Tebben et al. 2015). Regarding the associated biofilm it has long been shown to induce metamorphosis, particularly the tetrabromopyrrole (TBP) but it occurs in open-water, without settlement and thus other inducers are searched. Scale bars 500  $\mu$ m.

In Hydrozoa peptides with amidated glycine-leucine-tryptophan C-terminus motif (GLW-amide family), are hypothesized to be the internal signal that answer to external cues. It has been shown that synthetic GLW-amide induce *Hydractinia echinata* metamorphosis (Schmich et al., 1998). Furthermore this peptide was found to be common in *Cnidaria* and therefore tested against coral planulae. The *Hydra*-derived GLW-amide neuropeptide Hym-248 successfully induced metamorphosis of nine *Acropora* species. But it was not the case with other species like *Montastraea faveolata* and *Favia fragum* (Erwin and Szmant, 2010; Iwao et al., 2002) showing a species specific response. Nevertheless, like for TBP, most larvae do not settle properly on the substrate and there is an upregulation of a GABA genes in response to GLW-amide neuropeptide while

no significant up- or down-regulation happen when induction with CCA (Siboni et al., 2014; Tebben et al., 2015). This indicates that GLW-amides acts through GABA neurotransmitters to induce partial metamorphosis but that CCA induced metamorphosis goes through different pathways.

It is clear that there is dissociation between settlement and induction of scleractinian larvae metamorphosis. Although CCA is able of inducing both, the exact effect of TBP from CCA biofilm is unclear and its role as a neuroactive signaling compound remain speculative. Molecular signaling and metabolic pathways that transduce signals from external cues, physical or chemical, have still to be understood. GLW-amide partial effect leads us to look toward neuronal signal transduction but is not sufficient by itself to trigger proper metamorphosis. Metamorphosis induction is probably the result of multiple cues.

### **C. Calicodermis establishment during metamorphosis**

Scleractinian corals, also called hard or stony corals, are able to form this calcareous skeleton due to a specific cell layer, the calcicoblastic epithelium or calicodermis. A major fraction of the present thesis work focuses on calicodermis establishment. To date, little is known about the cellular mechanisms underlying the transition from the swimming planula to the calcifying polyp. Studies of calicodermis cell origin (local division or cell migration) and turnover are missing. Detailed histology of the forming calicodermis was presented for *P. damicornis* by Vandermeulen (1974, 1975). In this species, the aboral epithelium of the planula, i.e. the site of the future calicodermis, is described as a tall columnar epithelium composed of a heterogeneous cell population with cnidocytes, flagellated epithelial cells, secretory (gland cells) and mucus cells, with potential neurosecretory activity. Upon settling, the epithelium in contact with the substrate changes into a flattened epithelium made of interdigitated cells, the calcicoblast, containing vesicles of potential organic matrix and numerous mitochondrias. This cell layer also possesses anchoring cells, the desmocytes (Muscatine et al., 1997). Vandermeulen and Watabe underline the impressive speed at which this morphogenesis occurs; calcicoblast specific ultrastructural characteristics are visible only after settlement and the skeletogenesis starts within hours following settlement (Vandermeulen and Watabe, 1973).

### **D. Alternative study model: coral explant cultures**

Planula larvae are a great model to study calicodermis establishment because, under the right conditions, they naturally initiate the differentiation of this tissue layer during metamorphosis. But the supply in planulae can be irregular because not all corals have their life cycle completed in aquaria and field sampling requires adjustments to planulation or gametes broadcast periods. Finally, achieving settlement and metamorphosis in the laboratory can be a challenge in itself. Coral tissue culture appears as an alternative model to study morphogenesis.

Cell culture is the maintenance and growth *in vitro* of living cells and tissues. In *Bilateria*, cell cultures have served as a simplified system to study a broad range of topics, including ecotoxicology, drugs response of a

particular cell type, pathogens action, stem cells maintenance and differentiation, *etc.* In *Scleractinia*, such a model would avoid repetitive sampling in environment and/or coral growth in aquaria, which is not trivial and indeed time- and resource consuming. Unfortunately to date, no proliferative coral cell line exists, but primary cell or explant culture are being developed using different methodologies (Domart-Coulon and Ostrander, 2016; Vizel and Kramarsky-Winter, 2016). Briefly, samples are dissociated mechanically, chemically or enzymatically yielding either tissue (explant) or mixed cell type cultures (Figure 1-6). Cells can re-aggregate and explants round up into suspended multicellular aggregates with a smooth surface also called tissue ball due to its round shape. These structures possess an endoderm with symbionts and a ciliated ectoderm and rotate into the medium. These explants, are used in different studies, including biomineralization (Domart-Coulon et al., 2001; Helman et al., 2008; Mass et al., 2012). Vizel et al., 2011 succeeded to induce development of these explants into polyps (at low yield) without the use of chemicals, only using environmental parameters such as light and temperature cycling. A growing number of studies encourages the use of coral explant and assesses their viability (Feuillassier et al., 2014; Gardner et al., 2015).



Figure 1-6: Tissue ball formation.

(A) *P. damicornis* dissociated cells in culture, the black arrow indicates cells that have re-aggregated and start forming a tissue ball. (B) Two small spinning tissue balls after 24 h among multi-cellular cell culture, their brown color is due to the presence of dinoflagellates into their endoderm. Surrounding transparent ectoderm is also visible. (C) A large tissue ball moving into cell medium a few days after cell dissociation. cc: coral cell, d: dinoflagellate, cni: cnidocyte. Scale bars: 10, 50 and 100  $\mu\text{m}$  for A, B and C respectively.

Care must be taken during transposition of results obtain *in vitro* to the actual organism. Nevertheless, coral explant culture is a promising model to study different aspect of coral physiology (calicodermis establishment, symbiosis, biomineralization, environmental stress, cell de- or trans-differentiation, etc.).

### III. Role of the calicodermis in coral biomineralization

To study calicodermis establishment during polyp morphogenesis one goal was to develop new molecular markers of calicoblast precursors and thus we review below the role of the calicodermis and associated proteins. We distinguished three parts, proteins of the skeletal organic matrix (SOM), proteins involved in carbon transport and proteins involved in calcium transport.

#### A. Calicodermis and the skeletal organic matrix

Coral growth is supported by the external skeleton which is an accumulation of calcium carbonate in the form of aragonite. Biominerals include an organic and an inorganic matrix, in corals the organic matrix is made of proteins that must be synthesized and transported to the site of calcification (Al-Horani, 2015). The inorganic matrix is made of calcium carbonate ( $\text{CaCO}_3$ ). Skeletal formation is a biologically controlled process. However cellular mechanisms of biocalcification are not fully understood. Calicoblasts do not form aragonite crystals internally but rather secrete a skeletal organic matrix (SOM) made of proteins, that initiate biomineralization (Puverel et al., 2005). This SOM has received increasing interest and proteomic identification of the proteins that constitute it has been done in *A. millepora* and *S. pistillata* (Drake et al., 2013; Ramos-Silva et al., 2014) with the purpose to identify a biomineralization “toolkit”, i.e. an organic scaffold for aragonite deposition and orientation. This toolkit includes adhesion proteins -such as cadherins, integrins and contactin- and structural proteins -such as actin, tubulin, and collagen-. Moreover highly acidic proteins were found that are potentially specific to coral skeleton. They were named the coral acid-rich protein (CARP) subfamily and were only detected in coral transcriptomes (Drake et al., 2013). However the affiliation of proteins from the cytoskeleton (actin, tubulin, etc.) to the SOM is refuted by Ramos-Silva et al. (2013).

Another coral SOM protein was identified in *Galaxea fascicularis* and named galaxin. This protein is not a CARP and does not bind  $\text{Ca}^{2+}$  but its sequence analysis reveals that it is a protein made of a signal peptide, a propeptide, and a mature protein sequence, and it is suggested to be secreted by the calicodermis (Fukuda et al., 2003). This protein of 298 amino acids is rich in cysteine, the amino acid responsible for disulfide bridge formation, with 28 out of 30 cysteine residues forming tandem repeats (dicysteine sequences). Dicysteine repeats were also found in a protein of the SOM of Mollusca, the lustrin (Shen et al., 1997). All together these elements suggest that galaxin is a promising structural protein of the SOM. Galaxin-like proteins were found in other scleractinian species (e.g. *Acropora millepora*) and in the calcifying octocoral *Sinularia notanda* (Reyes-Bermudez et al., 2009; Kim et al., 2015).

In expressed sequence tag (EST) libraries of the *Montastrea faveolata* scleractinian coral, small cysteine-rich proteins (SCRiPs) were identified (Sunagawa et al., 2009). Furthermore these SCRiPs were found only in scleractinian species and might be involved in biomineralization, but their exact function remains to be elucidated.

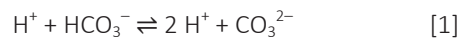
Finally, another cysteine-rich protein has been identified in adult polyps of *Pocillopora damicornis* (named Pdcyst-rich) where it is specifically expressed in the calicodermis (Vidal-Dupirol et al., 2009). Galaxin and Pdcyst-rich share features like the secretory protein-like structure with a peptide signal sequence. However, in contrast to galaxin, only 2 among the 16 cysteines residues form tandem repeats.

The discovery in calcifying corals of several cysteine-rich proteins, putatively involved in biomineralization as SOM structural proteins, is an interesting feature that merits more attention. In mammals, cysteine-rich ker-

atin-associated proteins (KRTAPs) are important components of hairs, and in birds feather epidermal differentiation cysteine-rich proteins (EDCRP) are conserved (Strasser et al., 2015). Although EDCRPs and KRTAPs have no common ancestor, cysteine-rich proteins are important components of skeletal organic matrices, in *Cnidaria* as well as outside of this phylum and this feature raises questions about the functional evolution of cysteine-rich proteins among *Metazoa* (Strasser et al., 2015).

## B. Carbon source of biomineralization

Calcium carbonate ( $\text{CaCO}_3$ ) is formed through precipitation from calcium and carbonate ions ( $\text{Ca}^{2+}$  and  $\text{CO}_3^{2-}$ ). Dissolved inorganic carbon (DIC) is thus necessary and can be obtained directly from seawater as bicarbonate ions ( $\text{HCO}_3^-$ ) or from cell respiration as carbon dioxide ( $\text{CO}_2$ ) which is then hydrated to bicarbonate ions. Finally bicarbonate ions will form carbonate ions ( $\text{CO}_3^{2-}$ ) as follow:



*In vivo* carbon dioxide hydration is catalyzed by carbonic anhydrase (CA) to form  $\text{HCO}_3^- + \text{H}^+$  and vice versa. The CA enzyme superfamily is widespread in *Metazoa* and has been identified in several corals (Weis et al., 1989). CA has two major roles: supplying  $\text{CO}_2$  to the symbiont for use in photosynthesis and supplying  $\text{HCO}_3^-$  for calcium bicarbonate formation (Weis et al., 1989). Evidence of CA in dinoflagellate membrane and in the calcidermis attest to these functions (Al-Moghrabi et al., 1996; Isa and Yamazato, 1984; Tambutté et al., 2007b). Interestingly, in sclerites of octocorals, some components of the SOM have been identified with a CA domain suggesting that SOM proteins are not only structural but also are able to locally hydrate carbon dioxide (Rahman et al., 2006).

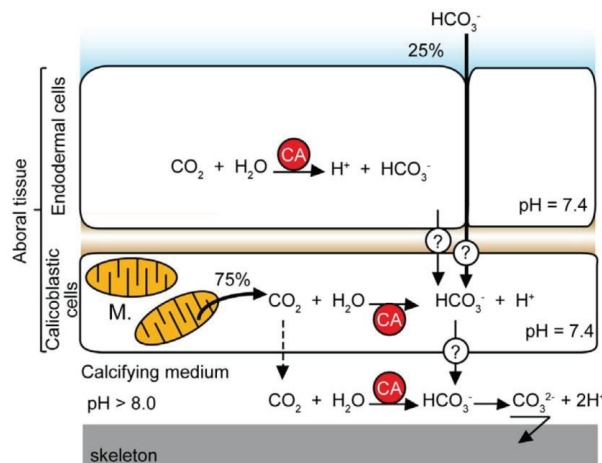


Figure 1-7: Dissolved inorganic carbon pathways.

Sources of dissolved inorganic carbon in the biomineralization process and transfer through aboral tissue according to Bertucci et al. 2013. CA: carbonic anhydrase.

While  $\text{HCO}_3^-$  can be obtained directly from seawater or indirectly from  $\text{CO}_2$  (Bertucci et al., 2013; Furla et al., 2000a, 2000b; Moya et al., 2008) it is not clear whether  $\text{HCO}_3^-$  can penetrate oral tissue and/or aboral gas-

trodermis through para-cellular or trans-cellular pathways.  $\text{CO}_2$  can be obtained by simple diffusion through tissue and come from either seawater or from mitochondrial respiration. Once inside the tissue, CA transforms  $\text{CO}_2$  in  $\text{HCO}_3^-$ . Sources and pathways of dissolved inorganic carbon are resumed in Figure 1-7 (according to Bertucci et al. 2013).

### **C. Calcium source of biomineralization**

Transport of calcium ions may be trans- or para-cellular and this topic is highly discussed in the literature. Both pathways have been shown in different corals making it difficult to conclude and/or generalize for all scleractinian coral species (Allemand et al., 2004, 2011). Even within the same species (*Stylophora pistillata*) both pathways may be used, with calcein-labeling of intercellular spaces indicating para-cellular pathway and  $\text{Ca}_2^+$ -ATPase enzyme immunolocalization indicating transcellular pathways through specific cell types (Tambutté et al., 2012).

Diffusion of  $\text{Ca}^{2+}$  through para-cellular pathways has been suggested in *Heliofungia actiniformis* and *S. pistillata* (Bénazet-Tambutté et al., 1996; Tambutté et al., 1995). On the other hand, active transport of  $\text{Ca}^{2+}$  through calcium ATPase and  $\text{Na}^+/\text{Ca}^{2+}$  exchange mechanisms are suggested in *G. fascicularis* and *S. pistillata* (Ip et al., 1991; Marshall, 1996; Zoccola et al., 2004). A plasma membrane calcium pump (PMCA) was localized in calicoblasts of *S. pistillata*. Likewise, in *P. damicornis*  $\text{Ca}^{2+}$  transporters are present (Vidal-Dupirol et al., 2013). It is likely that both passive diffusion and active transport of calcium occur in coral calicodermis.

We have seen that the components of the Skeletal Organic Matrix and the transport pathways of calcium ions and bicarbonate ions have received a lot of attention because these processes are of great importance in the comprehension of the molecular mechanisms of biocarbonate skeleton formation. Nevertheless, there is less consideration for the cellular mechanisms of calicodermis establishment, its differentiation, growth dynamics, and homeostasis (tissue maintenance through cell proliferation and death). This thesis work focused on these cellular aspects.

## **IV. Stem cell in *Cnidaria* and corals**

Stem cells are well studied in *Bilateria* models. Adult stem cells are pluripotent, i.e. they give rise to a limited number of cell types of differentiated, somatic or germinal, cells. In contrast, stem cells are poorly studied in scleractinian models where basic data are missing. Indeed, in *Cnidaria* attention has been mostly focused to hydrozoan models such as *Hydra* or *Hydractinia* species. The following section briefly presents stem cell systems and related genes identified in cnidarians.

### **A. Stem cell lineages in *Cnidaria***

In *Bilateria*, separation between germinal and somatic line is well defined, with germinal stem cells dedicated to gamete production. Questions regarding the origin of this separation pushed research toward



more ancient phyla, like *Cnidaria*, and is still a matter of debate (Gold and Jacobs, 2013). If it is presumed that all *Cnidaria* possess stem cells, the potency and separation between germinal and somatic lineages is not clear in all cases. These questions have been mostly studied in *Hydra* and in some other hydrozoan genera, and much less is known for scleractinian species. The following paragraphs report what is known in these species and a graphical summary is presented in Figure 1-8.

*Hydra* has three different stem cell lineages. The first two lineages consist of pluripotent epithelial stem cells, endodermal and ectodermal, respectively, that self-renew and give rise to endodermal and ectodermal cells. The “stemness” of these two types of epithelial stem cells is debated, as they are described as differentiated, epitheliomuscular cells (Gold and Jacobs, 2013). In classic *Bilateria* models, stem cells are undifferentiated cells that self-renew or commit to differentiation into specialized cell types. In *Hydra*, epithelial stem cells located in the body column give rise to epithelial cells that migrate basally towards the foot and apically towards the tentacles (Frank et al., 2009; Gold and Jacobs, 2013). The third type of stem cell lineage is located between epithelial cells and called interstitial cells (i-cells). These small, round, undifferentiated cells with large nucleus give rise to stinging cells (cnidocytes), gametes, neurons, secretory, and sensory cells but also to the gametes (Bode et al., 1987; Marcum and Campbell, 1978).

But the stem cell system is not homogenous in all *Hydrozoa*. In the colonial marine hydroid *Hydractinia*, i-cells give rise to the same differentiated cells as in *Hydra* but they also have the ability to replace epithelial cells from both endodermal and ectodermal origin (Müller et al., 2004). They are thus multipotent stem cells that give rise to all cell types. Although it has not been demonstrated yet, it seems possible that epithelial cells dedifferentiate into i-cells. In *Podocoryne carnea*, isolated striated muscle cells (ectodermal cells) cultured with endodermal cells will regenerate a manubrium, the sexual and feeding organ, including cell types such as, gametes, i-cells, cnidocytes, gland cells, secretory cells, showing the ability of striated muscle cells co-cultured with endodermal cells to transdifferentiate into diverse cell types (Schmid et al., 1982). It was also shown that *in vitro* collagenase treatment triggers transdifferentiation of striated muscle into all these cell types in the absence of endodermal cells (Schmid and Alder, 1984). These results show that separation between somatic and germ line is not clear in *P. carnea*, with germ line cells arising from somatic cells. The germ line cells come from somatic cells in the budding area of the female gonozoid polyp and migrate to the manubrium of the early medusa bud. Several possibilities have been discussed: male and female germ cells originating from somatic cells of the manubrial endoderm and/or sharing a common stem cell with all somatic cells, the i-cells (Gold and Jacobs, 2013; Seipel et al., 2004). *Clytia hemisphaerica* possesses i-cells at the base of the tentacles that differentiate into cnidocytes during migration from the proximal to the distal region of tentacles (Denker et al., 2008). But i-cells also give rise to the germ cells, indicating once again that in this species there is no separation between somatic and germ lines (Leclère et al., 2012).

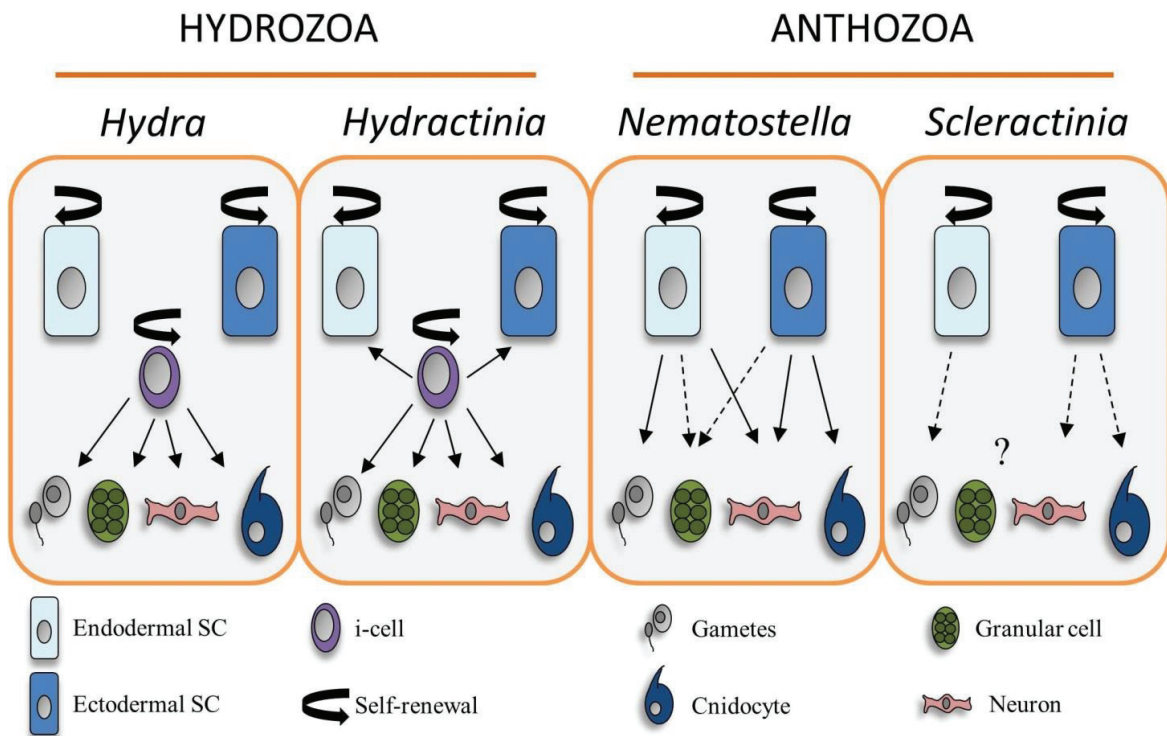


Figure 1-8: Stem cell systems in *Cnidaria*.

Hydrozoans possess three stem cell lineages, including i-cells. In *Hydra* they are well separated, epithelial stem cells (endodermal+ectodermal) self-renew and produce the epithelial cells. I-cells give rise to different cell types including cnidocytes, gametes, granular cells and neurons. In *Hydractinia* the separation between the three lineages does not exist anymore as i-cells can also produce epithelial cells. In *Anthozoa* the i-cell lineage was not found. Epithelial cells give rise to the different cell type. Separation of cell lineage is less clear. Concerning gametes production it has been observe to come from endodermal cell (Shikina et al. 2015) but another study argue in favor of a gametogenesis independent of epithelial cells (Barfield et al, 2016). Adapted from Gold and Jacobs 2013. SC: stem cell, i-cell: interstitial cell.

In *Anthozoa*, no i-cell lineage has been found so far (Gold and Jacobs, 2013; Technau and Steele, 2011). In the sea anemone *Nematostella vectensis*, neuron, sensory cell, cnidocytes and ganglion cells are formed from ectoderm but neurons can also be formed by endoderm in planulae (Marlow et al., 2009; Nakanishi et al., 2012). Primordial germ cell in *N. vectensis* are located in the endodermal mesenteries (Extavour et al., 2005).

In scleractinian corals studies are scarce. One recent study proposes that oocytes arise from an ovarian somatic cell located in the endodermal mesenteries of *Euphyllia ancora* (Shikina et al., 2015). Nevertheless, Barfield et al. (2016) observed that somatic mutants in *Orbicella faveolata* did not transfer their mutation to gametes and thus argue in favor of a separation between somatic stem cell lineage(s) and germ cell lineage. A few studies propose that amoebocyte cell types, found in epithelia and mesoglea at all life stages, could correspond to *Hydrozoa* i-cells, but this hypothesis is primarily based on histological studies, with no lineage tracing experiments to identify progeny. Furthermore, there amoebocytes are mostly reported to have phagocytosis abilities and thus are more likely involved in corals innate immune system rather than “true

stem cells” (Bruckner, 2015; Olano and Bigger, 2000). Stem cell systems in *Anthozoa* and particularly in *Scleractinia* are not well understood and need further study.

## B. Stem cell related genes

Identification of stem cells *in situ* can be done with morphological criteria. A “typical” stem cell, e.g. an i-cell, is described as small and round with a high nucleus/cytoplasm ratio corresponding to an undifferentiated cell. Nevertheless, in *Hydrozoa* epithelial stem cells do not match this morphological description. In order to identify stem cells, the use of genetic markers is more and more frequent. This requires knowledge about the genes that are expressed in stem cells. In *Cnidaria*, most studies have looked for gene homologs to *Bilateria* stem cell genes, based on the hypothesis that the stem cell system is ancestral, common to all metazoans. In the following paragraph we present some of the genes found in cnidarians.

*Nanos* and *Vasa* genes are involved in the gametogenesis of metazoans such as *Drosophila melanogaster*. In *Cnidaria* *nanos* homologs were found in the Hydrozoa *Hydra* (*Cnnos1*) and the *Anthozoa* *Nematostella* (*Nvnos1* and *Nvnos2*). *Cnnos1* is expressed in the germline cells (Hemmrich et al., 2012; Mochizuki et al., 2000). In *Nematostella*, *Nvnos1* and *Nvnos2* are expressed in primordial germ cells (PGCs) but also in somatic cells and thus potential ectodermal and endodermal stem cell respectively (Extavour et al., 2005). A *nanos* homolog is also expressed in *Hydractinia* i-cells (Plickert et al., 2012). *Vasa* homologs were also found. In *Hydra* *Cnvas1* and *Cnvas2* are expressed in germline cells as well as *Nvvas1* and *Nvvas2* in *Nematostella* (Extavour et al., 2005; Mochizuki et al., 2001). In *Hydractinia* *vasa* is expressed in i-cells (Rebscher et al., 2008).

The gene *c-myc* is described as a proto oncogene which is involved in stem cell self-renewal in metazoans such as *D. melanogaster* (Eilers and Eisenman, 2008). In *Cnidaria* it has been studied in *Hydra* where it is expressed in all stem cells (Hartl et al., 2010). More specifically *myc1* expression is restricted to i-cells (Hobmayer et al., 2012). *Hydractinia* i-cells also express *myc* (Plickert et al., 2012).

Wnt signaling supports the formation and maintenance of somatic stem cells in *Bilateria* but also their embryonic patterning (Wend et al., 2010). In *Hydra* it has been shown to be expressed in the head organizer and involved in the axis formation (Hobmayer et al., 2000). In *Clytia hemisphaerica* the Wnt signaling pathway, involving Frizzled receptor proteins and a Wnt ligand, is implicated in axial patterning through maternal RNA present in the egg and early embryos (Momose et al., 2008). The same receptors and ligand are expressed in *Hydractinia* i-cells (Plickert et al., 2012).

Another stem cell related gene is *piwi*. Piwi proteins are involved in stem cell maintenance in *Bilateria*. Also, *piwi* genes were detected in the cnidarian species previously cited, *Hydra*, *P. carnea*, *Hydractinia*, *Clytia hemisphaerica* and *N. vectensis* (Denker et al., 2008; Grimson et al., 2008; Hemmrich et al., 2012; Lim et al., 2014; Plickert et al., 2012; Seipel et al., 2004). In hydrozoans *piwi* was expressed in all stem cells. In the an-

thozoan *N. vectensis* three *piwi* genes were detected by transcriptomic analysis but not localized *in situ*. Contrary to the other stem cell related genes, *piwi* expression has also been identified in two scleractinian corals. It has been localized at the site of gametogenesis of *Euphyllia ancora* (Shikina et al., 2015) and detected in *S. pistillata* EST library (Liew et al., 2014).

This listing of stem cell related genes detected in *Cnidaria*, although not exhaustive, attests that these genes are strongly conserved among metazoans and confirm that they are potential tools to localize *in vivo* the stem cells.

# Chapter 1: Explant formation in primary coral cell culture

## I. Context

Cell culture from scleractinian corals offers the possibility to address coral physiology questions in simplified and controlled conditions. To date no coral cell line exists but primary mixed cell type cultures and explant (tissue) cultures are done and maintained in laboratory for days up to weeks without propagation (Vizel and Kramarsky-Winter, 2016). In certain conditions of light and temperature coral explants can be induced to develop into calcifying polyps (Vizel et al., 2011). Interestingly the formation of a mouth on explants obtained from *Fungia granulosa* fragments was described as a critical and necessary step to further obtain development of a polyp. If induced polyps can be maintained for months, explant cultures only allow short-term experiments, up to a few weeks. Cell proliferation activity in these round ciliated tissue explants (or tissue balls) is not known. This Chapter 1 presents a publication in the Cytotechnology journal in which cell proliferation during tissue ball formation was assessed (Lecointe et al., 2013).

PhD student's contribution: The PhD student designed the experiments with I. Domart-Coulon, A. Meibom and S. Cohen, carried out the experiments with IDC and SC and technical support of M. Gèze and C. Djediat, and analyzed statistically the data. All Authors contributed to drafting and editing the manuscript.

## II. Publication



## Scleractinian coral cell proliferation is reduced in primary culture of suspended multicellular aggregates compared to polyps

A. Lecointe · S. Cohen · M. Gèze · C. Djediat ·  
A. Meibom · I. Domart-Coulon

Received: 4 February 2013 / Accepted: 1 April 2013 / Published online: 12 June 2013  
© Springer Science+Business Media Dordrecht 2013

**Abstract** Cell cultures from reef-building scleractinian corals are being developed to study the response of these ecologically important organisms to environmental stress and diseases. Despite the importance of cell division to support propagation, cell proliferation in polyps and in vitro is under-investigated. In this study, suspended multicellular aggregates (tissue balls) were obtained after collagenase dissociation of *Pocillopora damicornis* coral, with varying yields between enzyme types and brands. Ultrastructure and cell type distribution were characterized in the tissue balls (TBs) compared to the polyp. Morphological evidence of cellular metabolic activity in their ciliated

cortex and autophagy in their central mass suggests involvement of active tissue reorganization processes. DNA synthesis was evaluated in the forming multicellular aggregates and in the four cell layers of the polyp, using BrdU labeling of nuclei over a 24 h period. The distribution of BrdU-labeled coral cells was spatially heterogeneous and their proportion was very low in tissue balls ( $0.2 \pm 0.1 \%$ ), indicating that suspended multicellular aggregate formation does not involve significant cell division. In polyps, DNA synthesis was significantly lower in the calicoderm ( $<1 \%$ ) compared to both oral and aboral gastroderm (about  $10 \%$ ) and to the pseudostratified oral epithelium ( $15\text{--}25 \%$  at tip of tentacle). DNA synthesis in the endosymbiotic dinoflagellates dropped in the forming tissue balls ( $2.7 \pm 1.2 \%$ ) compared to the polyp ( $14 \pm 3.4 \%$ ) where it was not different from the host gastroderm ( $10.3 \pm 1.2 \%$ ). A transient

---

I. Domart-Coulon was formerly affiliated with UMR 7208 BOREA Département Milieux et Peuplements Aquatiques, Muséum National d'Histoire Naturelle, Case Postale 26, 43 rue Cuvier, 75005 Paris, France

---

A. Lecointe · M. Gèze · I. Domart-Coulon (✉)  
UMR7245 MCAM Département RDDM, Muséum National D'Histoire Naturelle, Case Postale 54, 57 rue Cuvier, 75005 Paris, France  
e-mail: icoulon@mnhn.fr

A. Lecointe · S. Cohen · A. Meibom  
Laboratory for Biological Geochemistry, School of Architecture, Civil and Environmental Engineering (ENAC), Ecole Polytechnique Fédérale de Lausanne (EPFL), 1015 Lausanne, Switzerland

S. Cohen  
The Interuniversity Institute for Marine Science in Eilat, P.O. Box 469, 88103 Eilat, Israel

S. Cohen  
The Mina and Everard Goodman  
Faculty for Life Sciences, Bar-Ilan University,  
52900 Ramat Gan, Israel

C. Djediat  
Plateforme de microscopie électronique et d'imagerie, Département RDDM, Muséum National D'Histoire Naturelle, Case Postale 39, 12 rue Buffon, 75005 Paris, France

(24 h) increase was observed in the cell-specific density of dinoflagellates in individually dissociated coral cell cultures. These results suggest disruption of coral cell proliferation processes upon establishment in primary culture.

**Keywords** Primary culture · DNA synthesis · BrdU · Coral · Scleractinia · Dinoflagellate · Cell proliferation

## Introduction

Since the 1960s there have been multiple efforts to develop cell cultures from the scleractinian coral organisms, which build the structural framework of marine reefs. Coral cell cultures are potentially alternative tools to study the response of corals to environmental stress and diseases. In vitro experiments may complement and extend in vivo experiments in the aquarium or the natural reef environment. However, to date no coral cell lines have been established and isolated scleractinian coral cells can only be maintained in primary cultures on timescales from a few days to a few weeks, without continuous propagation.

Development of the methodology for coral cell cultures has been sporadic. Difficulties stem from a limited knowledge about cell nutritional requirements and physiology in vitro that lead to short-term functional viability (Domart-Coulon et al. 2004a). Limited tools for characterization of cell types, frequent overgrowth of contaminants (especially chytrid protists) (Rinkevich 1999, 2005), and a lack of characterization of the proliferating stem cell niches (Rinkevich 2011) add more complexities. Moreover, most unsuccessful strategies have remained unpublished.

To isolate cells, methods include mechanical detachment of soft tissue from the skeleton, either by pinching off tissue fragments with tweezers (Kramarsky-Winter and Loya 1996; Vizek et al. 2011) or by blasting the tissue with a jet of pressurized seawater (Nesa and Hidaka 2009). Alternately, coral soft tissue is chemically induced to detach, in response to removal of divalent cations (Gates and Muscatine 1992; Frank et al. 1994; Kopecky and Ostrander 1999; Domart-Coulon et al. 2001, 2004a; Mass et al. 2012) or exposure to a reducing agent, such as *N*-acetylcysteine (Peng et al. 2008). Enzymatic digestion has also

been widely used to dissociate the tissue into single cells (Gates and Muscatine 1992; Frank et al. 1994; Helman et al. 2008; Downs et al. 2010). Types and brand of enzymes used in dissociation studies vary between laboratories, and are often not detailed by authors, making it difficult to standardize protocols for coral cell isolation. Spontaneous dissociation has also been reported after freeze–thaw cycles (Frank et al. 1994) or after exposure of larvae to antibiotics (Reyes-Bermudez et al. 2009).

These methods yield either tissue (explant) cultures, or mixed cell type single dissociated cultures, which may be further enriched in specific cell types and for example applied to ecotoxicology testing (Downs et al. 2010). Suspended multicellular isolates (explants) are formed in cell culture medium within 3 days of culture initiation after divalent cation removal (Kopecky and Ostrander 1999; Domart-Coulon et al. 2001, 2004a). Similar structures (called tissue balls) are also formed in seawater via individual cell aggregation after mechanical dissociation (Nesa and Hidaka 2009) or rounding up and closure of soft tissue spheroids microdissected from the skeleton (Kramarsky-Winter and Loya 1996; Vizek et al. 2011).

Suspension cultures of multicellular aggregates have been applied to the study of symbiosis, the response to thermal stress, and interactions between coral and fungi (Kopecky and Ostrander 1999; Nesa and Hidaka 2009; Domart-Coulon et al. 2004b). Adherent cultures of multicellular aggregates have been used to develop models of in vitro biomineralization (Domart-Coulon et al. 2001; Helman et al. 2008; Mass et al. 2012). Decreasing in vitro viability usually limits the timescale of experiments using such primary cultures from a few days to a few weeks, enabling only short-term study of physiological mechanisms.

A major problem is the current lack of characterization of in vitro proliferation. Once the tissue is dissociated from the initial fragment, the biomass of primary cultures does not increase over time (in terms of cell number or protein content), so it is assumed that coral cells do not divide significantly. Clusters of cells have been reported to form in suspension in several models, including embryonic cells (Reyes-Bermudez et al. 2009) as well as adult cells (Kopecky and Ostrander 1999; Nesa and Hidaka 2009) or in adherent cultures on Primaria substrate (Domart-Coulon et al. 2001; Helman et al. 2008; Mass et al. 2012). In the soft



coral *Sinularia flexibilis*, these aggregates were interpreted as a sign of cell proliferation (Khalesi et al. 2008). Recent encouraging results have reported regeneration of polyps from suspended spheroid tissue cultured in seawater (Vizel et al. 2011). However cell division activity has not been investigated within these coral primary cultures and especially during formation of the multicellular aggregates.

Incorporation of BrdU (5-Bromo-2'-deoxy-uridine analogue of deoxythymidine) in the DNA of cell nuclei is an indicator of DNA synthesis and is widely used to estimate rates of cell division (Dolbeare and Selden 1994), although its interpretation requires caution as it may also detect DNA repair events not linked to S-phase of the cell cycle (Taupin 2007). Within the phylum Cnidaria, this method is commonly used in hydrozoans, for example in the marine species *Hydractinia echinata* and *Clytia hemisphaerica*, in short-term pulse (5 mM BrdU for 30 min to a few hours)—chase assays to detect mitotic activity and cellular self-renewal (Müller et al. 2004; Denker et al. 2008). In adult colonies of scleractinian corals the BrdU labeling method has recently been used, at much lower concentrations and longer exposure periods, to investigate cell proliferation activity in aquarium-based studies. DNA synthesis was detected in 2–4 % of the *Symbiodinium* dinoflagellate endosymbionts of *Montipora capitata*, via BrdU (50  $\mu$ M) labeling during 48 h (Santos et al. 2009). In another study, mitotic activity was assessed by expression of the conserved Proliferating Cell Nuclear Antigen (PCNA) protein in the species *Montipora foliosa* and *Acropora pulchra*, following creation of a lesion (D'Angelo et al. 2012). But in both cases, the spatial distribution of the proliferation activity was determined only at the level of the colony, comparing top versus underside and margin versus inner area of plate-forming *Montipora* corals, and comparing apex versus branch of branching *Acropora* corals. A very recent study reported differential cellular kinetics in the oral and aboral tissue layers of healthy and diseased corals (*Porites australiensis* and *Montipora informis*) exposed to BrdU (100  $\mu$ M) for 3 days, showing an increase in cell division and a decrease in apoptosis in growth anomaly lesions versus control tissue (Yasuda and Hidaka 2012).

In this study, we have evaluated the efficiency of different brands and types of collagenase to obtain cells and tissue balls (TBs) from adult colonies of the Indo-

Pacific scleractinian coral *Pocillopora damicornis*. The structure and cell type distribution of TBs were characterized and compared to polyps. The DNA synthesis activity was investigated via BrdU incorporation into nuclei over a 24 h period, at the onset of primary cultures in the forming TBs, and in vivo in the polyps. BrdU-labeled cells were localized and quantified in the cortex and the center of TBs, and in the four tissue-layers characteristic of coral polyps. The cell-specific density (CSD) of dinoflagellate symbionts was also monitored in vitro, during the first 2 days after establishment of single dissociated cell cultures. Implications for the proliferation activity of coral cells and their dinoflagellate endosymbionts in the polyp and in the TBs at the onset of primary cultures are discussed.

## Materials and methods

### Biological material

Small nubbins (~5 cm height) of the scleractinian coral *P. damicornis* (Linnaeus, 1758) were prepared by fragmentation from one large adult colony grown at the Aquarium Tropical, Palais de la Porte Dorée (ATPD), Paris, France. They were allowed to recover more than 3 weeks until completely covered with tissue, then used for cell isolation and BrdU labeling of DNA synthesis activity. Colony nubbins were cultured under a 12/12 h light/dark cycle (5000 Lux, provided by 6 fluorescent tubes, including 3 white light 10,000 K and 3 blue light 20,000 K) in equilibrated closed-circuit artificial seawater at 25 °C, salinity 35‰, pH 8.1  $\pm$  0.2 (daily pH fluctuations due to photosynthesis and respiration activity). During the 24 h BrdU labeling experiment, the light cycle was conserved, seawater was renewed every 6 h, and air was gently bubbled in for gas equilibration. Temperature and pH were monitored to remain within the recorded growing range (25–27.5 °C and pH 8.0–8.3).

### Coral cell isolation

The apex of branches (~5 mm height) from *P. damicornis* nubbins were sampled with scissors at the Aquarium Tropical, Palais de la Porte Dorée (ATPD, Paris) and placed for ~2–3 h at room temperature in 0.2  $\mu$ m filtered sea water (FSW)—sampled from a 1,500 L tank with artificial seawater (closed system)

equilibrated for a live stony coral exhibit. This seawater was supplemented with (v:v) 3 % antibiotics-antimycotics 100× solution (AB-AM, Gibco/Life Technologies, Carlsbad, CA, USA) corresponding to final concentrations of Amphotericin B <0.3 %, Penicillin 1.5–4.5 %, Streptomycin 1.5–4.5 %.

After three successive rinsing steps to remove loosely attached surface contaminants, the coral fragments were incubated at 24 °C in 5 mL collagenase 0.05–0.15 % (weight/volume) solution in FSW, stirred at 75 rpm with a magnetic stir bar, for periods ranging 10–30 min. Different types and commercial brands of collagenase were tested, with collagenase activity given either in Collagen Degrading Units (CDU) or in Wünsch units/mg of product. For comparison of the efficiency of collagenase digestion between brands, the Wünsch unit was converted in CDU (1 Wünsch unit/mg = 1,000 CDU/mg, after Roche manufacturer's manual). The enzyme percent concentration (weight/volume) traditionally used was standardized a posteriori per mg of wet tissue digested: this was calculated from the final weight of enzyme in a defined volume (5 mL) standardized to 100 mg of wet tissue. Here, wet tissue is defined by the difference between wet weight of coral fragments before ( $t = 0$ ) and after complete tissue dissociation ( $t = 3$  days), once the skeleton is bare. The range of activity for each enzyme was derived from repeated experiments with the same enzyme, on different batches of coral fragments.

The exact composition of collagenase blends is not specified by the provider(s). Collagenase type IV Sigma-Aldrich (C5138) from *Clostridium histolyticum* has a collagenase activity of 125 CDU per mg of product and also contains clostripain, a non-specific neutral protease and tryptic activities. Collagenase type IV Gibco (17104-019) from *Clostridium histolyticum* is prepared with low amount of tryptic activity and guaranteed to have at least 160 CDU per mg of product. Collagenase type I Sigma-Aldrich (C0130) from *Clostridium histolyticum* has 125 CDU per mg of product, and contains non-specific protease and clostripain activity. Two Liberase purified enzyme blends from Roche Diagnostics (Mannheim, Germany) were also used: Liberase DL (05401160001) and Liberase TM (05401119001). Both contain the same amount of collagenase activity (26 Wünsch units/5 mg of product, i.e. 5,200 CDU/mg of product) but differ in the type of combined neutral protease, its amount and its aggressiveness. According to the manufacturer,

Liberase DL contains low amount of dispase with weak aggressiveness and Liberase TM contains medium amount of thermolysin with high aggressiveness.

Tissue digestion was stopped by rinsing fragments 15 min with FSW at 75 rpm and 24 °C. Then each collagenase-treated apex was placed individually into separate wells of a 6-well plate (Nunclon/Thermo Fisher, Illkirch, France) in 5 mL of cell culture medium. These primary explant cultures were incubated at 24 °C under air, with a 10/14 h day/night light cycle under very low white light, 2–4 photosynthetic photon flux density (PAR)  $\mu\text{mol per m}^2$  per second (measured with LI-COR LI-250A light meter Quantum/Radiometer/Photometer). Tissue dissociation was monitored using an inverse phase contrast light microscope Olympus CK40 (Tokyo, Japan) and micrographs were acquired with Canon camera (Tokyo, Japan). Cell viability was determined by the trypan blue exclusion assay and cell counting on a Malassez hemacytometer.

The cell culture medium was modified from Domart-Coulon et al. (2001) and Helman et al. (2008). Its composition was based on filtered seawater (FSW) supplemented with commercial formula for vertebrate cell culture, with added salts to adjust osmolarity, and various amino-acid supplements, as well as trace amount of fetal calf serum to provide undetermined growth factors. Antibiotics-antimycotics mix (AB-AM, Gibco) was added to limit overgrowth of microbial contaminants. Prepared in FSW, this complex medium contained (v/v) 12.5 % modified DMEM (Gibco 11880 without phenol red and with 1 g L<sup>-1</sup> glucose and 100 mg L<sup>-1</sup> sodium pyruvate, to which were added NaCl 18.1 g L<sup>-1</sup>, KCl 0.35 g L<sup>-1</sup>, CaCl<sub>2</sub> 1.1 g L<sup>-1</sup>, Na<sub>2</sub>SO<sub>4</sub> 1 g L<sup>-1</sup>, MgCl<sub>2</sub>·6H<sub>2</sub>O 10.2 g L<sup>-1</sup>, aspartic acid 20 mg L<sup>-1</sup>, taurine 52 mg L<sup>-1</sup>, SrCl<sub>2</sub> 26 mg L<sup>-1</sup>) buffered with Hepes 5.96 g L<sup>-1</sup>, and pH adjusted to 7.9 and (v/v) 1.25 % Fetal Calf Serum (Sigma-Aldrich, St. Louis, MO, USA), (v/v) 1 % AB-AM (Gibco), (v/v) 1 % Glutamax (Gibco), and 50  $\mu\text{g/mL}$  ascorbic acid (Sigma-Aldrich) freshly prepared from frozen 5 mg/mL stock solution. Unless otherwise specified, all chemicals were from Sigma-Aldrich. Final concentration of antibiotics and antimycotics were Penicillin 0.5–1.5 %, Streptomycin 0.5–1.5 %, Amphotericin B <0.1 %. The culture medium was renewed every week by 50 %, with weekly addition of 50  $\mu\text{g/mL}$  ascorbic acid as antioxidant compound.

Isolated cells or tissue which detached from the skeleton were transferred into fresh culture medium in separate wells of a 6 or 24 well microplate (Nunclon), in order to limit contamination by ciliates, bacteria or chytrid-like protists associated with the original coral fragments. Substrate of culture dishes was plastic (Nunclon) or glass (autoclaved coverslips or Labtek chambers).

Scanning electron microscopy (SEM) and transmission electron microscopy (TEM) of coral polyps and multicellular aggregates formed in primary cultures

For ultrastructural observations, polyps at the apex of colony branches and cell aggregates formed in primary cultures were fixed overnight at 4 °C in 2.5 % glutaraldehyde and 0.2 % saturated picric acid in 0.1 M Sørensen-phosphate buffer at pH 7.9 (made with  $\text{NaH}_2\text{PO}_4\text{-}2\text{H}_2\text{O}$  and  $\text{Na}_2\text{HPO}_4\text{-}2\text{H}_2\text{O}$ ) containing 0.6 M sucrose. The skeleton of fixed colony fragments was decalcified in EDTA 0.5 M in 0.1 M Sørensen-phosphate buffer at pH 7.9 for 2 days at 4 °C. Polyps were then microdissected under a binocular. Fixed samples (polyps or cell aggregates) were rinsed three times in Sørensen-phosphate-sucrose buffer, post-fixed in 1 % osmium tetroxide ( $\text{OsO}_4$ ) in 0.1 M Sørensen-phosphate-0.6 M sucrose buffer for 1 h at room temperature, and dehydrated in a graded series of increasing ethanol concentrations.

For scanning electron microscopy (SEM), ethanol was substituted with liquid  $\text{CO}_2$  and samples were critical point dried, mounted on SEM stubs, fractured with a scalpel, and gold-coated. Observations were performed at 15 kV with a JEOL 840A scanning electron microscope (Tokyo, Japan) equipped with SEMAFORE image acquisition software at the electron microscopy platform (PIME) of the Muséum National d'Histoire Naturelle.

For transmission electron microscopy (TEM), dehydrated samples were embedded at 60 °C in Spurr resin. Semi-thin sections (0.5–1  $\mu\text{m}$ ) were cut with a 35° diamond blade (Diatome) on an ULTRACUT E Reichert-Jung microtome (Buffalo, NY, USA) and stained with 1 % toluidine blue containing sodium tetraborate (EMS, Fort Washington, PA, USA) followed by 0.1 % basic fuchsin (EMS). Ultra-thin sections (50–70 nm) were contrasted with saturated uranyl acetate 50 % in ethanol at room temperature,

and observed at 75 kV with a Hitachi H-7100 transmission electron microscope (Tokyo, Japan) equipped with a CCD Hamamatsu camera (Hamamatsu Photonics, Hamamatsu, Japan). Photos were taken with AMTV 542 image acquisition software, at the electron microscopy platform (PIME) of the Muséum National d'Histoire Naturelle.

Estimation of DNA synthesis via immunodetection of BrdU labeled cell nuclei

For primary cultures and coral colonies incubated, respectively, in cell culture medium and seawater, the BrdU labeling solution was renewed every 4–6 h, due to the reported instability of BrdU beyond 6 h after dilution in seawater (Santos et al. 2009). Reagents from the commercial 5-Bromo-2'-deoxy-uridine Labeling and Detection Kit II (Roche) were used, except that the colorimetric detection system was replaced by an epifluorescence detection system after preliminary assays revealed significant endogenous alkaline phosphatase activity in coral tissue, creating false positive labeling. Therefore a secondary (goat) antimouse antibody coupled to Alexa594 fluorochrome (Invitrogen/Life Technologies, Carlsbad, CA, USA) was used for detection of the primary antiBrdU mouse antibody (Roche).

In order to evaluate DNA synthesis at the onset of primary cultures, coral cells were incubated with 50  $\mu\text{M}$  BrdU labeling reagent in cell culture medium (5 mL), between Day 1 and Day 2 from collagenase treatment. Labeling was carried out during one diurnal cycle (24 h), with two successive changes of BrdU solution, first after 4 h then after 8 h, for an estimated exposure time of at least 14 h to active BrdU, covering the last 5 h of the dark photoperiod and 9 h of the light photoperiod. The experiment was repeated three times independently.

In order to evaluate DNA synthesis in situ in the polyps, coral nubbins were incubated with 25  $\mu\text{M}$  BrdU in seawater (250 mL) during one diurnal cycle (24 h), with four successive changes of the BrdU-labeled seawater, i.e. every 6 h starting with the 12 h light photoperiod and finishing with the 12 h dark photoperiod.

For immunohistological detection of BrdU incorporation, the apex of colony branches (four replicate nubbins exposed to BrdU and one unexposed control) and the multicellular aggregates were fixed overnight

at 4 °C with 0.5 % glutaraldehyde (Sigma-Aldrich), 2 % paraformaldehyde (Fluka/Sigma-Aldrich), and 0.2 % saturated picric acid (Sigma-Aldrich) in 0.1 M Sörensen-phosphate—0.6 M sucrose buffer at pH 7.9. Fixed tissue was rinsed in 0.1 M Sörensen-phosphate—0.6 M sucrose buffer, and the skeleton of colony fragments was decalcified in EDTA 0.5 M in 0.1 M Sörensen-phosphate buffer at pH 7.9 for 2 days at 4 °C, before microdissection of individual polyps under a binocular.

Samples were dehydrated in graded ethanol series and embedded at 37 °C under vacuum in LR-White medium grade resin (Fluka/Sigma-Aldrich). Serial semi-thin sections (1 µm) were cut with a 35° diamond knife (Diatome) on an ULTRACUT microtome and placed on Superfrost glass slides in five sets of five serial sections. One set was stained with toluidine blue—basic fuchsin for orientation in the tissue (cf. above for detailed stain composition), two sets were used for immunodetection of BrdU and the two other sets were used for internal immunolabeling negative controls, without antibodies (for autofluorescence) and without primary antibody. Finally, for each slide, the total tissue area examined to detect BrdU-positive nuclei corresponded to a surface of  $15 \times 10^4 \mu\text{m}^2$  by 5–10 µm depth, and consecutive areas were spaced by at least 30–40 µm. So, within an individual polyp or TB, each area corresponded in fact to a specific depth in the polyp or the TB.

Sections were permeabilized with PBS, 10 mM, pH 7.4, containing (v:v) 0.1 % Triton X100 (PBST), treated 10 min with HCl 2 M, washed with PBST, pre-incubated for 30 min in saturation solution (PBST with (w:v) 1 % BSA and (v:v) 2 % Normal Goat Serum), then incubated for 3 h at room temperature with the primary anti-BrdU mouse antibody (Roche kit no. 11299964001) diluted 1/50 in the saturation solution. Sections were washed three times in PBST then incubated 1 h at RT with the secondary goat anti-mouse antibody labeled with Alexa-594 (Invitrogen) diluted 1/100 in PBS. Sections were washed three times in PBS and slides were coverslipped in the mounting medium Prolong Gold Antifade with DAPI (Invitrogen).

Labeling was detected at  $\times 20$  and  $\times 40$  at the Centre de Microscopie de fluorescence et d'Imagerie numérique (PIME) of the Muséum National d'Histoire Naturelle with a Nikon Eclipse TE 300 inverse wide-field fluorescence microscope, equipped with a

mercury lamp, a z acquisition design, and a CDD camera. Images and image stacks were acquired using Metamorph software with MonoD excitation-emission settings ( $\lambda_{\text{ex}}$ : 340–380 nm,  $\lambda_{\text{em}}$ : 445–465 nm) for DAPI, with MonoR excitation-emission settings ( $\lambda_{\text{ex}}$ : 540–565 nm,  $\lambda_{\text{em}}$ : 580–620 nm) for dinoflagellates autofluorescence, and with HQ-APC excitation-emission settings ( $\lambda_{\text{ex}}$ : 563–617 nm  $\lambda_{\text{em}}$ : 632–697 nm) for Alexa-594. Selected optical planes were stacked to visualize BrdU-labeled structures. Localization of dinoflagellate cells was confirmed by overlay of chlorophyll autofluorescence images (MonoR settings) with DAPI images (MonoD settings). Specificity of BrdU signal was checked by colocalization of Alexa-594 (HQ-APC settings) with DAPI-counterstained nuclei (MonoD settings).

#### Evaluation of the cell specific density of dinoflagellate endosymbionts

The cell-specific density (CSD) is an estimation of the number of dinoflagellates contained in one host cell. CSDs were estimated at the onset of coral primary cultures in five independent collagenase experiments, with the method of Muscatine et al. (1998). The number of dinoflagellates per host cell was counted with an Olympus CK40 inverse phase contrast microscope (providing enhanced contrast of the host cell cytoplasmic membrane), in three to five hundred coral gastrodermal cells per well, in four to five replicate wells per culture. The cell-specific density data were expressed in terms of the frequency or percent distribution of host cells ( $f_i$ ) with a given number of dinoflagellates per cell ( $r_i$ ).

$$\text{CSD} = \sum (r_i * f_i) / \sum f_i$$

#### Data and statistical analysis

For quantification of the relative abundance of cells having engaged in DNA synthesis during the 24 h labeling period, BrdU-positive and DAPI-positive nuclei were counted using ImageJ image analysis software (U.S. National Institutes of Health, Bethesda, Maryland, USA, <http://www.rsb.info.nih.gov/ij/>) using the cell counting tool and checking for colocalization of Alexa-594 and DAPI signals with the colocalization plugin. Each slide was considered to represent one area in the depth of the polyp or the TB,

as it corresponded to 5–10 serial semi-thin (1  $\mu\text{m}$ ) sections, for which the total numbers of counted nuclei were pooled. Percentages of BrdU-labeled nuclei were compared after arcsine transformation and the data distribution was tested. Non-parametric statistical analyses of the data were performed with either Kruskal–Wallis test for comparison between more than two groups, or Mann–Whitney test for comparison between two non-paired groups, or signed Wilcoxon test between two paired groups (e.g. DNA synthesis data between tissue types from the same series of serial sections—same slide).

For CSDs of dinoflagellates measured over time in primary culture, data were transformed using arcsine. Data coherence between the five independent collagenase experiments was checked with a non-parametric Kruskal–Wallis test. When no significant differences were found, data were pooled. Differences between CSD at each time point were evaluated with non-parametric Mann–Whitney test, after at least one difference was found between timepoints with a Kruskal–Wallis test. In all statistical analyses, significance was associated with  $p$  values  $<0.05$ .

## Results

### Effect of collagenase type and commercial brand on tissue dissociation efficiency

Within 3 days from collagenase treatment, cells continued to detach from the polyp tissue, coming off the skeleton of the colony (Fig. 1a) as single dissociated individual cells and as tissue fragments. Derived primary cultures displayed a mixed cell type composition (Fig. 1b), including cnidocytes, brown-pigmented dinoflagellate endosymbionts of coral cells (about 8  $\mu\text{m}$  in diameter), and undetermined rounded clear or granulous coral cells (4–10  $\mu\text{m}$  in diameter).

Spontaneous aggregation of individual cells was observed in vitro, forming irregular cell clusters about 100  $\mu\text{m}$  in diameter (Fig. 1c) which fused on the second day (Fig. 1d) and developed a smooth surface on the third day of culture (Fig. 1e). Both these multicellular aggregates and the detached tissue fragments rounded up and closed into spherical or ellipsoidal tissue balls (TBs) delimited by a smooth surface and rotating in suspension. Fusion of TBs over the first 5 days of the primary cultures (Fig. 1f) led to

increase in TB size, reaching final diameters in the range of 250–900  $\mu\text{m}$ , and averaging  $520 \pm 230 \mu\text{m}$  ( $n = 133$ , pooled from all experiments), generally below the average diameter of apical polyps ( $620 \pm 70 \mu\text{m}$ ,  $n = 18$ ) and of branch lateral polyps ( $900 \pm 130 \mu\text{m}$ ,  $n = 27$ ). Dissociation of the initial colony fragment tissue was usually complete within 3–5 days, leaving the skeleton bare.

Results presented in Table 1 indicate that the dissociation efficiency varied depending on the type and brand of commercial collagenase enzyme used. Each collagenase type targets a specific type of collagen molecule, and commercial brands include varying amounts of other proteases (detailed in “[Material and methods](#)”). Standardized to collagenase digestive units (CDU) per mg wet coral tissue, the tissue dissociation yield varied depending on treatment, in terms of number of individual cells, and number and size of tissue balls. The viability of dissociated cells measured by the trypan blue exclusion assay was, however, similar between all treatments, in the range of 70–80 %. (The trypan blue assay has low precision, due to the differential staining reaction for different coral cell types and dinoflagellates.) The quantity of single dissociated cells obtained right after the incubation was low with collagenase Sigma type I and collagenase Gibco type IV and higher with collagenase Sigma type IV (for similar activity range), and was also high with Liberase TM and Liberase DL. Nevertheless, the three latter enzymes had distinct effects on the capacity of individual cells to reaggregate over time in primary culture. Aggregation of single dissociated cells into TBs was not observed for Liberase Roche TM, which contains high concentrations of additional proteases. Collagenase Sigma type IV and Liberase DL demonstrated the highest efficiency in terms of single cell numbers right after incubation (at  $t = 0$ ) but reproducibility in obtaining TBs in primary culture (at  $t = 2$  days) was better with collagenase Sigma type IV compared to Liberase DL. The average size of tissue balls did not vary with enzyme treatment, but their number was reproducibly highest after treatment with 0.15 % collagenase type IV from Sigma. As a conclusion, the treatment with (weight/vol) 0.15 % collagenase Sigma type IV had a good yield of single cell isolation at culture initiation and was the most efficient to obtain the formation of tissue balls in primary culture.

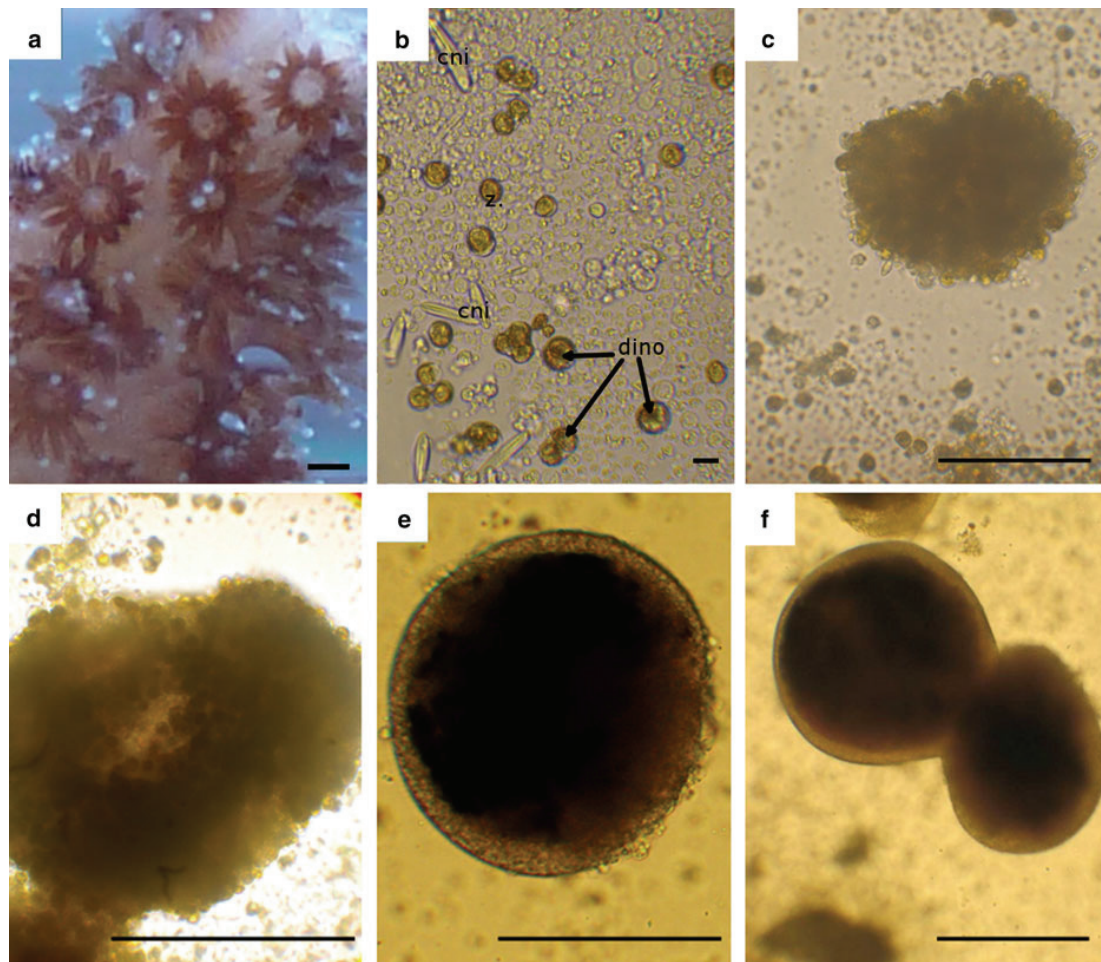


**Fig. 1** In vitro cell aggregation and the formation of tissue balls in primary cultures from *P. damicornis* scleractinian coral. **a** Polyps at the apex of a colony branch (scale bar 500  $\mu$ m). **b** Mixed morphological cell types in 1 day cell culture from collagenase type IV (Sigma) dissociated tissue (scale bar 15  $\mu$ m); brown spherical dinoflagellates (*dino*); spindle cells corresponding to various subtypes of cnidocytes (*cni*); clear rounded unidentified coral cells. **c** Irregular cluster formed by

aggregation of mixed cell types in 1 day cell culture (scale bar 100  $\mu$ m). **d** Cell aggregate formed by fusion of irregular cell clusters between first and second day of primary culture (scale bar 500  $\mu$ m). **e** Tissue balls are spheroid cell aggregates with a smooth surface, rotating in suspension in a 2 day primary culture (scale bar 500  $\mu$ m). **f** Fusion of suspended tissue balls in a 2 day primary culture (scale bar 500  $\mu$ m)

#### Morphology and structure of the tissue balls formed in vitro

The structure of tissue balls formed in vitro was compared to the structure of the polyps, visualized in scanning electron microscopy (SEM) after decalcification of the skeleton (Fig. 2). Typical of scleractinians, the polyp (Fig. 2a) is characterized by four cell layers organized in two tissues: the oral tissue facing

seawater, composed of the pseudostratified epithelium and the oral gastroderm containing dinoflagellate endosymbionts; the aboral tissue facing the skeleton, composed of the aboral gastroderm and the calicoderm. The gastroderm lines the internal gastric cavity (Fig. 2c). Comparatively, the organization of tissue balls formed in primary culture (Fig. 2b) was simpler, with only two distinct zones, described as a cortex and a central mass of cells. A small internal cavity was

**Table 1** Primary culture yield and viability, depending on collagenase type and commercial origin

Enzyme	Activity (Collagen degrading units per mg wet tissue)	Digestion protocol	Number of single dissociated cells at t = 0 (10 <sup>6</sup> viable cells per 100 mg wet tissue)	Cell viability (%)	Number of tissue balls (TB) at t = 2 days (per 100 mg wet tissue)	Diameter ( $\mu\text{m}$ ) of tissue balls (mean $\pm$ SD)
Collagenase Sigma type I (0.15 %)	7–8	1 $\times$ 30 min (+1 $\times$ 15 min rinse)	0.02–0.25	50–75	3–7	554 $\pm$ 195 (n = 14)
Collagenase Sigma type IV (0.15 %)	5–15	1 $\times$ 15 min (+1 $\times$ 15 min rinse)	3	75–80	5–15	336 $\pm$ 140 (n = 28)
Collagenase Gibco type IV (0.15 %)	5–15	1 $\times$ 30 min (+1 $\times$ 15 min rinse)	0.15–1.5	70	<1	500 (n = 1)
Liberase Roche DL (0.05 %)	120–130	1 $\times$ 30 min (+1 $\times$ 15 min rinse)	5–6	70–75	0–10	509 $\pm$ 79 (n = 10)
Liberase Roche TM (0.05 %)	70–150	1 $\times$ 30 min (+1 $\times$ 15 min rinse)	2–3	75–80	0	0

sometimes present inside the central mass (Fig. 2d, white hatched line). Both polyps and tissue balls displayed ciliae on their outer surface, facing respectively seawater or cell culture medium (Fig. 2e, f). The ciliary activity of the cells forming the cortex created TB rotation in suspension.

Histological observations (Fig. 3) confirmed differences in organization of the tissue balls as compared to the polyps (Fig. 3a), with an outer cortex differentiated from the central mass of cells, as visualized in semi-thin sections after aggregation of tissue fragments (Fig. 3b) or individual cells (Fig. 3e). The cortex ( $\sim 15 \mu\text{m}$  thick) was almost continuous, with the exception of an occasional small opening in TBs formed from tissue fragments (top in Fig. 3b). The spatial distribution of cell types was significantly different between polyp (Fig. 3a) and TBs (Fig. 3c, d, f). There was no recognizable pseudostratified epithelium in the TB. The cortex was rich in cells containing intracellular vesicles stained red with basic fuchsin and blue with toluidine blue borax, indicating basophilic content. The localization of dinoflagellate endosymbionts was restricted to the central mass, and the dinoflagellate-hosting gastrodermal cells were dispersed throughout the TB central mass instead of being grouped in specific layers (as in the gastrodermal layer of polyps). Cnidocytes were located underneath the cortex, in clusters at the periphery of the central mass. Mucocytes stained purple with basic fuchsin were distributed heterogeneously inside the central mass.

Ultrastructural observations (Fig. 4) confirmed the spatially differentiated cell type distribution inside tissue balls, with distinct cell types in the cortex and the central mass. The cortex was composed of interdigitated ciliated cells with apical microvilli and numerous mitochondria, joined together by apical intercellular septate junctions (Fig. 4a, b). Abundant electron-dense vesicles and fibrillar material were observed in proximity to Golgi structures in the cortex cells, indicating high secretory activity (Fig. 4c, d). In the central mass, few cnidocytes were detected underneath the cortex cells, mostly grouped in small clusters, with intact or partially lysed cnidocyst capsule (Fig. 4e). The central mass also contained coral cells hosting dinoflagellate symbionts (holobiont cells) (Fig. 4f). Intercellular spaces were abundant (Fig. 4g) and various types of autophagosomes were detected throughout the central mass (Fig. 4h), providing morphological evidence of autophagy processes.

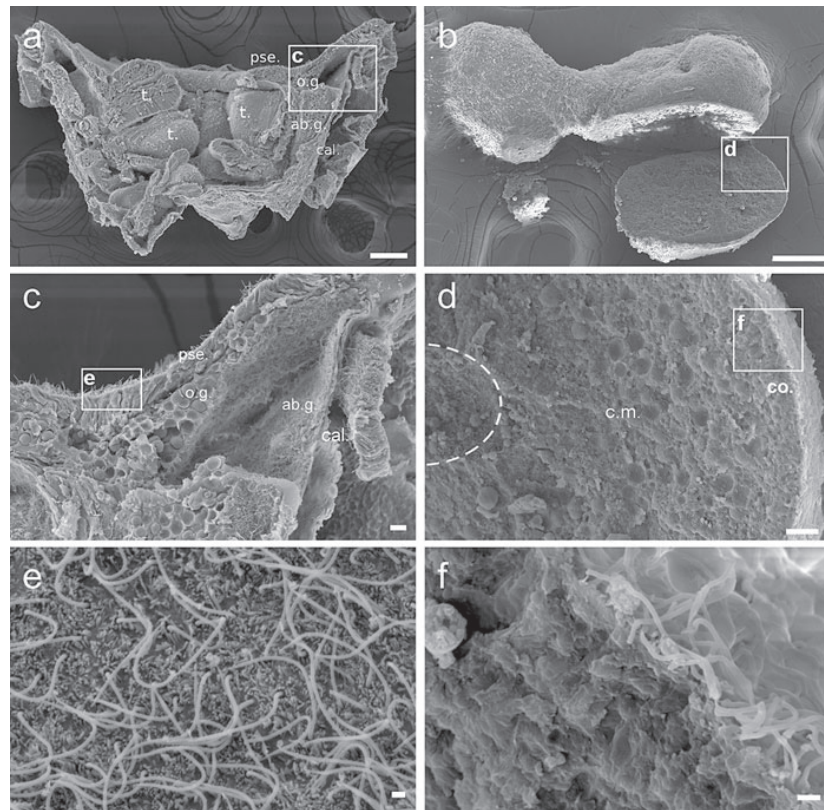


**Fig. 2** Structure of tissue ball (TB) compared to polyp. Scanning electron micrographs of **a** Fractured polyp of *P. damicornis* and **b** Fractured set of 2 fused tissue balls. *Insets* are higher magnifications showing **(c)** the polyp's four cell layers, including *pse.*: pseudo-stratified epithelium, *o.g.*: oral gastroderm, *ab.g.*: aboral gastroderm, *cal.*: calicoderm, and **(d)** the

TB's two zones, including *co.*: cortex, and *c.m.*: central mass, with a small internal cavity (*white dots*). Close-up on the ciliated external surface of respectively the polyp **e** and the TB **f**, facing respectively sea water or cell culture medium. *Scale bars*: **a**, **b** 100  $\mu\text{m}$ , **c**, **d** 10  $\mu\text{m}$ , and **e**, **f** 1  $\mu\text{m}$

Autofluorescence observations in epifluorescence microscopy of live material (Fig. 5) revealed differences between tissue balls and polyps in the spatial distribution of chlorophyll-containing dinoflagellates (in red) and of the coral cells containing Green Fluorescent Protein (GFP)-like molecules (in green). In the polyp, dinoflagellate density was highest in the oral tissue and tentacles (Fig. 5a), and GFP-like molecules were most concentrated at the apex of tentacles and at the periphery of the oral disk (Fig. 5c and overlay Fig. 5e). In the tissue balls, the distribution of dinoflagellates (Fig. 5b) and of GFP-like molecules (Fig. 5d and overlay Fig. 5f) was spatially highly heterogeneous, corresponding to individual cells dispersed throughout the tissue.

DNA synthesis in vitro in the tissue balls compared to in situ in the polyps

Detection of BrdU incorporation into cell nuclei in semi-thin sections of the polyps and of the tissue balls (Fig. 6) allowed localization of DNA synthesis both in situ in the polyp and in vitro, during formation of the tissue balls. Specific labeling of DAPI stained nuclei (Fig. 6a, b) with Alexa-594-conjugated anti-BrdU secondary antibody (Fig. 6c, d) was confirmed by co-localization of BrdU with DAPI (Fig. 6e, f) and absence of labeling in internal negative controls, and in tissue unexposed to BrdU (data not shown).

The percentage of cells having incorporated BrdU during 24 h was quantified in apical polyps from four



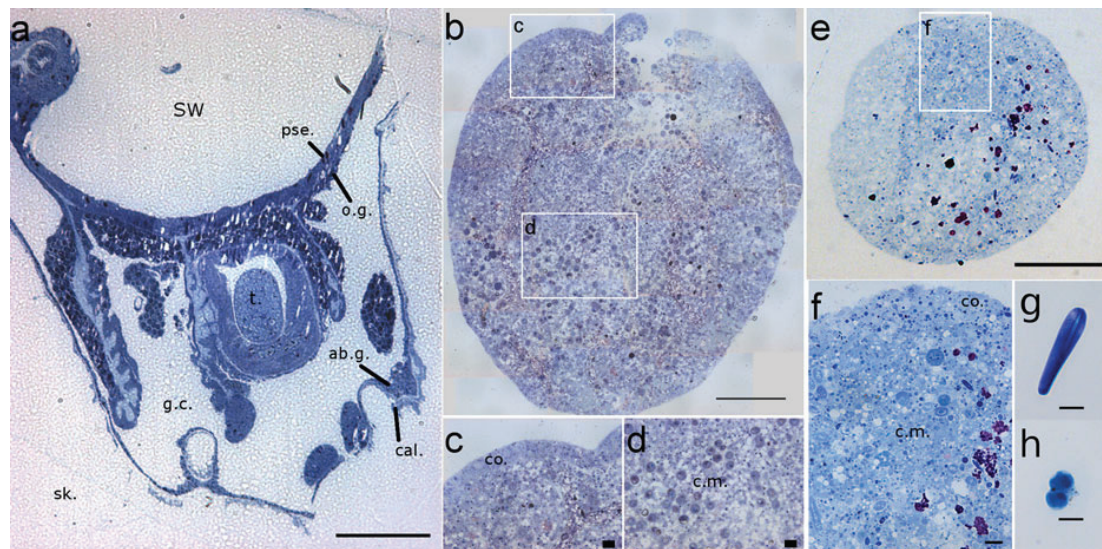


**Fig. 3** Histological organization of coral tissue balls compared to polyp. Optical micrographs of semi-thin sections (0.5–1  $\mu\text{m}$ ) stained with toluidine blue borax then basic fuchsin. Tangential section through (a) a polyp of *P. damicornis* and (b–f) a TB formed in vitro, either (b, c, d) via fusion and reorganization of detached tissue fragments or (e, f) via aggregation of single dissociated cells; g, h Single dissociated coral cell types

featuring a cnidocyte g and a gastrodermal host cell containing a doublet of symbiotic dinoflagellate (h) SW sea water, sk. decalcified skeleton, pse. pseudo-stratified epithelium, t. tentacle, o.g. oral gastroderm, ab.g. aboral gastroderm, g.c. gastric cavity, cal. calicoderm, co. cortex, c.m. central mass. Scale bars: a, b, e 100  $\mu\text{m}$  and c, d, f, g, h 10  $\mu\text{m}$

replicate colonies, and in three replicate TBs. Several areas corresponding each to data pooled from 5 to 10 serial sections were analyzed, corresponding each to a specific depth in the polyp or TB (see “Materials and methods”). Average relative abundance of BrdU-positive nuclei are reported in Table 2 for each cell layer and each zones of the polyp and the TB. Differences in average BrdU-labeling index between polyp cell layers or zones in the TBs, and between coral cells (oral gastroderm) and dinoflagellates are illustrated in Fig. 7. The percentage of BrdU-positive coral cell nuclei was counted separately for each cell layer of the polyp and each zone (cortex or central mass) of the TB (Fig. 7a). The BrdU-labeling index of dinoflagellate endosymbionts was also evaluated, to compare DNA synthesis rate of symbionts and host cells, in the polyp and in the TBs (Fig. 7b).

For TBs, no statistical differences in BrdU incorporation rates were found within similar zones (cortex or central mass) between the replicate TBs, so data were pooled. For comparison between zones, a similar very low rate of BrdU incorporation ( $0.2 \pm 0.1$  %, mean  $\pm$  standard error) was detected in nuclei of the

coral cells in the cortex and the central mass (Signed Wilcoxon,  $p$  value = 0.205,  $n = 40$  total sections). In the central mass, BrdU labeling index of dinoflagellate symbionts was significantly higher than BrdU labeling index of coral cells (Signed Wilcoxon, paired data,  $p$  value = 0.000,  $n = 38$  total sections), indicating that inside the tissue balls DNA synthesis activity was higher in dinoflagellates compared to coral cells.

For polyps, the average percentage of BrdU-positive nuclei was evaluated per area in the tissue depth and, within each area, the BrdU incorporation rates were collected separately for each cell layer. The BrdU labeling index of each cell layer varied between areas. All results are summarized in Table 2. For the pseudo-stratified oral epithelium (pse), BrdU incorporation rates ranged from 6.1 to 31.5 %, reaching 5.3 to 40.7 % at the tip of tentacles. In the oral gastroderm (o.g.), BrdU incorporation rates were similar in coral cells (from 5.1 to 15.9 %) and in dinoflagellate symbionts (from 5 to 21 %). In the aboral gastroderm (ab.g.), BrdU incorporation rates in coral cells ranged from 4 to 23.7 %. The calicoderm was the only cell layer with low variations in BrdU incorporation rates

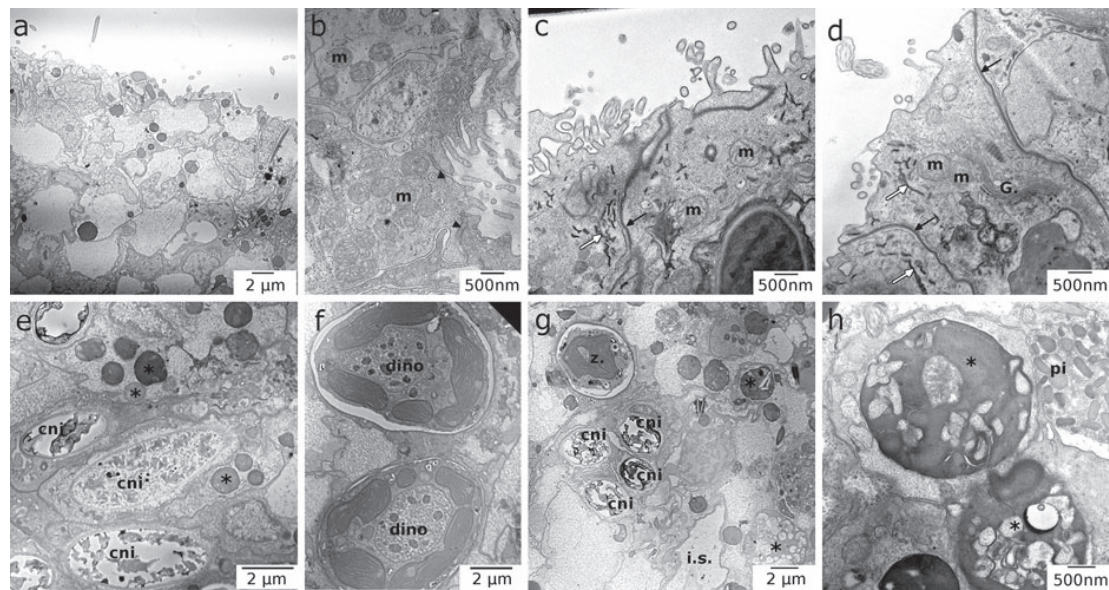


**Fig. 4** Ultrastructure of tissue balls. Transmission electron micrographs of TBs formed in vitro by **a** Aggregation of tissue fragments or **b** Aggregation of single dissociated cells; **c**, **d** Higher magnification of the cortex epithelium, composed of interdigitated ciliated cells joined by apical septate junctions (*black arrows*), and containing abundant mitochondria (*m*) and electron-dense fibrillar material (*white arrows*) in proximity to

Golgi structures (*G*.) Higher magnification of the central mass, with **e** Cnidocytes (*cni*) grouped in clusters, **f** a doublet of dinoflagellates (*dino*) in their coral host cell, **g** cnidocytes, dinoflagellate and intercellular spaces. **h** Autophagosome figures (*black stars*) are abundant inside cells of the central mass, and a few pigmented cells (*pi*) are observed. Scale bars **a**, **e**, **f**, **g** 2  $\mu$ m and **b**, **c**, **d**, **h** 500 nm

between areas (from 0 to 1.5 %). In order to evaluate differences in DNA synthesis activity between the four cell layers, arcsine transformed data averaged from all areas in the polyp replicates were compared with non-parametric tests. For coral cells, the calicoderm was the only cell layer statistically different from all others, with lowest BrdU labeling ( $0.8 \pm 0.4$  % mean  $\pm$  standard error,  $n = 6$  areas). In the pseudostratified epithelium, BrdU labeling was  $15.9 \pm 4.2$  % ( $n = 6$ ), reaching  $21.4 \pm 3.4$  % ( $n = 6$ ) at tip of tentacle. BrdU labeling index of coral cells was similar in the oral gastroderm ( $10.3 \pm 2.2$  %  $n = 5$ ), and the aboral gastroderm ( $10.3 \pm 3.3$  %  $n = 6$ ) (Mann–Whitney tests,  $p$  value  $< 0.0001$ ). The dinoflagellate symbionts displayed no statistically significant differences in BrdU incorporation rates compared to their host coral cells (oral gastroderm) (Signed Wilcoxon,  $p$  value = 0.584  $n = 4$ ).

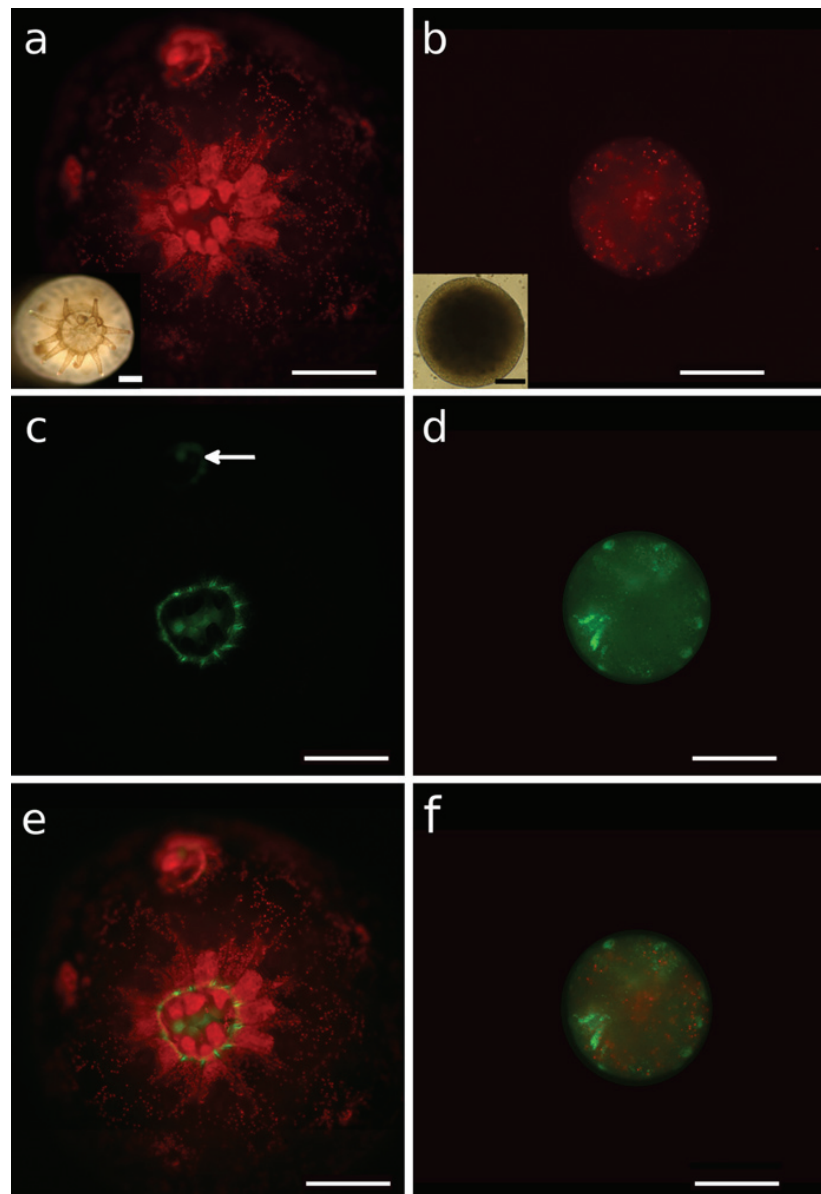
Compared to polyp coral cells, the DNA synthesis activity of coral cells in TBs was significantly reduced (Fig. 7a). The DNA synthesis activity of dinoflagellate

endosymbionts was also reduced in TBs compared to polyps, with rates of BrdU incorporation rates estimated at  $2.7 \pm 1.2$  % in vitro inside the central mass of TBs compared with  $14.0 \pm 3.4$  % in situ in the oral gastroderm of polyps (Fig. 7b). (The lower number of counted nuclei from dinoflagellates compared to coral cells was due to their lower relative abundance inside the TB central mass or the polyp, and to the lower number of semi-thin sections (1  $\mu$ m) passing through their nucleus.)

For polyps as well as for tissue balls, the important standard deviations noted for measured BrdU-labeling indexes were caused by the wide range of data distribution, due to high labeling variability between areas in the tissue depth. This large spatial variability indicates that the distribution of cells engaged in DNA synthesis is spatially highly heterogeneous, depending on their location in the polyp or the TB: within the same cell layer, cell proliferation rates vary locally.

In single dissociated cells, exposed to BrdU in parallel to tissue ball formation at the onset of primary

**Fig. 5** Compared auto-fluorescence of a live polyp and a tissue ball. Epifluorescence images of chlorophyll (*in red*), GFP-like molecules (*in green*) and their image overlay in a polyp of *P. damicornis* (**a**, **e**), and a tissue ball formed in primary cell culture (**b**, **d**, **f**), showing differences in the distribution of chlorophyll and GFP between the polyp and the TB. Scale bars 500  $\mu$ m



cultures, preliminary assessment of BrdU labeling of nuclei suggests that up to 20 % of the dinoflagellates had incorporated BrdU (14/70 total counted nuclei), but not the coral cells. The low number of counted nuclei (due to low cell yield of immunocytochemistry on suspended cells) will however require future confirmation of this preliminary observation.

#### Evolution of the cell specific density of dinoflagellate symbionts in primary cultures

The cell-specific density (CSD) of dinoflagellate endosymbionts was quantified in single dissociated gastrodermal cells (after the method of Muscatine et al. 1998) at the onset of primary cultures, over the

**Fig. 6** BrdU-labeled nuclei in polyp and in tissue ball formed in 2 days primary cell culture. Semi-thin ( $1\ \mu\text{m}$ ) sections stained with toluidine blue and basic fuchsin of **a** polyp and **b** TB. *Insets* are light micrographs indicating the orientation of the sections in respectively the *P. damicornis* polyp or the TB. Fluorescence of nuclei stained with DAPI (*in blue*) (**c**, **d**), immunolabeled with Alexa-594 (*in red*) (**e**, **f**) and their image overlay (**g**, **h**) in semi-thin sections of a polyp (**a**, **c**, **e**, **g**) and a tissue ball (**b**, **d**, **f**, **h**). *sk.* skeleton, *pse.* pseudo-stratified epithelium, *o.g.* oral gastroderm, *ab.g.* aboral gastroderm, *cal.* calicoderm, *g.c.* gastric cavity. *Scale bars*:  $100\ \mu\text{m}$

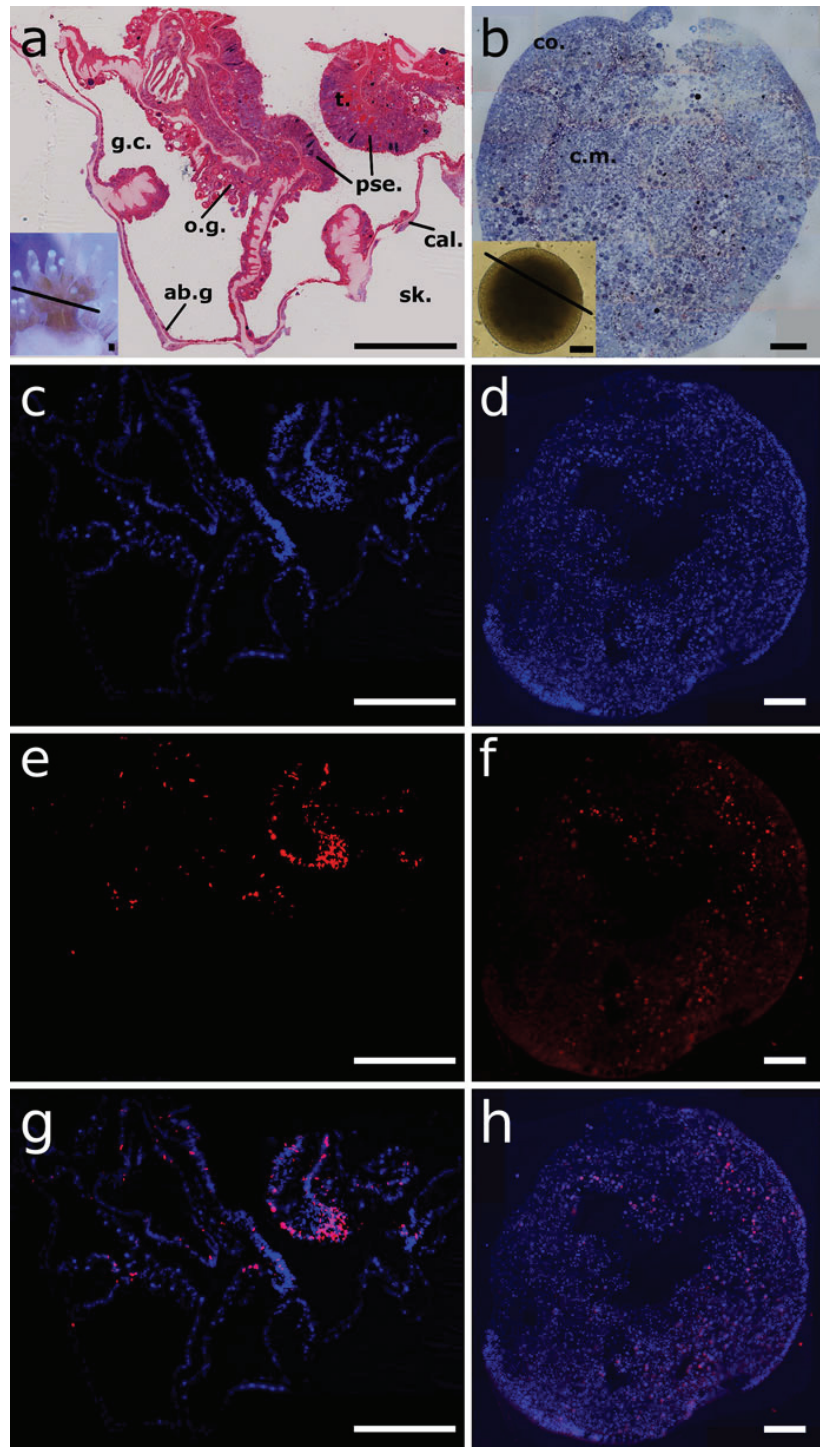


**Table 2** BrdU labeling index of nuclei of coral cells and dinoflagellate symbionts in the different tissue layers of the polyp and in vitro, during (2d) formation of the tissue balls

% BrdU-positive nuclei	Polyp				Tissue ball							
	Pseudo-stratified epithelium				Oral gastroderm		Calicoderm		Cortex		Central mass	
	Oral disk, coenosarc, tentacle	Tip of tentacle	Dinoflagellate endosymbionts	Coral cells	Aboral gastroderm	Aboral gastroderm	Coral cells	Dinoflagellate endosymbionts	Coral cells	Dinoflagellate endosymbionts	Coral cells	Dinoflagellate endosymbionts
Average	15.9 %	21.4 %	14.0 %	10.3 %	10.3 %	10.3 %	0.8 %	0.8 %	0.2 %	0.2 %	0.2 %	2.7 %
Standard error	4.2 %	5.6 %	3.4 %	2.2 %	3.3 %	3.3 %	0.4 %	0.4 %	0.1 %	0.1 %	0.1 %	1.2 %
Min-max	6.1–31.5 %	5.3–40.7 %	5–21 %	5.1–15.9 %	4.0–23.7 %	4.0–23.7 %	0–1.5 %	0–1.5 %	0–0.7 %	0–0.7 %	0–1.2 %	0–10 %
Standard deviation	10.3 %	13.6 %	6.8 %	4.9 %	8.2 %	8.2 %	0.9 %	0.9 %	0.3 %	0.3 %	0.4 %	3.4 %
Number of replicate tissue areas	6	6	4	5	6	6	6	6	8	8	8	8
Total counted nuclei	10,207	4,760	317	1,919	1,418	1,418	866	866	11,054	11,054	37,567	2,910

first 2 days from collagenase treatment. Data were averaged for three to five hundred gastrodermal (holobiont) cells counted per replicate well of a primary culture. No statistical difference was detected between the five independent collagenase experiments for each time point (Kruskal–Wallis test, *p* value >0.05 at *t* = 16, 20, 24 h; 40 and 45 h, *n* = 4–6), so data were pooled. Between time points there were statistically significant differences (Kruskal–Wallis test, *p* value <0.0001). The CSD at *t* = 0 h differed from the CSD at *t* = 16/20/24 h (Mann–Whitney test, *p* value = 0.001/0.010/0.043). Figure 8 illustrates the increase in average CSD during the first 20 h of primary culture, starting from 1.29 dinoflagellates per host cell at culture initiation and reaching 1.46 dinoflagellates per host cell at *t* = 16 h. After 40 h, the CSD returned to control level at beginning of culture.

**Discussion**

Cell dissociation methods are critical to the isolation of scleractinian coral cells and affect their in vitro survival and functionality. Enzyme digestion induces dissociation of individual cells and small cell clusters, which remain suspended or adhere to the culture substrate and may aggregate over time (Gates and Muscatine 1992; Frank et al. 1994; Helman et al. 2008; Downs et al. 2010). The mesoglea gel separating the two epithelial layers (epiderm and gastroderm) of cnidaria is an extracellular matrix (ECM) which, in *Hydra*, has been reported to contain collagen type IV (Fowler et al. 2000) associated to laminin in the subepithelial basal lamina and to fibrillar collagen type I (Shimizu et al. 2008; Sarras 2012). Collagenase is the most widely used enzyme for cnidarian tissue dissociation, with protocols first developed for hydrozoans, jellyfish and sea anemones, then adapted to the octocorals and stony corals (Gates and Muscatine 1992; Frank et al. 1994; Helman et al. 2008). Optimal reported concentrations of collagenase range from 0.05 to 0.15 % (dry weight/volume) with incubation times of 30 min to 4 h. However information on collagenase type and commercial brand is frequently missing from the literature. In this study, various collagenase-based cell dissociation methods were compared for their effects on cell yield and aggregation in primary culture. This study highlights

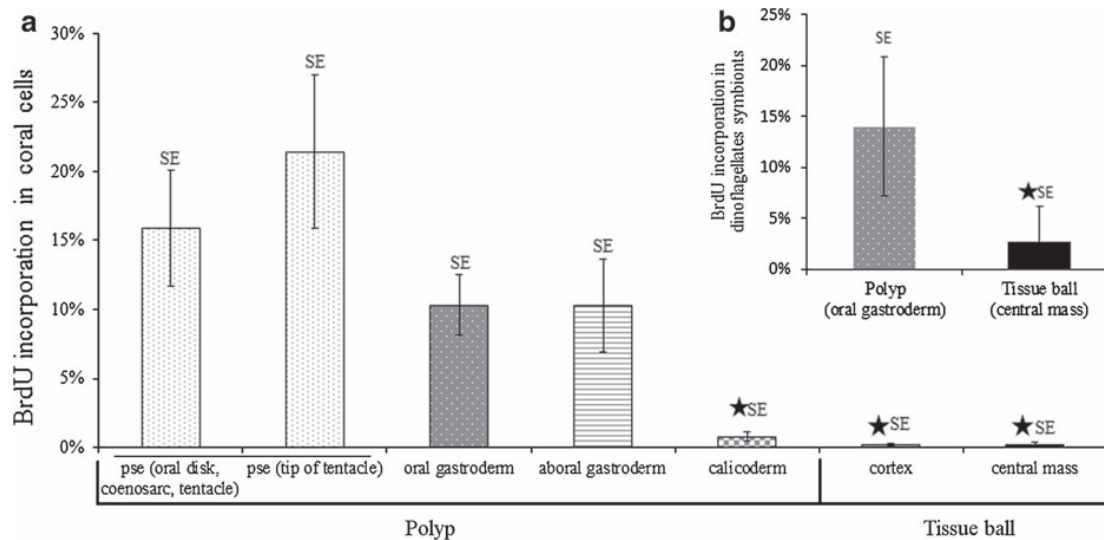


**Fig. 7** Compared BrdU incorporation rates of coral cells and dinoflagellates in polyps and in tissue balls obtained in 2 days primary culture. Data indicate mean  $\pm$  standard error (SE) for a coral cells in the different polyp tissue layers and the TB zones,

and **b** for dinoflagellates in the polyp oral gastroderm and in the TB (central mass). *pse* pseudo-stratified epithelium. *Black star* indicates significant difference between calicoderm and other tissue layers, and between TB and polyps

differences in the nature and yield of tissue versus single cell cultures obtained, depending on the collagenase type and commercial brand used. Aggregation of individual cells into suspended multicellular aggregates with a smooth surface (tissue balls) was optimized for *P. damicornis* after 15 min treatment with collagenase type IV (Sigma) adjusted to 5–15 collagen-degrading units (CDUs) per mg of wet tissue. These results confirm previous reports of the formation of adherent cell aggregates following collagenase (unspecified type) dissociation of tissue from the coral *Montipora digitata* (Helman et al. 2008). Compared to calcium removal treatment, after which dissociated cells failed to re-aggregate (Domart-Coulon et al. 2004a), this collagenase treatment preserves the coral cell adhesion capacities.

The timing of formation of suspended multicellular aggregates (tissue balls) in scleractinian coral primary cultures has been described (Kopecky and Ostrander 1999; Domart-Coulon et al. 2004a; Nesa and Hidaka 2009). Nevertheless mechanisms underlying formation of these structures are poorly understood, including potential involvement of in vitro proliferation. In this study, detailed morphological and ultrastructural observations of the forming cell aggregates highlight

their tissue-grade structure, with a cortex differentiated from the central mass by its cell type composition. Morphologically, these structures are similar to spheroids formed by wound healing of scleractinian soft tissue fragments manually peeled off the skeleton (Kramarsky-Winter and Loya 1996; Vizek et al. 2011), or to bailed out polyps (Sammarco 1982) after a few days incubation in seawater without attachment (data not shown).

Visualization of apical septate junctions between the interdigitated ciliated cells of the cortex indicates that this cell layer constitutes an epithelium, delimitating the surface of cell aggregates. A morphologically distinct underlying basal matrix was however not detected, in contrast to mesoglea observed in spheroids formed from *Fungia granulosa* tissue (Vizek et al. 2011), possibly reflecting species-specific differences in extra-cellular matrix abundance. Inside the cortex cells, abundance of mitochondria, electron-dense fibrillar material and Golgi apparatus are morphological indications of intense secretory activity. In a previous study, it was reported that the cells located at the surface of multicellular isolates formed from *P. damicornis* coral were immunoreactive to an antibody raised against the soluble organic matrix from the

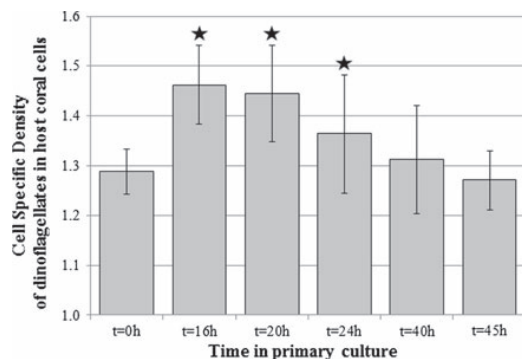


**Fig. 8** Cell Specific Density of dinoflagellate symbionts at initiation of coral primary cultures. For each time point, data were pooled from five independent experiments and are expressed as mean  $\pm$  standard deviation. A dark star indicates significant difference with control at  $t = 0$  h

skeleton of the related Pocilloporid coral *Stylophora pistillata* (Domart-Coulon et al. 2004b; Puverel et al. 2005). These cells might thus share features of calicoblast cell types.

Abundant autophagosomes in the central mass provide morphological evidence that autophagy events are involved in the formation of TBs. Combined with the spatially restricted distribution of cnidocytes and dinoflagellate endosymbionts to the center of tissue balls, these results suggest that cell sorting activities may exist, which could play a role during in vitro aggregation of scleractinian coral cells. Indeed, in the hydrozoan *Hydra* sp. homotypic interactions switching to heterotypic interactions have been reported during aggregation of epithelial cells (Hobmayer et al. 2001).

It was shown that a critical step for obtaining polyp regeneration from cultured spheroid explants is the development of a mouth, which can be induced by light and temperature cycling in seawater (Vizel et al. 2011). In the polyps of *P. damicornis*, we have observed that the oral disk was delimited by a concentrated ring of GFP-like molecules. According to D'Angelo et al. (2012), GFP-like proteins are concentrated in areas of growth and accelerated cell proliferation in several coral species (*Porites lobata*, *Montipora foliosa*, *Acropora pulchra/polystoma*) and could be used as a biomarker of locally accelerated growth and tissue regeneration. In the forming tissue balls of *P. damicornis*, we did not record any spatially differentiated pattern of distribution of GFP-like

molecules. Instead, cells containing GFPs were dispersed throughout the structure of the tissue balls, with a highly heterogeneous spatial distribution. These results indicate disorganization of tissue balls compared to polyps, with lack of an oral disk structure.

It is known that collagenase treatment of the extracellular matrix of cnidarian tissue may stimulate reprogramming and transdifferentiation of cell types, a process well described in the jellyfish (Scyphozoa) *Podocoryne carnea* (Schmid et al. 1999; Schmid and Reber-Müller 1995). In the jellyfish, collagenase treatment of isolated pieces of the umbrella triggers de-differentiation of striated muscle cells, followed by transdifferentiation to smooth muscle cells. In our case, collagenase may induce scleractinian coral tissue re-organization processes and the differentiation of cortex cells. Tissue re-organization may also be a common mechanism in scleractinian corals, triggered by several signals, after artificial or spontaneous detachment from skeleton.

Our results using BrdU labeling of nuclei show a very low level and high spatial heterogeneity of DNA synthesis activity inside the forming tissue balls, in our primary culture conditions. As DNA repair mechanisms in response to stress also involve limited DNA synthesis events before engagement in cellular apoptosis pathways, the BrdU labeling method cannot unambiguously detect cell proliferation activity in the coral primary cultures and should be complemented by other methods targeting proteins regulating progression through the cell cycle, to label cells engaged in mitosis. However, the low DNA synthesis rates measured for coral cells throughout the TB (about 0.2 %) indicate that the formation of these multicellular aggregates does not involve significant proliferation. Further analyses to investigate more precisely cell fate in longer-term cultures of tissue balls will be performed.

In situ labeling with BrdU of the polyps of *P. damicornis*, over a 24 h period in aquarium settings, revealed that DNA synthesis occurred in all four cellular layers composing the tissue, with a significantly lower rate in the calicoderm layer, which is involved in skeleton formation. No statistical differences of BrdU incorporation were found between the three other cell layers. The pseudostratified oral epithelium was highly labeled with  $15.9 \pm 4.2$  % BrdU-positive cells, reaching  $21.4 \pm 5.6$  % at tips of tentacles. Coral cells of the oral and aboral gastroderm

were characterized by respectively  $10.3 \pm 2.2 \%$  and  $10.3 \pm 3.3 \%$  BrdU incorporation rates. Our results are in agreement with the values reported for the BrdU labeling index of the gastroderm in polyps of *Montipora informis* and *Porites australiensis* healthy colonies (Yasuda and Hidaka 2012) but we report lower rates in the calicoderm and higher rates in the pseudostratified epithelium (oral epidermis). However this recent study used a longer exposure time to BrdU (3 days) than our study (24 h) and did not focus on differences between cell layers within an individual polyp. With long exposure periods, the distribution of BrdU positive cells is the result of combined cell division and migration, the cellular turnover masking potential differences in cell proliferation between cell layers (for example accumulation of BrdU positive cells may occur in regions of low turnover). The high variations of BrdU labeling index we observed from one area to the next within the same tissue layer of the same polyp suggest that there may be some highly proliferative clusters of cells inside each tissue layer. Additional experiments must be done to identify potential niche of stem cells and distinguish migration from division, with varying BrdU exposure times in pulse-chase labeling experiments.

Major differences in proliferation activity of the dinoflagellate endosymbionts were observed between in vitro and in situ conditions. Cell division of dinoflagellates was higher when located inside individually dissociated gastrodermal cells than when located inside the intact polyp or inside the tissue balls: the endosymbiont specific density (CSD) of gastrodermal cells peaked within the first day of individual cell culture and the proportion of dinoflagellate cells having incorporated BrdU seemed to increase from 14 % in intact polyp to 20 % in individually dissociated cells, whereas it dropped to 2.7 % inside the tissue balls. These combined BrdU labeling and CSD data suggest that tissue dissociation into individual gastrodermal cells induces an increase in dinoflagellate proliferation. Tissue dissociation is likely to disrupt the controls exerted by the coral host cell on its dinoflagellate symbiont proliferation, explaining the rapid and transient rise of CSDs. Restrictions of the intracellular availability of nitrogenous nutrients needed to undertake dinoflagellate cell cytokinesis is one of the processes which maintain dinoflagellates in a growth-limited state (Wooldridge

2010). In single dissociated cell cultures, the dissolved amino-acids contained in the complex cell culture medium are likely to be rapidly assimilated by the dinoflagellates (Grover et al. 2008), fueling their cell growth and division. The expulsion or degradation of dinoflagellates by the host cell after the peak of CSD could explain the return to initial CSD. Alternately, the coral host cell may die after the peak of CSD, releasing dividing dinoflagellates into the culture medium.

In this study, a nutrient-rich culture medium (containing (v:v) 12.5 % commercial DMEM) was used to establish primary coral cell cultures, under air and 10/14 h light/dark cycle, with very low white light intensity (2–4 photosynthetic photon flux density micromoles  $\text{m}^{-2} \text{s}^{-1}$ ). These conditions differ from the natural conditions for growth of the polyps and may contribute to limit the in vitro cellular DNA synthesis rate. Tissue-grade cell aggregates can also be obtained in seawater (Vizel et al. 2011; Nesa and Hidaka 2009), and they survive longest at low light intensity and constant low temperature as reported for the spheroid tissue from *Fungia granulosa* (Vizel et al. 2011). Nutrients and light intensity can have an impact on the survivorship of multicellular isolates from some coral species (e.g. *Acropora microphthalmia*) and not from others (e.g. *P. damicornis*) (Kopecky and Ostrander 1999). These observations confirm that cell culture conditions have to be adjusted between species, since optimal light- and temperature-range differ between scleractinian coral species.

Understanding processes leading to in vitro coral growth arrest and cellular senescence remains an exciting challenge (Rinkevich 2011). To date, most coral primary cultures are established from differentiated tissue from scleractinian adult colonies. In order to improve in vitro cell proliferation, it would be useful to differentiate more finely which area in the adult tissue layer has the highest proliferation potential, and attempt cultures from selected micro-dissected tissue fragments. Alternately, cultures could be established from highly proliferative larval tissue, as attempted on embryonic cells from *Acropora millepora* (Reyes-Bermudez et al. 2009) or hyperplastic tissue from growth anomalies (so-called ‘tumors’) for example of *Porites compressa* (Domart-Coulon et al. 2006), and *Porites australiensis* or *Montipora informis* (Yasuda and Hidaka 2012).



## Conclusion

In this study, spatial differences in DNA synthesis activity were detected in the different cell layers of scleractinian coral polyps with the BrdU labeling method (24 h exposure), with significantly lower proliferation in the calicoderm at the surface of skeleton compared to the pseudostratified epithelium facing seawater and the gastroderm lining the digestive cavity. BrdU incorporation rates evaluated during the process of formation of suspended multicellular aggregates in primary cultures initiated with collagenase were found to be very low, in both coral and dinoflagellate cells, indicating that cell aggregation does not imply simultaneous proliferation. Dissociation of the tissue into single cells was followed by a transient rise in the cell specific density of dinoflagellate symbionts of isolated gastrodermal cells. These results suggest that mechanisms controlling proliferation of coral cells and their dinoflagellate endosymbionts are disrupted by current in vitro primary culture conditions.

**Acknowledgments** This work was supported by the ATM Biomineralization of the Museum National d'Histoire Naturelle ('scleractinian coral' project) to I. Domart-Coulon, and by European Research Council Advanced Grant 246749 (BIOCARB) to A. Meibom. It was presented at the Symposium on 'Marine Invertebrate Cell Cultures', August 30–31 2012, at the Station de Biologie Marine du MNHN in Concarneau, France. We especially thank Michel Hignette and all the team from the Aquarium Tropical, Palais de la Porte Dorée, Paris, France, for access to biological material and facilities for aquarium experiments.

## References

- D'Angelo C, Smith EG, Oswald F, Burt J, Tchernov D, Wiedenmann J (2012) Locally accelerated growth is part of the innate immune response and repair mechanisms in reef-building corals as detected by green fluorescent protein (GFP)-like pigments. *Coral Reefs* 31(4):1045–1056
- Denker E, Manuel M, Leclère L, Le Guyader H, Rabet N (2008) Ordered progression of nematogenesis from stem cells through differentiation stages in the tentacle bulb of *Clytia hemisphaerica* (Hydrozoa, Cnidaria). *Dev Biol* 315:99–113
- Dolbear F, Selden JR (1994) Immunochemical quantitation of bromodeoxyuridine: application to cell-cycle kinetics. *Methods Cell Biol* 41:297–316
- Domart-Coulon IJ, Elbert DC, Scully EP, Calimlim PS, Ostrander GK (2001) Aragonite crystallization in primary cell cultures of multicellular isolates from a hard coral, *Pocillopora damicornis*. *Proc Natl Acad Sci USA* 98: 11885–11890
- Domart-Coulon IJ, Sinclair CS, Hill RT, Tambutte S, Puverel S, Ostrander GK (2004a) A basidiomycete isolated from the skeleton of *Pocillopora damicornis* (Scleractinia) selectively stimulates short-term survival of coral skeletogenic cells. *Mar Biol* 144:583–592
- Domart-Coulon I, Tambutte S, Tambutte E, Allemand D (2004b) Short term viability of soft tissue detached from the skeleton of reef-building corals. *J Exp Mar Biol Ecol* 309:199–217
- Domart-Coulon IJ, Traylor-Knowles N, Peters E, Elbert D, Downs CA, Price K, Stubbs J, McLaughlin S, Cox E, Aeby G, Brown PR, Ostrander GK (2006) Comprehensive characterization of skeletal tissue growth anomalies of the finger coral *Porites compressa*. *Coral Reefs* 25:531–543
- Downs CA, Fauth JE, Downs VD, Ostrander GK (2010) In vitro cell-toxicity screening as an alternative animal model for coral toxicology: effects of heat stress, sulfide, rotenone, cyanide, and cuprous oxide on cell viability and mitochondrial function. *Ecotoxicology* 19:171–184
- Fowler SJ, Jose S, Zhang X, Deutzmann R, Sarras MP Jr, Boot-Handford RP (2000) Characterization of *hydra* type IV collagen. Type IV collagen is essential for head regeneration and its expression is up-regulated upon exposure to glucose. *J Biol Chem* 275:39589–39599
- Frank U, Rabinowitz C, Rinkevich B (1994) In vitro establishment of continuous cell cultures and cell lines from 10 colonial cnidarians. *Mar Biol* 120:491–499
- Gates RD, Muscatine L (1992) 3 Methods for isolating viable anthozoan endoderm cells with their intracellular symbiotic dinoflagellates. *Coral Reefs* 11:143–145
- Grover R, Maguer JF, Allemand D, Ferrier-Pages C (2008) Uptake of dissolved free amino acids by the scleractinian coral *Stylophora pistillata*. *J Exp Biol* 211:860–865
- Helman Y, Natale F, Sherrell RM, LaVigne M, Starovoytov V, Gorbunov MY, Falkowski PG (2008) Extracellular matrix production and calcium carbonate precipitation by coral cells in vitro. *Proc Natl Acad Sci USA* 105:54–58
- Hobmayer B, Snyder P, Alt D, Happel CM, Holstein TW (2001) Quantitative analysis of epithelial cell aggregation in the simple metazoan *Hydra* reveals a switch from homotypic to heterotypic cell interactions. *Cell Tissue Res* 304:147–157
- Khalesi MK, Vera-Jimenez NI, Aanen DK, Beertink HH, Wijffels RH (2008) Cell cultures from the symbiotic soft coral *Simularia flexibilis*. *In Vitro Cell Dev Biol Anim* 44: 330–338
- Kopecky EJ, Ostrander GK (1999) Isolation and primary culture of viable multicellular endothelial isolates from hard corals. *In Vitro Cell Dev Biol Anim* 35:616–624
- Kramarsky-Winter E, Loya Y (1996) Regeneration versus budding in fungiid corals: a trade-off. *Mar Ecol-Prog Ser* 134:179–185
- Mass T, Drake JL, Haramaty L, Rosenthal Y, Schofield OM, Sherrell RM, Falkowski PG (2012) Aragonite precipitation by “proto-polyps” in coral cell cultures. *PLoS ONE* 7: e35049
- Müller WA, Teo R, Frank U (2004) Totipotent migratory stem cells in a hydroid. *Dev Biol* 275:215–224
- Muscatine L, Ferrier-Pages C, Blackburn A, Gates RD, Baghdasarian G, Allemand D (1998) Cell specific density of symbiotic dinoflagellates in tropical anthozoans. *Coral Reefs* 17(4):329–337

- Nesa B, Hidaka M (2009) High zooxanthella density shortens the survival time of coral cell aggregates under thermal stress. *J Exp Mar Biol Ecol* 368:81–87
- Peng SE, Luo YJ, Huang HJ, Lee IT, Hou LS, Chen WNU, Fang LS, Chen CS (2008) Isolation of tissue layers in hermatypic corals by *N*-acetylcysteine: morphological and proteomic examinations. *Coral Reefs* 27:133–142
- Puverel S, Tambutte E, Zoccola D, Domart-Coulon I, Bouchot A, Lotto S, Allemand D, Tambutte S (2005) Antibodies against the organic matrix in scleractinians: a new tool to study coral biomineralization. *Coral Reefs* 24:149–156
- Reyes-Bermudez A, Lin Z, Hayward DC, Miller DJ, Ball EE (2009) Differential expression of three galaxin-related genes during settlement and metamorphosis in the scleractinian coral *Acropora millepora*. *BMC Evol Biol* 9:178
- Rinkevich B (1999) Cell cultures from marine invertebrates: obstacles, new approaches and recent improvements. *J Biotechnol* 70:133–153
- Rinkevich B (2005) Marine invertebrate cell cultures: new millennium trends. *Mar Biotechnol (NY)* 7:429–439
- Rinkevich B (2011) Cell cultures from marine invertebrates: new insights for capturing endless stemness. *Mar Biotechnol (NY)* 13:345–354
- Sammarco PW (1982) Polyp bail-out—an escape response to environmental stress and a new means of reproduction in corals. *Mar Ecol Prog Ser* 10:57–65
- Santos SR, Toyoshima J, Kinzie RA III (2009) Spatial and temporal dynamics of symbiotic dinoflagellates (*Symbiodinium*: dinophyta) in the perforate coral *Montipora capitata*. *Galaxea. J Coral Reef Stud* 11:139–147
- Sarras MP (2012) Components, structure, biogenesis and function of the *Hydra* extracellular matrix in regeneration, pattern formation and cell differentiation. *Int J Dev Biol* 56:567–576
- Schmid V, Reber-Muller S (1995) Transdifferentiation of isolated striated muscle of jellyfish in vitro: the initiation process. *Semin Cell Biol* 6:109–116
- Schmid V, Ono SI, Reber-Muller S (1999) Cell-substrate interactions in cnidaria. *Microsc Res Tech* 44:254–268
- Shimizu H, Aufschnaiter R, Lib L, Sarras MP, Borza D-B, Abrahamson DR, Sadof Y, Zhang X (2008) The extracellular matrix of *Hydra* is a porous sheet and contains type IV collagen. *Zoology (Jena)* 111:410–418
- Taupin P (2007) BrdU immunohistochemistry for studying adult neurogenesis: paradigms, pitfalls, limitations, and validation. *Brain Res Rev* 53:198–214
- Vizel M, Loya Y, Downs CA, Kramarsky-Winter E (2011) A novel method for coral explant culture and micropropagation. *Mar Biotechnol (NY)* 13:423–432
- Wooldridge SA (2010) Is the coral-algae symbiosis really ‘mutually beneficial’ for the partners? *BioEssays* 32: 615–625
- Yasuda N, Hidaka M (2012) Cellular kinetics in growth anomalies of the scleractinian corals *Porites australiensis* and *Montipora informis*. *Dis Aquat Organ* 102:1–11

### III. Conclusion

Tissue explants obtained from *P. damicornis* branch apices require 3 days after cell dissociation to re-aggregate and/or round up. They are able to fuse together forming a round rotating tissue explant covered by a smooth ciliated surface, called tissue ball (TB). Cell proliferation was assessed during the first 24 h of TB formation using 5'-bromo-2'-deoxyuridine (BrdU) incorporation and data were compared between forming explants and the adult polyp. Main result is that TB formation does not require significant cell division. This lack of proliferation while the soft tissue detaches from the skeleton and rounds up into a sphere is similar to what was observed in *Hydra* head regeneration in which cell proliferation decrease during the first 24 h, also regeneration can occurs without cell proliferation (Cummings and Bode, 1984; Holstein et al., 1991). Investigation of cell proliferation in TB older than 24 h would provide information about cell division dynamics over longer periods of time *in vitro*.



# Chapter 2: Cell proliferation hot spots and cell migration during primary polyp morphogenesis

## I. Context

Metamorphosis is a critical step of coral life cycle during which the calicodermis cell layer, involved in skeleton formation, is established. Cellular mechanisms that support this step are not known. In the previous chapter heterogeneity of cell division pattern in the adult polyp of *P. damicornis* was revealed in close circuit aquarium conditions. Here we assessed cell division pattern of *S. pistillata* during metamorphosis using the same BrdU method in reef condition. Furthermore a chase experiment of BrdU signal was done at primary polyp stage to study cell migration.

PhD student's contribution: The PhD student designed the experiment with I. Domart-Coulon and A. Meibom, carried out the experiments and statistically analyzed the data with A. Paris. All authors contributed to drafting and editing the manuscript.

## II. Publication



## PROCEEDINGS B

[rspsb.royalsocietypublishing.org](http://rspsb.royalsocietypublishing.org)

### Research



**Cite this article:** Lecointe A, Domart-Coulon I, Paris A, Meibom A. 2016 Cell proliferation and migration during early development of a symbiotic scleractinian coral. *Proc. R. Soc. B* **283**: 20160206.

<http://dx.doi.org/10.1098/rspb.2016.0206>

Received: 29 January 2016

Accepted: 22 April 2016

#### Subject Areas:

cellular biology, developmental biology, environmental science

#### Keywords:

cell proliferation, BrdU, apoptosis, dinoflagellates, metamorphosis, scleractinia

#### Author for correspondence:

Isabelle Domart-Coulon

e-mail: [icoulon@mnhn.fr](mailto:icoulon@mnhn.fr)

Electronic supplementary material is available at <http://dx.doi.org/10.1098/rspb.2016.0206> or via <http://rspsb.royalsocietypublishing.org>.

THE ROYAL SOCIETY  
PUBLISHING

# Cell proliferation and migration during early development of a symbiotic scleractinian coral

Agathe Lecointe<sup>1,2</sup>, Isabelle Domart-Coulon<sup>2</sup>, Alain Paris<sup>2</sup>  
and Anders Meibom<sup>1,3</sup>

<sup>1</sup>Laboratory for Biological Geochemistry, School of Architecture, Civil and Environmental Engineering, École Polytechnique Fédérale de Lausanne (EPFL), Lausanne, Switzerland

<sup>2</sup>Unité MCAM UMR7245, Sorbonne Universités, Museum National d'Histoire Naturelle (MNHN), CNRS, Paris, France

<sup>3</sup>Center for Advanced Surface Analysis, Institute of Earth Sciences, University of Lausanne, Lausanne, Switzerland

In scleractinian reef-building corals, patterns of cell self-renewal, migration and death remain virtually unknown, limiting our understanding of cellular mechanisms underlying initiation of calcification, and ontogenesis of the endosymbiotic dinoflagellate relationship. In this study, we pulse-labelled the coral *Stylophora pistillata* for 24 h with BrdU at four life stages (planula, early metamorphosis, primary polyp and adult colony) to investigate coral and endosymbiont cell proliferation during development, while simultaneously recording TUNEL-positive (i.e. apoptotic) nuclei. In the primary polyp, the fate of BrdU-labelled cells was tracked during a 3-day chase. The pharynx and gastrodermis were identified as the most proliferative tissues in the developing polyp, and BrdU-labelled cells accumulated in the surface pseudostratified epithelium and the skeletogenic calicodermis during the chase, revealing cell migration to these epithelia. Surprisingly, the lowest cell turnover was recorded in the calicodermis at all stages, despite active, ongoing skeletal deposition. In dinoflagellate symbionts, DNA synthesis was systematically higher than coral host gastrodermis, especially in planula and early metamorphosis. The symbiont to host cell ratio remained constant, however, indicating successive post-mitotic control mechanisms by the host of its dinoflagellate density in early life stages, increasingly shifting to apoptosis in the growing primary polyp.

## 1. Introduction

Scleractinian corals are evolutionary ancient marine animals that build large reef structures in (sub-)tropical coastal waters, providing habitats for extremely diverse marine ecosystems [1]. The reefs are constructed through accumulation of aragonitic exoskeleton produced by the polyps, which are the fundamental physiological unit of scleractinian corals. The polyps host endosymbiotic photosynthetic dinoflagellates that strongly boost skeletal production [2]. However, the cellular processes initiating and driving skeletogenesis and controlling the density of *Symbiodinium* sp. endosymbionts remain obscure in both adult colonies and early life stages, which are critical to coral recruitment and reef survival. Studies on tissue homeostasis in scleractinians have mostly focused on the vulnerability of adults and their dinoflagellates to environmental stress, which can lead to symbiont loss and tissue bleaching (reviewed in [2] and [3]). Processes of cellular turnover, which include cell proliferation, migration and death, have hardly been investigated, and sparse existing work has focused on adult corals. Indeed, it was shown that colonies undergo apoptotic death in response to increased temperature and reduced pH [4,5], or changes in proliferation during disease and lesion repair [6,7]. Baseline levels of coral and dinoflagellate cell proliferation were recently experimentally determined at tissue scale in polyps from adult *Pocillopora damicornis* coral colonies, pulse-labelled for 24 h with BrdU [8].

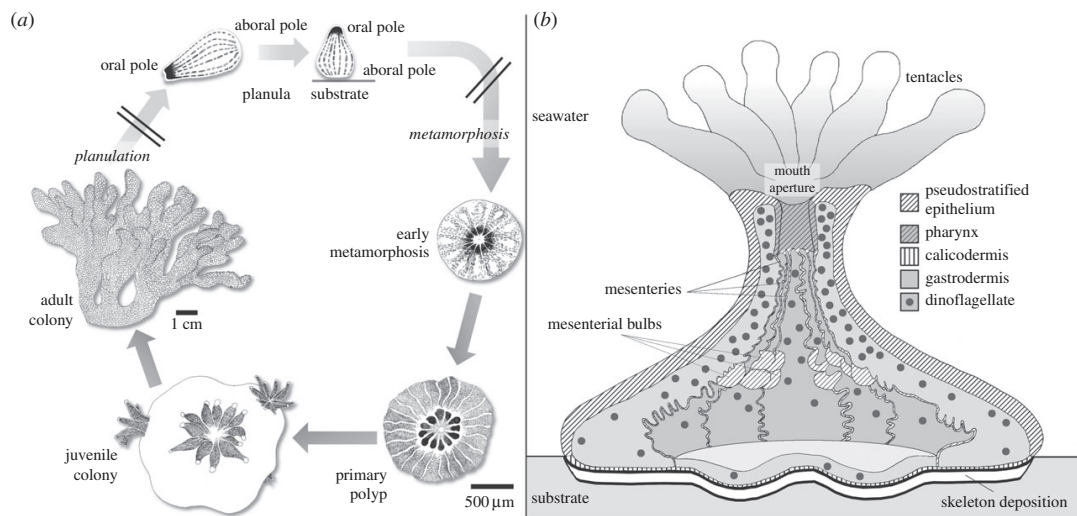


**Figure 1.** Tissue organization during *Stylophora pistillata* metamorphosis. (a) Coral cycle of development. The planula probes the substrate with its oral pole and, upon reception of suitable cues, flips over and flattens into a disc with its aboral pole pressed against the substrate, characteristic of the ‘early metamorphosis’ stage. Complete metamorphosis leads to the primary polyp stage, with tentacles budding around the mouth aperture, lateral spreading of the tissue and vertical extension of the body column. (b) Tissue structures in the primary polyp. Oral tissue, facing the seawater, is composed of a relatively thick bilayer of pseudostratified epithelium (pse, also called epidermis), with oral gastrodermis lining the gastric cavity. The mouth in the centre of the oral disc is connected to a ring of upward growing tentacles, while the pharynx grows inward and connects with radial mesenteries. Aboral tissue, facing the skeleton, is composed of a thin bilayer of calicodermis (skeletal tissue) and aboral gastrodermis. Dinoflagellate symbionts are hosted in the gastrodermal cells. Epithelial bilayers are separated by mesogleal gel.

However, early life stages offer the unique opportunity to investigate the ontogeny of morphogenetic processes in each specialized coral tissue, particularly with respect to the skeleton-forming calicodermis, and the host regulation of its *Symbiodinium* endosymbiont density.

The life cycle of a colonial reef-building scleractinian coral is illustrated in figure 1a, for species with internal fertilization, such as *Stylophora pistillata* (Esper, 1797), which releases swimming planktonic planula larvae from the brooding colony [9]. Metamorphosis-induced morphogenetic tissue changes enable the coral to rapidly initiate skeletal deposition [10,11]. Within 2–4 days, the primary polyp is fully functional and continues to grow vertically and horizontally (illustrated in figure 1b). Within 6–12 days, secondary polyps start to bud at the periphery of the primary polyp, forming a juvenile colony.

In this study, we evaluated cell turnover, by which we mean proliferation, migration and death (by apoptosis), in each forming epithelium during planula larval metamorphosis into primary polyp, permitting us to (i) identify reservoirs of high proliferation activity, (ii) infer cell migration patterns and (iii) quantitatively investigate the ontogeny of coral host control over its dinoflagellate symbiont density.

## 2. Material and methods

### (a) Biological material

Planula larvae of *S. pistillata* were collected at approximately 5 m depth in May 2013 from 7 to 11 parent colonies (greater than 30 cm width), on the reef of the Inter-University Institute for Marine Sciences, 5 km south the Coral Nature Reserve of Eilat, Israel, under permit number 2011/38182. Shallow-water (2–6 m) *S. pistillata* from the Gulf of Eilat contain clade A *Symbiodinium* sp., both at planula and adult colony stages [12]. Actively swimming planulae were distributed in batches of 10 larvae in 10 ml

seawater in plastic dishes (lumox Sarstedt, or classic Petri dishes, 5 cm diameter), fitted with underwater paper that had been exposed for 5 days to natural seawater to initiate biofilm formation. Dishes were incubated in shaded outdoor running seawater tables, at 23–25°C, with seawater renewal every 6 h. Inorganic nutrient concentrations at the seawater surface and 20 m depth, obtained for the week of the experiments from the Israel National Monitoring Program at the Gulf of Eilat (<http://www.iui-eilat.ac.il/Research/NMPmeteodata.aspx>), were 0.014–0.018 μM NH<sub>4</sub>, 0.007–0.011 μM NO<sub>2</sub>, 0.04–0.36 μM NO<sub>3</sub> and 0.023 μM PO<sub>4</sub>, corresponding to an oligotrophic environment. Salinity was 40.7‰, pH 8.17 and oxygen 218.5–219.9 μM. Ambient daylight intensity of approximately 500 μEinstein m<sup>-2</sup> s<sup>-1</sup> was measured at the water surface at midday with a LI-CORE 1000 Data Logger radiometer, corresponding to attenuation of direct sunlight by a factor three. Asynchronous larval metamorphosis and polyp development were monitored under the binocular microscope (5×) during 6 days. Replicates of each of three different early life stages, identified by their morphogenetic features, were collected: planula, early metamorphosis and primary polyp (figure 1a). Small colonies (less than 1 cm width and 0.5 cm tall), spontaneously settled in the outdoor seawater tables about two months earlier from another batch of *S. pistillata* planulae, were used as control adult life stage.

### (b) BrdU pulse-chase labelling to detect DNA synthesis and cell turnover

Cell proliferation during larval metamorphosis and primary polyp development was assessed using the BrdU (5-bromo-2'-deoxyuridine) labelling method, slightly modified from [8,13]. Larvae or recruits were incubated for 24 h at selected developmental stages in seawater containing 50 μM BrdU (Roche), renewed every 6 h. Corresponding unlabelled controls were incubated in normal seawater without BrdU. At the end of the 24 h pulse, three to five individual replicates and their corresponding controls were sampled for each life stage. Among the primary



polyps pulse-labelled with BrdU for 24 h, a few individuals were allowed to further grow in running seawater for a chase period of 48 h (two replicates; the third was lost) or 64 h (three replicates).

### (c) Serial tissue sectioning

At the end of the BrdU pulse or the chase, samples were fixed overnight at 4°C and prepared for serial sectioning following procedures detailed by Lecointe *et al.* [8]. Unicryl (EMS)-embedded samples were cut into semi-thin sections (1 µm thick) with a 35° diamond knife (Diatome) on an Ultracut microtome, at the MNHN PtME platform of electron microscopy (Paris). Serial sets of sections, obtained at three separate depths in each replicate, were used for (i) histological staining with toluidine blue-basic fuchsin (EMS) for identification and orientation in the larval/polyp structure, (ii) BrdU immunolocalization and (iii) apoptosis detection by terminal transferase-mediated dUTP nick end labelling (TUNEL) assay.

### (d) Immunolocalization of BrdU-labelled nuclei

The BrdU-labelling index measures the proportion of cell nuclei having incorporated BrdU in their newly synthesized DNA during the 24 h pulse. BrdU was immunodetected in tissue sections with primary anti-BrdU mouse antibody (Roche) and Alexa-594-labelled secondary goat anti-mouse antibody (Invitrogen), and nuclei were counterstained with DAPI (Invitrogen), following [8]. Sections were observed on a wide-field fluorescence microscope (Olympus XM10 slide scanner) at the EPFL PT-BIOP platform (Lausanne) using DAPI (Ex 377/50 nm, Em 440/40 nm), and CY3 filters (Ex 560/25 nm, Em 607/36 nm) at spatial lateral resolution of approximately 0.5 µm. A total of four to eight sections were imaged for each of three to five biological replicates per life stage, and analysed with IMAGEJ software (v. 1.49) using the cell counter plug-in to manually count BrdU-labelled nuclei among DAPI-counterstained total nuclei (for method, see electronic supplementary material, figure S1). Labelled nuclei were not detected in control tissue unexposed to BrdU (one negative control examined per life stage). Totals of 345–64 810 nuclei were counted per tissue type (depending on section orientation).

Dilution of BrdU labelling intensity was quantified during the 3 days chase in seawater. Dilution is caused by *de novo* synthesis of unlabelled DNA, through entry of cycling cells into S phase and division. An intensity drop by a factor of two can thus be attributed to one cell division. During the chase experiment, the fluorescent signal intensity of labelled nuclei was measured for BrdU and DAPI, background was subtracted and the CY3/DAPI signal intensity ratios were compared ( $n = 30$ –60 nuclei per tissue type, per chase time-point).

### (e) TUNEL assay for detection of apoptotic cell nuclei

Apoptosis was evaluated in the same biological samples previously analysed for BrdU labelling, using serial sections at similar depths in the tissue. Control samples not exposed to BrdU were also assessed for apoptosis (one control per life stage). Apoptosis is characterized by formation of DNA breaks (nick), and the TUNEL reaction uses the enzyme terminal deoxynucleotidyl transferase (TdT) to fill these gaps with fluorescein (FITC)-labelled dUTP. The TUNEL assay was performed for 1 h at 37°C according to kit instructions (*in situ* cell death detection—fluorescein, Roche). For negative controls, TdT enzyme was omitted from the reactive solution. For positive controls, sections were pre-incubated with recombinant DNase I (3 U ml<sup>-1</sup>, Ambion) for 10 min at room temperature. Treated sections were mounted with Prolong Gold Antifade reagent with DAPI (Invitrogen) and observed on a wide-field fluorescence microscope (Olympus XM10 slide scanner,

PT-BIOP, EPFL), using DAPI (Ex 377/50 nm, Em 440/40 nm) and FITC filters (Ex 485/20 nm, Em 525/30 nm), at spatial lateral resolution of approximately 0.3 µm. The proportion of TUNEL-positive cell nuclei was calculated from acquired images, using the counter cell plugin from IMAGEJ software. For each life stage, three biological replicates were assessed, with one to four sections imaged per replicate, and totals of 657 to 8219 nuclei counted per tissue type (depending on section orientation).

### (f) Mitotic index and abundance of dinoflagellates

For the endosymbiotic dinoflagellates, the mitotic index was calculated as the ratio of the number of dinoflagellate doublets (undergoing cytokinesis) to single dinoflagellate cells [14], in toluidine blue-stained sections of three replicates for each life stage (two to eight sections per replicate and 1200–2000 dinoflagellates counted per life stage). Results are presented as the mean  $\pm$  1 s.d. of doublet-to-single dinoflagellate ratio, for three biological replicates per life stage.

Dinoflagellate abundance (i.e. the number of symbiont nuclei relative to coral cell nuclei within the gastrodermal host tissue) was calculated using DAPI-stained nuclei counts previously obtained for assessment of the BrdU-labelling index (electronic supplementary material, table S1). Results are presented as mean  $\pm$  1 s.d. for three to five biological replicates per life stage.

### (g) Statistical analyses

Fluorescence images, acquired from BrdU and TUNEL assays in semi-thin sections at three different depths in each replicate sample, allow visualization of labelled or unlabelled nuclei according to tissue type. The data follow a binomial distribution with uneven variance and were statistically analysed using the generalized linear model (GLM) using the binomial family and logit link function in R software v. 3.2.0. Significance was assessed at  $\alpha = 0.05$  threshold *p*-value. Quantitative data for BrdU and TUNEL labelling are presented as boxplots, also reporting the means (as a cross) and outliers (detected outside the 1.5  $\times$  inter-quartile range). The CY3/DAPI signal intensity ratio does not follow a normal distribution, as cells are not synchronous and the quantity of BrdU incorporated into the DNA is time-dependent (during the 24 h pulse, a cell ending the S-phase will incorporate less BrdU than a cell that is just starting DNA replication). Therefore, non-parametric Kruskal–Wallis tests were used, followed by pairwise Wilcoxon's test when significant. For dinoflagellate mitotic index and abundance, the normality of residues and homoscedasticity of data allowed application of one-way ANOVA followed by Tukey HSD tests.

## 3. Results

### (a) Tissue organization and remodelling during metamorphosis

Major changes in tissue structure occur during coral lifestyle transition from swimming planula to sessile polyp, illustrated in figure 2 for four life stages: planula larva, early metamorphosis, primary polyp and adult polyp. The larval single bilayer of epithelia—pseudostratified epithelium (pse) and lipid-filled gastrodermis (g)—transforms into the polyp double bilayer of epithelia. Specialized areas connected to the surface pse develop from the larval oral and aboral poles during metamorphosis. The skeletogenic calicodermis (cal) differentiates in the basal floor at the interface with the

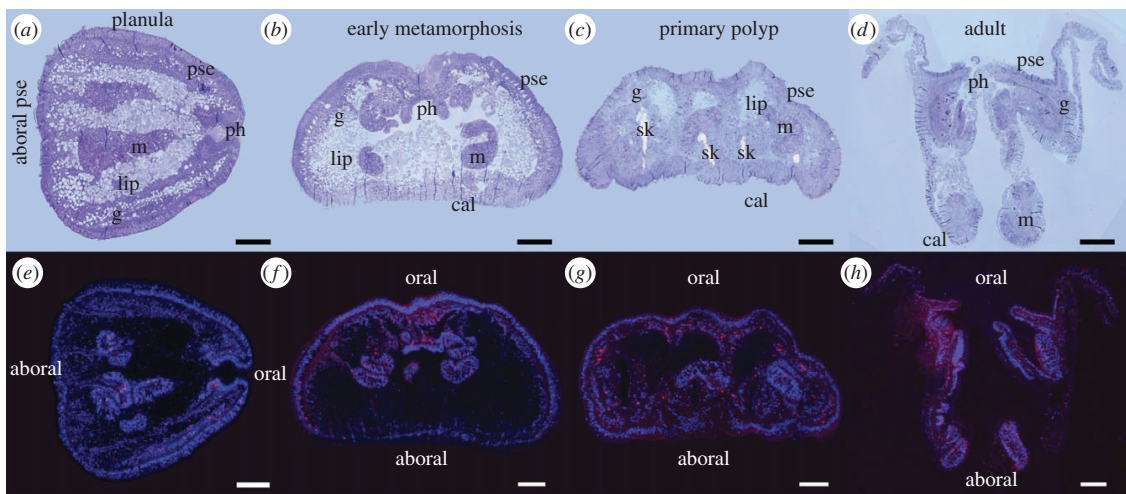


**Figure 2.** Distribution of BrdU-labelled nuclei in coral tissue from planula to adult polyp. (a–d) Toluidine blue-stained (1  $\mu\text{m}$ ) tissue sections. (e–h) BrdU-positive nuclei immunodetected with Alexa-594 fluorochrome (red) among nuclei counterstained with DAPI (blue). Scale bars, 100  $\mu\text{m}$ ; pse, pseudostratified epithelium; ph, pharynx; g, gastrodermis; m, mesentery; cal, calcicodermis; lip, lipids; sk, skeleton.

substrate, and the pharynx (ph) forms by inward invagination of the pse, just below the oral disc. Tentacles grow upward from the oral disc (figure 1*b*; electronic supplementary material, figure S1; not visible in figure 2 in the sections selected), but were not studied here because they retracted upon fixation, and thus were hard to distinguish from inner mesenterial bulbs (or cnidoglandular bands [15]), which were therefore also not included in this study (figure 1*b*).

The inner gastrodermis, lining the digestive cavity, forms a continuous epithelium from oral to aboral pole in the larva, and connects the oral disc with the basal floor in the polyp (figures 1*b* and 2*a–d*). The gastrodermis contains intracellular symbiotic dinoflagellates, which are more abundant in oral compared with aboral areas (figure 1*b*). Mesenteries, already present in this species at the planula stage, are radial inward-growing tissue folds attached below the pharynx and composed of gastrodermis and a thin layer of pse, forming radial partitions of the gastric cavity. In the polyp, these mesenteries connect the pharynx to the edges of the basal floor (figure 1*b* and figure 2*a–d*).

### (b) Coral cell proliferation and apoptosis

The spatial distribution of dividing cells, in the S phase of DNA synthesis (and thus labelled with BrdU during the 24 h pulse), is illustrated for each tissue structure and developmental stage in figure 2*e–h*, and electronic supplementary material, figure S1*b–e*, where BrdU is immunodetected (in red) among the DAPI-counterstained nuclei (in blue). Labelled nuclei were not detected in control tissue unexposed to BrdU (data not shown). Cell proliferation was found to be spatially and temporally highly heterogeneous, with scattered distribution of BrdU-positive nuclei, at densities depending on cell type and coral life stage.

The proportion of BrdU-positive nuclei is summarized for each tissue and developmental stage (figure 3*a–d*), along with the proportion of apoptotic nuclei, positive for the TUNEL enzymatic assay (figure 3*e–h*). Data are presented for the pharynx, pse and calcicodermis, which share a

common ectodermal origin, and for the gastrodermis, of endodermal origin. No significant differences were observed between oral and aboral gastrodermis, so these data were pooled. In planulae and early metamorphosis, less than 3% of coral cells from all three epithelia of ectodermal origin synthesized DNA within the 24 h pulse period, while in the gastrodermis up to 6% of the cells were BrdU-positive (figure 3*a–d*). However, in developing primary polyps, a peak of BrdU labelling was observed in the pharynx ( $19.3 \pm 7.3\%$ ) together with a significant increase in BrdU labelling of the gastrodermis ( $11.1 \pm 6.7\%$ ). Interestingly, this sudden increase in proliferation was not observed in other areas of the developing primary polyp, such as the pse, or the calcicodermis (despite active, ongoing skeleton deposition; see electronic supplementary material, figure S2). In adult polyps, BrdU labelling strongly decreased compared with in the primary polyp, in both pharynx (by a factor 4) and gastrodermis (by a factor 3), whereas it increased (by a factor 2) in the pse ( $7.3 \pm 1.6\%$ ). In adult polyps, the pse and the pharynx are the most proliferative tissue types, with  $7.3 \pm 1.6\%$  and  $5.5 \pm 2.0\%$  BrdU-labelled nuclei during the 24 h pulse, respectively, whereas the calcicodermis remains the least proliferative tissue (figure 3*a–d*; electronic supplementary material, table S1).

The number of TUNEL-positive, apoptotic nuclei did not increase in sections of tissue exposed to BrdU compared with control tissue unexposed to BrdU, indicating no effect of the BrdU-labelling protocol on apoptosis (data not shown). Globally, in all three epithelial tissues of ectodermal origin, the relative abundances of TUNEL-positive nuclei were lower than BrdU-positive nuclei, with less than 1% of apoptotic cells counted in the pse, less than 2% in the calcicodermis and a maximum of 2.5% in the pharynx of primary polyps, and non-significant differences between life stages (figure 3*a–c* and *e–g*; electronic supplementary material, table SII). In the gastrodermis, however, TUNEL labelling of nuclei was higher, at  $3.3 \pm 2.2\%$  in planulae, reaching  $5.1 \pm 2.4\%$  during early metamorphosis, and then decreasing in primary polyps, to below 2% in adults (figure 3*d,h*; electronic supplementary material, table SII).

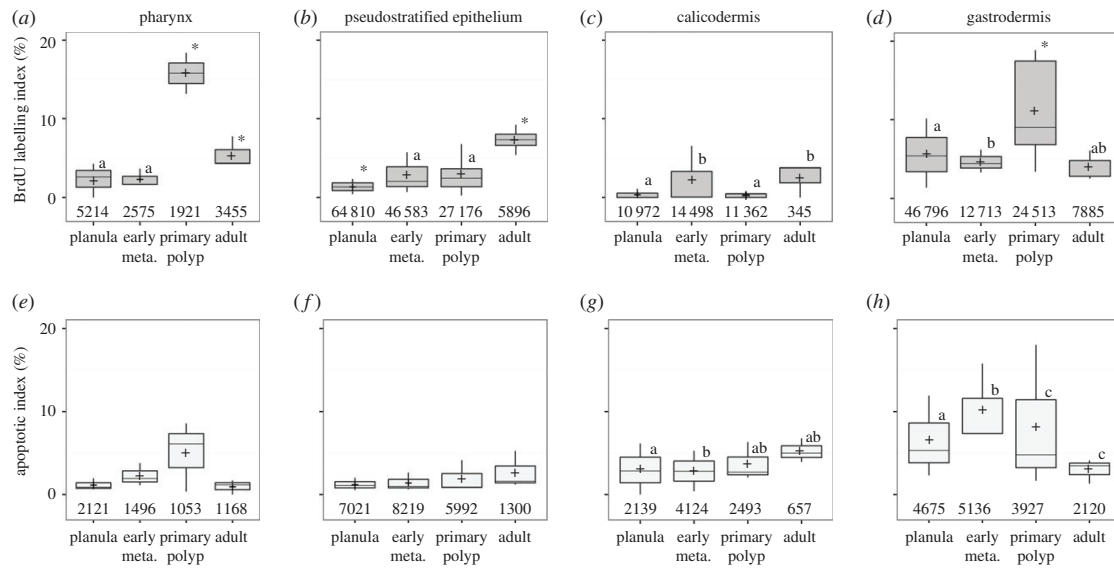


**Figure 3.** Tissue-specific cell turnover during metamorphosis. (a–d) BrdU-labelling index at the end of the 24 h pulse. (e–h) Apoptotic index in corresponding serial tissue sections of the same samples. In planula, the ‘calcicodermis’ is not yet differentiated and this term refers to the aboral pse. Early meta., early metamorphosis. Data are expressed as boxplots, with the average visualized as +, and total nuclei counts reported above the x-axis. An asterisk indicates significant differences with other averages. Significantly different groups are labelled with different letters (GLM,  $p < 0.05$ ).

### (c) Coral cell movements in the ectoderm-derived epithelia

The fate of BrdU-labelled cells was monitored at the primary polyp stage during a 64 h chase period in normal seawater, allowing tracking of labelled cells in the developing epithelia, particularly in the pharynx, the pse and the calcicodermis of the growing primary polyp (figure 4*a,c,e*). Accumulation or depletion of BrdU-labelled cells in specific tissue structures provide indirect evidence for cell import or loss, through cell death or export to other areas. De novo cell cycling in normal seawater dilutes the BrdU signal intensity because BrdU-labelled cells synthesize new, non-labelled DNA before division. The patterns of coral cell movements were thus recorded in these three connected epithelia in order to investigate the origin and turnover of cells in the skeletogenic calcicodermis. All data are provided in electronic supplementary material, tables SIII and SIV.

At the beginning of the chase, the pharynx of the primary polyp was highly BrdU-labelled ( $19.3 \pm 7.3\%$ ) compared with the pse ( $2.9 \pm 2.5\%$ ) and calcicodermis ( $0.4 \pm 0.4\%$ ). At 48 h into the chase, the proportion of BrdU-labelled nuclei remained stable in the pharynx ( $19.8 \pm 4.4\%$ ), whereas it increased by fivefold and sevenfold in the pse ( $15.6 \pm 5.7\%$ ) and calcicodermis ( $2.9 \pm 2.5\%$ ), respectively. At 64 h into the chase, the BrdU-labelling index had significantly decreased in the pharynx ( $11.4 \pm 6.6\%$ ), and returned to the initial low levels seen at the beginning of the chase in both pse and calcicodermis (figure 4*a,c,e*).

At 48 h into the chase, a twofold dilution of the BrdU signal intensity was observed in both pharynx and pse, indicating division of BrdU-positive cells, whereas a similar decrease was difficult to detect in the calcicodermis, in part due to high signal heterogeneity and lower initial BrdU-labelling levels (figure 4*b,d,f*).

### (d) Dinoflagellate cell turnover in the coral host gastrodermis

Comparative dynamics of cell proliferation and apoptosis in endosymbiotic dinoflagellates and coral gastrodermis are presented in figure 5, along with the evolution of dinoflagellate mitotic index and relative dinoflagellate abundances. All data are provided in electronic supplementary material, tables SI, SII and SV.

Rates of BrdU-labelled nuclei were systematically two to five times higher in endosymbiotic dinoflagellates than in host gastrodermis in all three early life stages (GLM analysis,  $p < 0.05$ ; figure 5*a*). In adult polyps, DNA synthesis was also twice as high in endosymbionts as in the host. High variability of the BrdU signal in dinoflagellates indicates spatial heterogeneity and asynchronous cell cycling during the 24 h pulse. No significant differences were observed for dinoflagellates between oral and aboral tissue, however. The mitotic index of dinoflagellates (representing a snapshot of the frequency of dinoflagellate doublets, i.e. visible mitotic figures at the time of tissue fixation) was lower than 2.5% at all stages, except in the primary polyp where it reached  $6.3 \pm 2.3\%$  (figure 5*b*). Owing to their small size, the mitotic index of coral cells could not be accurately estimated.

Higher apoptotic indices were observed for dinoflagellates than gastrodermis in planulae and at early metamorphosis (about 11–12% versus 3–5%, respectively). However, in primary polyps, apoptosis of dinoflagellates rose dramatically (up to 35%) compared with coral cells (approx. 4%). In adult polyps, apoptosis of the endosymbionts remained high at approximately 28% versus less than 2% for the gastrodermis (figure 5*c*; electronic supplementary material, table SII).

Interestingly, the dinoflagellate relative abundance (ratio of symbiont to host nuclei in the gastrodermis) remained stable throughout metamorphosis, at about 5–10% (one-way

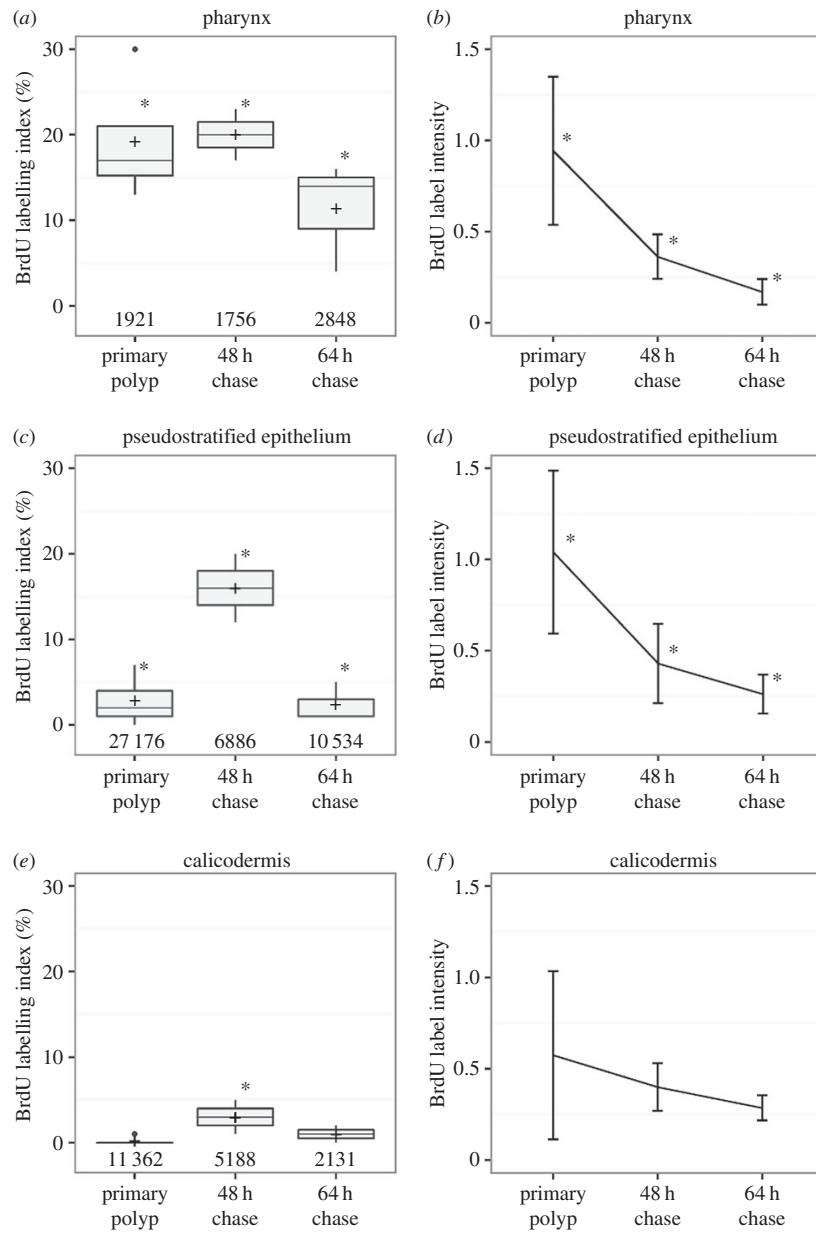


**Figure 4.** Chase of the BrdU label in the ectoderm-derived epithelia. (a,c,e) BrdU-labelling index in the primary polyp at the start, and 48 h and 64 h into the chase in normal seawater, respectively. Data are expressed as boxplots. An asterisk indicates a significantly different average from all other time points (GLM,  $p < 0.05$ ). (b,d,f) Dilution of the BrdU signal intensity. An asterisk indicates significant differences with other averages (Kruskal–Wallis and pairwise Wilcoxon test,  $p < 0.05$ ).

ANOVA,  $p = 0.2$ ; figure 5d), indicating a series of post-mitotic control mechanisms by the host of its endosymbiont population with an increasing role for apoptosis in the developing primary polyp.

During the chase in normal seawater, the proportion of BrdU-labelled dinoflagellate symbionts remained stable at 20–25% in the growing primary polyp, with very slow dilution of BrdU (significant only at 64 h; electronic supplementary material, figure S3a and table SIII), indicating decreased dinoflagellate division. By contrast, the combined depletion by a factor of 3 of BrdU-labelled gastrodermal cells and their corresponding BrdU signal dilution at the end of the chase (electronic supplementary material, figure S3b,c) indicate active cell division in the host gastrodermis. Taken together,

these results indicate decreasing cycling of endosymbiont cells relative to host cells in the growing primary polyp.

#### 4. Discussion

This work presents the first detailed assessment of cellular turnover at tissue scale during developmental morphogenesis in a scleractinian coral, and reveals the ontogenetic flexibility of its dinoflagellate-host density regulations. Cellular morphogenetic processes have mostly been characterized in Cnidaria during regeneration or development of medusozoans, such as freshwater *Hydra* and marine *Hydractinia* [16–18]. Proliferating cells from adult anthozoans, pulse-labelled

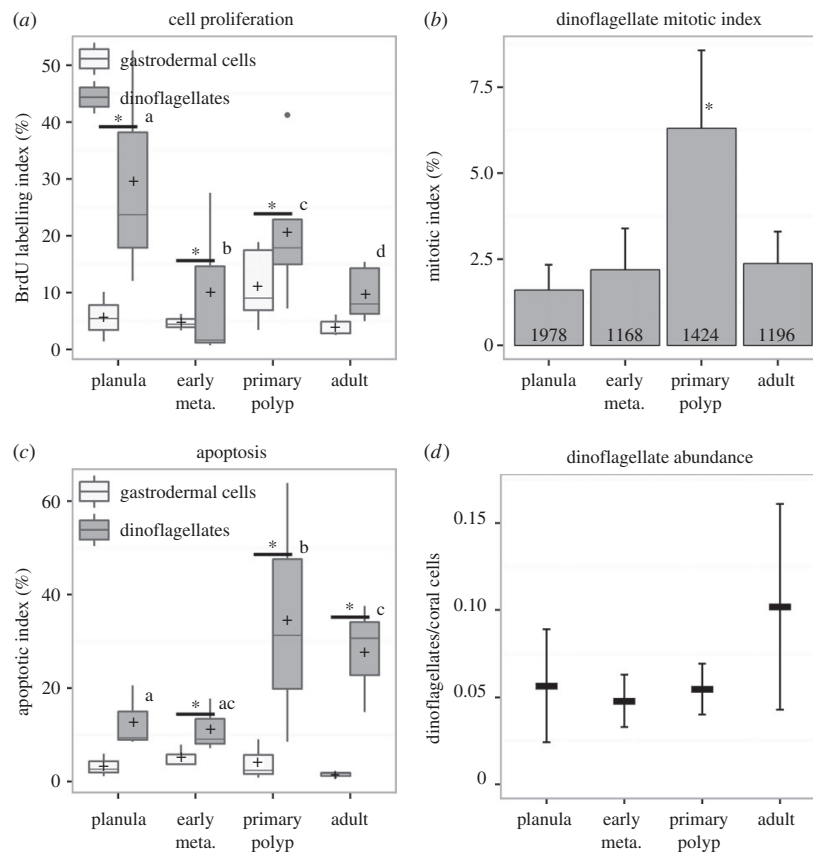


**Figure 5.** Dinoflagellate turnover in host gastrodermis during metamorphosis. (a) BrdU-labelling index in the gastrodermis after the 24 h pulse, for the dinoflagellates (dark grey) and the coral cells (light grey). An asterisk indicates a significant difference between dinoflagellates and gastrodermis (GLM,  $p < 0.05$ ). (b) Mitotic index of dinoflagellates. The asterisk indicates a significant difference with all other stages (Tukey HSD,  $p < 0.05$ ). (c) Apoptotic index in serial tissue sections of the same samples. An asterisk indicates a significant difference between dinoflagellates and gastrodermal cells. (d) Dinoflagellate relative abundance in the gastrodermis: no statistical differences were detected between stages (one-way ANOVA,  $p = 0.697$ ). Early meta., early metamorphosis.

with thymidine analogue EdU or BrdU, were monitored during wound-regeneration and post-bleaching recovery in oral tissue of sea anemones [19,20], and during growth anomaly disease in *Porites* or *Montipora* corals [7]. However, the spatial and temporal dynamics of cell proliferation, migration and death have never been investigated in the developing calcifying scleractinians. Larval metamorphosis requires extensive tissue remodelling to establish the primary polyp structures. Here, we quantify the cell turnover in each forming scleractinian coral epithelium, and the symbiont-to-host cell ratio, from initiation of larval metamorphosis to the fully developed primary polyp.

### (a) Identification of the pharynx as a hotspot of coral cell turnover during development

At the end of the 24 h BrdU pulse, a comparison of labelling levels between tissues from all life stages reveals enhanced coral cell proliferation in the primary polyp, with a hotspot of DNA synthesis localized in the pharynx (figure 3a). This specialized epithelium of ectodermal origin is the most productive tissue area, with up to 19% of cells undergoing DNA synthesis in the primary polyp, and low rates of cell death by apoptosis (less than 2.5%). In the rest of the pseudostratified epithelium (pse), DNA synthesis rates vary

from less than 3% in early life stages to 7.3% in the adult polyp, and few cells are lost via apoptosis (less than 1.5%).

The second highest proliferative tissue is the gastrodermis, of endodermal origin, which also displays the highest apoptotic index in early life stages (figure 3d). DNA synthesis rates in this cell layer vary between 3.8 and 11.1%, peaking in the developing primary polyp. Apoptotic indices peak in early metamorphosis and primary polyp (at about 5%), then drop to 1.5% in adult coral. These data indicate that developmental morphogenetic processes in the gastrodermis simultaneously involve coral cell apoptosis in the early life stages (planula to primary polyp), and proliferation peaking in the primary polyp.

During the chase, the pharynx maintains high proportions of BrdU-labelled cells, but with a twofold decrease in BrdU signal intensity, indicating that active cell division compensates for cells leaving the pharynx area (figure 4a,b). The duration of the cell cycle is not known for scleractinian coral cells and few data are available for other cnidarian species. In *Hydra* sp. the cell cycle has been estimated to last 3–4 days, up to 7 days for epithelial cells and 8.5 days for gastrodermal cells [21–23]. In our study, the twofold dilution of BrdU-labelling over a 2 days chase suggests a shorter cell cycle compared with *Hydra*, lasting about 2 days for the coral epithelial cells from the pse and pharynx

areas. Further flow cytometry experiments would shed more light on cell cycling times in scleractinian corals. In this study, we show that BrdU-labelled cells accumulate in the pse of the oral tissue and also in the calicodermis of the aboral tissue (figure 4c–f). Taken together, these results reveal cell movements, migrating away from the pharynx to the pse and calicodermis. Additional influx of cells to these tissue layers from the gastrodermis is also possible, as this epithelium is the second most proliferative tissue in the primary polyp.

These results are consistent with our earlier findings in another scleractinian species, in which the pse (including the pharynx area) was also observed to be the most proliferative tissue in adult polyps, followed by the gastrodermis [8]. Spatial patterns of cell division observed in *S. pistillata* are similar to patterns reported for another anthozoan, the sea anemone *Nematostella vectensis*, where scattered cell division is observed along the entire body, with a hotspot of DNA synthesis identified in the pharynx [19,24]. More restricted proliferation patterns are present in hydrozoans. For example, in the freshwater *Hydra* polyp, proliferating cells are restricted to the body column, in which there is constant renewal of cells and migration to the apical and basal end of the polyp [16,22]. In the marine *Clytia hemisphaerica*, cell division of interstitial i-cells occurs in the epithelium at the tentacle base, from which cells migrate and differentiate into mature nematocysts mounted at the tip of tentacles [25].

### (b) Cells in the skeletogenic calicodermis are non-cycling despite rapid growth of early life stages

The calicodermis appears to be essentially a non-proliferative epithelium (less than 2.5% of BrdU-positive cells), with non-cycling, terminally differentiated cells that are, however, actively producing skeleton (electronic supplementary material, figure S2). Cellular control of the coral biomineralization process has been proposed to involve highly localized proliferation or metabolic activity in the calicodermis [26]. Here, we demonstrate that active skeletal accretion is not associated with locally increased cellular proliferation in the overlying calicodermis. Moreover, our chase results indicate influx into the calicodermis of labelled cells from more proliferative reservoirs, primarily the pharynx and gastrodermis of the developing polyp. The exact migration pathway and number of divisions, from precursor cell until differentiated calicoblast, remains to be established. However, the BrdU signal intensity in calicoblast nuclei during the chase is lower by a factor of 2 to 4 compared with nuclei in more proliferative areas, which suggests one to two divisions during cell migration to the calicodermis. Correspondingly large standard deviations of the BrdU signal intensity in the calicodermis (figure 4f) indicate asynchronous cycling of the incoming cells. Migration may occur via displacement of epithelial cells in the pse, as in the *Hydra* body column [22], or through the mesenteries that connect the pharynx to the polyp basal floor [15,27].

The longevity of cells in quiescent calicodermis remains unclear. The calicodermis of the developing primary polyp is characterized by low rates of cell death via apoptosis (less than 3% TUNEL-positive nuclei). However, the transient accumulation, observed at 2 days into the chase, of BrdU-labelled cells imported from more proliferative reservoirs is followed by return to the initial low level at 64 h (figure 4c), indicating cell loss via a pathway different from apoptotic cell

death. Future experiments with autophagy markers would shed more light on these processes; autophagy is known to be an important process in vertebrate development [28].

### (c) Differential control of symbiont population by the host cells, depending on life stage

Constant dinoflagellate-to-gastrodermal cell ratio during metamorphosis indicates that the symbiont population is controlled by the host from the earliest life stages. In adult corals, it is known that a steady-state symbiont/host cell ratio is maintained through processes involving inorganic nutrient limitation (pre-mitotic control) and expulsion or cell death (post-mitotic control via autophagy or apoptosis) [2,28,29]. The dinoflagellate-to-gastrodermal cell ratio we observed through metamorphosis and development of *S. pistillata* was in the range 0.05–0.10 (figure 5d), with high variability in adult polyps reflecting high spatial heterogeneity of dinoflagellate abundance at colony level. This ratio is lower than the 0.15 ratio observed in adult *Acropora millepora* corals, but far above the ratio of bleached corals (0.005) [30]. The mitotic index we observed at all life stages is in agreement with values reported in adult scleractinian corals, typically being around or slightly below 5% [2]. However, the BrdU-labelling index was consistently higher for dinoflagellates compared with coral host (figure 5a), indicating that, early in development, the cell cycling activity of the endosymbionts surpasses that of the host cells.

During our experiments, inorganic nutrient concentrations in Eilat seawater were low, corresponding to an oligotrophic environment, and thus could not be responsible for the observed high *Symbiodinium* proliferation rates. The stability of dinoflagellate-to-gastrodermal cell ratio (figure 5d), despite higher DNA synthesis rates of endosymbionts (figure 5a), implies host regulation via post-mitotic control mechanisms. In planulae and during early metamorphosis, our results show that apoptosis is not the main endosymbiont regulation process, but that programmed cell death becomes essential for symbiont density regulation in the primary polyp and, to a lesser degree, in adult polyps (figure 5c). In planulae of *S. pistillata*, degradation of dinoflagellates has been reported [29] as well as release of symbionts into the water column [9]. Autophagy might also be involved in host regulation of the dinoflagellate population at early life stages, as it is known to be involved in adult coral bleaching [30]. Pre-mitotic control by host of dinoflagellate proliferation may be established only at the adult stage, when nutrient limitation and recycling mechanisms in the coral holobiont become fully developed [2].

## 5. Conclusion

This study has clearly identified the pharynx and gastrodermis as the most proliferative areas in the developing scleractinian polyp. Coral skeletal deposition does not involve proliferation of cells in the calicodermis, even during rapidly growing early life stages. Furthermore, our observations reveal an ontogenic succession of post-mitotic control mechanisms of the endosymbiotic dinoflagellate population density during host early development.

**Data accessibility.** The supporting datasets are summarized in the electronic supplementary material, tables SI–SV, and have been uploaded in the Dryad repository under the accession number <http://dx.doi.org/10.5061/dryad.d9v45>.

**Authors' contributions.** A.L., I.D.-C. and A.M. designed the experiment. A.L. carried out the experiments. A.P. and A.L. statistically analysed the data. All authors contributed to drafting and editing the manuscript.

**Competing interests.** We have no competing interests.

**Funding.** A.L. was funded by ERC Advanced grant no. 246749 'BIO-CARB' to A.M. Field labelling experiments, conducted at the marine station of the Inter-University Institute in Eilat, Israel, were funded through European ASSEMBLE call 6 programme

CORALCELLPROLIF to I.D.-C., with additional grants from the MNHN programmes ATM 'Biominalizations' and 'Formes'.

**Acknowledgements.** The PT-BIOP platform at EPFL Lausanne is acknowledged for access to and help with fluorescence microscopy. The PtME platform at MNHN is acknowledged for access to microtome and scanning electron microscope (electronic supplementary material, figure S2). We thank Shakib Djediat and Nicolas Rabet for discussions and Morgane Buet for drawing figure 1.

## References

- Stolarski J, Kitahara MV, Miller DJ, Cairns SD, Mazur M, Meibom A. 2011 The ancient evolutionary origins of Scleractinia revealed by azooxanthellate corals. *BMC Evol. Biol.* **11**, 316. (doi:10.1186/1471-2148-11-316)
- Davy SK, Allemand D, Weis VM. 2012 Cell biology of Cnidarian-dinoflagellate symbiosis. *Microbiol. Mol. Biol. Rev.* **76**, 229–261. (doi:10.1128/MMBR.05014-11)
- Falkowski PG, Dubinsky Z, Muscatine L, McCloskey L. 1993 Population control in symbiotic corals. *BioScience* **43**, 606–611. (doi:10.2307/1312147)
- Pernice M, Dunn SR, Miard T, Dufour S, Dove S, Hoegh-Guldberg O. 2011 Regulation of apoptotic mediators reveals dynamic responses to thermal stress in the reef building coral *Acropora millepora*. *PLoS ONE* **6**, e16095. (doi:10.1371/journal.pone.0016095)
- Kvitt H *et al.* 2015 Breakdown of coral colonial form under reduced pH conditions is initiated in polyps and mediated through apoptosis. *Proc. Natl Acad. Sci. USA* **112**, 2082–2086. (doi:10.1073/pnas.1419621112)
- D'Angelo C, Smith EG, Oswald F, Burt J, Tchernov D, Wiedenmann J. 2012 Locally accelerated growth is part of the innate immune response and repair mechanisms in reef-building corals as detected by green fluorescent protein (GFP)-like pigments. *Coral Reefs* **31**, 1045–1056. (doi:10.1007/s00338-012-0926-8)
- Yasuda N, Hidaka M. 2012 Cellular kinetics in growth anomalies of the scleractinian corals *Porites australiensis* and *Montipora informis*. *Dis. Aquat. Organ.* **102**, 1–11. (doi:10.3354/dao02530)
- Lecoq A, Cohen S, Gèze M, Djediat C, Meibom A, Domart-Coulon I. 2013 Scleractinian coral cell proliferation is reduced in primary culture of suspended multicellular aggregates compared to polyps. *Cytotechnology* **65**, 705–724. (doi:10.1007/s10616-013-9562-6)
- Rinkevich B, Loya Y. 1979 The reproduction of the Red Sea coral *Stylophora pistillata*. II. Synchronization in breeding and seasonality of planulae shedding. *Mar. Ecol. Prog. Ser.* **1**, 145–152. (doi:10.3354/meps001145)
- Vandermeulen JH, Watabe N. 1973 Studies on reef corals. I. Skeleton formation by newly settled planula larva of *Pocillopora damicornis*. *Mar. Biol.* **23**, 47–57. (doi:10.1007/BF00394111)
- Gilis M, Meibom A, Domart-Coulon I, Grauby O, Stolarski J, Baronnet A. 2014 Biomineralization in newly settled recruits of the scleractinian coral *Pocillopora damicornis*. *J. Morphol.* **275**, 1349–1365. (doi:10.1002/jmor.20307)
- Byler KA, Carmi-Veal M, Fine M, Goulet TL. 2013 Multiple symbiont acquisition strategies as an adaptive mechanism in the coral *Stylophora pistillata*. *PLoS ONE* **8**, e59596. (doi:10.1371/journal.pone.0059596)
- Santos SR, Toyoshima J, Kinzie RALII. 2009 Spatial and temporal dynamics of symbiotic dinoflagellates (*Symbiodinium*: Dinophyta) in the perforate coral *Montipora capitata*. *Galaxea J. Coral Reef Stud.* **11**, 139–147. (doi:10.3755/galaxea.11.139)
- Wilkerson FP, Kobayashi D, Muscatine L. 1988 Mitotic index and size of symbiotic algae in Caribbean Reef corals. *Coral Reefs* **7**, 29–36. (doi:10.1007/BF00301979)
- Peters EC. 2016 Anatomy. In *Diseases of coral* (eds CM Woodley, CA Downs, AW Bruckner, JW Porter, SB Galloway), pp. 85–107. New York, NY: John Wiley & Sons, Inc.
- David CN, Campbell RD. 1972 Cell cycle kinetics and development of *Hydra attenuata* I. Epithelial cells. *J. Cell Sci.* **11**, 557–568.
- Plickert G, Krohner M, Munck A. 1988 Cell proliferation and early differentiation during embryonic development and metamorphosis of *Hydractinia echinata*. *Development* **103**, 795–803.
- Chera S, Ghila L, Dobretz K, Wenger Y, Bauer C, Buzgariu W, Buzgariu W, Martinou J-C, Galliot B. 2009 Apoptotic cells provide an unexpected source of Wnt3 signaling to drive *Hydra* head regeneration. *Dev. Cell.* **17**, 279–289. (doi:10.1016/j.devcel.2009.07.014)
- Passamaneck YJ, Martindale MQ. 2012 Cell proliferation is necessary for the regeneration of oral structures in the anthozoan cnidarian *Nematostella vectensis*. *BMC Dev. Biol.* **12**, 34. (doi:10.1186/1471-213X-12-34)
- Fransolet D, Roberty S, Herman A-C, Tonk L, Hoegh-Guldberg O, Plumier J-C. 2013 Increased cell proliferation and mucocyte density in the sea anemone *Aiptasia pallida* recovering from bleaching. *PLoS ONE* **8**, e65015. (doi:10.1371/journal.pone.0065015)
- Bosch TC, David CN. 1984 Growth regulation in *Hydra*: relationship between epithelial cell cycle length and growth rate. *Dev. Biol.* **104**, 161–171. (doi:10.1016/0012-1606(84)90045-9)
- Holstein TW, Hobmayer E, David CN. 1991 Pattern of epithelial cell cycling in *Hydra*. *Dev. Biol.* **148**, 602–611. (doi:10.1016/0012-1606(91)90277-A)
- Govindasamy N, Murthy S, Ghanekar Y. 2014 Slow-cycling stem cells in *Hydra* contribute to head regeneration. *Biol. Open* **3**, 1236–1244. (doi:10.1242/bio.201410512).
- Singer II. 1971 Tentacular and oral-disc regeneration in the sea anemone, *Aiptasia diaphana*. 3. Autoradiographic analysis of patterns of tritiated thymidine uptake. *J. Embryol. Exp. Morphol.* **26**, 253–270.
- Denker E, Manuel M, Leclère L, Le Guyader H, Rabet N. 2008 Ordered progression of nematogenesis from stem cells through differentiation stages in the tentacle bulb of *Clytia hemisphaerica* (Hydrozoa, Cnidaria). *Dev. Biol.* **315**, 99–113. (doi:10.1016/j.ydbio.2007.12.023)
- Tambutté E, Allemand D, Zoccola D, Meibom A, Lotto S, Caminiti N, Tambutté S. 2007 Observations of the tissue-skeleton interface in the scleractinian coral *Stylophora pistillata*. *Coral Reefs* **26**, 517–529. (doi:10.1007/s00338-007-0263-5)
- Seipel K, Schmid V. 2006 Mesodermal anatomies in cnidarian polyps and medusae. *Int. J. Dev. Biol.* **50**, 589. (doi:10.1387/ijdb.062150ks)
- Aburto MR, Hurlé JM, Varela-Nieto I, Magariños M. 2012 Autophagy during vertebrate development. *Cells* **1**, 428–448. (doi:10.3390/cells1030428)
- Titlyanov EA, Titlyanova TV, Loya Y, Yamazato K. 1998 Degradation and proliferation of zooxanthellae in planulae of the hermatypic coral *Stylophora pistillata*. *Mar. Biol.* **130**, 471–477. (doi:10.1007/s002270050267)
- Dunn SR, Schnitzler CE, Weis VM. 2007 Apoptosis and autophagy as mechanisms of dinoflagellate symbiont release during cnidarian bleaching: every which way you lose. *Proc. R. Soc. B* **274**, 3079–3085. (doi:10.1098/rspb.2007.0711)

### III. Supplementary material

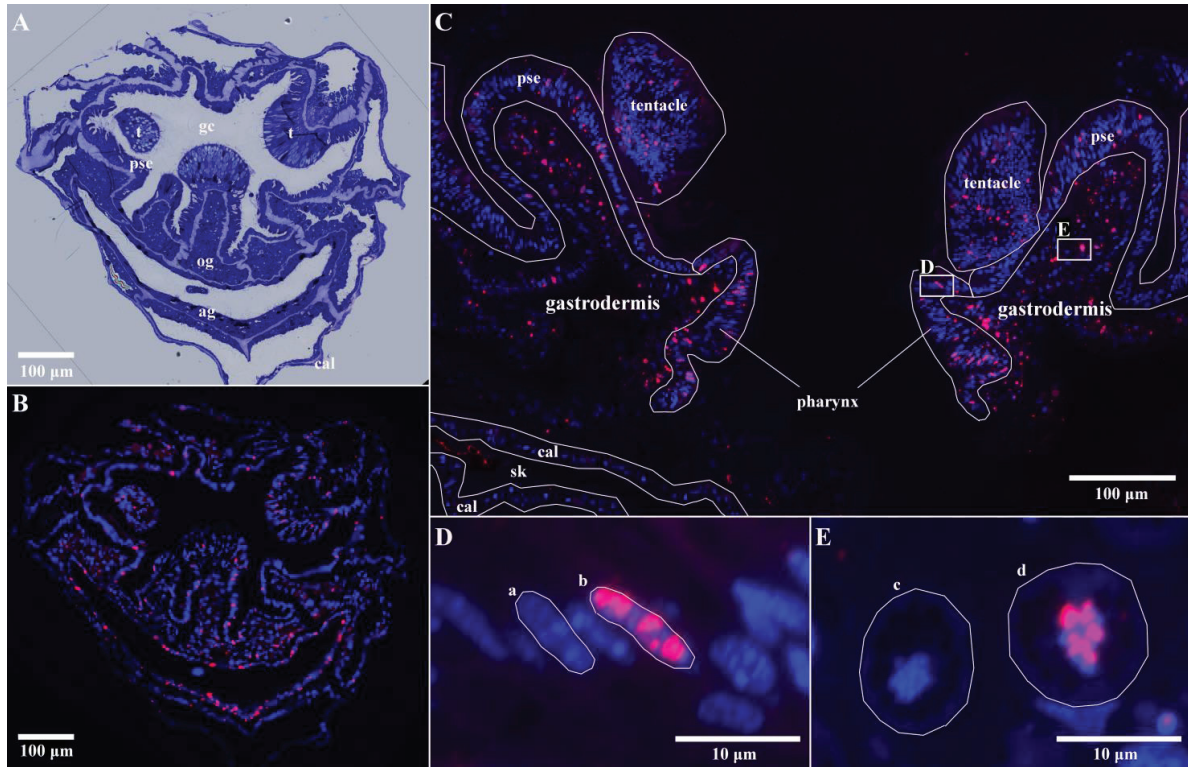


Figure 3-S1: Imaging method for quantification of BrdU-labeled nuclei immunodetected in the coral tissue layers.

(A) Toluidine blue semi-thin section (1 µm) of *S. pistillata* adult polyp. (B-E) BrdU is detected with Alexa-594 (red) co-localized with DAPI-stained nuclei (blue) in (B) the corresponding serial transverse section from the same adult polyp, (C) longitudinal section from a primary polyp, oriented through the highly labeled pharynx area (cell layers are outlined in white). (D-E) Magnified view highlighting in (D) the pharynx with (a) unlabeled nuclei (b) BrdU-labeled nuclei, and in (E) the gastrodermis with (c) a dinoflagellate cell with unlabeled nuclei (d) a dinoflagellate cell with BrdU labeled nuclei. t: tentacle, gc: gastric cavity, pse: pseudostratified epithelium, og: oral gastrodermis, ag: aboral gastrodermis, cal: calicodermis, sk: decalcified skeleton. Alexa-594 labeling which does not co-localize to nuclei is considered an artefact.



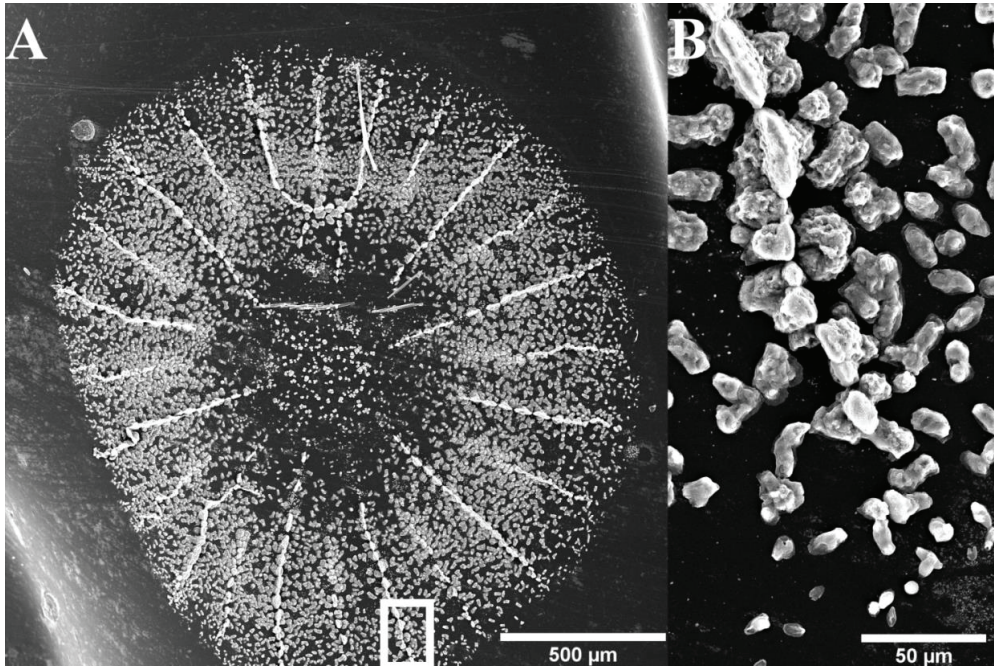


Figure 3-S2: Skeleton deposition during metamorphosis. (A) Scanning electron micrograph of skeleton already deposited by *Stylophora pistillata* at the early metamorphosis stage. (B) Magnified view of growing septa.

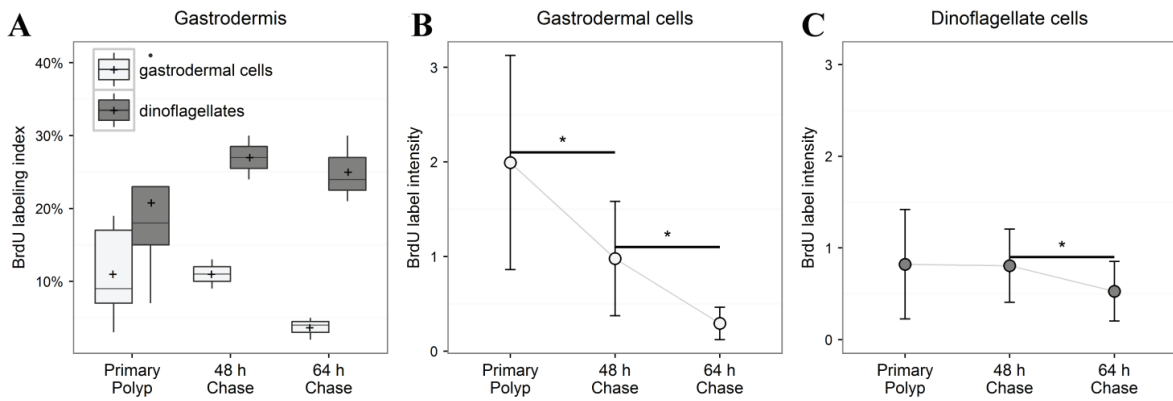


Figure 3-S3: Chase of the BrdU labeling in the gastrodermis. (A) BrdU-labeling index in the primary polyp at the start, 48 h and 64 h into the chase in normal seawater. Data are expressed as boxplots (c.f. M&M in main text) for the dinoflagellates (dark grey) and the gastrodermal coral cells (light gray). A star indicates statistical difference between gastrodermal cells and dinoflagellates (glm,  $p$ -value $<0.05$ ). (B) Dilution of BrdU signal intensity for the gastrodermal coral cells and (C) for the dinoflagellates. A star indicates a statistical difference between two consecutive time points (Kruskal-Wallis and pairwise Wilcoxon test,  $p$ -value $<0.05$ ).

**Supplementary table I: BrdU 24h-labeling index of coral and dinoflagellate cells**

Tissue	Planula			Early metamorphic			Primary polyp			Adult		
	mean	SD	#nuclei	mean	SD	#nuclei	mean	SD	#nuclei	mean	SD	#nuclei
pharynx	2.3% ± 2.2%		5214	2.4% ± 1.2%		2575	19.3% ± 7.3%		1921	5.5% ± 2.0%		3455
pseudostratified epithelium	1.4% ± 1.0%		64810	2.9% ± 2.6%		46583	2.9% ± 2.5%		27176	7.3% ± 1.6%		5896
calicodermis	0.4% ± 0.7%		10972	2.2% ± 3.8%		14498	0.4% ± 0.4%		11362	2.5% ± 2.2%		345
gastrodermis	5.7% ± 4.4%		46796	4.7% ± 1.5%		12713	11.1% ± 6.7%		24513	3.8% ± 1.6%		7885
dinoflagellates	29.5% ± 20.9%		1793	10.0% ± 15.2%		669	20.8% ± 12.8%		1204	9.8% ± 4.8%		737

nuclei pooled from 2-6 sections per replicate, 3-5 replicates per timepoint

**Supplementary table II: Apoptotic index of coral and dinoflagellate cells**

Tissue	Planula			Early metamorphic			Primary polyp			Adult		
	mean	SD	#nuclei	mean	SD	#nuclei	mean	SD	#nuclei	mean	SD	#nuclei
pharynx	0.6% ± 0.4%		2121	1.1% ± 0.7%		1496	2.5% ± 2.1%		1053	0.5% ± 0.4%		1168
pseudostratified epithelium	0.6% ± 0.4%		7021	0.7% ± 0.5%		8219	1.0% ± 0.9%		5992	1.4% ± 1.1%		1300
calicodermis	1.5% ± 1.5%		2139	1.4% ± 1.2%		4124	1.9% ± 1.1%		2493	2.6% ± 0.7%		657
gastrodermis	3.3% ± 2.5%		4675	5.1% ± 2.4%		5136	4.1% ± 4.3%		3927	1.5% ± 0.7%		2120
dinoflagellates	12.8% ± 6.7%		172	11.3% ± 5.6%		149	34.5% ± 27.8%		209	27.7% ± 11.6%		172

nuclei pooled from 1-4 sections per replicate, 3 replicates per timepoint

**Supplementary table III: BrdU labeling index during the chase experiment**

Tissue	Primary polyp (t0)			48 h Chase			64 h Chase		
	mean	SD	#nuclei	mean	SD	#nuclei	mean	SD	#nuclei
pharynx	19.3% ± 7.3%		1921	19.8% ± 4.4%		1756	11.4% ± 6.6%		2848
pseudostratified epithelium	2.9% ± 2.5%		27176	15.6% ± 5.7%		6886	2.3% ± 2.4%		10534
calicodermis	0.4% ± 0.4%		11362	2.9% ± 2.5%		5188	1.0% ± 1.0%		2131
gastrodermis	11.1% ± 6.7%		24513	10.9% ± 2.8%		9032	3.5% ± 1.7%		6563
dinoflagellates	20.8% ± 12.8%		1204	26.7% ± 4.4%		656	25.1% ± 4.7%		365

nuclei pooled from 4-6 sections per replicate, 2-5 replicates per time-point

**Supplementary table IV: Nuclei BrdU-labeling intensity**

Tissue	Primary polyp			48 h Chase			64 h Chase		
	mean	SD	#nuclei	mean	SD	#nuclei	mean	SD	#nuclei
pharynx	0.94 ± 0.40		30	0.36 ± 0.12		30	0.18 ± 0.06		30
pseudostratified epithelium	1.04 ± 0.45		54	0.44 ± 0.21		60	0.26 ± 0.10		37
calicodermis	0.57 ± 0.46		19	0.40 ± 0.12		21	0.28 ± 0.08		7
gastrodermis	1.99 ± 1.13		59	0.98 ± 0.60		60	0.30 ± 0.17		58
dinoflagellates	0.8 ± 0.6		30	0.8 ± 0.4		30	0.5 ± 0.3		30

7-60 nuclei measured per replicate, 3 replicates per time-point

**Supplementary table V: Mitotic index of dinoflagellates**

	Planula			Early metamorphosis			Primary polyp			Adult		
	mean	SD	#nuclei	mean	SD	#nuclei	mean	SD	#nuclei	mean	SD	#nuclei
dinoflagellates	1.6% ± 0.7%		1978	2.2% ± 1.2%		1168	6.3% ± 2.3%		1424	2.4% ± 0.9%		1196

mitotic index evaluated in 2-8 sections per replicate, 3 replicates per time-point

## IV. Conclusion

Cell proliferation rates at the site of the future calicodermis remain low through metamorphosis. But active skeleton deposition attests for an early establishment of a functional calicodermis. Thus calicoblasts and desmocytes that constitute this cell layer more likely come from transdifferentiation of the aboral pseudostratified epithelium of *S. pistillata* planula. In the primary polyp the pharynx is the most proliferative area from which cells migrate through pseudostratified epithelium and/or mesenterial filaments up to the calicodermis. This pattern of cell division and migration in a scleractinian coral is put forward here for the first time.



# Chapter 3: Calicodermis establishment during *Pocillopora damicornis* metamorphosis: towards the development of precursor cell markers

## I. Abstract

Successful coral larval recruitment is crucial for reef maintenance and growth. Metamorphosis from the planktonic swimming planula to the sessile calcifying polyp implies important transformations supporting the differentiation of a specialized skeletogenic epithelial cell layer, the calicodermis, which forms the massive calcium carbonate exoskeleton typical of *Scleractinia*. Nevertheless the cellular mechanisms underlying this calicodermis differentiation process are not known. Here we recorded cell proliferation at tissue-scale in the metamorphosing polyp of *Pocillopora damicornis* exposed to a 24 h BrdU pulse, and developed molecular markers of proliferative cells and calicodermis differentiation. Cell proliferation does not start at the onset of metamorphosis but with a delay, and the calicodermis remains the lowest proliferative cell layer at all stages. These results suggest that calicodermis establishment follows a sequential process, involving first a direct transdifferentiation of the pseudostratified epithelium at the planula aboral pole, and then an influx of cells migrating out from other tissue areas in the developing polyp. We located *piwi*-expressing cells at two tissue sites in the adult polyp, at the base of tentacle bulbs, and inside the mesenteries near the cnidoglandular band. Both sites displayed a high proliferation index, and may function as potential somatic stem cell reservoirs. We detected a cysteine-rich protein named “Pdcyst-rich”, previously reported in adult corals and showed that its expression was restricted to calcifying life stages: Pdcyst-rich was absent from planula larvae but expressed in the developing primary polyp at the calicodermis interface with the skeleton, and later inside the calicodermis of polyps from adult colonies. Hypotheses are discussed regarding potential precursor cell migration from reservoirs in the pseudostratified epithelium and the mesenteries, towards the polyp basal floor, but the exact lineage of the calicodermis needs further investigation.

## II. Introduction

Reef-building corals are threatened by sea surface temperature elevation and ocean acidification both being consequences of global warming. Elevated temperatures disrupt existing coral endosymbiosis with *Symbiodinium* sp. dinoflagellates, while reduced pH slows down or stops calcification and these combined parameters thus affect coral growth and larval recruitment. Metamorphic transition from the swimming planula larva to the sessile polyp is a critical step of coral life cycle that includes important morphological changes, most notably with the establishment of the skeletogenic tissue, the calicodermis, which controls rapid skeleton deposition on the substrate. Nevertheless, the calicodermis cell lineage is not known. In *Hydra*, interstitial stem cells (i-cells) are scattered throughout the polyp body column and proliferation is re-

stricted to this column from which cells migrate to the apical and basal end of the polyp (David and Campbell, 1972; Holstein et al., 1991). In scleractinian corals, stem cells have not been formally identified. Proliferative cell types are more likely to be sensitive to DNA mutation due to high cell division rates. RNA silencing systems, such as the transposon silencing system, protect DNA of dividing cells. In *Bilateria*, repeat-associated small interfering RNAs (rasiRNAs) are involved in maintaining genomic stability through silencing of transposons (Vagin et al. 2006). These rasiRNAs, also called piwi-interacting RNAs (piRNAs), interacts with Piwi proteins to form the piRNA-induced silencing complex (piRISC) that will detect and degrade transposons, thus protecting the genome integrity (Siomi et al. 2011). Consequently we used *piwi* expression as a potential marker for undifferentiated precursor cells. This gene family may have a broader role in *Cnidaria* than in *Bilateria*. In the scleractinian *Euphyllia ancora*, *piwi* expression was recently localized in the mesenteries, and thus associated with germline production (Shikina et al., 2015). In the ctenophoran *Pleurobrachia pileus*, *piwi* expression was also associated with the germline, with piwi paralogues expressed in somatic territories (Alié et al. 2011).

During metamorphosis, initiation of skeleton deposition by the settled larvae (Vandermeulen and Watabe, 1973; Gilis et al., 2014) implies rapid differentiation of the polyp skeletogenic tissue. How this calicodermis cell layer is formed, and whether it involves processes of direct differentiation of cells at the aboral pseudo-stratified epithelium and/or rapid cell proliferation are unclear. In *Stylophora pistillata* cell migration from highly proliferative tissue areas to the forming, non-proliferative calicodermis has been shown (Lecoïnte et al., 2016). Nevertheless the location of potential multipotent stem cells and the temporal characterization of events supporting calicodermis differentiation are missing. Galaxin, Small Cysteine-Rich Proteins (SCRiPs) and Pdcyst-rich protein are secreted proteins restricted to scleractinian corals and characterized by high cysteine amino-acid residue proportions, withan N-terminal peptide signal sequence. These proteins are thought to be involved in skeletal biomineralization (Fukuda et al., 2003; Kim et al., 2015; Reyes-Bermudez et al., 2009; Sunagawa et al., 2009; Vidal-Dupiol et al., 2009). The Pdcyst-rich protein was localized in tissue sections of adult colonies of *Pocillopora damicornis* and found to be restricted to the skeletogenic epithelium at the interface with the skeleton (Vidal-Dupiol et al., 2009), making it a potential calicodermis differentiation marker.

Here, we assessed cell proliferation at tissue scale in the metamorphosing larva of *Pocillopora damicornis* (Linnaeus, 1758) via BrdU pulse-labeling aquarium experiments. Novel *piwi* gene markers were developed to locate potential proliferative precursor cells and their expression was localized in polyp tissue of adult colonies. Experiments are presented to validate Pdcyst-rich protein as a marker of calicodermis differentiation.

### III. Materials and Methods

#### A. Biological material

Planula larvae were obtained from the Aquarium Tropical du Palais de la Porte Dorée (ATPD, Paris, France) or from Océanopolis (Brest, France), where larvae are periodically emitted from large colonies of *Pocillopora damicornis* coral, grown in aquarium under 12 h/12 h light/dark period. Settlement of planulae was promoted by placing them in contact with biofilm-covered underwater paper or plastic dishes incubated for more than three months in aquaria at ATPD. Metamorphosis was monitored under the binocular (at 5x magnification), and larvae were sorted by developmental stage, classified as “planula”, “early metamorphosis”, “forming polyp”, and “primary polyp” according to morphological characteristics.

#### B. BrdU pulse to assess cell proliferation

To assess cell proliferation during metamorphosis, coral samples of each of developmental stage were incubating in artificial seawater (ASW) with 50  $\mu$ M of 5-bromo-2'-deoxyuridine (BrdU) for a 24 h pulse (12h day /12h night). This thymidine analog is incorporated in DNA during the S-phase of dividing cells. Pulse-labeled and control unlabeled samples were rinsed and fixed overnight at 4°C in 0.5% glutaraldehyde, 2% paraformaldehyde and 0.2% saturated picric acid in 0.1 M Sörensen-phosphate-0.6 M sucrose buffer (after Lecointe et al., 2013). For adult colony controls, pulse-labeled branch apices were fixed similarly, then decalcified in EDTA 0.5 M in Sörensen-phosphate buffer at pH 8 for several days at 4°C and individual polyps were microdissected under the binocular. Samples were dehydrated in graded ethanol series, embedded in Unicryl resin at 37°C, and semi-thin sections (1  $\mu$ m) were cut with a 35° diamond knife (Diatom) on an ULTRACUT microtome. Alternately, thicker (3-5  $\mu$ m) tissue sections were cut with a Leica microtome from paraffin (ParaplastPlus, Leica) – embedded samples.

#### C. Immunolocalisation of BrdU and Pdcyst-rich protein

For immunolocalization of BrdU in the cell nuclei, a commercial primary anti-BrdU mouse monoclonal antibody from the 5-Bromo-2'-deoxy-uridine Labeling and Detection Kit II (Roche) was used, according to the protocol described in Lecointe et al. 2013. For immunolocalization of the Pdcyst-rich protein in the differentiating calicodermis, a rabbit polyclonal antibody was custom-generated (Proteogenics, France) using the following synthetic peptide target sequence, 5'- MRNCSSSLVCDQAQSDL-3'. This target sequence, selected after bioinformatics analysis of published Pdcyst-rich protein sequences from *Pocillopora damicornis* and *Acropora digitifera*, is different from the peptide sequence used in Vidal-Dupiol et al. 2009 although also located in the protein extracellular domain.

Coral tissue sections were permeabilized with PBS 10mM pH 7.4 containing 0.2% Triton X100 (PBSt) and treated for 10 min with HCl 2 M or 0.02-0.2 M (for respectively BrdU and Pdcyst-rich immunolocalization), then blocked for 30 min in saturation solution (PBSt containing 1% Bovine Serum Albumin and 1% Natural

Goat Serum) and incubated 3 h at room temperature with primary antibody diluted 1/100 in saturation solution. After rinsing steps, sections were incubated 1 h at room temperature with secondary antibody coupled with either Alexafluor-594 (BrdU) or Alexafluor-660 (Pdcyst-rich) diluted 1/200 in PBSt, rinsed and finally mounted with Prolong Gold antifade reagent with DAPI (Roche). Alternately, a Horse-Raddish Peroxydase (HRP) amplification step was added for Pdcyst-rich protein immunolocalization, using an HRP-conjugated anti-rabbit secondary antibody, reacted with tyramide-conjugated fluorochrome Alexafluor-488 (Molecular Probes, TSAkit #12). Slide acquisitions were done at the BIOP platform (EPFL, Lausanne) and at the CeMIM platform (MNHN, Paris). For BrdU, images were acquired on a wide-field fluorescence microscope (Olympus Slide Scanner) using DAPI (Ex 377/50 nm, Em 440/40 nm), and CY3 filters (Ex 560/25 nm, Em 607/36 nm) at spatial lateral resolution of approximately 0.5  $\mu\text{m}$ . Three sections at different tissue depths were imaged per life stage and the proportion of BrdU containing cell nuclei (i.e. the labeling index) was manually counted for each cell layers and tissue areas using the cell counter plugin from ImageJ software (v1.49). The data followed a binomial distribution with uneven variance and were statistically analyzed using the generalized linear model (glm) with binomial family and logit link function in R software v. 3.2.0. Significance was assessed at  $\alpha=0.05$  threshold  $p$ -value. For Pdcyst-rich protein immunolocalization, images of thin sections (1  $\mu\text{m}$ ) were acquired on a ZEISS LSM710 confocal microscope using DAPI (Ex. 405 nm Em. 450/40 nm) and Far red (Ex. 633 nm Em. 695/45 nm) filters. Images of thicker sections (5  $\mu\text{m}$ ) were acquired in z series (0.2 to 0.5  $\mu\text{m}$  step) on a Nikon Eclipse 350 wide-field fluorescence microscope using DAPI and FITC settings of a quadruple dichroic filter set.

#### **D. Bioinformatics identification of *piwi* gene related sequences in *Pocillopora damicornis* transcriptome and phylogenetic study.**

Piwi protein sequences were first obtained from NCBI. *Clytia hemisphaerica piwi* sequence was blasted against the NGS-based transcriptome dataset PocilloporaBase available at <http://cnidarians.bu.edu/PocilloporaBase/cgi-bin/index.cgi> (Traylor-Knowles et al., 2011) and two *piwi* sequences (named *piwi1* and *piwi2*) were identified and assembled from EST sequences. Corresponding translated nucleotide sequences were blasted against NCBI with a cut-off value of at least  $2e-100$ . Additional Piwi sequences from *Cnidaria* (*Scleractinia*, *Actinaria*, *Hydrozoa*) but also from *Porifera* and *Bilateria* were selected for phylogenetic tree construction and rooted with three argonaute sequences. Selected sequences were aligned using BioEdit (v.7.2.5), restricted to the piwi-like Eukaryote domain (397 amino acid) and maximum-likelihood phylogenetic tree constructed on Mega (v7.0.14) using the Jones-Taylor-Thornton (JTT) model of amino-acid substitution with a bootstrap of 100.

#### **E. Semi-quantitative RT-PCR**

For total RNA extraction, branch apexes from adult colonies and batches of 5 larvae/post-larvae were sampled in RNA later (Invitrogen) and stored at  $-20^{\circ}\text{C}$  until use. Extractions were carried out using Tri-



zol (Invitrogen) according to manufacturer's instructions. RNA quality was checked on agarose gel and absence of DNA contamination was checked with PCR. Total cDNA was obtained by RT-PCR using the SuperScript® III Reverse Transcriptase and random hexamer (Invitrogen).

Specific primers (supplementary table 1) were designed for RT-PCR, using Primer3Plus software, to amplify *piwi1* and *piwi2* from the cDNA of our *Pocillopora damicornis* model, as well as primers for *Pdcyst-rich* cDNA (modified from (Vidal-Dupiol et al., 2009). Amplicons were cloned and cDNA sequences of these three genes will be deposited in Genbank. To compare gene expression levels at different stages of the metamorphosis, semi-quantitative reverse transcriptase PCR (sqRT-PCR) were performed. The following program was used: Denaturation (95°C, 2 min), amplification (95°C for 15 s, 50°C for 15 s, and 72°C for 30 s) and final extension at 72°C for 5 min. In sqRT-PCR saturation must not be reached, hence the number of amplification steps (i.e. cycles) necessary to reach the exponential phase of the amplification reaction was first experimentally determined for each gene. Then, the same amount of cDNA was added for each PCR reaction/each developmental stage and the amplicons of target and housekeeping genes at all developmental stages were visualized simultaneously on the same 1% agarose electrophoresis gel. After migration, images of the gel were acquired using E-box Vilber and analyzed using the gel analyzer plugin of ImageJ software. Normalized gene expression was obtained by dividing target gene expression (*piwi1* or *piwi 2*, or *pdcyst-rich*) with housekeeping gene expression (*18S rRNA* or *ef5*). Three independent sqRT-PCR experiments were carried out using independent sets of coral sample replicates and the mean and standard deviation of the normalized expression were calculated at each developmental stage for *piwi 1* and *piwi 2* and *pdcyst-rich* genes. Data were checked for normality and homoscedasticity followed by one-way ANOVA test and Tukey HSD test when significant ( $\alpha < 0.05$ ) using R software.

#### **F. Whole-mount *in situ* hybridization (ISH) of *piwi 1* and *piwi 2* mRNA**

DIG-labeled antisense RNA probes were synthesized from linearized pGEM-T Easy plasmid (Promega) using T7 or SP6 polymerase and the RNA DIG-labeling mix (Roche). Total sense and antisense probe sequences are given in supplementary Figure S1. Branch apices (0.5 cm long) of adult colonies were fixed in 4% paraformaldehyde, 275 mM EDTA in saline buffer (0.1 M MOPS, 2 mM MgSO<sub>4</sub>, 1 mM EDTA, 0.5 M NaCl) for 24 h at 4°C, washed thoroughly in the saline buffer and stored in methanol at -20°C. Tissues were not demineralized. After stepwise rehydration to PBST (PBS pH 7.4, 0.1% tween 20) and 10 min digestion with 10 µg/ml Proteinase K in PBST at 37°C, samples were washed in PBST with 2 mg/ml glycine and transferred progressively to hybridization buffer (HB, 5X Saline Sodium Citrate (SSC) pH 7.4, 50% deionized formamide, 0.1% tween 20), pre-hybridized for 2 h at 52°C in HB (containing 0.1% SDS, 50 µg/mL heparin, 100 µg/mL salmon DNA and 1% dextran sulfate), then hybridized with 1 ng/µL DIG-labeled RNA probes for 19 h at 52°C. Sense probes were used as a control. Tissues were washed in HB at 52°C and at RT, in consecutive washing buffers (WB) WB1 (2X SSC, 50% deionized formamide, 0.1% tween 20) and WB2 (2X SSC, 0.1%

tween 20). After transfer in MABt buffer (100 mM maleic acid, 150 mM NaCl, pH7.5, 0.1% triton X100) and blocking in MABt + 2X blocking reagent (Roche) samples were incubated 3 h in MABt + 2X blocking reagent containing 1/2000 anti-DIG-alkaline phosphatase (Roche) at RT. After five washing in MABt and transfer to TMNT (100 mM Tris-HCl, 100 mM NaCl, 0.1% Tween 20, pH 9.5), color was developed using 225 µg/mL NBT, 175 µg/mL BCIP, 50 mM MgCl<sub>2</sub> in TMNT. Reaction was stopped by washing with distilled water and samples were post-fixed with 4% formaldehyde in PBS overnight at 4°C before PBS washes and mounting in 50% glycerol/PBS. Coral tissue was pulled out from the skeleton of hybridized apexes and polyps were individually dissected for observation at the MNHN with an Olympus SZX12 binocular (x63, x90) equipped with a CCD camera.

## **IV. Results**

### **A. Cell proliferation in the different tissues through metamorphosis**

Five life stages were differentiated according to morphological characteristics, from the free-swimming planula larva to the benthic calcifying polyp from adult colonies, as illustrated in Figure 4-1A. At the onset of settlement, the disc-shaped larva corresponds to the “early metamorphosis” stage. During metamorphosis, the “forming polyp” is characterized by visible budding of tentacle structures around the mouth aperture. The “primary polyp” is characterized by extended tentacles and vertically growing body column. This metamorphosis process spans about 2-3 days since induction by natural cues from biofilm-covered substrate, but development is asynchronous among larvae from the same batch. Later, within 5 to 10 days, secondary polyps will bud at the periphery of the primary polyp, forming the juvenile colony (“adult polyp” stage).

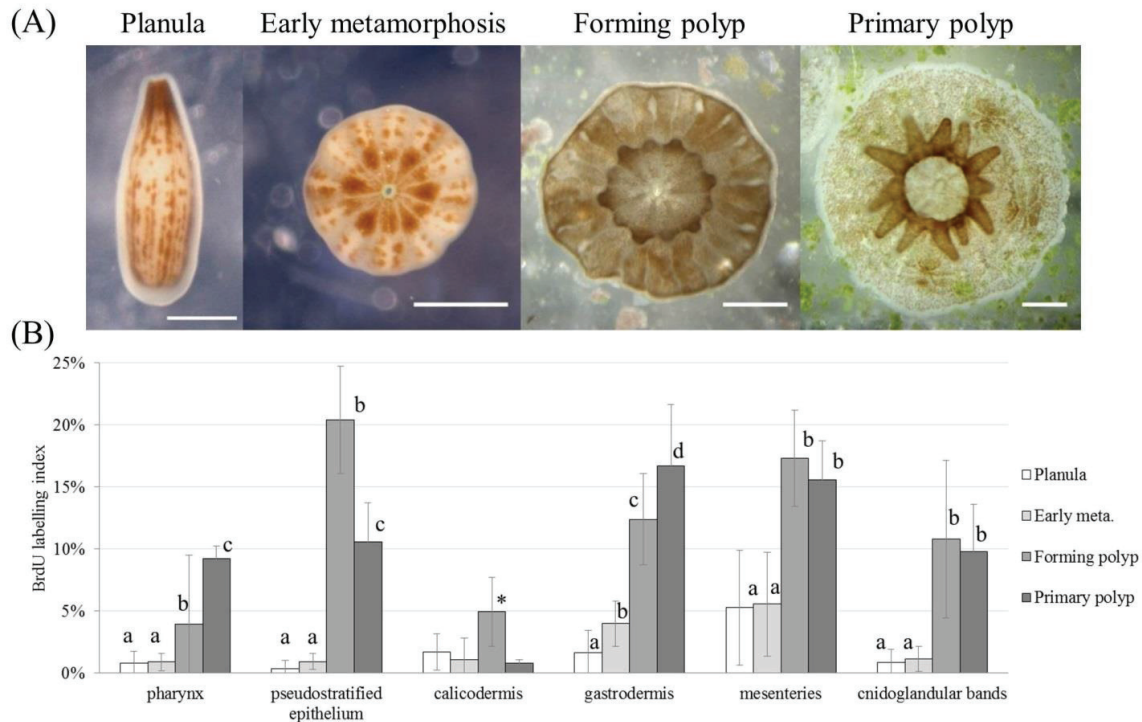


Figure 4-1: Cell proliferation through metamorphosis.

(A) Pictures of studied life stages, scale bars: 500  $\mu$ m. (B) BrdU labeling index after a 24 h pulse in all cell layers/tissue areas at the different life stages. For each tissue areas significant differences between life stages are labeled with different letters and a star when different from all other stages (generalized linear model,  $p$ -value < 0.05). Early meta.: early metamorphosis.

Major changes occur at tissue scale, notably with transformation of the larval single bilayer of epithelia—pseudostratified epithelium (pse) and lipid-filled gastrodermis (g)—into the polyp double bilayer of epithelia. The skeletogenic epithelium, the calicodermis (cal), differentiates at the interface with the substrate. A few specialized structures are already present in the planula of *P. damicornis*, such as the pharynx, formed by inward invagination of the pse, and the mesentery filaments attached below the pharynx and which extend in the primary polyp to its basal floor (cf schematic representation of the primary polyp of *Stylophora pistillata*, a related Pocilloporid species, in Lecoite et al., 2016).

Figure 4-1B presents the BrdU labeling index, i.e. the proportion of cell nuclei having incorporated BrdU during the 24 h pulse, in the different cell layers/tissue areas through metamorphosis. Planula and “early metamorphosis” stages present the lowest BrdU labeling index in all tissue areas (< 6%), suggesting that the beginning of metamorphosis is not a proliferative process. Cell proliferation significantly increases in the “forming polyp”, with a three to tenfold increase of the labeling index in almost all tissues areas. Most drastic increases are observed in the pse (from  $0.9 \pm 0.6\%$  up to  $20.4 \pm 4.3\%$ ) and the cnidoglandular bands of the mesenteries (from  $1.1 \pm 1.0\%$  up to  $10.8 \pm 6.4\%$ ) while a threefold increase is observed in the rest of the mesenterial filaments ( $5.6 \pm 4.2\%$  to  $17.3 \pm 3.9\%$ ) and the gastrodermis ( $4.0 \pm 1.8\%$  to  $12.4 \pm 3.7\%$ ). At the “primary polyp” stage, the labeling index is maintained at high level in the whole mesentery, but continues to increase

in the gastrodermis (to  $16.7\pm 5.0\%$ ) and the pharynx ( $3.9\pm 5.6\%$  to  $9.2\pm 1.0\%$ ) while it decreases in the pse (to  $10.6\pm 3.1\%$ ). Interestingly, despite active skeleton deposition since the onset of metamorphosis (Gilis et al., 2014), the calicodermis is one of the least proliferative tissue, with a labeling index remaining below 2% except at the “forming polyp” stage when it transiently increases to  $4.9\pm 2.8\%$ .

### **B. Identification and expression localization of *piwi* genes from *P. damicornis***

Two *piwi* genes were identified *in silico* from the available transcriptomic data base PocilloporaBase (Traylor-Knowles et al., 2011) using BLAST. The alignment of these translated sequences with Piwi sequences obtained on NCBI from other *Cnidaria*, is available as supplementary data 1, and includes representative species of *Scleractinia*, *Hydrozoa* and *Actinaria*, but also *Porifera* and *Bilateria*. Maximum likelihood analysis was limited to the piwi-like eukaryote domain conserved between all families. The resulting phylogenetic tree presented in Figure 4-2, and rooted using Argonaute sequences - as this family is close to the Piwi family - places both *piwi 1* and *piwi 2* with homologues from *Scleractinia* among *Cnidaria*.

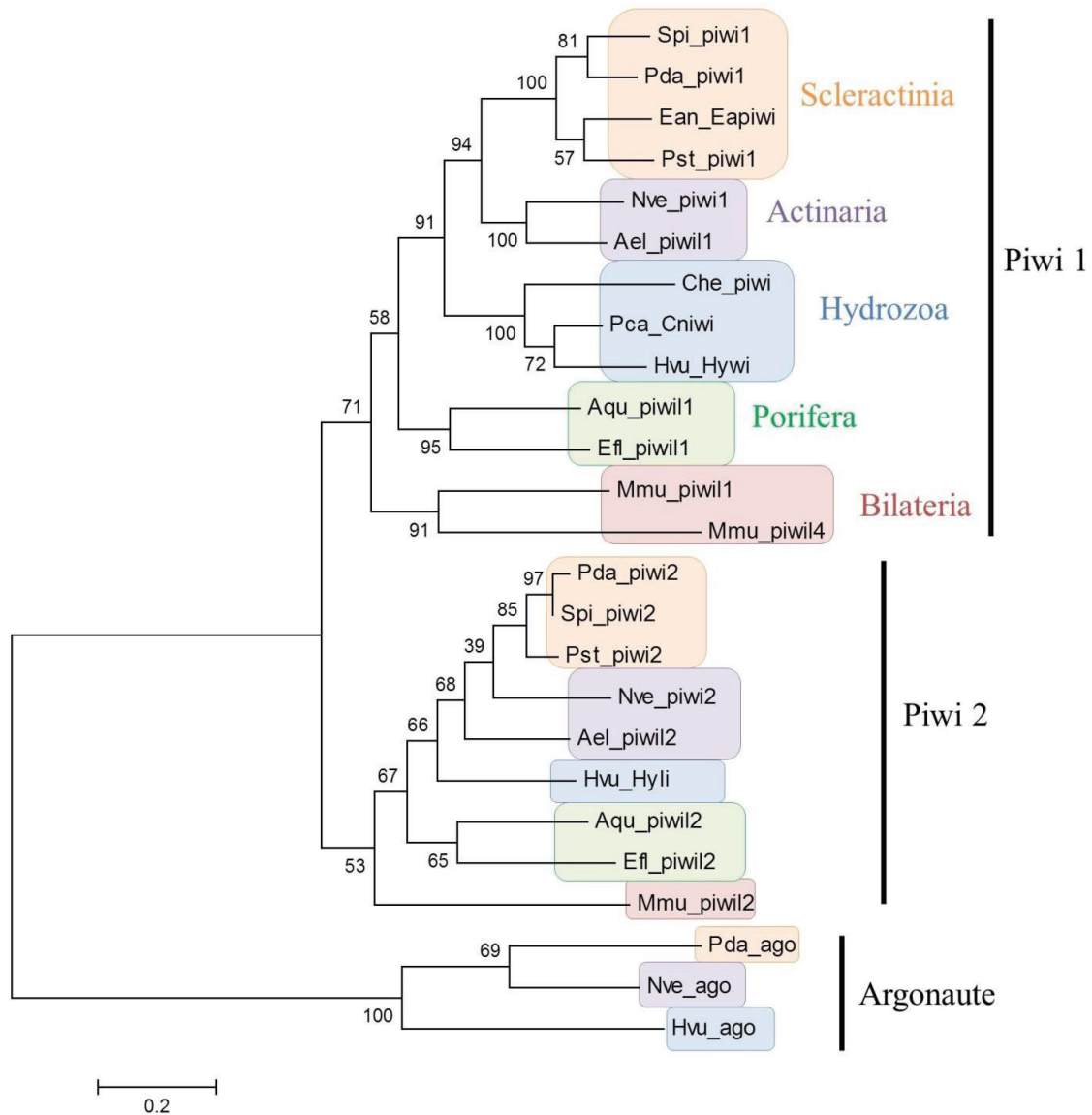


Figure 4-2: Piwi maximum-likelihood phylogeny.

Constructed using the Jones-Taylor-Thornton (JTT) model of amino-acid substitution with bootstrap (100) support values above branches, on the piwi-like Eucaryote conserved domain (397 amino acids). Ael: "*Anthopleura elegantissima*", Aqu: "*Amphimedon queenslandica*", Che: "*Clytia hemisphaerica*", Ean: "*Euphyllia ancora*", Efl: "*Ephydatia fluviatilis*", Hvu: "*Hydra vulgaris*", Mmu: "*Mus musculus*", Nve: "*Nematostella vectensis*", Pca: "*Podocoryna carnea*", Pda: "*Pocillopora damicornis*", Pst: "*Pseudodiploria strigosa*", Spi: "*Stylophora pistillata*".

Expression levels of *piwi 1* and *piwi 2*, assessed by semi-quantitative RT-PCR, were constant through metamorphosis (Figure 4-3, one-way ANOVA *p*-value 0.21 and 0.79 respectively). In the adult polyp, expression of both *piwi* genes was visualized by whole mount *in situ* hybridization (ISH), and was spatially restricted to the tentacles, below their terminal bulb (also called acrosphere) and inside the mesenteries, near the cnidoglandular bands (Figure 4-4). These results must be considered as preliminary as only the adult life stage was tested, and the labeling was not consistently detected in the concerned polyp structures. Improvements to

the protocol have to be made particularly regarding RNA preservation and sample permeabilization/hybridization conditions. Moreover, early life stages should also be tested

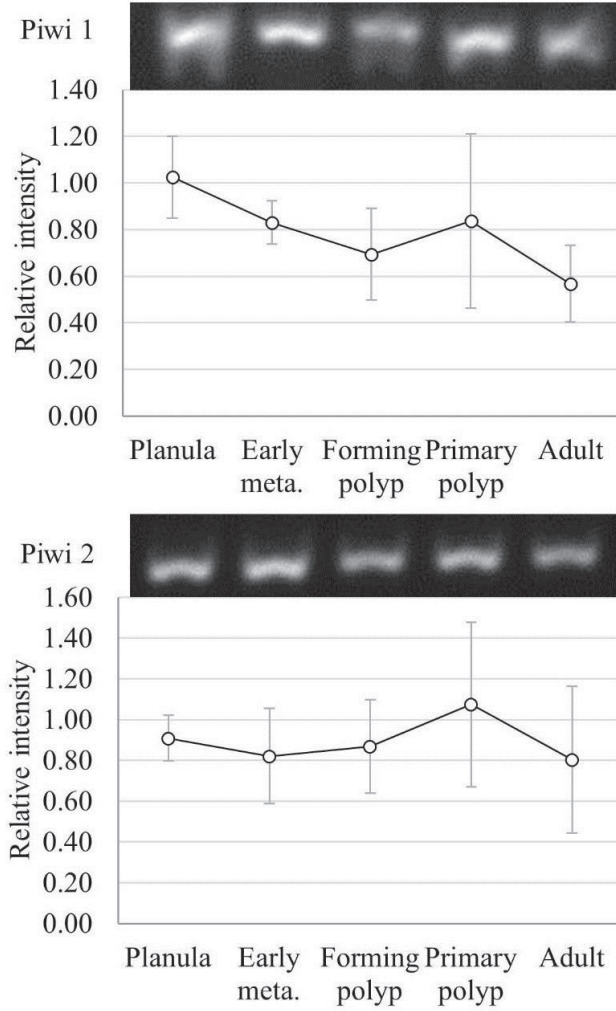


Figure 4-3: *piwi 1* and *piwi 2* expression through metamorphosis. Intensities were normalized using *eif5* as house-keeping gene. Data are expressed in mean relative intensity  $\pm$  1SD. No significant differences were detected between stages in both cases (ANOVA, p-value=0.21 and 0.79 for *piwi 1* and *piwi 2* expressions respectively). Early meta.: early metamorphosis.

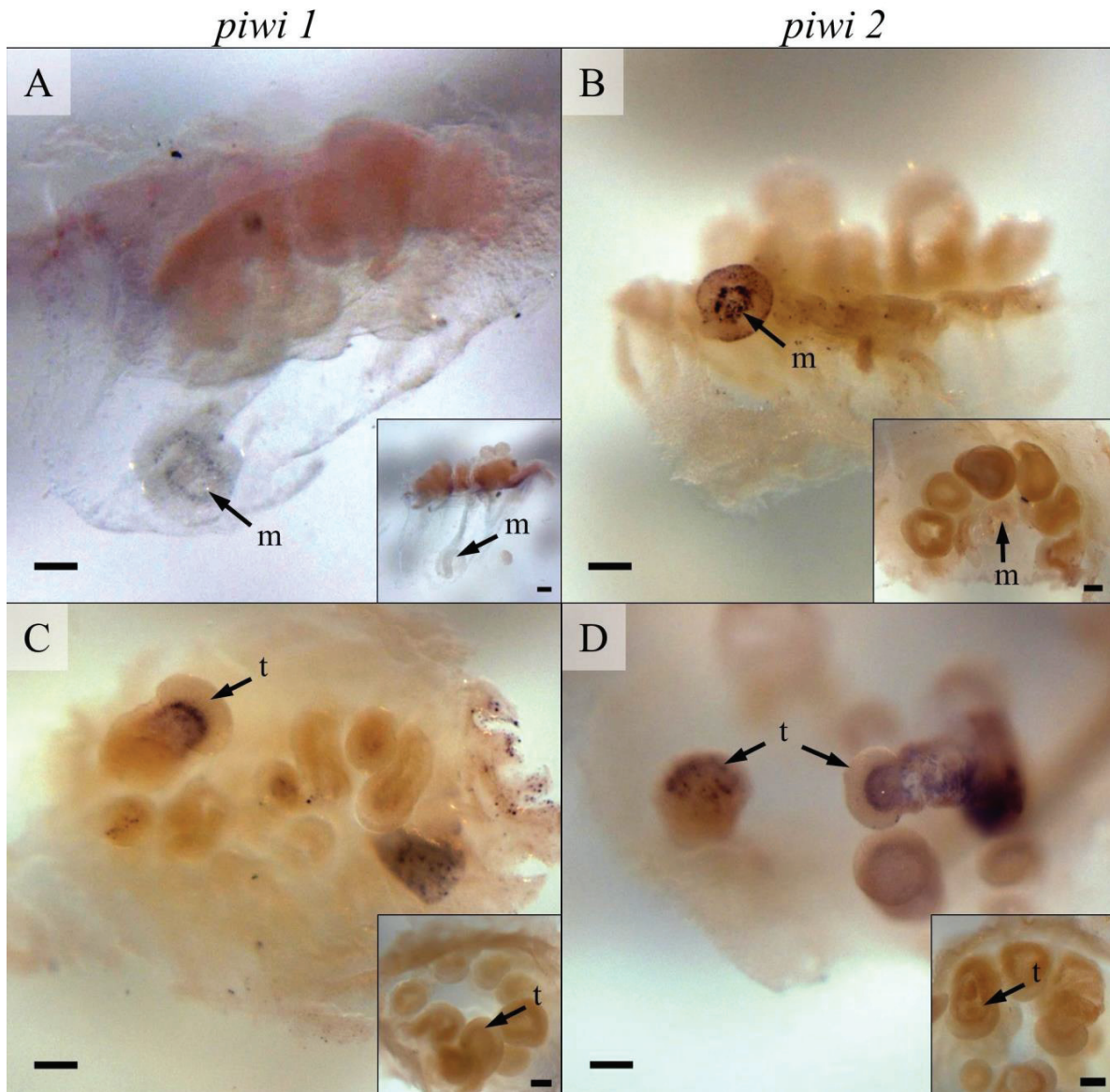


Figure 4-4: *piwi* expression pattern in *P. damicornis* adult polyps. Expression of *piwi 1* and *piwi 2* were localized in mesenteries, respectively illustrated in (A) and (B), and in tentacles tips, respectively illustrated in (C) and (D) Black arrows points to labeled areas. Insets present corresponding controls using sense probe. m: mesentery, t: tentacle. Scale bars 10  $\mu$ m.

### C. *pdcyst-rich* gene expression and protein localization

Expression levels of *pdcyst-rich* gene, assessed by semi-quantitative RT-PCR, reached a peak right after settlement, at the beginning of the metamorphosis (Figure 4-5) then it decreased in the forming polyp, before a slight increase at the primary polyp and adult stages. At the protein level of regulation, the Pdcyst-rich protein was immunolocalized in the cytoplasm of cells of the calicodermis in the adult demineralized polyp (Figure 4-6E) but not in the pse at the aboral pole of the planula (Figure 4-6A). In the primary polyp, it was detected at skeleton location against the calicodermis (Figure 4-6D). Surprisingly we could not detect it in thin sections (1  $\mu$ m) at the “early metamorphosis” stage nor the “forming polyp” stage (Figure 4-6B-C).

However, by using thicker histological sections (5  $\mu\text{m}$ , in paraffin) and a horseradish peroxidase (HRP) amplification step, we detected a signal at the apical pole of cells in the differentiating calicodermis, facing the skeleton (Figure 4-7). Interestingly, this Pdcyst-rich protein label is heterogeneously distributed along the calicodermis, with spatial discontinuity at all stages, from the forming primary polyp to the polyp of adult colonies and may react with specific cell types. These results must be confirmed, as the paper substrate on which coral larvae had settled was autofluorescent, and only the portion of tissue areas detached from it could be read unambiguously. Thus non fluorescent settlement substrates should be used. Additionally, the Pdcyst-rich protein could be detected by Western Blots of tissue extracts and its presence/absence compared across life stages.

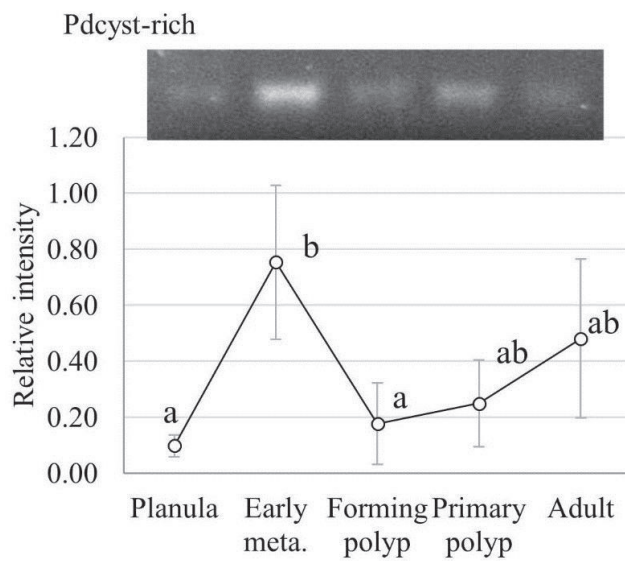


Figure 4-5: *pdcyst-rich* expression through metamorphosis. Intensities were normalized using *18S* as a house-keeping gene. Data are expressed in mean relative intensity  $\pm$  1SD. Different letters mean a significant difference (ANOVA followed by TukeyHSD test,  $p$ -value $<$ 0.05). Early meta.: early metamorphosis.



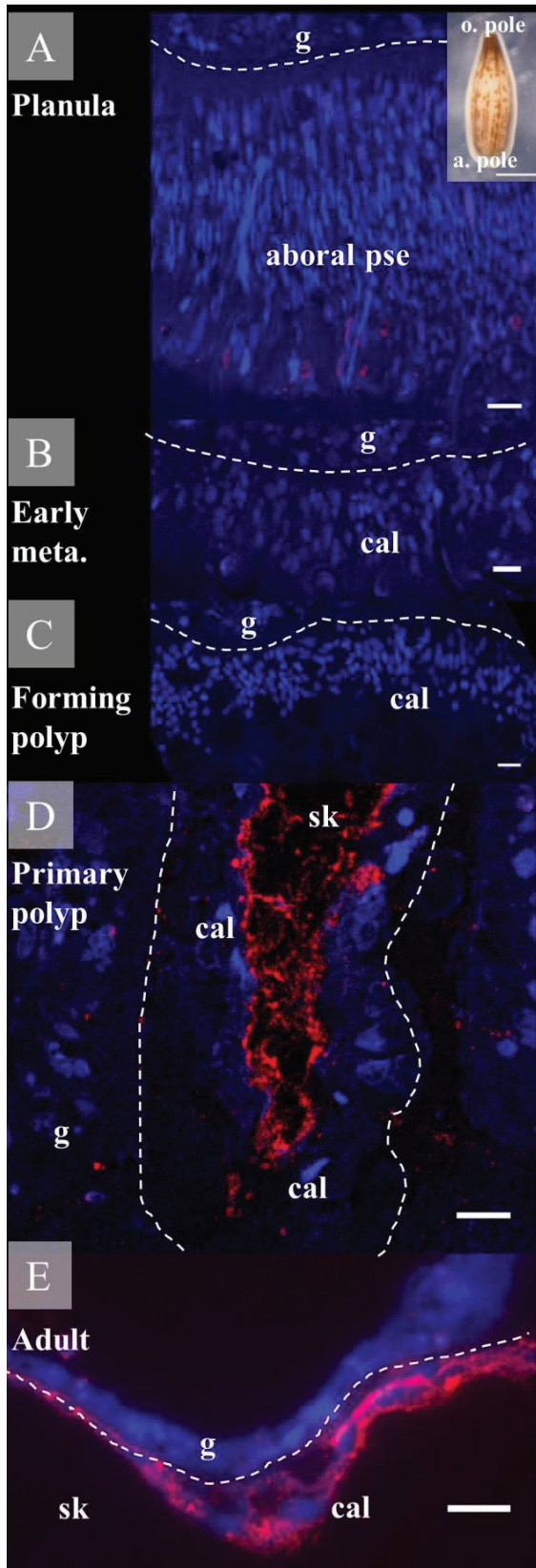


Figure 4-6: Pdcyst-rich protein localization through coral metamorphosis.

No signal in the aboral pseudostratified epithelium of the planula larva (A) neither in the calicodermis of both early metamorphosis (B) and forming polyp (C) stages. Pdcyst-rich protein was localized against the calicodermis in the non-demineralized primary polyp (D) and inside the calicodermis of the demineralized adult polyp (E). Dashed white lines indicate mesoglea and thus delimit cell layers. Early meta: early metamorphosis, o.pole: oral pole, a.pole: aboral pole, pse: pseudostratified epithelium, g: gastrodermis, cal: calicodermis, sk: skeleton location. Scale bars 10  $\mu\text{m}$ , 500  $\mu\text{m}$  in inset of (A).

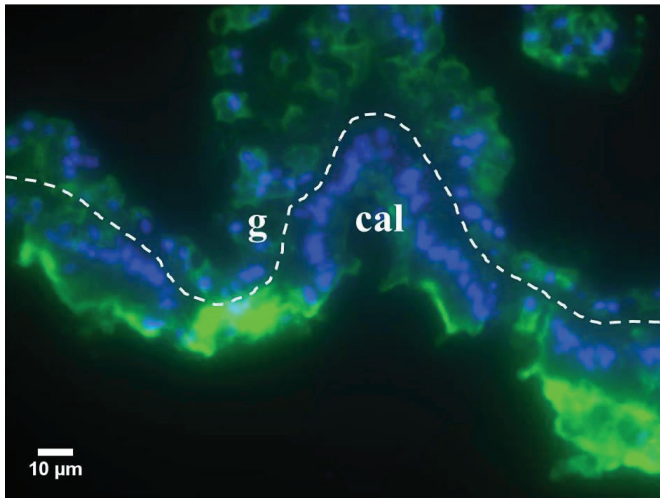


Figure 4-7: Pdcyst-rich protein localization in the forming polyp stage in thicker section and using an HRP amplification system. Nuclei are stained in blue (DAPI) and Pdcyst-rich is localized in green (Alexa 488). Dashed white line indicates mesoglea and thus delimits cell layers. g: gastrodermis, cal: calicodermis

## V. Discussion

### A. Proliferation and candidate precursor cells

In early metamorphosis, within the few hours following the initiation of larval settlement, the majority of cells in all tissue areas do not proliferate (Figure 4-1B) suggesting that onset of metamorphosis does not require cell division but rather implies tissue remodelling, including rapid transdifferentiation of the aboral pseudostratified epithelium of the planula, which will form the initial skeletal deposits. Growth of the calicodermis can then be explained, at least at primary polyp stage, by cell influx from highly proliferative tissue areas. These results are consistent with processes observed in another pocilloporid species, *Stylophora pistillata*, during metamorphosis in reef settings (Lecoite et al., 2016). Similar delayed proliferation processes have also been observed in the marine hydrozoan *Hydractinia echinata* where larval cells go directly through differentiation without dividing, and cell proliferation is recorded only nine hours after the onset of metamorphosis (Kroiher et al., 1990; Plickert et al., 1988). In *S. pistillata* growing primary polyp, cell migration from proliferative areas (mostly the pharynx) to the calicodermis has been highlighted, suggesting that precursor cells originate from outside this skeletogenic tissue, and pointing to a metabolic trade-off limiting cell division in favour of rapid skeleton deposition (Lecoite et al., 2016). In *P. damicornis*, our results indicate that cell proliferation is not restricted to the pharynx of the forming polyp, as a higher level of cell division was recorded in the surrounding pseudostratified epithelium (Figure 4-1). Low levels (< 5%) of proliferation in the calicodermis were observed, in agreement with the previous study on *Stylophora pistillata*, with a transient increase at the “forming polyp” stage, a developmental stage which was not examined in the former study. Moreover, here our results reveal high proliferation inside the mesenterial filaments and their associated cnidoglandular bands, two specific tissue areas that were not examined in Lecoite et al., 2016 and where gametogenesis of scleractinian corals is known to take place (Harrison, 2011).

In *Bilateria*, somatic and germinal cell lineages are well studied and both are separated, however the origin of this separation in early metazoans is still debated (Gold and Jacobs, 2013). In Hydrozoa, the freshwater *Hydra sp.*, which is the historically studied developmental model in *Cnidaria*, possesses three stem cell (SC) lineages (ectodermal, endodermal and interstitial (i-cell) stem cell lineages) which are well separated, with specific progeny. These are pluripotent SCs and one SC cannot differentiate into another SC type. Nevertheless in the marine *Hydractinia* model, this separation is less clear, with the possibility for i-cells to also differentiate into epithelial SC and hence all cell types; these cells are thus considered multipotent (Müller et al., 2004). Furthermore the “stemness” of *Hydra* epithelial lineages is discussed as these cells possess characteristics of differentiated cells. In *Anthozoa*, no i-cell lineage has been found so far, and only pluripotent epithelial cells have been described. In *Nematostella vectensis* (*Actinaria*, *Anthozoa*) gametes arise from endodermal cells. In *Orbicella faveolata* (*Scleractinia*, *Anthozoa*) Barfield et al., 2016 observed that somatic mutants did not transfer their mutation to gametes and thus argue in favor of a separation between somatic and germ stem cell lineages. The existence of i-cells could be restricted to *Hydrozoa*, and *Anthozoa* could contain only epithelial “stem cell” lineages. Further studies focused on anthozoan species are needed to answer this question. In *Hydra*, the three SC lineages express *piwi* homologues, *Hyli* and *Hywi* (Hemrich et al., 2012; Juliano et al., 2014). In other *Cnidaria*, like medusozoans *Podocoryne carnea* and *Clytia hemisphaerica*, but also in the ctenophore *Pleurobrachia pileus*, *piwi* is expressed in germ and somatic cells (Alié et al., 2011; Leclère et al., 2012; Seipel et al., 2004). Thus *piwi* expression does not seem to be restricted to one cell lineage. In *Scleractinia*, only one study localized *piwi* expression, in the solitary species *Euphyllia ancora*, only in the endodermal part of the mesenteries (Shikina et al., 2015), corresponding to an extension of the gastrodermis. Hence caution must be taken with the use of the term “stem cell” in *Anthozoa*.

In this study, we found two *piwi* genes, with preliminary expression pattern obtained for both in at least two tissue locations in the scleractinian coral *P. damicornis*, inside the mesenteries and at the base of the tentacle terminal bulb. Interestingly, inside the mesenteries, increased cell proliferation was recorded during late metamorphosis, both in the mesenterial filament and its cnidoglandular band compartments, where high proportions of BrdU labeled cells were detected (Figure 4-1B). These sites could be involved in the formation of dividing precursor cells, migrating to terminally differentiated epithelia, such as the calicodermis, or they could be involved in gametogenesis. Morphological characterization of the *piwi*-expressing territories in mesenteries by thin section and/or TEM is needed. Similarly, we propose that *piwi* expressing cells located near the tentacle terminal bulbs are likely to be involved as precursor cells for the nematocyte lineage (cnidarian stinging cells): indeed nematoblasts are known to differentiate while they migrate to their final position at the tip of tentacles. In the jellyfish *C. hemisphaerica*, *piwi* expression is localized at the base of tentacle bulbs, called the nematogenic ectoderm, which is the area that supply nematocytes to the tentacles (Denker et al., 2008; Leclère et al., 2012). Unfortunately, in this study of the coral *Pocillopora damicornis*,

tentacles retracted inside the polyp during fixation for the BrdU labeling experiments, preventing accurate assessment of cell proliferation in these areas.

In the “forming polyp” and “primary polyp”, tissues such as the pharynx and surrounding pse, and the cnidoglandular bands inside the mesenteries are all highly proliferative (Figure 4-1B), they share a common ectodermal ontogeny and connect with the calicodermis in the polyp basal floor. It is possible that precursors of the calicodermis originate from these areas and migrate while dividing to finally differentiate in the calicodermis, as suggested for *S. pistillata* (Lecoite et al., 2016). However, no *piwi*-expressing cells were detected in the pharynx of *Pocillopora damicornis*. If proliferative cells are scattered through the pharynx and surrounding pse, this dispersion could have prevented their detection with our current protocol of whole mount ISH, as this method is sensitive to revelation time and acquisition system sensitivity/resolution. Further experimentations are needed to investigate this hypothesis.

### **B. Pdcyst-rich protein and calicodermis differentiation**

There is more and more evidence about the involvement of proteins rich in cysteine residues in the calcium carbonate biomineralization process of scleractinian species. Fukuda et al., 2003 identified galaxin in *Galaxea fascicularis*, a cysteine-rich protein with cysteine tandem repeats and a potential role in calcification. A galaxin homologue and two galaxin-like proteins were later identified in the acroporid species *Acropora millepora* (Reyes-Bermudez et al., 2009). More recently, galaxin and a galaxin-like proteins have been found in the calcifying octocoral *Sinularia notanda* (Kim et al., 2015). A phylogenetically distinct family of Small Cysteine-Rich Proteins (SCRiPs) was also discovered in *Montastrea faveolata*, restricted to scleractinian corals, and hence was proposed to be involved in biomineralization (Sunagawa et al., 2009). In *Pocillopora damicornis*, our results confirm that another cysteine-rich protein, called Pdcyst-rich, is expressed in the calicodermis of polyps from adult colonies (Figure 4-6E, Vidal-Dupiol et al., 2009). Moreover, our new data show that this protein is absent from the planula larva and is expressed only in the calcifying life stages, at larval metamorphosis into primary polyp and during subsequent growth of the colony. This temporal expression pattern supports its validation as a biological marker for calicodermis differentiation. The new antibody developed against this protein cross-reacted with material located at the interface of the calicodermis and the skeleton in developing primary polyps of *P. damicornis*, as well as inside the calicodermis of adult colonies. Interestingly, this spatial distribution was highly heterogeneous, in the form of discontinuous hotspots along the calicodermis. The mRNA expression peak of *pdcyst-rich* recorded at early metamorphosis stage is expected to be correlated with a peak in protein translation, in the forming polyp. Using thin sections (1  $\mu\text{m}$ ) we did not detect Pdcyst-rich protein in the forming polyp. However, by using thicker paraffin-embedded tissue sections (5  $\mu\text{m}$  instead of 1  $\mu\text{m}$ ) and an additional amplification step of the fluorescent immunolabeling signal (mediated by horseradish peroxidase reaction with tyramide-conjugated fluorochromes in the presence of  $\text{H}_2\text{O}_2$ ), we were able to identify a signal in the calicodermis of the forming polyp (Figure 4-7),

which was also present in adult calicodermis and absent in the planula. One hypothesis is that the abundance of this Pdcyst-rich protein is too low in the early stages of metamorphosis to be detected without the use of thick sections and an amplification step. Future complementary Western Blot experiments are needed to further investigate this protein expression in tissue extract across life stages. Also, the skeleton is very rapidly deposited at the early stages (Gilis et al., 2014) and hence the corresponding low intracellular labeling intensity of the calicodermis may be explained by a potentially higher turnover of the protein at these early stages. In the adult, this protein amount might be higher and/or its turnover may slow down.

Preliminary bioinformatics analyses indicate that the Pdcyst-rich protein from *Pocillopora damicornis* clusters with predicted keratine-like proteins from another coral species *Acropora digitifera* (see supplementary Figure 3). In mammals and birds, cysteine-rich proteins with a keratin domain have been shown to have a role as structural proteins in respectively hair and feather mineralization (Strasser et al., 2014, 2015). Several studies on lizards, chicken, and humans have suggested the diversification of a gene cluster called epidermal differentiation complex, providing major structural proteins to the cornified layers of the epidermis. Genes with a cysteine/proline content superior to 50%. and involved in keratinocyte cornification have indeed been shown, in the western painted turtle *Chrysemys picta bellii*, to have evolved from this complex (Holthaus et al., 2015). The high cysteine content in organic matrix proteins of a broad range of Metazoans, including Pdcyst-rich protein in scleractinian coral, suggests a potential common ancestral role in the structural protein toolkit and for skeletogenic epithelium differentiation.

In conclusion, this study provides tissue-scale characterization of cell proliferation in the metamorphosing polyp of *Pocillopora damicornis* coral exposed to a 24 h BrdU pulse, and preliminary results on new molecular markers of putative somatic stem cells and calicodermis differentiation in scleractinian corals.

### Acknowledgements

A. Lecointe was funded by ERC Advanced grant no. 246749 'BIOCARB' to A.M. The PT-BIOP platform at EPFL Lausanne and the CeMIM platform at MNHN Paris are acknowledged for access to and help with fluorescence microscopy. We also thank the team of aquarist of the ATPD and Océanopolis for providing coral larvae and colonies and for access to and maintenance of aquaria.

## VI. Supplementary material

Table 4-S1 : PCR primer sequences used in semi-quantitative RT-PCR

<i>P. damicornis</i> Genes	PCR forward primer	PCR reverse primer
<i>pdyst-rich</i>	5' -CGCAAAGCCTTTCTTAGTTG-3'	5' -AGGCTCAAGGGAAAGACTGT-3'
<i>piwi 1</i>	5' -TCCCAGGTCATTGTTGGC-3'	5' -GCAACAAATCCACCAACAG-3'
<i>piwi 2</i>	5' -ACAATTGAAGACTGTGGC-3'	5' -AACTCTGACTTGTTCGTGT-3'
<i>Eif5</i>	5' -AGTCAATCATGGCTCTCGTC-3'	5' -TGCAAGGCTTTGGCAATTTC-3'
<i>18S</i>	5' -AATCCTGACTCAGGGAGGT-3'	5' -CACCAGACTTGCCCTCCAAT-3'

> anti-sense piwi 1 probe

5' -

CAGGAAACAGCTATGACCATGATTACGCCAAGCTATTTAGGTGACACTATAGAATACTCAAGCTATGCATCCAACGCGTTGGGAGCTCT  
CCCATATGGTCGACCTGCAGGCGGCCGCACTAGTGATTGCAACAAATCCACCAACAGAGCGGCCCTTCTGCAGACTATCATGATAAGTG  
TCAATTCCTATCACCATAGTCTCTTTCATAGGAATTTGACAGCCACGCTTCACCACCAAGTTTACAGTTTACAGTTTGGATGCCAATTT  
GGTGATACACTCATTACCATATTCTTCTTTGAGATGGTTCGGCCAACAATGACCTGGGAATCCCGCGGCCATGGCGGCCGGGAGCATG  
CGACGTCGGGCCCAATTCG-3'

> sense piwi 1 probe

5' -

TGTAAAACGACGGCCAGTGAATTGTAATACGACTCACTATAGGGCGAATTGGGCCCGACGTCGCATGCTCCCGGCCGCATGGCCGCGG  
GATTCACAGGTCATTGTTGGCCGAACCATCTCAAAGAAGAATATGGTAATGAGTGTATGCACCAAAATTTGGCATCCAGCTAAACTGTAA  
ACTTGGTGGTGAAGCGTGGGCTGTCGAAATTCCTATGAAAGGACTATGGTGATAGGAATTGACACTTATCATGATAGTCTGCAGAAGG  
GCCGCTCTGTTGGTGGATTTGTTGCAATCACTAGTGCAGCCGCTGCAGGTCGACCATATGGGAGAGCTCCCAACGCGTTGGATGCATA  
GCTTGAGTA-3'

> anti-sense piwi 2 probe

5' -

CAGGAAACAGCTATGACCATGATTACGCCAAGCTATTTAGGTGACACTATAGAATACTCAAGCTATGCATCCAACGCGTTGGGAGCTCT  
CCCATATGGTCGACCTGCAGGCGGCCGCACTAGTGATTAACCTCTGACTTGTGCGTGTACAATAATGTAAACGGGTTGGGGTAACTGTTCCC  
TGCCGTACATGCTGACTGACGAGGTAAAAGTGTACCACTCTCTCCTTGTGATTGTTGGTCCAGTATGGTGCAGGACCGGGGTTATC  
AAGTTTGGGCTGGGCCACCTCCCTGAGCTGCAAAGATTGCTGCATTGATTCTCTTTGACACGATCACCACCTGCCATCTTGGGGTGT  
AGTTACCACCAAGTGGACAAAACACTCGGAGAGCTGTTGCATTCATACCCAGCCACAGTCTTCAATTGAATCCCGCGGCCATGGCGG  
CCGGAGCATGCGACGTCGGGCCAATTCG-3'

> sense piwi 2 probe

5' -

TGTAAAACGACGGCCAGTGAATTGTAATACGACTCACTATAGGGCGAATTGGGCCCGACGTCGCATGCTCCCGGCCGCATGGCCGCGG  
GATTCGAATTGAAGACTGTGGCTGGGTATGAAAGTGCAACAGCTCTCCGAGTGTGTTTGTCCACTTTGGTGGTAACTATCACCCCAAGATGG  
CAGTGGTGTATCGTGTCAAAGAGAATCAATGCACGAATCTTTGCAGCTCAGGGAGGTGGGCCAGGCCAAACTTGATAACCCCGGTCCC  
GGCACCATACTGGACCACAAATCACAAGGAGAGACTGGTACGACTTTTACCTCAGTCAGTCAGCATGTACGGCAGGGAACAGTTACCCC  
AACCCGTTACATTATTGTACACGACAAGTCAGAGTTAATCACTAGTGCAGCCGCTGCAGGTCGACCATATGGGAGAGCTCCCAACGCG  
TTGGATGCATAGCTTGAGTA-3'

Figure 4-S1: Probe sequences used to target *piwi* mRNA in whole mount *in situ* hybridization

10 20 30 40 50 60 70 80 90 100

```

Ael_piwi1 KSADWSRETRGNALHSTVNLNEN--WLIVHTARDTNIANDFKSTIERVCGPMGKVKPKMIPIDNDRDITLRLAKNELDADR--PQIVTITVPTNRKDRY
Ael_piwi2 NTADWGRDATRQQVISAVDLHS--WVVVFKRDKQSKALEFISTMRQVIFVMGIVRDPHMIELRDDRTETYLRISIRENLHPR--VQMVVITFPTSRDDRY
Nve_piwi1 KSADWSREIRGAPLHSTVNLNEN--WVIVHTNRDSGVAITDFQQLTARVCGPMGINTIKPRMVPNLNDRDITSYLKALSNEIQADF--PQIVTIVPTNRKDRY
Nve_piwi2 DQADWGRDATREKVISAVNLNEN--WVVFTQRDSGKANDEFVQTMKICAPAMGIQVNQPKMNQLRDDRTETYLRISIRENLHQ--VQVVVVITFPTSRDDRY
Aqu_piwi1 AGADWSRDMRGKSMISSVNLKN--YLI VCTNRDAGVAEEFIGITIKRIGPMPGIMIDEQVEVLRNDRDITSFLRAVSGQLRDKS--TQMVIVLPQQKQKDL
Aqu_piwi2 LDADWSRQLVKEHVISAVPLTH--WLLLVTKRDSGKAVDFIEMMKKVCPPMGIEVKEPVIEIQTDKTELRLAIRENMSS--LQVVAIFPTQRDDRY
Efl_piwi1 GEPDWSREMRGASLISAVNHQN--YLMVFTSRDADKADQLFQTLIRVGPMPGMRFDEPQLAELPNDRITQFLQGIERQLTP--E--TQMVIVLPDLRDKDRY
Efl_piwi2 MEADWSRECLKEHVISAVSLD--WAVLIVRDKQKATDFVNMILSKVCPPIGMEVHEPKMVVEVNDRTESYLRAELIAPR--LQMVVITFPTSRDDRY
Che_piwi GNADWQKERTRGLLITSTFMNMQ--WVLIVSRQDEKVAQDFLRILTQTASPMGMRVADPQLCRDQSQDPRQYIQSLKEIQIKP--TEIIVCIVPNNRKDRY
Pca_Cniwi QFADWSRETRGKELISTVNMTN--WLLVYTKRDSNIANDFKQTLQRVCGPMGQVADPQMCRLNSDSAQTYFSTLKEQINPQ--TQIVVCI VPNNRKDRY
Hvu_Hyli READWGREATREAVITIGDINS--WVIVTKRDQPKAEFVQTMKQCCPQMGKFCGDPFFLALNDRDITETYLRITIRENLNQK--VQCVVITFPTSRDDRY
Hvu_HyWi SDADWTKESRGKMLLSFVSIK--WLLVFSQRDSNIAQDFKNTLQKVCGPMGMVAEPQLCRNLQDNAKAFITALKENITND--LQIVCIVPNNRKDRY
Pst_piwi1 KSADWSREMRGNPLHSTVNLKREKWLITRDKDTASAKDFALTLKKVCGPMGVNI EQPMEILPLDDRTDSYLVNVIKKNYDDD--LQMVVITLPTNRKDRY
Pst_piwi2 -----
Pda_piwi1 KTADWSREMRGNPLQSTVNLDS--WLLIYSSRDSGNAKDFAQTLNPKVCGPMGIVKSKSVECLQNLNDRITESYLEAIKGNFSDS--LQMVVITLPTNRKDRY
Pda_piwi2 -----
Spi_piwi1 RTAEWSREMRGNPLQSTVNLNEN--WLLIYNNRDSGNAKDFAQLTRVCKVCGPMGIQVSKPEYFELNNDRTESYLHAINERYNS--LQMVVVITLPTNRKDRY
Spi_piwi2 PQADWQGOAVKEQVITPVPLRN--WLLVYNNRDSKSAVEFVSMKIVTIPAMGIEVHPNMLELRDDRTETYLRIMIREHLNQQ--TQVWVITFPTSRDDRY
Mmu_piwi1 QFADWQKERTRGAFLISVPLDN--WLLIYTRRNYEAANSILIQLFKVTPAMGIQMKKAIMIEVD--DRTEAYLRALQQKVTSD--TQIVVCLLSNRKDRY
Mmu_piwi2 EDLHWKVEVTRDASILTIPMHF--WALFYPKRAMDQARELVNMLEKIAGPIGMIRISPPAWVELKDDRTIETYIRTISQLLGVGEKI QMVVCIIMGTRDDLY
Mmu_piwi4 FAADWSKDMRSCCKVLSQPLNR--WLVCCNRAEHLIEAFSLCLRRVGGSMGFNMGYPKIKVD--ETPAFLRAIQVHGDDP--VQLVMCILPBNQKNY
Pda_ago -----SLHDGARIEKVALACFCRR--CREDQLRXFSKQMGVNSRRQLRMSEEPVVVRYGRDAREVESLFSKVVWDIPGLQLIMAILPERDKQIY
Hvu_ago -----NGAWNMKGRRLYGKAIKKWGLIVYDIIKPLQNEVLIKFKQTEI LKSAKIEIGQIDN--PVYQARAPELPESVISKAFKKDKDIELLVTLPKGTIP--FY
Nve_ago -----GGVNDMRGRQQLFHGIEIRIWAIAACFVKQMQCTEDSLRRFSNQLMKISVQCGMPISCPVVFVFRYARNPDEVERMFRRLKEAHPDLQMLLVLPGKTI--VY

```

110 120 130 140 150 160 170 180 190 200

```

Ael_piwi1 DAIKKLCLEK-----PVPSQVIVSRITLSKKQMLMSVCTKIGIQLNCKLGGEAWALE-----IPLKLMVIGDVTYHDSA--E
Ael_piwi2 -----
Nve_piwi1 DSIKKLCLEK-----GVPSQVIVSRITLSKKQMLMSVCTKIGIQLNCKLGGEAWAVD-----IPLKNLMVIGIDTYHDS--Q
Nve_piwi2 AAVKKLCVES-----PVPSQVIVSRITLSKTSNPTKLRVSVQKIALQINVKLGGEALWALD-----IPTSRLMVCIGIDVYHDKA--R
Aqu_piwi1 DAVKKLCVDA-----PVPSQVIVSRITLSKKQMLMSVCTKIGIQLNCKLGGEALWALD-----IPLKNLMVIGIDTYHDSA--S
Aqu_piwi2 SSLLKLCVCE-----PVPQVINARTISQQLKRSVTQKVALQINVKLGGEALWAVK-----TPLENAMVIGIDVYHDS--R
Efl_piwi1 DAIKKFCCVDH-----PVPSQCVTARVLTKKQGLMSVATKIALQLDCKLGGEALWALE-----IPMNVMVIGIDYADHDIV--T
Efl_piwi2 SAIKKLCVES-----PVPQVLIARTITQQLKRSVQKVALQINVKLGGEALWAVE-----IPLKSMVIGIDVYHDKS--Y
Che_piwi DAIKKITCVEN-----PVPSQVIVSRITLSKKQMLMSVCTKIGIQLNCKLGGEVWATE-----IPVKKLMVIGIDVYHDSM--N
Pca_Cniwi DAIKKLCVER-----PVPSQVIVSRITLSKKQMLMSVCTKIGIQLNCKLGGEVWAVD-----IPLKNVMVIGIDVYHDSA--T
Hvu_Hyli AAVKKLCVIES-----PVPSQVINARTISQANKLRVSVQKVALQINVKLGGEALWALN-----IPMNVMVIGIDVYHDS--K
Hvu_HyWi DAIKKLCCVER-----PVPQVIVSRITLSKKQMLMSVCTKIGIQLNCKMGGNVWAVD-----IPIQ--VMVIGIDVYHDSL--T
Pst_piwi1 DAIKKLCLEK-----PVPSQVIVGRTISKKQMLMSVCTKIGIQINVKLGGEAWAVE-----IPLQKTVMVIGIDCYHDSL--T
Pst_piwi2 -----SQKIALQINCKLGGEALWALD-----IPLKSMVIGIDVYHDSA--R
Pda_piwi1 DAIKKLCLET-----PVPSQVIVGRTISKKQMLMSVCTKIGIQLNCKLGGEAWAVE-----IPMKRTVMVIGIDTYHDSL--Q
Pda_piwi2 SAVKKLCVES-----PVPSQVINARTISQQLKRSVTQKIALQINCKLGGEALWALD-----IPLKSMVIGIDVYHDSA--R
Spi_piwi1 DAIKKCCLEK-----PVPSQVIVSRITLSKKQMLMSVCTKIGIQLNCKLGGEAWAVE-----IPLKSMVIGIDTYHDSL--Q
Spi_piwi2 SAVKKLCVES-----PVPSQVINARTISQQLKRSVTQKIALQINCKLGGEALWALD-----IPLKSMVIGIDVYHDSA--R
Mmu_piwi1 DAIKKYLCIDC-----PTPSQCVVARTLGKQVTMAIATKIALQMNCKMGGELWVRVD-----MPLKLMVIGIDCYHDTT--A
Mmu_piwi2 DAIKKLCVQS-----PVPSQVINVRTIGQPTLRVSVQKILLQMNCKLGGEALWAVD-----IPLKSMVIGIDVYHDS--R
Mmu_piwi4 DSIKKYLSDC-----PVPSQCVLRTLNKQGIMLSVATKIAMQMTCKLGGEALWSVE-----IPLKSMVIGIDICRDLA--N
Pda_ago PEIKRVDGN-----VIGIPTQCQVQSKHVNRTN--PQVCANIALKINSKLGGINHVIDPGVKSPP--VFREPVIIFGADVTHPSPTEN
Hvu_ago GDIKRLCETENGFNQSDPGVQNLINKNGVCTCQIQSKNLKCN--PMTLAQCLKINSRMGGTNNVDSNNKIRPLNVPFKEPVIFLGDVTHPELGLGK
Nve_ago AEVKRVGDT-----MLGVITCQIQGNVTKPS--PQTLNLKLIKINAKLGGVNNILAPEIRPP--VFREPAIFLGDVTHPPAAGD

```

210 220 230 240 250 260 270 280 290 300

```

Ael_piwi1 KGRSVGGFVASLNQTLTR--YYSRCTFQHSG----QELIDGLKVCMAAALRKYQEING--MLPDKIIMYRDGVGDDQLLQVIVTEHEVSQLCQFKI IQSG
Ael_piwi2 -----
Nve_piwi1 KGRSVGGFVASLNKPCTRQREYYSRCTFQHSG----QELVDGLKVCMTAALRQWQING--VLPDKIIVFRDGVGDDQLRAVIEHEVPQILSTFKFQDQ
Nve_piwi2 GGRSVGGLVCSMNRSLTR--WYSDVCFQSPG----QELIDGLKMLLIRKIRKWHVNM--ALPERIIVYRDGVGDDQLKVAVAGVEVQFEECFASFGES
Aqu_piwi1 KGRSVAAFIASNSTLIR--YYSQTMFQSSG----QELGDNLMKACMIMALKKYSINN--TFPDRIVVYRDGVGDDQLHIVKEHEVQMLESFSSSTSGD
Aqu_piwi2 GKRSVLFVGSSTNKFFTR--WYSRVITQGAN----QEIGDLKICFQSLSRKYEINH--NLPDRIIVFRDGVGDDQVKTIVVEFEIPQMKSCLMFMGES
Efl_piwi1 RGRSVCGFIASNTQSLR--YYSQCFQHTG----QELADNLKVMASKALQKYYHINK--VLPDRIIVYRDGVGDDQLAMVVNYEVPQMDTDFKQFSSG
Efl_piwi2 GNKSIAGFVASTNPFTR--WYSRVAMQESQ----QELIDGLKMLCQALAKKYEMNQ--SLPERIIVFRDGVGDDQLEIVSNEYVQQLQDQCFLLNDS
Che_piwi KGQSIGGFVASTNDSLIR--YYSRITKQRSH----QEICDQKICMGTGALKKYEYVNG--HDPDRIIVYRDGVGDDQIVDVKDHEVPQFKAALQEFENP
Pca_Cniwi KGKSIGGFVASTNRYLIR--YYSRITSQISH----QEICNQKLCVMTGALKKYEYVNH--TLPDRIIVYRDGVGDDQNSDGYEHELPLQKASFSAQAN
Hvu_Hyli GRSVGGFVASTNSTFTR--WYSRVCFQNGI--QELIDGLKLCFVGLKYYHEDNH--SLPEKIIVFRDGVGDDQLEIVSNEYVQQLQDQCFLLNDS
Hvu_HyWi KGKSIGGFVASTNKLIR--YYSRITAHTSH----QEICDQKICMGTGALKKYEYVNH--TLPDRIIVYRDGVGDDQLEIVSNEYVQQLQDQCFLLNDS
Pst_piwi1 KGRSVGGFVASMNKLIR--YHSRVTQHTG----MELIDELKTCMTAALKKYEYVNH--DLPDRIIVYRDGVGDDQLRIVVEHEVPQLKASFQIAGG
Pst_piwi2 GGRSVGGFVASMNKLIR--WFSRVCVQSPG----QELIDGLKMLTASLKKYEYVNH--TLPDRIIVFRDGVGDDQLRTVAGVEVQQLSECYTLFGES
Pda_piwi1 KGRSVGGFVASTNATLIR--YYSRVTQHTG----MELIDGLKMTAALKKYEYVNH--GLPDRIIVYRDGVGDDQLKVVNHVEVPQLKASFQDLPTD
Pda_piwi2 GGRSVGCFVASMNKLIR--WNSRVCVQSPG----QELIDGLKMCVSVSLKKYEYVNH--ALPDRIIVYRDGVGDDQLKIVVAGVEVQQLSECVFHFGEN
Spi_piwi1 KGRSVGGFVASTNPTLIR--YYSRVTQHTG----MELIDGLKMTSMTGSSSI-----
Spi_piwi2 KGRSVGCFVASMNKLIR--WNSRVCVQSPG----QELIDGLKMLSVSLSKKYEYVNH--TLPDRIIVYRDGVGDDQLKIVVAGVEVQQLSECFVHFVGN
Mmu_piwi1 GRRSIAGFVASINEMTR--WFSRVCVQDRG----QELVDGLKVCQALRAWSGCNE--YMSRVIIVYRDGVGDDQLKTVNVEVQDLCKLKSVMG
Mmu_piwi2 GMRVVGGFVASINLTIR--WYSRVQMPH----QEIVDSLKLCVGSLSKKYEYVNH--CLPEKIVVYRDGVGDDQLKTVNVEVQDLKQCFEAFDN
Mmu_piwi4 KVVVVGGFVASINRIR--WFSRVCVQRTA----ADTADCLKVCMTGALNRWYRNH--DLPDRIIVYRDGVGDDQLKIVVAGVEVQQLSECVFHFVCG
Pda_ago GIPSIAAVASMNDANATK--YCARVRAQNHKSGKAQEIIINDLAVMVELLIDIFYKANRKLKPKNIIFYRDGVSEGGFQDQVILVHEVRAVQQAICMLEDK
Hvu_ago SPSIAAVGSIDEVPSR--YSACVRIQTHR-----VEVIDENLVITELLQKDYRHMK--VKPKIIMFRDGVSEGGFQVQLVHEMVAIQKACIKLEK
Nve_ago KRPSVAAVVGSMADHLSR--YASRVRQTHR----QEIIAELAAMVRELLVQFVYRSTR--HKPQIRIVYRDGVSEGGFQVQLVHELKAIREACTIKLEV

```

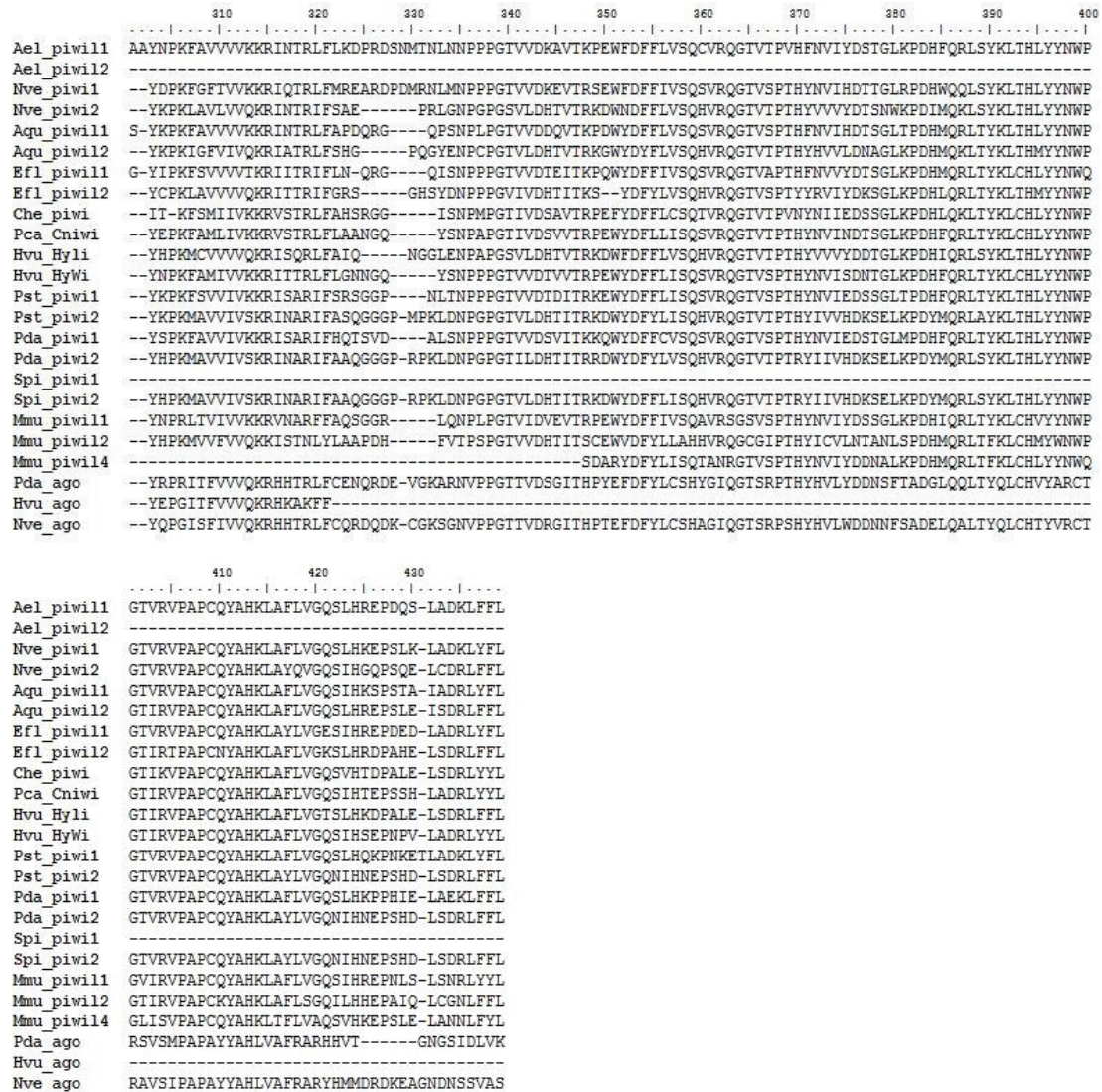


Figure 4-S2: Piwi-like Eukaryote domain alignment used to generate phylogenetic tree of Figure 4-2. Ael: "*Anthopleura elegantissima*", Aqu: "*Amphimedon queenslandica*", Che: "*Clytia hemisphaerica*", Ean: "*Euphyllia ancora*", Efl: "*Ephydatia fluviatilis*", Hvu: "*Hydra vulgaris*", Mmu: "*Mus musculus*", Nve: "*Nematostella vectensis*", Pca: "*Podocoryna carnea*", Pda: "*Pocillopora damicornis*", Pst: "*Pseudodiploria strigosa*", Spi: "*Stylophora pistillata*"



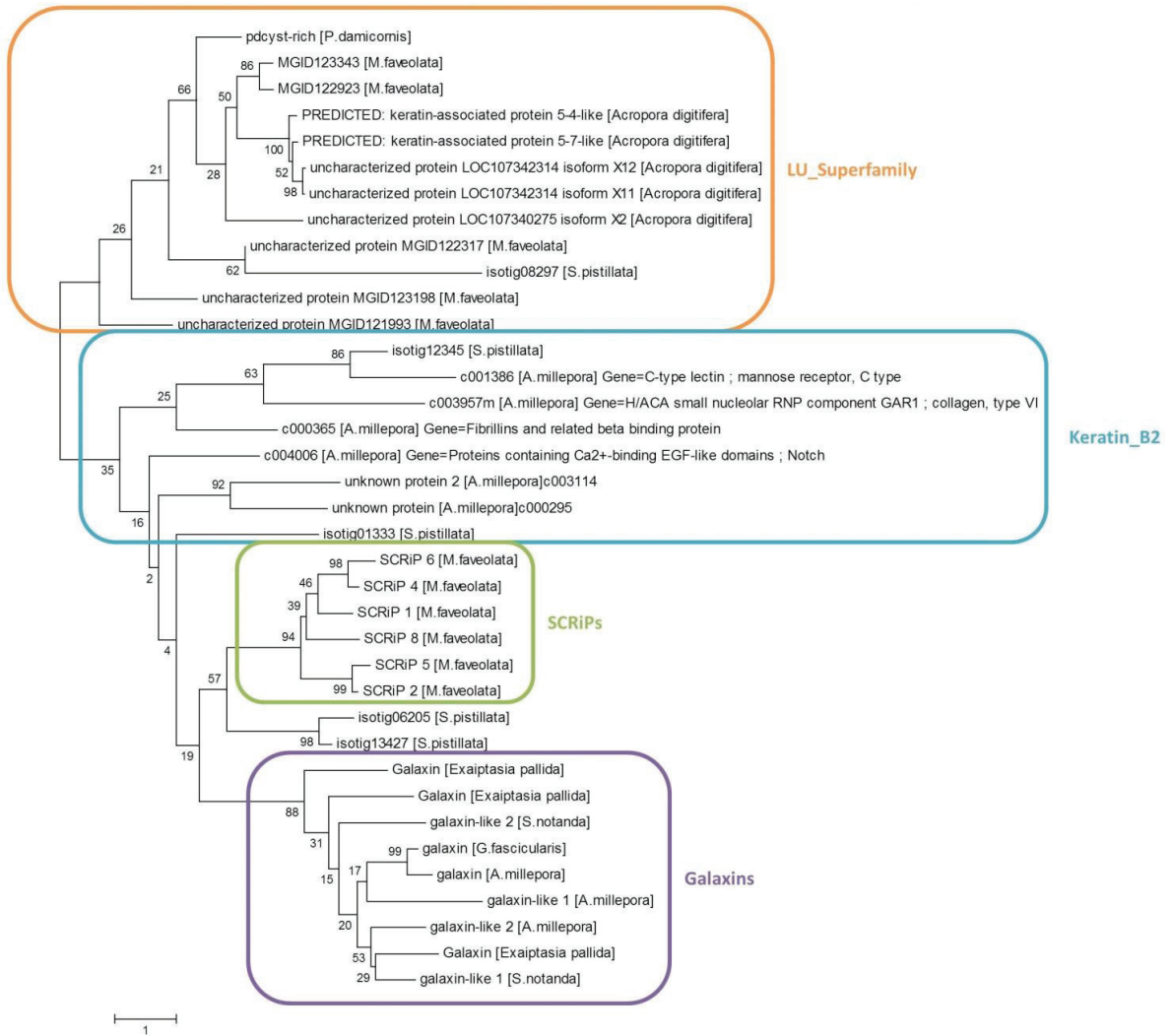


Figure 4-S3: Pdcyst-rich associated protein maximum likelihood tree. Preliminary results. Constructed using the Jones-Taylor-Thornton (JTT) model of amino-acid substitution with bootstrap (1000) support values above branches. Pdcyst-rich protein is clustered with keratin-associated proteins of *Acropora digitifera*.



# Chapter 4: Tracing isotopically labeled biofilm compounds into coral host tissue during settlement

## I. Abstract

Larval recruitment is a critical step in the life cycle of reef-building corals. Location of settlement of the scleractinian planula larva will determine the chances of survival and the probability of successful establishment of colony. Environmental cues, physical or chemical, play a major role in this process (Hadfield and Paul, 2001) and their study is important in the context of reef decline. The metabolic pathways involved in larval settlement remain to be elucidated and whether the chemical cues are acting at the cell surface or intracellularly in planula tissue is not known. In this study, newly released *Pocillopora damicornis* planulae were exposed to isotopically labeled ( $^{15}\text{N}$ ,  $^{13}\text{C}$ ) mature crustose coralline algae-containing biofilms. High resolution isotopic imaging with NanoSIMS allowed us to visualize a few  $^{13}\text{C}$  and/or  $^{15}\text{N}$  enrichment spots (<1  $\mu\text{m}$  diameter) in the calicodermis of metamorphosed larva. An unsettled planula showed similar enrichment spots in its pharynx, with the rest of the tissue unlabeled. Although preliminary, these results indicate that there are transferable cues, from biofilm to the larva that are potentially involved in the induction of metamorphosis in scleractinian corals.

## II. Introduction

In the search for determining settlement inducers of coral metamorphosis, most studies have focused on chemical cues from bacterial biofilms growing on surfaces or associated with crustose coralline algae (CCA) (Baird and Morse, 2004; Grasso et al., 2011; Tebben et al., 2011). Several chemical cues have been identified, such as tetrabromopyrrole (TBP) produced by bacterial genus *Pseudoalteromonas* isolated from CCA surface biofilm (Sneed et al., 2014; Tebben et al., 2011). However, a recent study in five coral species (*Acropora millepora*, *A. tenuis*, *A. globiceps*, *A. surculosa*, and *Leptastrea purpurea*) pointed out that metamorphosis induced by TBP was not ecologically realistic because it occurred without settlement of the larvae on the substrate, on the contrary when induced by CCA or CCA cell wall-associated compounds (glycoglycerolipids and polysaccharides) larvae properly settled and underwent metamorphosis (Tebben et al., 2015). Also they obtained same metamorphosis rates with CCA treated or not with antibiotics, showing that the associated biofilm was not involved in the process. Nevertheless, if bacterial cell wall components are the metamorphosis cues, they are still present after antibiotics treatment. In *Acropora microphthalmia* settlement and metamorphosis was induced with 8-weeks old biofilms in the absence of CCA (Webster et al., 2004). If CCA and/or associated biofilms can induce proper metamorphosis it is not clear what are the compounds involved.

Regarding potential internal responses to such cues, the GLW-amide neuropeptide family has been shown to induce metamorphosis in hydrozoans and a few scleractinian corals, e.g. *Acropora* sp., *Montastrea faveolata*, and is thought to act as a hormone (Erwin and Szmant, 2010; Iwao et al., 2002). Environmental cues might trigger neuropeptide secretion from planula neuro-epithelial cells which will act on the tissue to provoke metamorphosis (Takahashi et al., 2011). Nevertheless, in contrast with CCA induced metamorphosis, metamorphosis induced by exposure to neuropeptides is not always combined with settlement (Erwin and Szmant, 2010; Iwao et al., 2002). A study on gene regulation after either a CCA-induced or a TBP-induced metamorphosis indicates that GABA (gamma-aminobutyric acid) transporters, which are involved in neurotransmission process, are upregulated in the presence of TBP, whereas there are no changes in expression after CCA extract inducement (Siboni et al., 2014). The change of expression from TBP- to CCA-induced metamorphosis indicates that TBP inducement uses a different signaling pathway than CCA-inducement. Thus, it is clear that chemical compounds can induce partial or complete metamorphosis in coral larvae, but the identification of these cues is still under debate and the molecular mechanisms underlying this conversion of external cues into internal signals are generally poorly understood. Whether the molecular signal is integrated inside the larval tissue or not is not known. To begin answering this question, we labeled a mature biofilm (containing CCA) with stable isotopes ( $^{13}\text{C}$  and  $^{15}\text{N}$ ) and exposed *Pocillopora damicornis* planula larvae to it. The presence of stable isotopic enrichments within the tissue of unsettled planulae and properly settled and metamorphosed larvae was investigated with high resolution secondary ion mass spectrometry (NanoSIMS) imaging.

### III. Material and methods

#### A. Biofilm labeling with stable isotopes and larvae exposure

Planulae were obtained from the public aquarium of Océanopolis (Brest, France) where larvae are emitted regularly from large colonies of *P. damicornis* scleractinian coral. Mature biofilms were grown in closed-circuit aquaria and recirculating artificial seawater equilibrated in large exhibit tanks during 5 months on under-water papers (~10x15 cm) at the Aquarium Tropical du Palais de la Porte Dorée (ATPD, Paris, France). At the time of the experiment underwater papers were totally covered with recognizable crustose coralline algae (CCA), filamentous red and green algal turf (See supplementary Figure 5-S1, pictures from A. Massé). Biofilms were then transferred in beaker filled with 300 mL of artificial seawater (ASW) modified from Harrison et al., (1980) made of 355.6 mM NaCl, 24.4 mM Na<sub>2</sub>SO<sub>4</sub>, 7.9 mM KCl, 46.2 mM MgCl<sub>2</sub>, 9 mM CaCl<sub>2</sub>·2H<sub>2</sub>O and completed with isotopically labeled 1.3 mM sodium bicarbonate ( $^{13}\text{CHNaO}_3$ ), 5 μM ammonium chloride ( $^{15}\text{NH}_4\text{Cl}$ ) and 5 μM potassium nitrate ( $\text{K}^{15}\text{NO}_3$ ) (ASWi), final salinity 28‰. Unlabeled control biofilms were exposed to similar concentrations of unlabeled sodium bicarbonate, ammonium chloride, and potassium nitrate. During 5 days ASWi was renewed twice a day and experimental settings were as follows: pH 8.29±0.2, temperature 25.5±0.6°C, under 12/12h light period. After the 5 days enrichment period, bio-

film were rinsed several times and 3 mm diameter discs of biofilm were sampled in a fixative solution of 2.5% glutaraldehyde, 0.8% paraformaldehyde, 0.2% picric acid, 10 mM  $\text{CaCl}_2 \cdot 2\text{H}_2\text{O}$  in 0.1 M Sørensen-phosphate-0.6 M sucrose pH 8. Rest of biofilm was used for incubation with freshly released planula larvae ( $n=30$ ) from the morning or the day before. Control experiments were achieved in the same conditions with unlabeled biofilm ( $n=30$ ). The following morning ( $t=16$  h), after 3 h light–12 h dark–1 h light, 3 mm diameter discs of biofilm were again sampled in fixative solution, as well as unsettled planulae, and metamorphosed larvae that had settled on the substrate. The latter are characterized by a disc-shape structure with no tentacles yet developed and refers as “early metamorphosis” stage.

### **B. Histological procedures**

After 24 h at 4°C in the fixative solution, samples were prepared for microscopy and NanoSIMS as follows: rinsed in PBS (Phosphate buffered saline, pH 8) and post-fixed in osmium ( $\text{OsO}_4$ ) 4% in Sørensen 0.1 M, rinsed and dehydrated in graded series of ethanol before embedding in Spurr resin with polymerization for a few days at 60°C. Resin blocs were cut in semi-thin sections (1  $\mu\text{m}$ ) with a 35° diamond knife (Diatom) on an ULTRACUT microtome at the MNHN PtME platform for electron microscopy (Paris, France). A longitudinal section going through the pharynx was put on a glass slide and stained 10 s with toluidine blue stain (1% in sodium borate 1% buffer) and the following serial section was placed on 10 mm diameter coverslip, suitable for both NanoSIMS holders and SEM holders. Stained sections were mounted with Eukitt medium and acquired under light microscope Olympus Slide Scanner (Objectif 40x) at the Bioimaging and optics platform (BIOP, EPFL, Lausanne).

### **C. Scanning electron microscopy in backscattered electron mode (SEM, BSE)**

For tissue orientation and ultrastructure identification, semi-thin tissue and biofilm sections were first observed on a scanning electron microscope (SEM) Hitachi SU 3500 from the Electron Microscopy Platform (PtME, MNHN, Paris, France) using back-scattered electron detector (BSE), in collaboration with Dr. S. Djediat. The SEM was operated at 10 kV under 50 Pa.

### **D. NanoSIMS isotopic imaging**

The tissue and biofilm sections observed in SEM were then coated with ~10 nm gold before analysis with the NanoSIMS 50L ion microprobe (Cameca) in the Laboratory for Biological Geochemistry (EPFL, Lausanne, Switzerland). Samples were bombarded with a 16-keV primary ion beam of caesium (1 to 3 pA). Secondary molecular ions  $^{12}\text{C}_2^-$ ,  $^{13}\text{C}^{12}\text{C}^-$ ,  $^{12}\text{C}^{14}\text{N}^-$ , and  $^{12}\text{C}^{15}\text{N}^-$  were simultaneously collected in electron multipliers at a mass resolution sufficient to avoid potentially problematic isobaric interferences on  $^{13}\text{C}^{12}\text{C}^-$  and  $^{12}\text{C}^{15}\text{N}^-$ . Isotopic images (256 × 256 pixels) of 40 × 40  $\mu\text{m}^2$  were obtained. Distribution maps of the  $^{13}\text{C}/^{12}\text{C}$  and  $^{15}\text{N}/^{14}\text{N}$  ratios were obtained by taking the ratio between the drift-corrected  $^{13}\text{C}^{12}\text{C}^-$  and  $^{12}\text{C}_2^-$  images and the  $^{12}\text{C}^{15}\text{N}^-$  and  $^{12}\text{C}^{14}\text{N}^-$  images, respectively.  $^{13}\text{C}$  and  $^{15}\text{N}$  enrichments were expressed in the  $\delta$  notation

$$\delta X(\text{‰}) = \left( \frac{X_{mes}}{X_{nat}} - 1 \right) \times 1000 \quad (1)$$

where  $\delta X$  is either  $\delta^{13}\text{C}$  or  $\delta^{15}\text{N}$ ,  $X_{mes}$  is the measured  $^{13}\text{C}/^{12}\text{C}$  or  $^{15}\text{N}/^{14}\text{N}$  ratio, and  $X_{nat}$  is the average natural  $^{13}\text{C}/^{12}\text{C}$  or  $^{15}\text{N}/^{14}\text{N}$  ratio measured in non-labeled samples. To obtain quantitative enrichment of a specific area, region of interest (ROI) where delimited.  $\delta$  value are reported as mean  $\pm$  1SD of total pixels included in the selected ROIs.

### E. Transmission electron microscopy (TEM)

In parallel, ultrathin (70 nm) sections of early metamorphosis larva were cut, contrasted with saturated uranyl acetate 50 % in ethanol at room temperature and acquired using a TEM Hitachi H-7100 at 75 kV at the PtMe (MNHN, Paris, France).

## IV. Results

After 5 days incubation with isotopically labeled ASW, isotopic enrichment in bacteria from the biofilm surface was measured with NanoSIMS. The  $\delta^{13}\text{C}$  and  $\delta^{15}\text{N}$  enrichments averaged  $741 \pm 220\text{‰}$  and  $7361 \pm 2472\text{‰}$ , respectively (Figure 5-1). Carbon enrichment is lower than nitrogen probably because of  $^{13}\text{C}$  dilution due to fixation and epoxy embedding that adds additional  $^{12}\text{C}$  atoms (Pernice et al., 2015). After 16 h exposure to the isotopically labeled biofilm, 19 larvae settled on UWP and started metamorphosis (63%), only one did not settle. In a similar control experiment using biofilm with normal isotopic composition 26 (87%) settled in the same 16 h time interval, only one did not settle. Note that, after 16 h in isotopically normal ASW, the biofilm was still enriched, with a slight decrease due to dilution of  $^{13}\text{C}$  and  $^{15}\text{N}$  with  $^{12}\text{C}$  and  $^{14}\text{N}$ , respectively, yielding average  $\delta^{13}\text{C}$  and  $\delta^{15}\text{N}$  enrichments of  $515 \pm 85\text{‰}$  and  $4992 \pm 1381\text{‰}$ , respectively (Figure 5-1). Both planulae and metamorphosed larvae presented  $^{13}\text{C}$  enrichment in some of their dinoflagellates, localized in the primary starch around the pyrenoid (Figure 5-2).

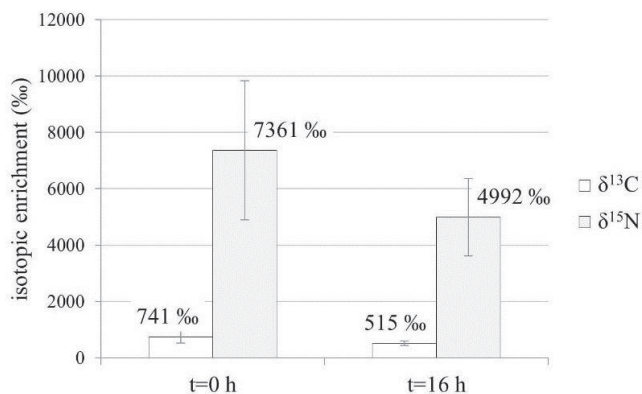
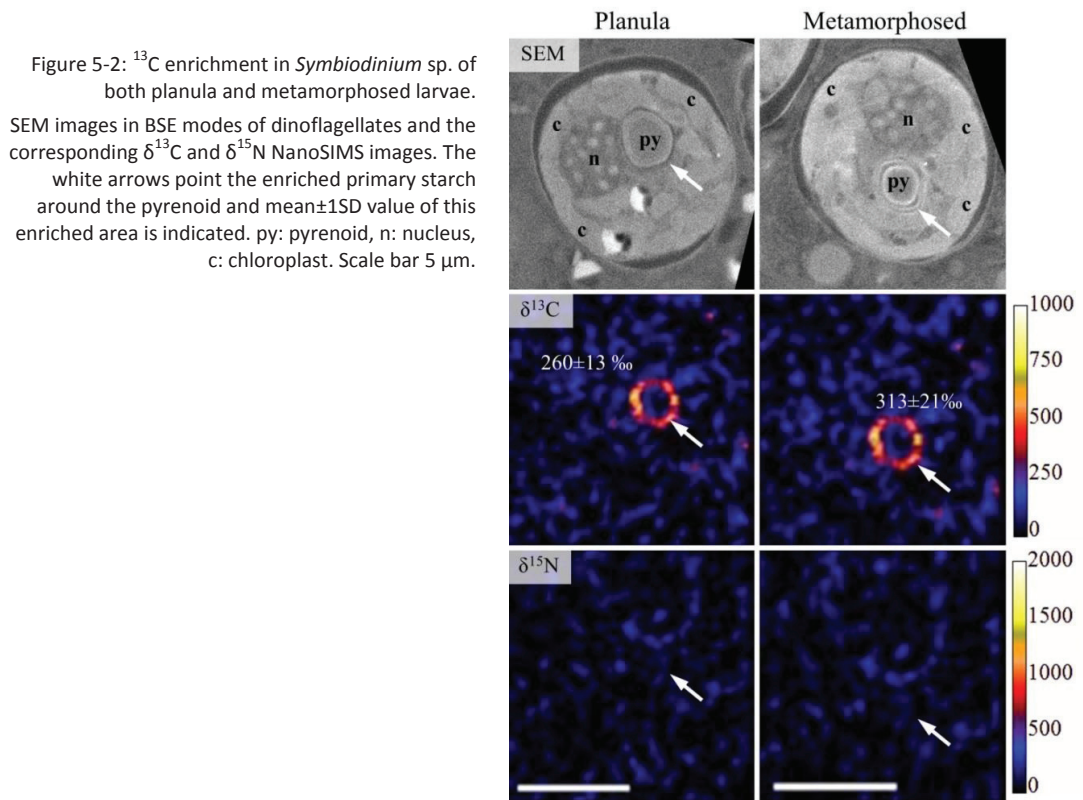


Figure 5-1: Isotopic enrichment in bacteria from biofilm after 5 days incubation with stable isotopes (t=0 h) and 16 h after transfer in normal seawater in the presence of planulae.



In the planula, no enrichment was observed in the future calcicodermis, i.e. the aboral pseudostratified epithelium (pse) neither the gastrodermis. Nevertheless, one spot of  $\delta^{15}\text{N}$  was observed with an enrichment of  $657 \pm 87\%$  in the pharynx area of the oral pse (Figure 5-3). Although this represents a clear detection, it has been observed only once in the all pharynx surface of the section imaged (pharynx area:  $3000 \mu\text{m}^2$ ) and calls for further investigation.

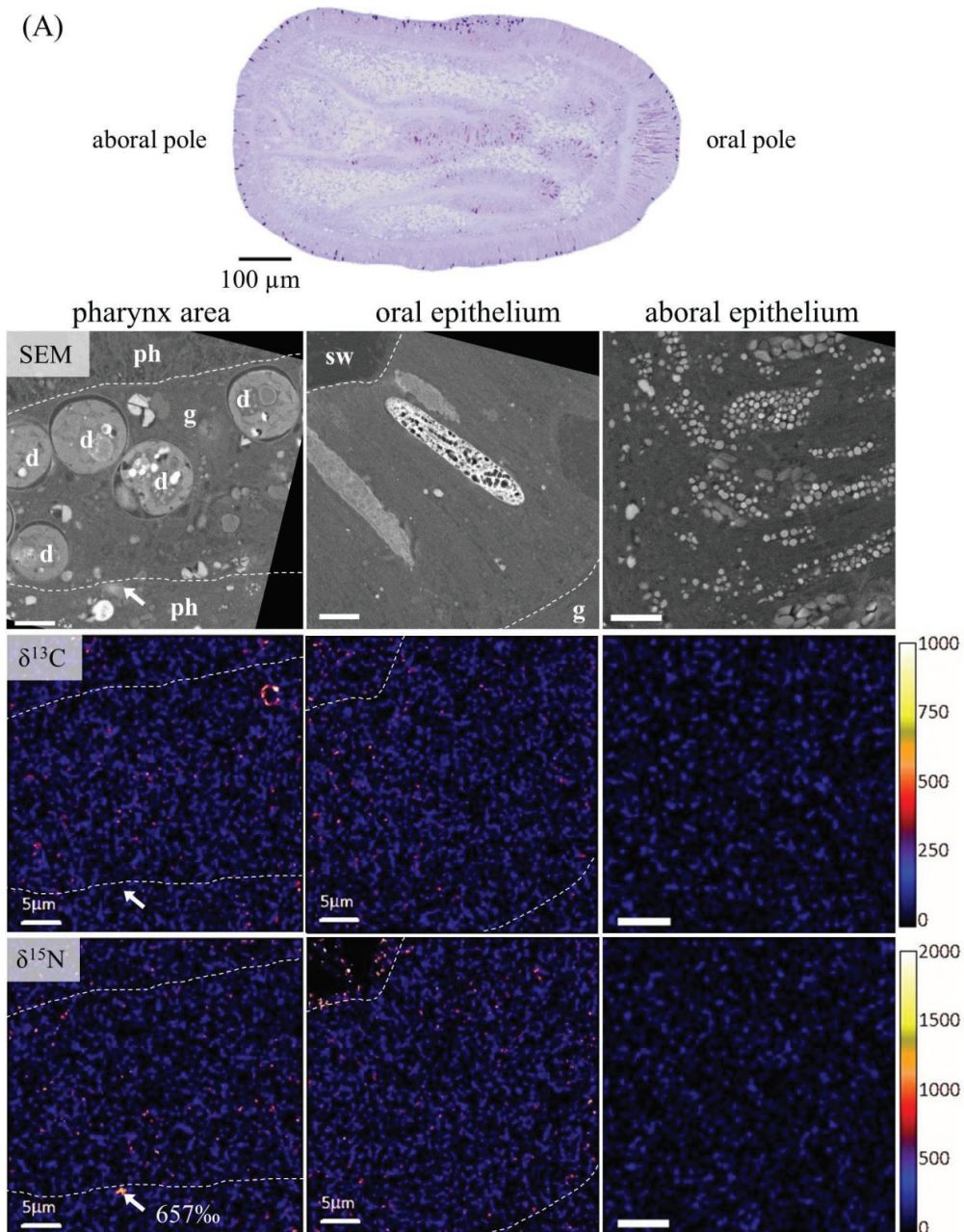


Figure 5-3: Isotopic ratios in the unsettled planula.

(A) Toluidine blue stained semi-thin ( $1\ \mu\text{m}$ ) section of a *P. damicornis* planula. Panel underneath shows SEM and corresponding NanoSIMS images of the different epithelium in the planula. A spot of  $^{15}\text{N}$  enrichment ( $657\pm 87\text{‰}$ ) is observed in the pharynx area (white arrow). ph: pharynx, g: gastrodermis, d: dinoflagellate, sw: seawater. Dotted line indicates mesoglea and thus cell layer limits. Scale bars: (A)  $100\ \mu\text{m}$ , panel  $5\ \mu\text{m}$ .

In the metamorphosed larva, no enrichment was observed in the pharynx, neither in the pse nor in the gastrodermis. Several enrichment spots were observed in the differentiating calicoderms (Figure 5-4). Total surface of calicoderms available on the section was about  $40,000\ \mu\text{m}^2$  and 11 images ( $40\times 40\ \mu\text{m}$ ) were acquired, covering around a third of the surface ( $13,200\ \mu\text{m}^2$ ). Five of these images exhibited 1 to 3 enrichment spots with sizes under  $1\ \mu\text{m}^2$ . Among these enrichment spots, two types were identified: 1) structure-



associated  $^{15}\text{N}$ -enrichment spots without  $^{13}\text{C}$ -enrichment (Figure 5-4, columns I-II), and 2) spots not associated with visible structures and enriched in both  $^{13}\text{C}$  and  $^{15}\text{N}$  (Figure 5-4, columns III-IV). In the former case, the enriched structures appear strongly stained with toluidine blue indicating acidic tissue components and with surrounding structures indicative of cnidocytes (Figure 5-S2).

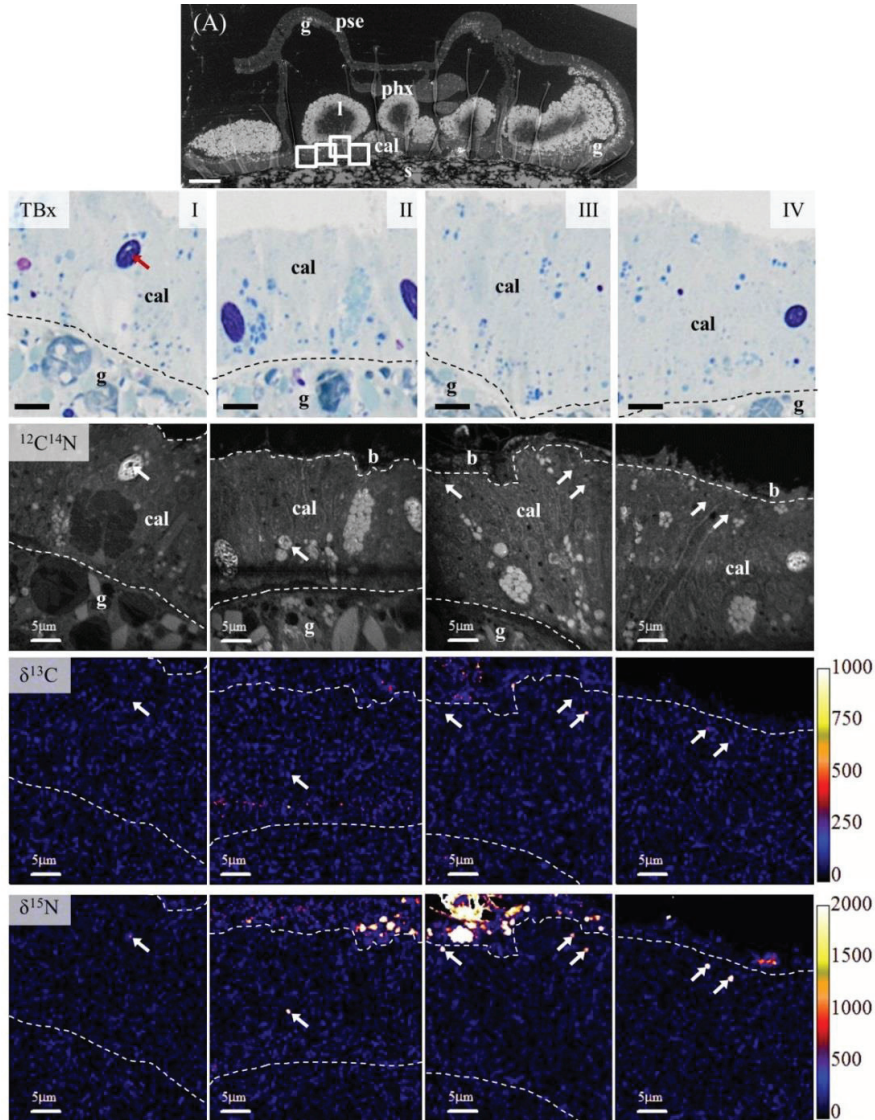


Figure 5-4: Isotopic enrichment in the metamorphosed larva.

(A) SEM image of a semi-thin ( $1\ \mu\text{m}$ ) section of a *P. damicornis* metamorphosed larva, scale bars  $100\ \mu\text{m}$ . Panel underneath shows toluidine blue/sodium borate stain (TBx) of four areas in the calicodermis, followed by  $^{14}\text{N}/^{12}\text{C}$  topography of and corresponding NanoSIMS images presenting enrichment spots (white arrows) in  $^{13}\text{C}$  and/or  $^{15}\text{N}$ , scale bars  $5\ \mu\text{m}$ . The red arrow point the structure in TBx stained section in which a  $^{15}\text{N}$  enrichment has been detected. Dotted line indicates mesoglea and thus cell layer limits. pse: pseudostratified epithelium, phx: pharynx, b: biofilm, g: gastrodermis, l: lipids, cal: calicodermis.

## V. Discussion

This data presented above are to be considered preliminary results illustrating a methodology that might prove helpful in identifying possible pathways taken by chemical cues that trigger coral larva settle-

ment and metamorphosis. In the following discussion, it is cautioned that only one section was imaged with the NanoSIMS for each, unique, sample. Nevertheless, it is the first time that such an experimental design has been carried out and these preliminary observations outcomes are discussed qualitatively.

The results show unambiguously that unidentified molecules from the mature biofilm were transferred to the settled metamorphosing larva. In the presence of crustose coralline algae (CCA) (and associated bacterial biofilm) settlement and metamorphosis of *P. damicornis* planulae was induced. The presence of  $^{13}\text{C}$  labeling in the primary starch surrounding the pyrenoid of dinoflagellates was observed in both unsettled planula and metamorphosed larva. Most likely, this is due to rapid photo-assimilation of  $^{13}\text{CO}_2$  respired by the labeled biofilm. Unsettled planula did not display any isotopic enrichment from the biofilm in their aboral pseudostratified epithelium (pse) - which is the future site of calicodermis differentiation - but did exhibit one  $^{15}\text{N}$  enrichment spot ( $< 1 \mu\text{m}$ ) in the pharynx area of the oral pole. Before settlement, planulae probe substrate surface with their oral pole. This  $^{15}\text{N}$ -enrichment in the pharynx may be due to a potential cue or inhibitor (as they did not settle) of metamorphosis. We did not observe any enrichment in the oral pse surrounding the pharynx.

Settled and metamorphosed larvae exhibited a few spots with isotopic enrichment in its calicodermis. Two kind of spots where observed:  $^{15}\text{N}$ -enrichment without  $^{13}\text{C}$ -enrichment or both  $^{13}\text{C}$  and  $^{15}\text{N}$ -enrichments, which most likely indicates that more than one type of molecules were transferred to the coral tissue. In some cases the former type of enrichment was associated with structures of the calicodermis that are interpreted to be cnidocytes (Figure 5-4, 5-S2), although this hypothesis should be confirmed with transmission electron microscopy of serial ultra-thin sections. Hexacorallia have two types of cnidocytes (Peters, 2016) that are thought to be involved in settlement (Vandermeulen, 1974). It is possible that settlement and metamorphosis involve two distinct induction pathways, because a chemical cue such as TBP generally induces metamorphosis without settlement. No enrichment was observed in the other cell layers of the metamorphosed larva, including the pharynx, indicating that most of the chemical cues for settlement go through the aboral epithelium/differentiating calicodermis. Nevertheless due to the small size of enrichment spots, ( $<1 \mu\text{m}$ ), and the fact that only one section was imaged per sample, we cannot rule out the possibility that other enrichment spots are present in other cell layers.

This study is the first revealing a transfer of molecules from the biofilm to the metamorphosing scleractinian larva with a spatial resolution that allow subcellular structures to be resolved. Further replicates and analysis are needed, but this approach could bring more information about the chemical cues involved in settlement and metamorphosis induction.

## VI. Supplementary material

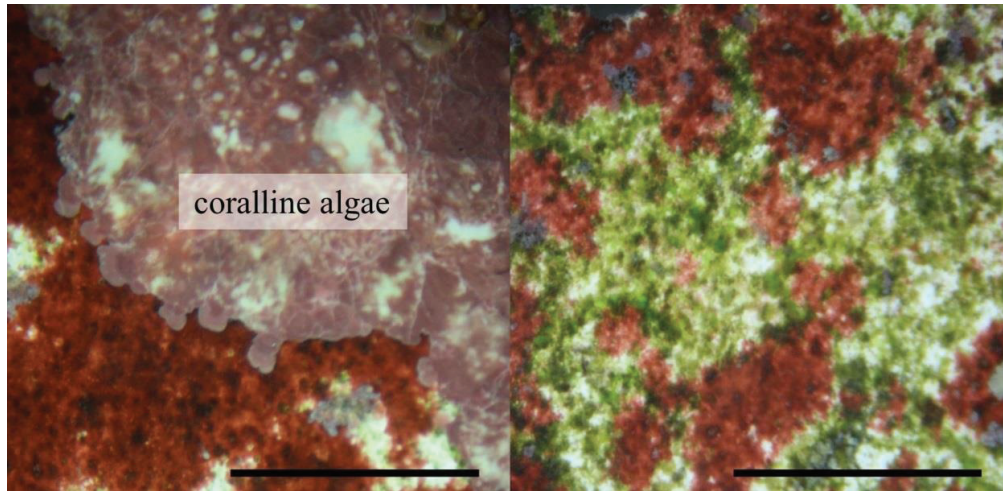


Figure 5-S1: Mature biofilm grown on underwater paper in aquaria conditions at the Aquarium Tropical du Palais de la Porte Dorée (Paris, France). Scale bars: 1 cm.

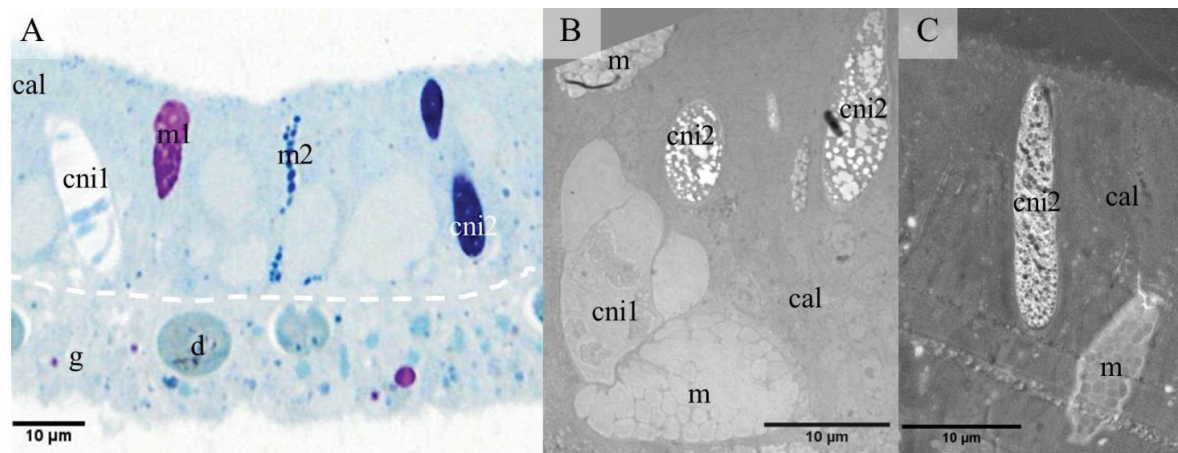


Figure 5-S2: Early metamorphosis calicodermis with some of its cnidocyte and mucous cells. (A) Semi-thin section (1  $\mu\text{m}$ ) stained with toluidine blue in which we can see at least two types of cnidocyte and mucocyte. Dashed white line indicates mesoglea location and thus delimits cell layers. (B) Transmission electron microscopy of an ultra-thin section (70 nm) with the corresponding type 1 and 2 cnidocytes and unidentified mucocytes. (C) SEM BSE acquisition of a cnidocyte type 2 and a mucocyte. cal: calicodermis, g: gastrodermis, cni: cnidocyte type 1 or 2, m: mucocyte type 1 or 2, d: dinoflagellate.



# General discussion and conclusion

A critical step in the coral life cycle is the metamorphosis of the planula into a benthic polyp and future colony. However the cellular mechanisms that support this step, and particularly the formation of the skeletogenic cell layer, are not understood. The global objective of this thesis was to increase knowledge about the establishment of the calicodermis during polyp morphogenesis and a fundamental question that initiated this thesis work was: By which cellular mechanisms do corals develop from a non-calcifying swimming planula larva into a benthic calcifying polyp? Two pocilloporid scleractinian coral species (*Pocillopora damicornis* and *Stylophora pistillata*) were studied using fluorescence and electron microscopy techniques, tissue homeostasis assays (BrdU labeling, TUNEL), molecular biology tools and NanoSIMS isotopic imaging. The work contributes to better understand cellular processes during coral metamorphosis and, as discussed in the introduction, is set in a context of high coral mortality and stress from both local and global anthropogenic environmental impact, including climate change.

## I. Metamorphosis induction

Environmental cues induce coral metamorphosis (Heyward and Negri, 1999; Mason et al., 2011; Morse et al., 1988; Mundy and Babcock, 1998; Nozawa and Harrison, 2007; Nozawa et al., 2011; Vermeij et al., 2010; Whalan et al., 2012, 2015). How these physical and chemical cues trigger coral settlement and metamorphosis remain poorly understood. In Chapter 4, a molecular transfer from an isotopically labeled biofilm containing coralline crustose algae (CCA) to the forming calicodermis of a settled early metamorphosis stage recruit was visualized for the first time using nanoscale secondary ion mass spectrometry (NanoSIMS). This finding, although representing relatively low levels of detection, supports an internalization of unidentified biofilm-derived compounds, which can provoke morphogenetic changes associated with coral settlement and metamorphosis. The NanoSIMS detection in the coral tissue of at least two types of signals, one enriched exclusively in  $^{15}\text{N}$  and another enriched in both  $^{15}\text{N}$  and  $^{13}\text{C}$ , suggests that multiple inducers might be involved in metamorphosis. The existence of distinct cues for settlement and metamorphosis is a likely possibility, based on the observation that different cues can induce complete (settlement *and* metamorphosis) or incomplete metamorphosis (no settlement but metamorphosis). In *Porites astreoides* CCA always induce complete metamorphosis whereas tetrabromopyrrole isolated from CCA-associated biofilm induces both complete and uncomplete settlement ,(Sneed et al., 2014; Tebben et al., 2015). To further strengthen the significance of the preliminary NanoSIMS observations presented in Chapter 4, a study would have to be established to include more replicate samples with precise TEM or SEM-BSE identification of the structures associated with the observed isotopic signals. Chemical identification of the labeled molecules transferred from the biofilm to the host coral would be another essential step to better understand this pro-

cess. This could be achieved with, for example, MALDI-TOF mass spectrometry (matrix-assisted laser desorption/ionization time-of-flight) that allows metabolite imaging in tissue sections.

## II. Calicodermis establishment during metamorphosis

Establishment of the calicodermis is required to be a fast process given that skeleton deposition is visible as early as 6 hours after settlement (Vandermeulen and Watabe, 1973, Gilis et al. 2014). Results of Chapters 2 and 3 indicate that cell division at the early metamorphosis stage stays low, similar to the planula stage. This demonstrates that, in the two species studied, formation of the calicodermis does not require cell proliferation. Thus it is more likely that this cell layer initially emerges from direct trans-differentiation of the aboral pseudostratified epithelium of the planula. To our knowledge, no published studies exist on cell proliferation during metamorphosis in scleractinian corals. However, similar cell behavior has been observed in *Hydractinia* metamorphosis, during which some cells directly trans-differentiate into post-metamorphosis cells and cell proliferation activity increases only 9 h after beginning of the metamorphosis (Kroiher et al., 1990; Plickert et al., 1988). Thus, in *Cnidaria* it is not uncommon that in the metamorphosis process existing larval cells rapidly trans-differentiate and that only hours later, proliferation significantly increases in the cnidarian tissues. Interestingly, results from primary cell cultures in Chapter 1 show that explant formation does not imply cell proliferation. Similarly, it has been shown in *Hydra* that the regeneration process, i.e. after head ablation, can occur without cell proliferation (Cummings and Bode, 1984). Together this data demonstrate great cell plasticity of corals and other *Cnidaria*.

Primary polyps grow rapidly while supporting active skeleton formation. However, the calicodermis remains the cell layer with the least proliferation activity at all stages for both species investigated (Chapters 2 and 3), raising questions about the origin of calciblasts. Direct trans-differentiation of the aboral pseudostratified epithelium might supply calciblasts during early metamorphosis, but in the developing primary polyp, the low cell division rate in calicodermis cannot sustain its growth. As possible solution to this problem, supported by the observations presented in Chapter 2, is that differentiating cells migrate from regions characterized by high proliferation rates (such as the pharynx), through the pseudostratified epithelium and/or the mesenterial filaments, to the calicodermis.

Cell proliferation patterns seem to be diverse in cnidarians. In *Clytia hemisphaerica* cnidocyte progenitors divide fast locally, at the base of tentacle and in the tentacle bulb, and progenies migrate and differentiate on their way up to the tentacle tip (Denker et al., 2008). In *Hydra*, all cell types are formed from interstitial cells dividing in the body column and progeny cells migrate either to the polyp tentacles or to the foot (Frank et al., 2009; Gold and Jacobs, 2013); there is no cell proliferation activity outside the body column. In the anthozoan *Nematostella vectensis*, cell migration was not assessed but cell proliferation occurs broadly distributed throughout the polyp, with the highest rate in the pharynx area (up to  $49.0 \pm 3.9\%$ ) (Fritz et al., 2013;

Passamanek and Martindale, 2012). It seems that in scleractinians, there is an intermediate system between the hydrozoan system (with locally restricted areas of proliferation) and the more homogeneous proliferation pattern observed in the anthozoan *N. vectensis*. According to our results (Chapters 2 and 3) low levels of cell division occur in the entire polyp but with areas of high proliferation in the pharynx and pseudostratified epithelium from which cells may migrate. It is the first time such a pattern of cell division and migration has been proposed in scleractinian corals.

To monitor the establishment of the calicodermis during early life stages, a calicodermis cell differentiation marker (anti-Pdcyst-rich antibody) was developed and PCR primers were designed (Chapter 3). Semi-quantitative reverse transcriptase PCR revealed gene expression starting at early metamorphosis stage. Localization in the adult calicodermis was confirmed by immunolocalization in semi-thin (1  $\mu\text{m}$ ) sections. At primary polyp stage, Pdcyst-rich protein was localized at the interface with the newly formed skeleton. However, in the forming primary polyp stage localization was only possible in thicker sections using a HRP signal amplification method. Difficulties in immunohistocalizing Pdcyst-rich protein in polyp of early life stages could be explained by a low level of protein translation and/or a rapid protein secretion due to high skeleton deposition at earlier life stages. These findings need further investigations and additional western blotting experiments.

### III. Stem cells in *Scleractinia*

Identification of high proliferation areas from which cells migrate indicates the existence of localized precursor cell sources or niches. In *S. pistillata*, this source is most likely the pharynx area. In *P. damicornis*, the source is less localized but the highest division rate was observed in the pseudostratified epithelium. Only one previous study has localized stem cells in the coral *Euphyllia ancora* (Shikina et al., 2015) with a focus on germ cell lineages and the gametogenesis and without studying epithelial cells. It is therefore the first time that the pharynx is put forward as a potential precursor cell pool in the scleractinian coral *S. pistillata*. Assays to localize *piwi* expression in *P. damicornis* polyp revealed other precursor cell pools, near the cnidoglandular bands of the mesenteries and just below the tentacle tips (Chapter 3). Mesenteries were identified as highly proliferative areas and are the site of gametogenesis, consistent with the findings of Shikina et al. (2015), it is therefore not surprising to have found *piwi* expression in this area. Here, based on the observations in Chapter 3, the hypothesis is presented that *P. damicornis* may also possess germline precursors in the mesenteries.

In tentacles, the observation of *piwi* expression just below the terminal bulb could indicate a nematogenesis site (i.e. cnidocyte production). The high proliferation rate (up to 20%) observed in the tentacle tips of *P. damicornis* in Chapter 1 (Figure 7) support this hypothesis. In *Hydra* and *Hydractinia*, cnidocytes are progeny of stem cells, referred to as i-cells, that divide in the epithelium of the body column and then migrate to the

tentacle tip while differentiating (Gold and Jacobs, 2013). In *C. hemisphaerica*, nematogenesis is restricted to the base of the tentacle, the area referred to as 'tentacle bulb'. In this jellyfish species, cnidocytes are formed from stem cells in the proximal zone and migrate while differentiating to the distal zone, i.e. the tentacle tip (Denker et al., 2008). Furthermore, the stem cells of the tentacle bulb express *piwi*. In *Anthozoa* there are no i-cells (Gold and Jacobs, 2013) and nematogenesis is less studied. In *N. vectensis*, cnidocytes derive from ectodermal stem cells, but it is not clear if their formation occurs at the base of the tentacle or throughout the epithelium (Marlow et al., 2009). In scleractinian corals, the location of the cells giving rise to cnidocytes is not known. Here it is proposed that a pool of precursor cells is located just below the tentacle tips in *P. damicornis*. Location of these *piwi*-expressing cells needs to be confirmed, for example by ultrastructure in transmission electron microscopy. If confirmed, the progeny of these cells may migrate while differentiating up to tentacle base and tip.

#### **IV. Symbiont regulation during metamorphosis**

While coral-dinoflagellate symbiosis was not the main focus of this work, interesting observations of the symbiont cell population arose from the work in Chapter 2.

High division rates of *Symbiodinium in hospite* at planula, early metamorphosis, and primary polyp stages indicate an absence of proliferation regulating mechanisms for this cell population (Chapter 2, Figure 5(a)). At the same time, the observation of a constant symbiont/host ratio in the same samples indicates regulation and points to a post-mitotic control mechanism (Chapter 2, Figure 5(d)). Regulation of the symbiont population density by the host occurs through different processes; nutrient limitation (nitrogen and/or phosphorus) prevents dinoflagellate division *in hospite* (Cook et al., 1988; Hoegh-Guldberg and Smith, 1989; Jackson et al., 1989) and expulsion or degradation eliminates symbionts in situations with overabundance (Davy et al., 2012; Dunn et al., 2007; Gates et al., 1992; Titlyanov et al., 1998). Degradation and death of symbionts occur through apoptosis or autophagy. In Chapter 2, low apoptotic indices for the symbionts during at planula and early metamorphosis stages (Chapter 2, Figure 5(c)) indicate that this post-mitotic regulation is probably not the main process regulating the population in these stages, with autophagy a more likely alternative (Klionsky et al., 2012). Future work to clarify these aspects should include autophagic structures identification using transmission electron microscopy and/or the use of autophagy-blockers such as e.g. wortmannin (Dunn et al., 2007) to test if dinoflagellate population increases in the planula when autophagy is blocked. The increasing rates of apoptosis in the primary and adult polyps (Chapter 2, Figure 5(c)) imply that regulation through apoptosis increases in significance during later developmental stages.

This interesting pattern of symbiont proliferation and regulation during coral metamorphosis raises the question of its ecological significance. What could be the advantage of letting symbionts proliferate at early life stages? *S. pistillata* from the Gulf of Aqaba, Red Sea, inherits its symbionts primarily by vertical transmis-



sion, i.e. from the mother colony, but also by horizontal transmission i.e. from the environment (Byler et al., 2013). In *S. pistillata* larvae from shallow waters of the Gulf of Aqaba, which are the one studied in Chapter 2, Byler et al. (2013) observed that planulae were only harboring one dominant clade (A or C), which always corresponded to the dominant clade of the parent colony. However a shift in clade domination in juvenile colonies was observed with juvenile hosting clade A symbiont whereas their parental colonies were dominated by clade C. Hence *S. pistillata* juveniles are capable of selecting clades from the environment and shifting their dominant population. Combination of both types of symbiont acquisition is most advantageous to the future colony: obtaining the necessary symbionts from the mother colony while acquiring a perhaps even more suitable clade from the environment and transmitting such new symbiont type(s) to the next generation (Byler et al., 2013). The fact that symbionts proliferate rapidly *in hospite* but with a post-mitotic control of the population (Chapter 2), could be a way for the host to select an appropriate clade from the environment. Released planula can swim for a few days before settling (Richmond and Hunter, 1990) and thus during this time can acquire symbionts from the environment. Nevertheless Byler et al. (2013) did not observe any background clades in the collected planula, hence either the symbiont acquisition occurs during early metamorphosis or they only studied freshly released planulae that did not start to acquire new symbionts. This hypothesis has to be tested e.g. by exposing *S. pistillata* planulae hosting clade C *Symbiodinium* to clade A *Symbiodinium* while preventing metamorphosis for a few days.

The new data on symbiont regulation in a scleractinian coral presented here raises new questions about the acquisition, selection and maintenance of dinoflagellates in early life stages.

## V. Conclusion

This work assessed cellular mechanisms supporting calicodermis establishment during primary polyp morphogenesis. Cell-proliferation and death patterns in two pocilloporid corals were quantified at the tissue level. Initiation of metamorphosis does not require active cell proliferation. However, primary polyp growth is supported by areas of high cell division activity, localized to the pharynx and pseudostratified epithelium, from which cells may migrate to reach the calicodermis. Cell markers were developed and potential proliferative precursor cells have been localized in two areas: The mesenteries, potentially involved in gametogenesis, and right below the tentacle tips, potentially involved in nematogenesis, opening new questions regarding their commitment to specific lineages of differentiated cell types.



## References

### - A -

- Al-Horani, F.A. (2015). Physiology of skeletogenesis in scleractinian coral. In *Diseases of Coral*, pp. 192–205.
- Alié, A., Leclère, L., Jager, M., Dayraud, C., Chang, P., Le Guyader, H., Quéinnec, E., and Manuel, M. (2011). Somatic stem cells express *Piwi* and *Vasa* genes in an adult ctenophore: Ancient association of “germline genes” with stemness. *Dev. Biol.* *350*, 183–197.
- Allemand, D., Ferrier-Pagès, C., Furla, P., Houlbrèque, F., Puverel, S., Reynaud, S., Tambutté, É., Tambutté, S., and Zoccola, D. (2004). Biomineralisation in reef-building corals: from molecular mechanisms to environmental control. *Comptes Rendus Palevol* *3*, 453–467.
- Allemand, D., Tambutté, É., Zoccola, D., and Tambutté, S. (2011). Coral calcification, cells to reefs. In *Coral Reefs: An Ecosystem in Transition*, Z. Dubinsky, and N. Stambler, eds. (Springer Netherlands), pp. 119–150.
- Al-Moghrabi, S., Goiran, C., Allemand, D., Speziale, N., and Jaubert, J. (1996). Inorganic carbon uptake for photosynthesis by the symbiotic coral-dinoflagellate association II. Mechanisms for bicarbonate uptake. *J. Exp. Mar. Biol. Ecol.* *199*, 227–248.
- Ayre, D.J., and Resing, J.M. (1986). Sexual and asexual production of planulae in reef corals. *Mar. Biol.* *90*, 187–190.

### - B -

- Baghdasarian, G., and Muscatine, L. (2000). Preferential expulsion of dividing algal cells as a mechanism for regulating algal-cnidarian symbiosis. *Biol. Bull.* *199*, 278–286.
- Baird, A.H., and Morse, A.N.C. (2004). Induction of metamorphosis in larvae of the brooding corals *Acropora palifera* and *Stylophora pistillata*. *Mar. Freshw. Res.* *55*, 469–472.
- Barfield, S., Aglyamova, G.V., and Matz, M.V. (2016). Evolutionary origins of germline segregation in Metazoa: evidence for a germ stem cell lineage in the coral *Orbicella faveolata* (Cnidaria, Anthozoa). *Proc. R. Soc. Lond. B Biol. Sci.* *283*, 20152128.
- Bénazet-Tambutté, S., Allemand, D., and Jaubert, J. (1996). Permeability of the oral epithelial layers in cnidarians. *Mar. Biol.* *126*, 43–53.
- Berkelmans, R., De'ath, G., Kininmonth, S., and Skirving, W.J. (2004). A comparison of the 1998 and 2002 coral bleaching events on the Great Barrier Reef: spatial correlation, patterns, and predictions. *Coral Reefs* *23*, 74–83.
- Bertucci, A., Moya, A., Tambutté, S., Allemand, D., Supuran, C.T., and Zoccola, D. (2013). Carbonic anhydrases in anthozoan corals—A review. *Bioorg. Med. Chem.* *21*, 1437–1450.
- Bode, H.R., Heimfeld, S., Chow, M.A., and Huang, L.W. (1987). Gland cells arise by differentiation from interstitial cells in *Hydra attenuata*. *Dev. Biol.* *122*, 577–585.
- Bongaerts, P., Carmichael, M., Hay, K.B., Tonk, L., Frade, P.R., and Hoegh-Guldberg, O. (2015). Prevalent endosymbiont zonation shapes the depth distributions of scleractinian coral species. *R. Soc. Open Sci.* *2*, 140297.
- Bruckner, A.W. (2015). History of Coral Disease Research. *Dis. Coral* *52*.

Byler, K.A., Carmi-Veal, M., Fine, M., and Goulet, T.L. (2013). Multiple symbiont acquisition strategies as an adaptive mechanism in the coral *Stylophora pistillata*. PLoS ONE 8, e59596.

- C -

Carpenter, K.E., Abrar, M., Aeby, G., Aronson, R.B., Banks, S., Bruckner, A., Chiriboga, A., Cortés, J., Delbeek, J.C., DeVantier, L., et al. (2008). One-third of reef-building corals face elevated extinction risk from climate change and local impacts. Science 321, 560–563.

Cesar, H.S.J. (2002). Coral reefs: their functions, threats and economic value. Neth. Cesar Environ. Econ. Consult.

Cohen, A.L., and Holcomb, M. (2009). Why corals care about ocean acidification: uncovering the mechanism. Oceanography 22, 118–127.

Cook, C.B., D’Elia, C.F., and Muller-Parker, G. (1988). Host feeding and nutrient sufficiency for zooxanthellae in the sea anemone *Aiptasia pallida*. Mar. Biol. 98, 253–262.

Cooper, E., Burke, L., and Bood, N. (2008). Belize’s coastal capital: the economic contribution of Belize’s coral reefs and mangroves. World Resour. Inst.

Costanza, R., d’Arge, R., de Groot, R., Farber, S., Grasso, M., Hannon, B., Limburg, K., Naeem, S., O’Neill, R.V., Paruelo, J., et al. (1997). The value of the world’s ecosystem services and natural capital. Nature 387, 253–260.

Cressey, D. (2016). Coral crisis: Great Barrier Reef bleaching is “the worst we’ve ever seen.” Nature.

Cummings, S.G., and Bode, H.R. (1984). Head regeneration and polarity reversal in *Hydra attenuata* can occur in the absence of DNA synthesis. Wilhelm Roux Arch. Dev. Biol. 194, 79–86.

- D -

Daly, M., Fautin, D.G., and Cappola, V.A. (2003). Systematics of the Hexacorallia (Cnidaria: Anthozoa). Zool. J. Linn. Soc. 139, 419–437.

Darwin, C. (1897). The structure and distribution of coral reefs (New York: D. Appleton and company).

David, C.N., and Campbell, R.D. (1972). Cell Cycle Kinetics and Development of *Hydra attenuata* I. Epithelial Cells. J. Cell Sci. 11, 557–568.

Davy, S.K., Allemand, D., and Weis, V.M. (2012). Cell biology of cnidarian-dinoflagellate symbiosis. Microbiol. Mol. Biol. Rev. 76, 229–261.

Denker, E., Manuel, M., Leclère, L., Le Guyader, H., and Rabet, N. (2008). Ordered progression of nematogenesis from stem cells through differentiation stages in the tentacle bulb of *Clytia hemisphaerica* (Hydrozoa, Cnidaria). Dev. Biol. 315, 99–113.

Domart-Coulon, I., and Ostrander, G.K. (2016). Coral cell and tissue culture methods. In Diseases of Coral, (Wiley Blackwell), pp. 489–505.

Domart-Coulon, I.J., Elbert, D.C., Scully, E.P., Calimlim, P.S., and Ostrander, G.K. (2001). Aragonite crystallization in primary cell cultures of multicellular isolates from a hard coral, *Pocillopora damicornis*. Proc. Natl. Acad. Sci. 98, 11885–11890.

Drake, J.L., Mass, T., Haramaty, L., Zelzion, E., Bhattacharya, D., and Falkowski, P.G. (2013). Proteomic analysis of skeletal organic matrix from the stony coral *Stylophora pistillata*. *Proc. Natl. Acad. Sci.* *110*, 3788–3793.

Dunn, S.R., Schnitzler, C.E., and Weis, V.M. (2007). Apoptosis and autophagy as mechanisms of dinoflagellate symbiont release during cnidarian bleaching: every which way you lose. *Proc. R. Soc. Lond. B Biol. Sci.* *274*, 3079–3085.

## - E -

Eilers, M., and Eisenman, R.N. (2008). Myc's broad reach. *Genes Dev.* *22*, 2755–2766.

Erwin, P.M., and Szmant, A.M. (2010). Settlement induction of *Acropora palmata* planulae by a GLW-amide neuropeptide. *Coral Reefs* *29*, 929–939.

Extavour, C.G., Pang, K., Matus, D.Q., and Martindale, M.Q. (2005). *vasa* and *nanos* expression patterns in a sea anemone and the evolution of bilaterian germ cell specification mechanisms. *Evol. Dev.* *7*, 201–215.

## - F -

Fabricius, K.E. (2005). Effects of terrestrial runoff on the ecology of corals and coral reefs: review and synthesis. *Mar. Pollut. Bull.* *50*, 125–146.

Fautin, D.G. (2002). Reproduction of *Cnidaria*. *Can. J. Zool.* *80*, 1735–1754.

Feuillassier, L., Martinez, L., Romans, P., Engelmann-Sylvestre, I., Masanet, P., Barthélémy, D., and Engelmann, F. (2014). Survival of tissue balls from the coral *Pocillopora damicornis* L. exposed to cryoprotectant solutions. *Cryobiology*.

Finnerty, J.R., Pang, K., Burton, P., Paulson, D., and Martindale, M.Q. (2004). Origins of bilateral symmetry: *Hox* and *Dpp* expression in a sea anemone. *Science* *304*, 1335–1337.

Fox, R., Barnes, R.D., and Ruppert, E.E. (2003). *Invertebrate zoology: a functional evolutionary approach* (Belmont, CA: Brooks/Cole).

Frank, U., Plickert, G., and Mueller, W.A. (2009). *Cnidarian interstitial cells: the dawn of stem cell research*. (Springer).

Fritz, A.E., Ikmi, A., Seidel, C., Paulson, A., and Gibson, M.C. (2013). Mechanisms of tentacle morphogenesis in the sea anemone *Nematostella vectensis*. *Development* *140*, 2212–2223.

Fukuda, I., Ooki, S., Fujita, T., Murayama, E., Nagasawa, H., Isa, Y., and Watanabe, T. (2003). Molecular cloning of a cDNA encoding a soluble protein in the coral exoskeleton. *Biochem. Biophys. Res. Commun.* *304*, 11–17.

Furla, P., Allemand, D., and Orsenigo, M.-N. (2000a). Involvement of H<sup>+</sup>-ATPase and carbonic anhydrase in inorganic carbon uptake for endosymbiont photosynthesis. *Am. J. Physiol.-Regul. Integr. Comp. Physiol.* *278*, R870–R881.

Furla, P., Galgani, I., Durand, I., and Allemand, D. (2000b). Sources and mechanisms of inorganic carbon transport for coral calcification and photosynthesis. *J. Exp. Biol.* *203*, 3445–3457.

## - G -

Gardner, S.G., Nielsen, D.A., Petrou, K., Larkum, A.W.D., and Ralph, P.J. (2015). Characterisation of coral explants: a model organism for cnidarian–dinoflagellate studies. *Coral Reefs* *34*, 133–142.

Gates, R.D., Baghdasarian, G., and Muscatine, L. (1992). Temperature stress causes host cell detachment in symbiotic cnidarians: implications for coral bleaching. *Biol. Bull.* 182, 324–332.

Gilis, M., Meibom, A., Domart-Coulon, I., Grauby, O., Stolarski, J., and Baronnet, A. (2014). Biomineralization in newly settled recruits of the scleractinian coral *Pocillopora damicornis*. *J. Morphol.* 275, 1349–1365.

Gilis, M., Meibom, A., Alexander, D., Grauby, O., Stolarski, J., and Baronnet, A. (2015). Morphology, microstructure, crystallography, and chemistry of distinct CaCO<sub>3</sub> deposits formed by early recruits of the scleractinian coral *Pocillopora damicornis*. *J. Morphol.* 276, 1146–1156.

Gold, D.A., and Jacobs, D.K. (2013). Stem cell dynamics in Cnidaria: are there unifying principles? *Dev. Genes Evol.* 223, 53–66.

Gómez-Cabrera, M. del C., Ortiz, J.C., Loh, W.K.W., Ward, S., and Hoegh-Guldberg, O. (2008). Acquisition of symbiotic dinoflagellates (*Symbiodinium*) by juveniles of the coral *Acropora longicyathus*. *Coral Reefs* 27, 219–226.

Grasso, L.C., Negri, A.P., Fôret, S., Saint, R., Hayward, D.C., Miller, D.J., and Ball, E.E. (2011). The biology of coral metamorphosis: Molecular responses of larvae to inducers of settlement and metamorphosis. *Dev. Biol.* 353, 411–419.

Grimson, A., Srivastava, M., Fahey, B., Woodcroft, B.J., Chiang, H.R., King, N., Degnan, B.M., Rokhsar, D.S., and Bartel, D.P. (2008). Early origins and evolution of microRNAs and Piwi-interacting RNAs in animals. *Nature* 455, 1193–1197.

## - H -

Hadfield, M.G., and Paul, V.J. (2001). Natural chemical cues for settlement and metamorphosis of marine invertebrate larvae. *Mar. Chem. Ecol.* 431–461.

Harrison, P.L. (2011). Sexual reproduction of scleractinian corals. In *Coral Reefs: An Ecosystem in Transition*, Z. Dubinsky, and N. Stambler, eds. (Springer Netherlands), pp. 59–85.

Harrison, P.J., Waters, R.E., and Taylor, F.J.R. (1980). A broad spectrum artificial sea water medium for coastal and open ocean phytoplankton. *J. Phycol.* 16, 28–35.

Hartl, M., Mitterstiller, A.-M., Valovka, T., Breuker, K., Hobmayer, B., and Bister, K. (2010). Stem cell-specific activation of an ancestral myc protooncogene with conserved basic functions in the early metazoan *Hydra*. *Proc. Natl. Acad. Sci.* 107, 4051–4056.

Helman, Y., Natale, F., Sherrell, R.M., LaVigne, M., Starovoytov, V., Gorbunov, M.Y., and Falkowski, P.G. (2008). Extracellular matrix production and calcium carbonate precipitation by coral cells *in vitro*. *Proc. Natl. Acad. Sci. U. S. A.* 105, 54–58.

Hemrich, G., Khalturin, K., Boehm, A.-M., Puchert, M., Anton-Erxleben, F., Wittlieb, J., Klostermeier, U.C., Rosenstiel, P., Oberg, H.-H., Domazet-Lošo, T., et al. (2012). Molecular signatures of the three stem cell lineages in *Hydra* and the emergence of stem cell function at the base of multicellularity. *Mol. Biol. Evol.* 29, 3267–3280.

Heyward, A.J., and Negri, A.P. (1999). Natural inducers for coral larval metamorphosis. *Coral Reefs* 18, 273–279.

Hirose, M., Kinzie, R.A., and Hidaka, M. (2000). Early development of zooxanthella-containing eggs of the corals *Pocillopora verrucosa* and *P. eydouxi* with special reference to the distribution of zooxanthellae. *Biol. Bull.* 199, 68–75.

Hobmayer, B., Rentzsch, F., Kuhn, K., Happel, C.M., von Laue, C.C., Snyder, P., Rothbacher, U., and Holstein, T.W. (2000). WNT signaling molecules act in axis formation in the diploblastic metazoan *Hydra*. *Nature* *407*, 186–189.

Hobmayer, B., Jenewein, M., Eder, D., Eder, M.-K., Glasauer, S., Gufler, S., Hartl, M., and Salvenmoser, W. (2012). Stemness in hydra — a current perspective. *Int. J. Dev. Biol.* *56*, 509.

Hoegh-Guldberg, O., and Smith, G.J. (1989). Influence of the population density of zooxanthellae and supply of ammonium on the biomass and metabolic characteristics of the reef corals *Seriatopora hystrix* and *Stylophora pistillata*. *Mar. Ecol. Prog. Ser.* *57*, 173–186.

Hoegh-Guldberg, O., Mumby, P.J., Hooten, A.J., Steneck, R.S., Greenfield, P., Gomez, E., Harvell, C.D., Sale, P.F., Edwards, A.J., Caldeira, K., et al. (2007). Coral reefs under rapid climate change and ocean acidification. *Science* *318*, 1737–1742.

Holstein, T.W., Hobmayer, E., and David, C.N. (1991). Pattern of epithelial cell cycling in *Hydra*. *Dev. Biol.* *148*, 602–611.

Holthaus, K.B., Strasser, B., Sipos, W., Schmidt, H.A., Mlitz, V., Sukseree, S., Weissenbacher, A., Tschachler, E., Alibardi, L., and Eckhart, L. (2015). Comparative genomics identifies epidermal proteins associated with the evolution of the turtle shell. *Mol. Biol. Evol.* msv265.

#### - I -

Ip, Y.K., Lim, A.L.L., and Lim, R.W.L. (1991). Some properties of calcium-activated adenosine triphosphatase from the hermatypic coral *Galaxea fascicularis*. *Mar. Biol.* *111*, 191–197.

Isa, Y., and Yamazato, K. (1984). The distribution of carbonic anhydrase in a staghorn coral, *Acropora hebes* (Dana). *Galaxea* *3*, 25–36.

Iwao, K., Fujisawa, T., and Hatta, M. (2002). A cnidarian neuropeptide of the GLWamide family induces metamorphosis of reef-building corals in the genus *Acropora*. *Coral Reefs* *21*, 127–129.

#### - J -

Jackson, A.E., Miller, D.J., and Yellowlees, D. (1989). Phosphorus metabolism in the coral-zooxanthellae symbiosis: characterization and possible roles of two acid phosphatases in the algal symbiont *Symbiodinium* sp. *Proc. R. Soc. Lond. B Biol. Sci.* *238*, 193–202.

Juliano, C.E., Reich, A., Liu, N., Götzfried, J., Zhong, M., Uman, S., Reenan, R.A., Wessel, G.M., Steele, R.E., and Lin, H. (2014). PIWI proteins and PIWI-interacting RNAs function in *Hydra* somatic stem cells. *Proc. Natl. Acad. Sci.* *111*, 337–342.

#### - K -

Karako-Lampert, S., Zoccola, D., Salmon-Divon, M., Katzenellenbogen, M., Tambutté, S., Bertucci, A., Hoegh-Guldberg, O., Deleury, E., Allemand, D., and Levy, O. (2014). Transcriptome analysis of the scleractinian coral *Stylophora pistillata*. *PLoS ONE* *9*, e88615.

Kayal, E., Roure, B., Philippe, H., Collins, A.G., and Lavrov, D.V. (2013). Cnidarian phylogenetic relationships as revealed by mitogenomics. *BMC Evol. Biol.* *13*, 5.

Kim, J.-W., Kim, S.H., Jung, M., Kim, H.S., Han, S.-J., Moon, T.S., Kim, B.-S., Nam, B.-H., and Park, C.-I. (2015). Gene discovery in the finger leather coral *Sinularia notanda* by construction and sequencing of a normalized cDNA library. *Mar. Genomics* 19, 1–4.

Klionsky, D.J., Abdalla, F.C., Abeliovich, H., Abraham, R.T., Acevedo-Arozena, A., Adeli, K., Agholme, L., Agnello, M., Agostinis, P., Aguirre-Ghiso, J.A., et al. (2012). Guidelines for the use and interpretation of assays for monitoring autophagy. *Autophagy* 8, 445–544.

Kroiher, M., Plickert, G., and Müller, W.A. (1990). Pattern of cell proliferation in embryogenesis and planula development of *Hydractinia echinata*. *Roux's Arch. Dev. Biol.* 199, 156–163.

## - L -

LaJeunesse, T.C. (2001). Investigating the biodiversity, ecology, and phylogeny of endosymbiotic dinoflagellates in the genus *Symbiodinium* using the ITS region: in search of a “species” level marker. *J. Phycol.* 37, 866–880.

Leclère, L., Jager, M., Barreau, C., Chang, P., Le Guyader, H., Manuel, M., and Houliston, E. (2012). Maternally localized germ plasm mRNAs and germ cell/stem cell formation in the cnidarian *Clytia*. *Dev. Biol.* 364, 236–248.

Lecointe, A., Cohen, S., Gèze, M., Djediat, C., Meibom, A., and Domart-Coulon, I. (2013). Scleractinian coral cell proliferation is reduced in primary culture of suspended multicellular aggregates compared to polyps. *Cytotechnology* 65, 705–724.

Lecointe, A., Domart-Coulon, I., Paris, A., and Meibom, A. (2016). Cell proliferation and migration during early development of a symbiotic scleractinian coral. *Proc. R. Soc. Lond. B Biol. Sci.* 283, 20160206.

Lesser, M.P., Weis, V.M., Patterson, M.R., and Jokiel, P.L. (1994). Effects of morphology and water motion on carbon delivery and productivity in the reef coral, *Pocillopora damicornis* (Linnaeus): Diffusion barriers, inorganic carbon limitation, and biochemical plasticity. *J. Exp. Mar. Biol. Ecol.* 178, 153–179.

Liew, Y.J., Aranda, M., Carr, A., Baumgarten, S., Zoccola, D., Tambutté, S., Allemand, D., Micklem, G., and Woolstra, C.R. (2014). Identification of MicroRNAs in the Coral *Stylophora pistillata*. *PLoS ONE* 9, e91101.

Lim, R.S.M., Anand, A., Nishimiya-Fujisawa, C., Kobayashi, S., and Kai, T. (2014). Analysis of *Hydra* PIWI proteins and piRNAs uncover early evolutionary origins of the piRNA pathway. *Dev. Biol.* 386, 237–251.

## - M -

Magalon, H., Baudry, E., Husté, A., Adjrou, M., and Veuille, M. (2005). High genetic diversity of the symbiotic dinoflagellates in the coral *Pocillopora meandrina* from the South Pacific. *Mar. Biol.* 148, 913–922.

Marcum, B.A., and Campbell, R.D. (1978). Development of *Hydra* lacking nerve and interstitial cells. *J. Cell Sci.* 29, 17–33.

Marlow, H.Q., Srivastava, M., Matus, D.Q., Rokhsar, D., and Martindale, M.Q. (2009). Anatomy and development of the nervous system of *Nematostella vectensis*, an anthozoan cnidarian. *Dev. Neurobiol.* 69, 235–254.

Marshall, A.T. (1996). Calcification in hermatypic and ahermatypic corals. *Science* 271, 637.

Mason, B., Beard, M., and Miller, M.W. (2011). Coral larvae settle at a higher frequency on red surfaces. *Coral Reefs* 30, 667–676.



- Mass, T., Drake, J.L., Haramaty, L., Rosenthal, Y., Schofield, O.M., Sherrell, R.M., and Falkowski, P.G. (2012). Aragonite precipitation by “proto-polyps” in coral cell cultures. *PLoS ONE* 7, e35049.
- McLaughlin, J.J.A., and Zahl, P.A. (1959). Axenic zooxanthellae from various invertebrate hosts. *Ann. N. Y. Acad. Sci.* 77, 55–72.
- Mochizuki, K., Sano, H., Kobayashi, S., Nishimiya-Fujisawa, C., and Fujisawa, T. (2000). Expression and evolutionary conservation of nanos-related genes in *Hydra*. *Dev. Genes Evol.* 210, 591–602.
- Mochizuki, K., Nishimiya-Fujisawa, C., and Fujisawa, T. (2001). Universal occurrence of the vasa-related genes among metazoans and their germline expression in *Hydra*. *Dev. Genes Evol.* 211, 299–308.
- Momose, T., Derelle, R., and Houliston, E. (2008). A maternally localised Wnt ligand required for axial patterning in the cnidarian *Clytia hemisphaerica*. *Development* 135, 2105–2113.
- Morse, D.E., Hooker, N., Morse, A.N., and Jensen, R.A. (1988). Control of larval metamorphosis and recruitment in sympatric agariciid corals. *J. Exp. Mar. Biol. Ecol.* 116, 193–217.
- Moya, A., Tambutté, S., Bertucci, A., Tambutté, E., Lotto, S., Vullo, D., Supuran, C.T., Allemand, D., and Zoccola, D. (2008). Carbonic anhydrase in the scleractinian coral *Stylophora pistillata* characterization, localization and role in biomineralization. *J. Biol. Chem.* 283, 25475–25484.
- Müller, W.A., Teo, R., and Frank, U. (2004). Totipotent migratory stem cells in a hydroid. *Dev Biol* 275, 215–224.
- Mundy, C.N., and Babcock, R.C. (1998). Role of light intensity and spectral quality in coral settlement: implications for depth-dependent settlement? *J. Exp. Mar. Biol. Ecol.* 223, 235–255.
- Muscatine, L. (1990). The role of symbiotic algae in carbon and energy flux in reef corals. *Ecosyst. World* 25, 75–87.
- Muscatine, L., Tambutté, E., and Allemand, D. (1997). Morphology of coral desmocytes, cells that anchor the calicoblastic epithelium to the skeleton. *Coral Reefs* 16, 205–213.
- Muscatine, L., Ferrier-Pagès, C., Blackburn, A., Gates, R.D., Baghdasarian, G., and Allemand, D. (1998). Cell specific density of symbiotic dinoflagellates in tropical anthozoans. *Coral Reefs* 17, 329–337.

## - N -

- Nakanishi, N., Renfer, E., Technau, U., and Rentzsch, F. (2012). Nervous systems of the sea anemone *Nematostella vectensis* are generated by ectoderm and endoderm and shaped by distinct mechanisms. *Development* 139, 347–357.
- Nishikawa, A., Katoh, M., and Sakai, K. (2003). Larval settlement rates and gene flow of broadcast-spawning (*Acropora tenuis*) and planula-brooding (*Stylophora pistillata*) corals. *Mar. Ecol. Prog. Ser.* 256, 87–97.
- Nozawa, Y., and Harrison, P.L. (2007). Effects of elevated temperature on larval settlement and post-settlement survival in scleractinian corals, *Acropora solitaryensis* and *Favites chinensis*. *Mar. Biol.* 152, 1181–1185.
- Nozawa, Y., Tanaka, K., and Reimer, J.D. (2011). Reconsideration of the surface structure of settlement plates used in coral recruitment studies. *Zool. Stud.* 50, 53–60.

- O -

Olano, C.T., and Bigger, C.H. (2000). Phagocytic activities of the gorgonian coral *Swiftia exserta*. *J. Invertebr. Pathol.* *76*, 176–184.

- P -

Passamaneck, Y.J., and Martindale, M.Q. (2012). Cell proliferation is necessary for the regeneration of oral structures in the anthozoan cnidarian *Nematostella vectensis*. *BMC Dev. Biol.* *12*, 34.

Pernice, M., Dunn, S.R., Tonk, L., Dove, S., Domart-Coulon, I., Hoppe, P., Schintlmeister, A., Wagner, M., and Meibom, A. (2015). A nanoscale secondary ion mass spectrometry study of dinoflagellate functional diversity in reef-building corals. *Environ. Microbiol.* *17*, 3570–3580.

Peters, E.C. (2016). Anatomy. In *Diseases of Coral*, C.M. Woodley, C.A. Downs, A.W. Bruckner, J.W. Porter, and S.B. Galloway, eds. (John Wiley & Sons, Inc), pp. 85–107.

Plickert, G., Kroihner, M., and Munck, A. (1988). Cell proliferation and early differentiation during embryonic development and metamorphosis of *Hydractinia echinata*. *Development* *103*, 795–803.

Plickert, G., Frank, U., and Müller, W.A. (2012). *Hydractinia*, a pioneering model for stem cell biology and reprogramming somatic cells to pluripotency. *Int. J. Dev. Biol.* *56*, 519.

Puverel, S., Tambutté, E., Zoccola, D., Domart-Coulon, I., Bouchot, A., Lotto, S., Allemand, D., and Tambutté, S. (2005). Antibodies against the organic matrix in scleractinians: a new tool to study coral biomineralization. *Coral Reefs* *24*, 149–156.

- R -

Rahman, M.A., Isa, Y., and Uehara, T. (2006). Studies on two closely related species of octocorallians: biochemical and molecular characteristics of the organic matrices of endoskeletal sclerites. *Mar. Biotechnol.* *8*, 415–424.

Ramos-Silva, P., Marin, F., Kaandorp, J., and Marie, B. (2013). Biomineralization toolkit: The importance of sample cleaning prior to the characterization of biomineral proteomes. *Proc. Natl. Acad. Sci.* *110*, 2144–2146.

Ramos-Silva, P., Kaandorp, J., Herbst, F., Plasseraud, L., Alcaraz, G., Stern, C., Corneillat, M., Guichard, N., Durlet, C., Luquet, G., et al. (2014). The skeleton of the staghorn coral *Acropora millepora*: molecular and structural characterization. *PLOS ONE* *9*, e97454.

Rebscher, N., Volk, C., Teo, R., and Plickert, G. (2008). The germ plasm component *Vasa* allows tracing of the interstitial stem cells in the cnidarian *Hydractinia echinata*. *Dev. Dyn.* *237*, 1736–1745.

Reyes-Bermudez, A., Lin, Z., Hayward, D.C., Miller, D.J., and Ball, E.E. (2009). Differential expression of three galaxin-related genes during settlement and metamorphosis in the scleractinian coral *Acropora millepora*. *BMC Evol Biol* *9*, 178.

Richmond, R.H., and Hunter, C.L. (1990). Reproduction and recruitment of corals: Comparisons among the Caribbean, the Tropical Pacific, and the Red Sea. *Mar. Ecol. Prog. Ser.* Oldendorf *60*, 185–203.

Rowan, R., and Powers, D.A. (1991). A molecular genetic classification of zooxanthellae and the evolution of animal-algal symbioses. *Science* *251*, 1348–1351.

- Sarkis, S., van Beukering, P.J., McKenzie, E., Hess, S., Brander, L., Roelfsema, M., van der Putten, L.L., and Bervoets, T. (2010). Total economic value of Bermuda's coral reefs: valuation of ecosystem services (Department of Conservation Services, Government of Bermuda).
- Schmich, J., Trepel, S., and Leitz, T. (1998). The role of GLWamides in metamorphosis of *Hydractinia echinata*. *Dev. Genes Evol.* 208, 267–273.
- Schmid, V., and Alder, H. (1984). Isolated, mononucleated, striated muscle can undergo pluripotent transdifferentiation and form a complex regenerate. *Cell* 38, 801–809.
- Schmid, V., Wydler, M., and Alder, H. (1982). Transdifferentiation and regeneration *in vitro*. *Dev. Biol.* 92, 476–488.
- Seipel, K., Yanze, N., and Schmid, V. (2004). The germ line and somatic stem cell gene *Cniwi* in the jellyfish *Podocoryne carnea*. *Int. J. Dev. Biol.* 48, 1–7.
- Shen, X., Belcher, A.M., Hansma, P.K., Stucky, G.D., and Morse, D.E. (1997). Molecular cloning and characterization of lustrin A, a matrix protein from shell and pearl nacre of *Halotis rufescens*. *J. Biol. Chem.* 272, 32472–32481.
- Shikina, S., Chung, Y.-J., Wang, H.-M., Chiu, Y.-L., Shao, Z.-F., Lee, Y.-H., and Chang, C.-F. (2015). Localization of early germ cells in a stony coral, *Euphyllia ancora*: potential implications for a germline stem cell system in coral gametogenesis. *Coral Reefs* 1–15.
- Siboni, N., Abrego, D., Motti, C.A., Tebben, J., and Harder, T. (2014). Gene expression patterns during the early stages of chemically induced larval metamorphosis and settlement of the coral *Acropora millepora*. *PLOS ONE* 9, e91082.
- Siomi, M.C., Sato, K., Pezic, D., and Aravin, A.A. (2011). PIWI-interacting small RNAs: the vanguard of genome defence. *Nat Rev Mol Cell Biol* 12, 246–258.
- Sneed, J.M., Sharp, K.H., Ritchie, K.B., and Paul, V.J. (2014). The chemical cue tetrabromopyrrole from a biofilm bacterium induces settlement of multiple Caribbean corals. *Proc. R. Soc. Lond. B Biol. Sci.* 281, 20133086.
- Spalding, M., Ravilious, C., and Green, E.P. (2001). *World Atlas of Coral Reefs* (CA: University of California Press).
- Stoddart, J.A. (1983). Asexual production of planulae in the coral *Pocillopora damicornis*. *Mar. Biol.* 76, 279–284.
- Stolarski, J., Kitahara, M.V., Miller, D.J., Cairns, S.D., Mazur, M., and Meibom, A. (2011). The ancient evolutionary origins of *Scleractinia* revealed by azooxanthellate corals. *BMC Evol. Biol.* 11, 316.
- Strasser, B., Mlitz, V., Hermann, M., Rice, R.H., Eigenheer, R.A., Alibardi, L., Tschachler, E., and Eckhart, L. (2014). Evolutionary origin and diversification of epidermal barrier proteins in amniotes. *Mol. Biol. Evol.* msu251.
- Strasser, B., Mlitz, V., Hermann, M., Tschachler, E., and Eckhart, L. (2015). Convergent evolution of cysteine-rich proteins in feathers and hair. *BMC Evol. Biol.* 15, 1.

Sunagawa, S., DeSalvo, M.K., Voolstra, C.R., Reyes-Bermudez, A., and Medina, M. (2009). Identification and gene expression analysis of a taxonomically restricted cysteine-rich protein family in reef-building corals. *PLoS ONE* 4, e4865.

**- T -**

Takahashi, T., Hatta, M., Takahashi, T., and Hatta, M. (2011). The importance of GLWamide neuropeptides in cnidarian development and physiology. *J. Amino Acids* 2011, 2011, e424501.

Tambutté, E., Allemand, D., Bourge, I., Gattuso, J.-P., and Jaubert, J. (1995). An improved <sup>45</sup>Ca protocol for investigating physiological mechanisms in coral calcification. *Mar. Biol.* 122, 453–459.

Tambutté, E., Tambutté, S., Segonds, N., Zoccola, D., Venn, A., Erez, J., and Allemand, D. (2012). Calcein labeling and electrophysiology: insights on coral tissue permeability and calcification. *Proc. R. Soc. Lond. B Biol. Sci.* 279, 19–27.

Tambutté, S., Tambutté, E., Zoccola, D., Caminiti, N., Lotto, S., Moya, A., Allemand, D., and Adkins, J. (2007). Characterization and role of carbonic anhydrase in the calcification process of the azooxanthellate coral *Tubastrea aurea*. *Mar. Biol.* 151, 71–83.

Tebben, J., Tapiolas, D.M., Motti, C.A., Abrego, D., Negri, A.P., Blackall, L.L., Steinberg, P.D., and Harder, T. (2011). Induction of larval metamorphosis of the coral *Acropora millepora* by tetrabromopyrrole isolated from a *Pseudoalteromonas* bacterium. *PLoS ONE* 6, e19082.

Tebben, J., Motti, C.A., Siboni, N., Tapiolas, D.M., Negri, A.P., Schupp, P.J., Kitamura, M., Hatta, M., Steinberg, P.D., and Harder, T. (2015). Chemical mediation of coral larval settlement by crustose coralline algae. *Sci. Rep.* 5.

Technau, U., and Steele, R.E. (2011). Evolutionary crossroads in developmental biology: *Cnidaria*. *Development* 138, 1447–1458.

Titlyanov, E.A., Titlyanova, T.V., Loya, Y., and Yamazato, K. (1998). Degradation and proliferation of zooxanthellae in planulae of the hermatypic coral *Stylophora pistillata*. *Mar. Biol.* 130, 471–477.

Traylor-Knowles, N., Granger, B.R., Lubinski, T.J., Parikh, J.R., Garamszegi, S., Xia, Y., Marto, J.A., Kaufman, L., and Finnerty, J.R. (2011). Production of a reference transcriptome and transcriptomic database (PocilloporaBase) for the cauliflower coral, *Pocillopora damicornis*. *BMC Genomics* 12, 585.

**- V -**

Vagin, V.V., Sigova, A., Li, C., Seitz, H., Gvozdev, V., and Zamore, P.D. (2006). A distinct small rna pathway silences selfish genetic elements in the germline. *Science* 313, 320–324.

Vandermeulen, J.H. (1974). Studies on reef corals. II. Fine structure of planktonic planula larva of *Pocillopora damicornis*, with emphasis on the aboral epidermis. *Mar. Biol.* 27, 239–249.

Vandermeulen, J.H. (1975). Studies on reef corals. III. Fine structural changes of calicoblast cells in *Pocillopora damicornis* during settling and calcification. *Mar. Biol.* 31, 69–77.

Vandermeulen, J.H., and Watabe, N. (1973). Studies on reef corals. I. Skeleton formation by newly settled planula larva of *Pocillopora damicornis*. *Mar. Biol.* 23, 47–57.

Vermeij, M.J.A., Marhaver, K.L., Huijbers, C.M., Nagelkerken, I., and Simpson, S.D. (2010). Coral Larvae Move toward Reef Sounds. *PLOS ONE* 5, e10660.

Veron, J.E.N. (2000). *Corals of the World Vol. 1 2 3* (Townsville: Odyssey Publishing).

Vidal-Dupiol, J., Adjeroud, M., Roger, E., Foure, L., Dural, D., Mone, Y., Ferrier-Pagès, C., Tambutté, E., Tambutté, S., Zoccola, D., et al. (2009). Coral bleaching under thermal stress: putative involvement of host/symbiont recognition mechanisms. *BMC Physiol.*

Vidal-Dupiol, J., Zoccola, D., Tambutté, E., Grunau, C., Cosseau, C., Smith, K.M., Freitag, M., Dheilly, N.M., Allemand, D., and Tambutté, S. (2013). Genes related to ion-transport and energy production are Upregulated in response to CO<sub>2</sub>-driven pH decrease in corals: new insights from transcriptome analysis. *PLoS ONE* 8, e58652.

Vizel, M., and Kramarsky-Winter, E. (2016). Coral tissue culture and micropropagation. *Dis. Coral* 482–488.

Vizel, M., Loya, Y., Downs, C.A., and Kramarsky-Winter, E. (2011). A novel method for coral explant culture and micropropagation. *Mar Biotechnol NY* 13, 423–432.

## - W -

Webster, N.S., Smith, L.D., Heyward, A.J., Watts, J.E.M., Webb, R.I., Blackall, L.L., and Negri, A.P. (2004). Metamorphosis of a scleractinian coral in response to microbial biofilms. *Appl. Environ. Microbiol.* 70, 1213–1221.

Weis, V.M. (1993). Effect of dissolved inorganic carbon concentration on the photosynthesis of the symbiotic sea anemone *Aiptasia pulchella* Carlgren: Role of carbonic anhydrase. *J. Exp. Mar. Biol. Ecol.* 174, 209–225.

Weis, V.M., Smith, G.J., and Muscatine, L. (1989). A “CO<sub>2</sub> supply” mechanism in zooxanthellate cnidarians: role of carbonic anhydrase. *Mar. Biol.* 100, 195–202.

Wend, P., Holland, J.D., Ziebold, U., and Birchmeier, W. (2010). Wnt signaling in stem and cancer stem cells. *Semin. Cell Dev. Biol.* 21, 855–863.

Whalan, S., Webster, N.S., and Negri, A.P. (2012). Crustose coralline algae and a cnidarian neuropeptide trigger larval settlement in two coral reef sponges. *PLoS ONE* 7, e30386.

Whalan, S., Wahab, M.A.A., Sprungala, S., Poole, A.J., and Nys, R. de (2015). Larval settlement: the role of surface topography for sessile coral reef invertebrates. *PLOS ONE* 10, e0117675.

Wiedenmann, J., D’Angelo, C., Smith, E.G., Hunt, A.N., Legiret, F.-E., Postle, A.D., and Achterberg, E.P. (2013). Nutrient enrichment can increase the susceptibility of reef corals to bleaching. *Nat. Clim. Change* 3, 160–164.

Wilkinson, C.R. (2008). *Status of coral reefs of the world 2008* (Australian Institute of Marine Science Townsville).

## - Z -

Zapata, F., Goetz, F.E., Smith, S.A., Howison, M., Siebert, S., Church, S.H., Sanders, S.M., Ames, C.L., McFadden, C.S., France, S.C., et al. (2015). Phylogenomic analyses support traditional relationships within *Cnidaria*. *PLOS ONE* 10, e0139068.

Zoccola, D., Tambutté, E., Kulhanek, E., Puvarel, S., Scimeca, J.C., Allemand, D., and Tambutté, S. (2004). Molecular cloning and localization of a PMCA P-type calcium ATPase from the coral *Stylophora pistillata*. *Biochim. Biophys. Acta-Biomembr.* 1663, 117–126.



## Curriculum Vitae

LECOINTE Agathe

30 rue Geoffroy Saint Hilaire 75005, Paris

French

agathe.lecointe@epfl.ch

17.10.1989 (26 years old)

+33 6 29 99 30 94

### EMPLOYMENT HISTORY

- 2012-present      PhD student : Scleractinian coral morphogenesis: Searching for stem cells and precursors of the skeletogenic calicodermis
- Collaborations with Aquariums: Océanopolis (Brest), Aquarium tropical du palais de la porte dorée (Paris).
- Field experiments in Red Sea.
- Thesis Director: Anders Meibom  
Thesis Co-Director: Isabelle Domart-Coulon
- 2012 January-June      Establishment of primary coral cell culture and assessment of cell division in adult polyps and coral explant. UMR 7208 BOREA · Evolution of Biomineralisation · National Museum of Natural History, 75005 Paris. Supervisor: Isabelle Domart-Coulon
- 2011 January-June      Study of two transmembrane proteins specific of filamentous cyanobacteria. Laboratorio de Ecología Microbiana y Toxicología Ambiental · Dpto. Genética Molecular y Microbiología · Facultad de Ciencias Biológicas Pontificia Universidad Católica de Chile. Lab Director: Mónica Vásquez. Supervisor: Dinka Mandakovic
- 2010 July              Internship at the “Grand Aquarium de Saint-Malo” (35400 Ille-et-Vilaine) Education

### PUBLICATIONS

Lecoinge, A., Cohen, S., Gèze, M., Djediat, C., Meibom, A., and Domart-Coulon, I. (2013). Scleractinian coral cell proliferation is reduced in primary culture of suspended multicellular aggregates compared to polyps. *Cytotechnology* 65, 705–724.

Lecoinge, A., Domart-Coulon, I., Paris, A., and Meibom, A. (2016). Cell proliferation and migration during early development of a symbiotic scleractinian coral. *Proc. R. Soc. B* 283, 20160206.

### TALKS AND POSTERS

- 2016      International Coral Reef Symposium (ICRS), oral presentation “Cell proliferation and turnover in early life stages of a symbiotic scleractinian coral”

- 2015 Union of French Aquarium Curators (UCA), oral presentation, "Scleractinian corals larvae emission in artificial conditions and study of metamorphosis"
- 2013 International conference on coelenterate biology (ICCB), oral presentation, "Cell proliferation in polyp and larval tissues of scleractinian corals"
- 2013 Poster "Proliferation activity among the four cell layers of the coral *Pocillopora damicornis* (*Scleractinia*)" for CASA days (EPFL) and UMR MCAM (MNHN).
- 2012 International congress, Marine Invertebrate Cell Culture Symposium, oral presentation "Coral cell proliferation *in situ* (polyp) and in primary cultures"
- 2011 Poster "Morphometric changes of *Nostoc* sp. PCC7120 and genetic expression analysis of *filA* and *filB*, cell membrane protein coding genes specific of filamentous cyanobacteria"

### EDUCATION

- 2012-present PhD in marine biology at EPFL. In co-direction with Isabelle Domart-Coulon the National Museum of Natural History, Paris, France. Thesis director: Anders Meibom.
- 2010-2012 Master. in marine biology. University Pierre et Marie Curie, Paris, France.
- 2007-2010 Bachelor in life Science. University Pierre et Marie Curie, Paris, France.

### LANGUAGES

English: fluent  
 Spanish: moderate  
 German: basic

### MISCELLANEOUS

Scuba-diving (PADI lvl 2, >50 dives in Mediterranean Sea and Red Sea),  
 Theater (5 years).



